

**An Antibiotic Discovery Campaign Targeting VirF, the Main Transcriptional
Regulator of Virulence in *Shigella flexneri***

By

Anthony A. Emanuele

A dissertation submitted in partial fulfillment
of the requirements for the degree of
Doctor of Philosophy
(Medicinal Chemistry)
in the University of Michigan
2016

Doctoral Committee:

Professor George A. Garcia, Chair
Professor Gordon L. Amidon
Professor Anna K. Mapp
Professor Hollis D. Showalter
Professor Ronald W. Woodard

A piece of advice that helped me through my last year of graduate school:

***No amount of regret can change the past,
and no amount of anxiety can change the future***

© Anthony A. Emanuele

2015

**For my biggest fan,
My Mother
(who is more excited than I am about my graduation)**

ACKNOWLEDGEMENTS

I would not be where I am today without the support of a lot of people. First and foremost, I would like to thank my advisor, Dr. George Garcia. I cannot thank you enough for all you have done for me over the years. You allowed a young undergraduate student, who had no idea how to do anything, into your lab and gave him a chance to prove himself. Throughout my time in your lab, you have provided me guidance, in science and in life, and have taught what it means to be a good scientist. I could not have asked for a better mentor, thank you for everything. I'd also like to thank the members of my committee for all the advice and support they provided me during the course of my dissertation research: Dr. Hollis Showalter, Dr. Ronald Woodard, Dr. Gordon Amidon, and Dr. Anna Mapp.

It would not be right if I did not acknowledge the many former and current members of the Garcia lab that made getting through each day a little easier. Dr. Julie Hurt for dealing with me as an undergraduate; I did not realize how annoying I must have been until after I was in your role, my apologies. Dr. Yi-Chen Chen for being the nicest and kindest person I have ever met in my life; lab morale really dropped off after you left. Dr. Suman Atwal for being someone I could always count on to go to No Thai with. Nathan Scharf for splitting rent and all the awesome baked goods; you should probably switch careers. Maxwell Stefan for making me feel not quite so old and his cheerful personality. Nicholas Ragazzone for being my successor... don't disappoint me. Lastly, Andrew Pratt (the former adopted lab member) for teaching

me how to convince people that I am right, even though, I may have no idea what I'm talking about.

From the bottom of my heart I'd also like to thank all my friends and family that have supported me throughout my life. Specifically my parents, Leslie and Bernie, I obviously wouldn't be the man I am today without you; my siblings, Tracy and Michael, for accepting my status as the golden child; and my grandparents. I also have to thank all my friends from back home for always finding a way to keep me grounded and never letting my head get "too" big. Lastly, I'd like to thank my beautiful wife, Katelyn, for all of her support. Over the past year, there were many stressful and discouraging days but, no matter what, you always found a way to make me smile. Words cannot describe how much this meant to me.

The research presented in this dissertation was supported by the National Institutes of Health (AI85179), the Pharmacological Sciences Training Program (T32-GM007767), the American Foundation for Pharmaceutical Education, the Rackham Merit Fellowship, and the University Of Michigan College Of Pharmacy.

TABLE OF CONTENTS

DEDICATION.....	ii
ACKNOWLEDGEMENTS.....	iii
LIST OF FIGURES.....	viii
LIST OF TABLES.....	xi
ABSTRACT.....	xiii
CHAPTER	
I. Introduction.....	1
The Need for Novel Antibiotics.....	1
Shigellosis.....	2
<i>Shigella</i> Pathogenesis.....	4
VirF: Structure, Regulation, and Function.....	4
VirF: A Potential Anti-Virulence Target?	8
Research Objectives.....	9
References.....	11
II. Small Molecule High-Throughput Screening Campaign Targeting VirF..	20
Materials and Methods.....	22
Results.....	26
Discussion.....	31
Notes to Chapter II.....	36
References.....	36

Appendix.....	39
III. Tissue Culture-Based Models of the <i>Shigella flexneri</i> Invasion Process	41
.....	41
Materials and Methods.....	42
Results.....	46
Discussion.....	51
Notes to Chapter III.....	57
References.....	57
Appendix.....	61
IV. The Expression, Purification, and Characterization of VirF.....	64
Materials and Methods.....	66
Results.....	76
Discussion.....	81
Notes to Chapter IV.....	88
References.....	88
Appendix.....	92
V. Mechanism of Inhibition Determination and Resulting SAR Studies.....	94
Materials and Methods.....	96
Results.....	103
Discussion.....	116
Notes to Chapter IV.....	123
References.....	123
Appendix.....	126

VI. HTS of ~20,000 Marine Natural Product Extracts Against <i>Shigella flexneri</i>: Identification of Globomycin and Desferrioxamine E.....	131
Materials and Methods.....	133
Results.....	143
Discussion.....	151
Notes to Chapter IV.....	158
References.....	158
Appendix.....	162
VII. Concluding Summary.....	188
References.....	193

LIST OF FIGURES

Figure

I-1.	Schematic Representation of <i>Shigella</i> Pathogenesis.....	5
I-2.	Co-crystal Structure of MarA Bound to <i>mar</i> Promoter.....	6
II-1.	Maps of the Reporter and Positive Control Plasmids Used in the HTS....	21
II-2.	Flow Chart Depicting the Hit Identification Process for the HTS.....	27
II-3.	Representative Dose-Response Curves from the Reconfirmation Study	31
II-4.	Comparison of Controls for HTS Pilot Screen and 100K Small Molecule Screen	32
III-1.	<i>S. flexneri</i> 2457T Invasion Assay Results.....	48
III-2.	<i>S. flexneri</i> 2457T Plaque Formation Assay Results.....	50
III-3.	Size of Plaques from Plaque Formation Assay with <i>S. flexneri</i> 2457T....	51
IV-1.	SDS-PAGE Analysis of the MalE-VirF Purification from pMALvirF in <i>E. coli</i> BL21(DE3) Cells.....	77
IV-2.	SDS-PAGE Analysis of the VirF(154-263) Purification from pET19b- VirF(154-263) in <i>E. coli</i> BL21(DE3) Cells.....	78
IV-3.	SDS-PAGE Analysis of MalE-VirF Purifications (KS1000 vs. BS103)....	79
IV-4.	Electrophoretic Mobility Shift Assay (EMSA) PAGE of MalE-VirF Binding to <i>pvirB</i> DNA Probe.....	82
IV-5.	Plot of MalE-VirF Binding to the <i>pvirB</i> DNA Probe.....	83
V-1.	Schematic Depicting Presumptive Steps in the Activation of Transcription by VirF.....	95

V-2.	Electrophoretic Mobility Shift Assay (EMSA) PAGE of MalE-VirF Binding to <i>pvirB</i> DNA Probe in Presence of Small Molecule Hit Compounds.....	104
V-3.	Characterization of Compound 19615.....	110
V-4.	Maps of Control Plasmids Used in GFP Reassembly Assay.....	112
V-5.	Maps of Test Plasmids Used in the GFP Reassembly Assay.....	113
V-6.	Typical Results Seen in GFP Reassembly Assay.....	114
V-7.	Figure Depicting Deduced SAR.....	119
VI-1.	Flow Chart Depicting the Results of the HTS Campaign.....	137
VI-2.	HPLC Trace and Yield of Active Peptidic Molecules.....	140
VI-3.	Crystal Structure (Ellipsoid) of Globomycin A (1).....	146
VI-4.	Chemical Structures of Globomycins A-C (1, 2, and 3).....	147
VI-5.	Chemical Structure of Desferrioxamine E.....	147
VI-6.	Plots Depicting Fold VirF Activation (solid-line, right y-axis) versus % Growth Inhibition (dotted-line, left y-axis) for Globomycins A-C (1, 2, and 3).....	148
VI-7.	Electrophoretic Mobility Shift Assay (EMSA) of MalE-VirF Binding to <i>pvirB</i> DNA Probe in Presence of Desferrioxamine E (Des).....	151
VII-1.	Genes Regulated by VirF and their Roles in Pathogenesis.....	189

Appendix Figure

II-1.	Representative Dose-Response Curves From Reconfirmation Stud.....	40
III-1.	Bacterial Toxicity of Compounds.....	63
IV-1.	Analytical Gel Filtration Results.....	92
IV-2.	Negative Controls for FP Assay.....	93
V-1.	EMSA Depicting <i>E. coli</i> RNA Polymerase (RNAP) Binding to the <i>lac</i> Promoter (<i>plac</i>) in the Presence of 19615.....	130
VI-1.	HRMS Spectrum of Globomycin A (1).....	178

VI-2.	HRMS Spectrum of Globomycin B (2).....	179
VI-3.	HRMS Spectrum of Globomycin C (3).....	180
VI-4.	¹ H NMR Spectrum of Globomycin A (1) Recorded at 700 MHz (in DMSO-d6).....	181
VI-5.	¹³ C NMR Spectrum of Globomycin A (1) Recorded at 700 MHz (in DMSO-d6).....	182
VI-6.	g-COSY Spectrum of Globomycin A (1) Recorded at 700 MHz (in DMSO-d6).....	183
VI-7.	HRMS Spectrum of Desferrioxamine E.....	184
VI-8.	¹ H NMR Spectrum of Desferrioxamine E Recorded at 700 MHz (in DMSO-d6).....	185
VI-9.	¹³ C NMR Spectrum of Desferrioxamine E Recorded at 700 MHz (in DMSO-d6).....	186
VI-10.	g-COSY Spectrum of Desferrioxamine E Recorded at 700 MHz (in DMSO-d6).....	187

LIST OF TABLES

Table

II-1.	Hits from 100K ChemDiv Screen that were Rescreened from Fresh Samples.....	28
II-2.	Reconfirmation Compound IC ₅₀ Values and Toxicities from Fresh Samples.....	30
III-1.	MTT Cell Viability Assay Results for Caco-2 Cell Growth in Presence of Compounds.....	47
IV-1.	Oligonucleotides Used in EMSA and FP Experiments.....	73
V-1.	Primers Used in TOPO Plasmid Construction.....	97
V-2.	Constructed TOPO Vectors.....	98
V-3.	Oligonucleotides Used in EMSA, FP, and FID Experiments.....	100
V-4.	Results of 19615 Analog Testing in FP Assay.....	105
V-5.	Results of the FID Assay.....	111
V-6.	List of All Plasmid Combinations Used in GFP Reassembly Assay.....	114
V-7.	Solubility of Selected 144092/144143 Analogs.....	115
VI-1.	MIC ₉₀ Values for Compounds 1, 2, and 3.....	150
VI-2.	Results of Siderophore Testing in Presence of Iron.....	151
VII-1.	Summary of Most Promising Compounds Identified in this Work.....	192

Appendix Table

II-1.	Log(IC ₅₀) and Associated Error for the Reconfirmation Dose-Response Study.....	39
III-1.	Cytotoxicity Estimates of Compounds in HeLa and L2 Cells.....	61

V-1.	FID Assay with 10 bp <i>pvirB</i> Probes.....	126
V-2.	SAR Table for 144143 Analogs.....	126
V-3.	SAR Table for 144092 Analogs.....	127
V-4.	SAR Table for Pyrimidine Analogs.....	128
VI-1.	Crystal Data and Structure Refinement for Globomycin A (1).....	162
VI-2.	Atomic Coordinates ($\times 10^4$) and equivalent isotropic displacement parameters ($\text{Å}^2 \times 10^3$) for Globomycin A (1).....	163
VI-3.	Bond Lengths [Å] and Angles [deg] for Globomycin A (1).....	165
VI-4.	Hydrogen Coordinates ($\times 10^4$) and isotropic displacement parameters ($\text{Å}^2 \times 10^3$) for Globomycin A (1).....	173
VI-5.	Torsion Angles [deg] for Globomycin A (1).....	175
VI-6.	Hydrogen Bonds for Globomycin A (1) [$d = \text{Å}$ and $\angle = \text{deg}$].....	177

ABSTRACT

An Antibiotic Discovery Campaign Targeting VirF, the Main Transcriptional Regulator of Virulence in *Shigella flexneri*

By

Anthony A. Emanuele

Chair: George A. Garcia

Shigella flexneri is a gram-negative enteropathogen that infects the human colonic epithelium. It is estimated that *Shigella* spp. infect 165 million people a year worldwide. Symptoms of shigellosis include bloody dysentery, dehydration, and ultimately death if the infection is not treated properly. The current recommended first-line treatment for shigellosis is ciprofloxacin; however, many new multi-drug resistant strains of *Shigella* have begun to emerge. The emergence of these strains, along with the lack of novel antibiotics in the drug pipeline, makes the need for new effective treatments for shigellosis a priority.

Genetic knockout studies have shown that VirF, the main transcriptional activator of the *Shigella* pathogenesis cascade, is necessary for virulence, but not bacterial viability. We hypothesized that a novel anti-virulence therapy for shigellosis could be developed through the inhibition of VirF. To identify inhibitors of VirF, we performed a high-throughput screening (HTS) campaign testing over 140,000 small molecules and 20,000 natural product extracts using a *Shigella*-based, VirF-driven, β -galactosidase reporter assay. Following a series of confirmation screens, we identified five

compounds from the HTS campaign that had VirF inhibitory properties. Using tissue culture-based models of the *S. flexneri* infection process, we were able to show that three of compounds were able to attenuate the virulence of *S. flexneri*, thereby, validating VirF as a target for the treatment of shigellosis.

To further characterize the hits from the HTS campaign a series of established *in vitro* assays were adapted and optimized for VirF. An electrophoretic mobility shift assay and a fluorescence polarization assay were used to monitor VirF binding to the *virB* promoter, and a fluorescence intercalator displacement assay was used to determine if the hits could directly bind DNA. Using these assays, we were able to determine the mechanism of inhibition (blockade of VirF binding to the *virB* promoter) and preliminary structure-activity relationship trends for one of the hits, and report the first dissociation constant for VirF binding to the *virB* promoter ($2.8 \pm 1.0 \mu\text{M}$).

CHAPTER I

Introduction

The Need for Novel Antibiotics

“A post-antibiotic era-in which common infections and minor injuries can kill, far from being an apocalyptic fantasy, is instead a very real possibility for the 21st century.”

-World Health Organization, 2014¹

The misuse of prescription antibiotics and the overuse of antibiotics in livestock feed have greatly contributed to the rapid increase in drug-resistant bacteria in the environment. This global rise of multi-drug resistant pathogens is a serious challenge to human health. The emergence and spread of resistance to drugs considered to be last resort, such as carbapenems²⁻⁴ and vancomycin,^{5, 6} has resulted in infections that are completely resistant to all known medications.⁷ Exacerbating this problem is the slow rate at which new antibiotics are being discovered. Since the 1960s, no new class of broad-spectrum antibiotics has been discovered and only five classes of narrow-spectrum antibiotics (streptogramins: streptogramin B, oxazolidinones: linezolid, lipopeptides: daptomycin, fidaxomicin, and diarylquinolines: bedaquiline) have had compounds approved for clinical use.^{8, 9} Unfortunately, resistance to all five newly approved compounds has already been observed.¹⁰⁻¹⁴ While a promising new antibiotic has been recently discovered (teixobactin)¹⁵ it has yet to be approved for clinical use

and is ineffective at targeting gram-negative pathogens. Clearly, there is an urgent need for new antibiotic treatments.

All current antibiotics negatively affect bacterial viability, and as such, any organisms that mutate to become resistant to the antibiotic will have a selective growth advantage. This can contribute to the rapid emergence of resistant strains. A potential method to combat bacterial infection while potentially minimizing the emergence of resistance is to target virulence instead of bacterial viability. It is hypothesized (by us and others¹⁶) that targeting virulence will result in less selective pressure for the emergence of new drug-resistant strains as they are expected to have little or no growth advantage. Also, virulence therapies should not harm the normal microbiota of the host, since the therapy targets virulence pathways that do not exist in the non-pathogenic microbiota. This has the potential to eliminate the development of secondary infections often associated with previous antibiotic exposure, such as infections caused by *Clostridium difficile*.¹⁷ Although virulence-directed therapies appear promising, they are still in the early phases of development; however, recent studies have provided encouraging evidence that this strategy could be effective. Virstatin, a small molecule inhibitor of ToxT (a transcriptional activator of critical virulence factors in *V. cholerae*) was shown to protect infant mice from intestinal colonization by *V. cholera*.¹⁸ Also, a series of benzimidazole compounds were shown to limit infection in a murine model of *Yersinia pseudotuberculosis* pneumonia through the inhibition of the transcriptional regulator of the *Yersinia* type III secretion system, LcrF.¹⁹⁻²¹

Shigellosis

Shigella flexneri is a gram-negative pathogenic bacterium that is a member of the *Enterobacteriaceae* family. There are approximately 165 million cases of *Shigella* spp.

infection worldwide and these infections claim more than one million lives per year.^{1, 22} The primary route of transmission for *Shigella* is fecal-to-oral, so it is not surprising that a majority of outbreaks occur in areas with poor sanitation conditions such as in underdeveloped nations or at day-care centers (children under five years of age represent 69% of all cases and 61% of all deaths).¹ *Shigella* infects the human gastrointestinal tract by invading the mucosal cells and spreading through the colonic epithelium. Upon infection, the host may experience severe bloody dysentery, dehydration, and ultimately death if not administered proper treatment. The current WHO recommended first-line treatment for *Shigella* infections include quinolones, such as ciprofloxacin and norfloxacin;²³ however, quinolone-resistant and multi-drug resistant strains of *Shigella* are being isolated. Recently, a *S. flexneri* clinical isolate was reported in China to be resistant to ciprofloxacin, third-generation cephalosporins (common second-line therapy), and nalidixic acid (previous first-line therapy).²⁴ Although these infections are commonly thought to be isolated to developing regions of the world, multi-drug resistant strains of *Shigella* are being found across the United States.^{25, 26} The Centers for Disease Control and Prevention issued a press release on April 2, 2015 warning US citizens of a multi-drug resistant strain of *Shigella* spreading across the country.²⁷ The appearance of multi-drug resistant strains coupled with the highly virulent nature of *Shigella* (exposure to only 10-100 bacteria is needed to establish an infection²⁸) has caused the National Institute of Allergy and Infectious Diseases (NIAID) to classify *Shigella* spp. as a Category B priority pathogen.

Shigella Pathogenesis

The essential parts of the molecular machinery required for *Shigella* pathogenesis are encoded on the 230 kb *Shigella* virulence plasmid.²⁹⁻³¹ Of the genes encoded on this plasmid, the *virF* gene may be the most important. VirF is an AraC family transcriptional activator that regulates (directly and indirectly) the transcription of all downstream virulence factors in *Shigella* spp.³²⁻³⁵ VirF directly activates two downstream virulence genes, *virB* and *icsA*.^{36, 37} VirB is a secondary transcriptional activator that is responsible for activating the transcription of other virulence genes, such as *ipaB*, *ipaC*, and, *ipaD*,³⁸ whose gene products are involved in the construction of the Type III Secretion System (which is required for initial bacterial invasion) and escape from host-cell defense systems.³⁹⁻⁴¹ IcsA assembles actin polymerase on one pole of the bacterium and propels the bacterium through the infected host cells via the polymerization of host cell actin; allowing the bacterium to spread to adjacent cells.⁴²⁻⁴⁴ Gene silencing studies have shown that the lack of VirB expression leads to a loss of virulence,^{32, 45} and that the lack of IcsA expression blocks the intra- and inter-cellular movement of *Shigella*.^{46, 47} A schematic representation of the *Shigella* spp. pathogenesis cascade is provided in Figure I-1.

VirF: Structure, Regulation, and Function

The three-dimensional structure of VirF has not yet been determined. However, based on sequence similarity, VirF is classified as an AraC family transcriptional regulator.⁴⁸ AraC family transcriptional regulators can function either as monomers or as homodimers. VirF is believed to function as a homodimer and, by homology, has two domains: an N-terminal dimerization domain and a C-terminal DNA-binding domain.

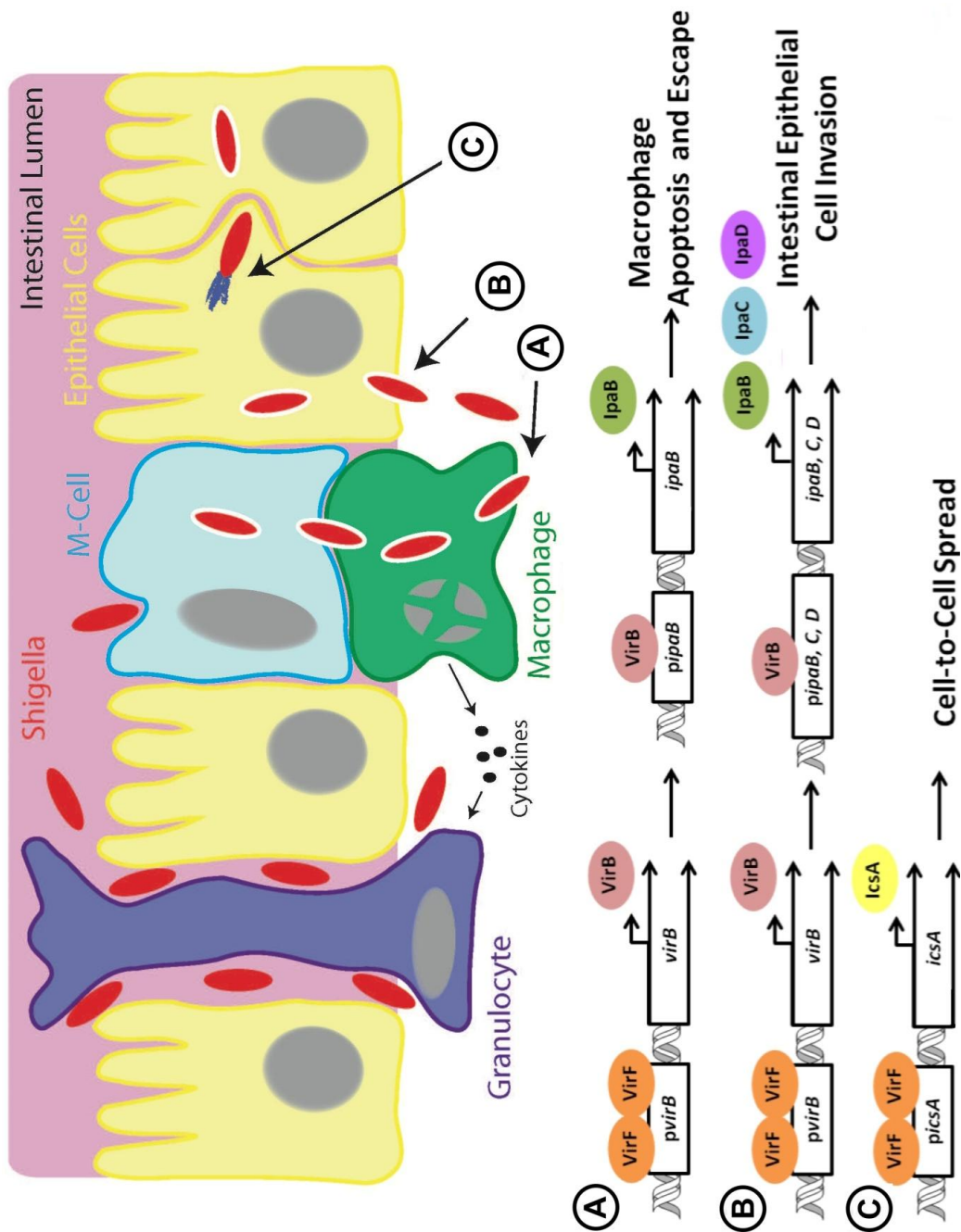


Figure I-1: Schematic Representation of *Shigella* Pathogenesis.

The C-terminal DNA-binding domain is highly conserved across all AraC-family members and contains two helix-turn-helix (HTH) motifs that insert into adjacent major groove segments of the DNA.^{49, 50} Figure I-2 provides the first high-resolution structure for an AraC-family transcriptional regulator (MarA) and highlights the interactions between the HTH motifs and the DNA.⁵¹ The N-terminal domain, not depicted in Figure

I-2 (MarA has only one domain and functions as a monomer), is much less conserved across AraC-family members.

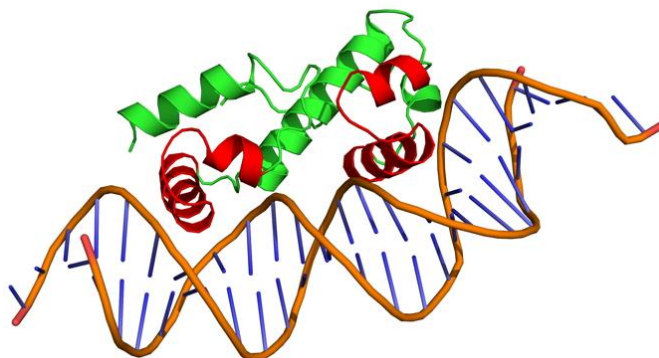


Figure I-2: Co-crystal Structure of MarA Bound to *mar* Promoter.⁵¹ Helix-turn-helix motifs are highlighted in red and are shown to interact in two adjacent major grooves of the *mar* promoter. Each HTH motif is made up of 20 amino acids and combined span approximately 20 nucleotides. Upon binding MarA bends the DNA by approximately 35°. The structure was refined to a resolution of 2.3 Å and the image depicted was made from the following PDB file: 1BL0.

There are three classes of AraC family members: monomeric, chemically-modulated, and physically-modulated.^{49, 52} MarA, depicted in Figure I-2, is an example of the monomeric class. Most members of this class are involved in bacterial stress-response pathways.^{52, 53} AraC is the poster child for the chemically-modulated class. AraC functions as a homodimer, but can only activate transcription after binding arabinose and undergoing a conformational shift.⁵⁴ Most members of this class are activated by small carbohydrates, such as, RhaS and RhaR from *E. coli*, which are modulated by L-rhamnose.⁵⁵ VirF is a member of the physically-modulated class and can only activate transcription under the correct environmental signals (pH, temperature, osmolarity), specifically signals commonly encountered in the host cell environment.^{38, 56-58}

Transcription of the *virF* gene is repressed by the temperature dependent binding of the H-NS protein to two sites in the *virF* promoter.⁵⁸⁻⁶⁰ H-NS binds to the *virF* promoter at temperatures below 32°C preventing RNA polymerase from binding and activating transcription. However, when the temperature increases to 37°C there is a change in DNA topology that frees H-NS from the promoter, allowing *virF* mRNA to be transcribed by RNA polymerase. Once VirF is expressed it can activate the transcription of two genes, *virB* and *icsA*.

To activate the transcription of *virB*, VirF binds upstream of the transcription start site between positions -17 to -105 and aids in the recruitment of RNA polymerase.³⁶ This transcriptional activation process is further regulated by temperature and osmolarity. Similarly to *virF* transcriptional regulation, H-NS also represses the transcription of *virB* at temperatures below 32°C.³⁶ When the temperature shifts to 37°C, there is a change in the local negative supercoiling of the DNA that results in the displacement of H-NS, the binding of VirF, and the recruitment of RNA polymerase by VirF.⁶¹ It has been shown that conditions of high osmolarity enhance the change in DNA topology,⁵⁷ and that the supercoiling of the DNA is necessary for VirF to activate transcription (however, VirF can still bind to non-supercoiled DNA).⁶¹ It has also recently been shown that VirB itself can participate in positive feedback regulation at both the *virB* and *virF* promoters by antagonizing H-NS mediated repression.⁶²

VirF-mediated activation of the *icsA* promoter appears to be more complex than the activation of the *virB* promoter. Recently, the lab of Dr. Maurizio Falconi has identified a 450-nucleotide antisense RNA, RnaG, which is transcribed *in cis* from *icsA* and attenuates the transcription of *icsA*.^{37, 63} As with both *virF* and *virB*, H-NS also

represses the transcription of *icsA* at temperatures below 32°C.^{59, 64} The exact mechanism of how VirF, H-NS, and RnaG control transcription of *icsA* is not completely understood; however, the Falconi lab has identified four distinct binding sites for both VirF and H-NS within the *icsA*/RnaG promoter and coding regions.³⁷ They have also shown that H-NS and VirF both repress the transcription of RnaG.³⁷ It is possible that RnaG serves as a fine-tune control mechanism for the *icsA* promoter that helps prevent the transcription of *icsA* after only temperature-mediated dissociation of H-NS.

VirF: A Potential Anti-Virulence Target?

Genetic knockout studies have shown that VirF is required for host cell infection, but not bacterial viability.⁶⁵ This trait, combined with a number of other factors, makes VirF an attractive target for an anti-virulence therapy. For one, the likelihood of resistance to VirF inhibitors developing environmentally (outside of an infected host) should be quite low. Absent conditions that mimic those of an infected host, there should be little or no expression of VirF;^{38, 56-58} therefore, the VirF-selective inhibitors should have no effect on *Shigella* spp. in the environment. Additionally, targeting virulence gene expression does not impair bacterial viability or impact non-virulent organisms,^{66, 67} and hence, there should be little selective pressure in the environment for resistance development. Also, in the infected host, *Shigella* utilize VirF-induced IpaB to escape from macrophages.⁴⁰ Inhibition of VirF should block this and increase the efficiency of macrophage killing *Shigella* and thereby reduce the development of resistance. Although no one has attempted to target the VirF-activated *Shigella* pathogenesis cascade with a small molecule, there has been promising vaccine-based approaches.^{68, 69} Several researchers have used *icsA*-knockout strains of *Shigella* as live-attenuated vaccine candidates (bacteria can initially invade epithelial cells and

generate an immune response, but cannot spread intra- or inter-cellularly).⁷⁰⁻⁷³ In fact, two *icsA*-knockout vaccine candidates are scheduled to enter phase I clinical trials in the near future (Clinicaltrials.gov identifier: NCT01336699). It may be possible that a small molecule targeting VirF could replicate this *icsA*-knockout phenotype, as well as, prevent initial bacterial invasion. Of course, these are all postulates and require experimental testing to determine their validity.

Research Objectives

It is clear that VirF is an attractive target for therapeutic intervention. However, at the time this dissertation research began, VirF's potential as a therapeutic target had yet to be validated. Therefore, there were two main goals for this dissertation research: 1) to identify, characterize, and develop small molecule inhibitors of VirF, and 2) to validate VirF as a novel anti-virulence target for the treatment of shigellosis. Over the course of the project, we also sought to gain a better understanding of how VirF activates transcription and looked to develop tools to monitor VirF activity at all levels (biochemical, bacterial, and cellular). The primary objective described in each chapter follows:

Chapter 2: To identify small molecule inhibitors of VirF.

Using our lab's previously developed *Shigella*-based, VirF-driven, β -galactosidase reporter assay,⁷⁴ we tested over 100,000 small molecules in a high-throughput screening campaign and identified five inhibitors of VirF-driven transcriptional activation.

Chapter 3: To validate VirF as a potential small molecule therapeutic target.

We evaluated the hits from our high-throughput screen in a series of tissue culture-based models of the *S. flexneri* invasion process and determined that small molecule inhibitors of VirF can attenuate the virulence of *Shigella*.

Chapter 4: To develop tools to monitor VirF binding to the *virB* promoter at the biochemical level.

We developed a homologous *Shigella*-based expression system to express and purify VirF and then characterized VirF in a series of *in vitro* DNA-binding assays. We also determined the first experimental dissociation constant for VirF binding to the *virB* promoter ($2.8 \pm 1.0 \mu\text{M}$).

Chapter 5: To determine the mechanism of inhibition of our hits and to identify structure-activity relationship trends.

We determined that one hit inhibited VirF activity by preventing VirF from binding to the *virB* promoter. We also screened analogs of our most promising hits and identified structure-activity relationship trends.

Chapter 6: To identify natural product extracts that inhibit the activity of VirF or the growth of *Shigella flexneri*.

Using our lab's previously developed *Shigella*-based, VirF-driven, β -galactosidase reporter assay,⁷⁴ we tested over 20,000 natural product extracts in a high-throughput screen. We identified extracts that have inhibitory effects on VirF, apparent activating effects on VirF, and that inhibit the growth of *S. flexneri*. Lastly, in collaboration with the Sherman lab (Life Sciences Institute, University of Michigan Ann Arbor), we identified the active components from two of our natural product extract hits.

References

1. WHO. Antimicrobial Resistance Global Report On Surveillance. **2014**.
2. Kumarasamy, K. K.; Toleman, M. A.; Walsh, T. R.; Bagaria, J.; Butt, F.; Balakrishnan, R.; Chaudhary, U.; Doumith, M.; Giske, C. G.; Irfan, S.; Krishnan, P.; Perry, C.; Pike, R.; Rao, B.; Ray, U.; Sarma, J. B.; Sharma, M.; Sheridan, E.; Thirunarayan, M. A.; Turton, J.; Upadhyay, S.; Warner, M.; Welfare, W.; Livermore, D. M.; Woodford, N. Emergence of a new antibiotic resistance mechanism in India, Pakistan, and the UK: a molecular, biological, and epidemiological study. *Lancet Infect Dis* **2010**, 10, 597-602.
3. Yigit, H.; Queenan, A. M.; Anderson, G. J.; Domenech-Sanchez, A.; Biddle, J. W.; Steward, C. D.; Alberti, S.; Bush, K.; Tenover, F. C. Novel Carbapenem-Hydrolyzing Beta-Lactamase, KPC-1, from a Carbapenem-Resistant Strain of *Klebsiella pneumoniae*. *Antimicrobial Agents and Chemotherapy* **2001**, 45, 1151-1161.
4. Arnold, R. S.; Thom, K. A.; Sharma, S.; Phillips, M.; Johnson, K. J.; Morgan, D. J. Emergence of *Klebsiella pneumoniae* Carbapenemase (KPC)-Producing Bacteria. *Southern Medical Journal* **2011**, 104, 40-45.
5. Leclercq, R.; Derlot, E.; Duval, J.; Courvalin, P. Plasmid-Mediated Resistance to Vancomycin and Teicoplanin in *Enterococcus Faecium*. *New England Journal of Medicine* **1988**, 319, 157-161.
6. Frieden, T. R.; Munsiff, S. S.; Williams, G.; Faur, Y.; Kreiswirth, B.; Low, D. E.; Willey, B. M.; Warren, S.; Eisner, W. Emergence of vancomycin-resistant enterococci in New York City. *The Lancet* **1993**, 342, 76-79.
7. Udhwadia, Z. F.; Amale, R. A.; Ajbani, K. K.; Rodrigues, C. Totally Drug-Resistant Tuberculosis in India. *Clinical Infectious Diseases* **2012**, 54, 579-581.
8. Lewis, K. Platforms for antibiotic discovery. *Nature Reviews Drug Discovery* **2013**, 12, 371-387.
9. Center for Disease Dynamics, E. P. State of the World's Antibiotics, 2015. **2015**.
10. Jenssen, W. D.; Thakker-Varia, S.; Dubin, D. T.; Weinstein, M. P. Prevalence of macrolides-lincosamides-streptogramin B resistance and *erm* gene classes

- among clinical strains of Staphylococci and Streptococci. *Antimicrob Agents Chemother* **1987**, 31, 883-888.
11. Marty, F. M.; Yeh, W. W.; Wennersten, C. B.; Venkataraman, L.; Albano, E.; Alyea, E. P.; Gold, H. S.; Baden, L. R.; Pillai, S. K. Emergence of a clinical daptomycin-resistant *Staphylococcus aureus* isolate during treatment of methicillin-resistant *Staphylococcus aureus* bacteremia and osteomyelitis. *J Clin Microbiol* **2006**, 44, 595-597.
 12. Petrella, S.; Cambau, E.; Chauffour, A.; Andries, K.; Jarlier, V.; Sougakoff, W. Genetic basis for natural and acquired resistance to the diarylquinoline R207910 in Mycobacteria. *Antimicrob Agents Chemother* **2006**, 50, 2853-2856.
 13. Tsiodras, S.; Gold, H.; Sakoulas, G. Linezolid resistance in a clinical isolate of *Staphylococcus aureus*. *Lancet* **2001**, 358, 207-208.
 14. Goldstein, E. J.; Babakhani, F.; Citron, D. M. Antimicrobial Activities of Fidaxomicin. *Clinical Infectious Diseases* **2012**, 61, S143-S148.
 15. Ling, L. L.; Schneider, T.; Peoples, A. J.; Sporeing, A. L.; Engels, I.; Conlon, B. P.; Mueller, A.; Schaberle, T. F.; Hughes, D. E.; Epstein, S.; Jones, M.; Lazarides, L.; Steadman, V. A.; Cohen, D. R.; Felix, C. R.; Fetterman, K. A.; Millet, W. P.; Nitti, A. G.; Zullo, A. M.; Chen, C.; Lewis, K. A new antibiotic kills pathogens without detectable resistance. *Nature* **2015**, 517, 455-459.
 16. Clatworthy, A. E.; Pierson, E.; Hung, D. T. Targeting virulence: a new paradigm for antimicrobial therapy. *Nature Chemical Biology* **2007**, 3, 541-548.
 17. Lo Vecchio, A.; Zacur, G. M. Clostridium difficile infection: an update on epidemiology, risk factors, and therapeutic options. *Current Opinion in Gastroenterology* **2012**, 28, 1-9.
 18. Hung, D. T.; Shakhnovich, E. A.; Pierson, E.; Mekalanos, J. J. Small-Molecule Inhibitor of *Vibrio cholerae* Virulence and Intestinal Colonization. *Science* **2005**, 310, 670-674.
 19. Bowser, T. E.; Bartlett, V. J.; Grier, M. C.; Verma, A. K.; Warchol, T.; Levy, S. B.; Alekshun, M. N. Novel anti-infection agents: small-molecule inhibitors of bacterial transcription factors. *Bioorganic & Medicinal Chemistry Letters* **2007**, 17, 5652-5.

20. Garrity-Ryan, L. K.; Kim, O. K.; Balada-Llasat, J. M.; Bartlett, V. J.; Verma, A. K.; Fisher, M. L.; Castillo, C.; Songsunthong, W.; Tanaka, S. K.; Levy, S. B.; Mecsas, J.; Alekshun, M. N. Small Molecule Inhibitors of LcrF, a *Yersinia pseudotuberculosis* Transcription Factor, Attenuate Virulence and Limit Infection in a Murine Pneumonia Model. *Infection and Immunity* **2010**, 78, 4683-4690.
21. Kim, O. K.; Garrity-Ryan, L. K.; Bartlett, V. J.; Grier, M. C.; Verma, A. K.; Medjanis, G.; Donatelli, J. E.; Macone, A. B.; Tanaka, S. K.; Levy, S. B.; Alekshun, M. N. N-hydroxybenzimidazole inhibitors of the transcription factor LcrF in *Yersinia*: novel antivirulence agents. *J Med Chem* **2009**, 52, 5626-34.
22. Kotloff, K. L.; Winickoff, J. P.; Ivanoff, B.; Clemens, J. D.; Swerdlow, D. L.; Sansonetti, P. J.; Adak, G. K.; Levine, M. M. Global burden of *Shigella* infections: implications for vaccine development and implementation of control strategies. *Bull World Health Organ* **1999**, 77, 651-666.
23. WHO. Guidelines for the control of shigellosis, including epidemics due to *Shigella dysenteriae* type 1. In *Weekly Epidemiological Record*, 2005; pp 1-64.
24. Qiu, S.; Xu, X.; Wang, Y.; Yang, G.; Wang, Z.; Wang, H.; Zhang, L.; Liu, N.; Chen, C.; Liu, W.; Li, J.; Su, W.; Jia, L.; Wang, L.; Jin, H.; Keim, P.; Yuan, Z.; Huang, L.; Song, H. Emergence of resistance to fluoroquinolones and third-generation cephalosporins in *Shigella flexneri* subserotype 1c isolates from China. *Clin Microbiol Infect* **2012**, 18, E95-E98.
25. CDC. Outbreaks of multidrug-resistant *Shigella sonnei* gastroenteritis associated with day care centers-Kansas, Kentucky, and Missouri, 2005. *MMWR Morb Mortal Wkly Rep* **2006**, 55, 1068-1071.
26. Replogle, M. L.; Fleming, D. W.; Cieslak, P. R. Emergence of antimicrobial-resistant shigellosis in Oregon. *Clinical Infectious Diseases*. **2000**, 30, 515-9.
27. CDC. Importation and Domestic Transmission of *Shigella sonnei* Resistant to Ciprofloxacin - United States. *MMWR. Morbidity and Mortality Weekly Report* **2015**, 64.
28. DuPont, H. L.; Myron, M. L.; Hornick, R. B.; Formal, S. B. Inoculum Size in Shigellosis and Implications for Expected Mode of Transmission. *The Journal of Infectious Diseases* **1989**, 159, 1126-1128.

29. Sansonetti, P. J.; Kopecko, D. J.; Formal, S. B. Involvement of a plasmid in the invasive ability of *Shigella flexneri*. *Infection and Immunity* **1982**, 35, 852-860.
30. Sasakawa, C.; Kamata, K.; Sakai, T.; Murayama, S. Y.; Makino, S.; Yoshikawa, M. Molecular alteration of the 140-megadalton plasmid associated with loss of virulence and congo red binding-activity in *Shigella flexneri*. *Infection and Immunity* **1986**, 51, 470-475.
31. Buchrieser, C.; Glaser, P.; Rusniok, C.; Nedjari, H.; D'Hauteville, H.; Kunst, F.; Sansonetti, P.; Parsot, C. The virulence plasmid pWR100 and the repertoire of proteins secreted by the type III secretion apparatus of *Shigella flexneri*. *Molecular Microbiology* **2000**, 38, 760-771.
32. Adler, B.; Sasakawa, C.; Tobe, T.; Makino, S.; Komatsu, K.; Yoshikawa, M. A dual transcriptional activation system for the 230 kb plasmid genes coding for virulence-associated antigens of *Shigella flexneri*. *Molecular Microbiology* **1989**, 3, 627-35.
33. Schroeder, G. N.; Hilbi, H. Molecular Pathogenesis of *Shigella* spp.: Controlling Host Cell Signaling, Invasion, and Death by Type III Secretion. *Clin Microbiol Rev* **2008**, 21, 134-156.
34. Porter, M. E.; Dorman, C. J. Differential regulation of the plasmid-encoded genes in the *Shigella flexneri* virulence regulon. *Molecular & General Genetics* **1997**, 256, 93-103.
35. Sakai, T.; Sasakawa, C.; Yoshikawa, M. Expression of four virulence antigens of *Shigella flexneri* is positively regulated at the transcriptional level by the 30 kiloDalton virF protein. *Mol Microbiol* **1988**, 2, 589-597.
36. Tobe, T.; Yoshikawa, M.; Mizuno, T.; Sasakawa, C. Transcriptional control of the invasion regulatory gene virB of *Shigella flexneri*: activation by virF and repression by H-NS. *Journal of Bacteriology* **1993**, 175, 6142-9.
37. Tran, C. N.; Giangrossi, M.; Prosseda, G.; Brandi, A.; Di Martino, M. L.; Colonna, B.; Falconi, M. A multifactor regulatory circuit involving H-NS, VirF and an antisense RNA modulates transcription of the virulence gene icsA of *Shigella flexneri*. *Nucleic acids research* **2011**, 39, 8122-8134.

38. Tobe, T.; Nagai, S.; Okada, N.; Adler, B.; Yoshikawa, M.; Sasakawa, C. Temperature-regulated expression of invasion genes in *Shigella flexneri* is controlled through the transcriptional activation of the *virB* gene on the large plasmid. *Molecular Microbiology* **1991**, 5, 887-893.
39. Blocker, A.; Gounon, P.; Larquet, E.; Niebuhr, K.; Cabaux, V.; Parsot, C.; Sansonetti, P. The Tripartite type III secretion of *Shigella flexneri* inserts IpaB and IpaC into host membranes. *J Cell Biol* **1999**, 147, 683-693.
40. Hilbi, H.; Moss, J. E.; Hersh, D.; Chen, Y.; Arondel, J.; Banerjee, S.; Flavell, R. A.; Yuan, J.; Sansonetti, P. J.; Zychlinsky, A. Shigella-induced apoptosis is dependent on caspase-1 which binds to IpaB. *J Biol Chem* **1998**, 273, 32895-32900.
41. Espina, M.; Olive, A. J.; Kenjale, R.; Moore, D. S.; Ausar, F. S.; Kaminski, R. W.; Oaks, E. V.; Middaugh, R. C.; Picking, W. D.; Picking, W. L. IpaD Localizes to the tip of the Type III Secretion System Needle of *Shigella flexneri*. *Infection and Immunity* **2006**, 74, 4391-4400.
42. Bernardini, M. L.; Mounier, J.; d'Hauteville, H.; Coquis-Rondon, M.; Sansonetti, P. J. Identification of icsA, a plasmid locus of *Shigella flexneri* that governs bacterial intra- and intercellular spread through interaction with F-actin. *Proceedings of the National Academy of Sciences of the United States of America* **1989**, 86, 3867-3871.
43. May, K. L.; Morona, R. Mutagenesis of the *Shigella flexneri* Autotransporter IcsA Reveals Novel Functional Regions Involved in IcsA Biogenesis and Recruitment of Host Neural Wiscott-Aldrich Syndrome Protein. *Journal of Bacteriology* **2008**, 190, 4666-4676.
44. Zumsteg, A. B.; Goosmann, C.; Brinkmann, V.; Morona, R.; Zychlinsky, A. IcsA is a *Shigella flexneri* Adhesion Regulated by the Type III Secretion System and Required for Pathogenesis. *Cell Host & Microbe* **2014**, 15, 435-445.
45. Colonna, B.; Casalino, M.; Fradiani, P. A.; Zagaglia, C.; Naitza, S.; Leoni, L.; Prosseda, G.; Coppo, A.; Ghelardini, P.; Nicoletti, M. H-NS regulation of virulence gene expression in enteroinvasive *Escherichia coli* harboring the virulence plasmid integrated into the host chromosome. *Journal of Bacteriology* **1995**, 177, 4703-12.

46. Sansonetti, P. J.; Arondel, J.; Fontaine, A.; d'Hauteville, H.; Bernardini, M. L. OmpB (osmo-regulation) and icsA (cell-to-cell spread) mutants of *Shigella flexneri*: vaccine candidates and probes to study the pathogenesis of shigellosis. *Vaccine* **1991**, 9, 416-22.
47. Makino, S.; Sasakawa, C.; Kamata, K.; Kurata, T.; Yoshikawa, M. A genetic determinant required for continuous reinfection of adjacent cells on large plasmid in *S. flexneri* 2a. *Cell* **1986**, 46, 551-5.
48. Dorman, C. J.; Porter, M. E. The *Shigella* virulence gene regulatory cascade: a paradigm of bacterial gene control mechanisms. *Molecular Microbiology* **1998**, 29, 677-684.
49. Gallegos, M. T.; Schleif, R.; Bairoch, A.; Hofmann, K.; Ramos, J. L. AraC/XylS family of transcriptional regulators. *Microbiology & Molecular Biology Reviews* **1997**, 61, 393-410.
50. Tobes, R.; Ramos, J. L. AraC-XylS database: a family of positive transcriptional regulators in bacteria. *Nucleic Acids Research* **2002**, 30, 318-321.
51. Rhee, S.; Martin, R. G.; Rosner, J. L.; Davies, D. R. A novel DNA-binding motif in MarA: The first structure for an AraC family transcriptional activator. *Proceedings of the National Academy of Sciences of the United States of America* **1998**, 95, 10413-10418.
52. Martin, R. G.; Rosner, J. L. The AraC transcriptional activators. *Current Opinion in Microbiology* **2001**, 4, 132-137.
53. Martin, R. G.; Gillette, W. K.; Rhee, S.; Rosner, J. L. Structural requirements for marbox function in transcriptional activation of mar/sox/rob regulon promoters in *Escherichia coli*: sequence, orientation and spatial relationship to the core promoter. *Molecular Microbiology* **1999**, 34, 431-441.
54. Schleif, R. AraC protein, regulation of the l-arabinose operon in *Escherichia coli*, and the light switch mechanism of AraC action. *Fems Microbiology Reviews* **2010**, 34, 779-796.
55. Holcroft, C. C.; Egan, S. M. Interdependence of Activation at rhaSR by Cyclic AMP Receptor Protein, the RNA Polymerase Alpha Subunit C-Terminal Domain, and RhaR. *Journal of Bacteriology* **2000**, 182, 6774-6782.

56. Nakayama, S.; Watanabe, H. Involvement of CpxA, a sensor of a 2-component regulatory system, in the pH-dependent regulation of expression of *Shigella sonnei* virF gene. *Journal of Bacteriology* **1995**, 177, 5062-5069.
57. Porter, M. E.; Dorman, C. J. A role for H-NS in the thermo-osmotic regulation of virulence gene expression in *Shigella flexneri*. *Journal of Bacteriology* **1994**, 176, 4187-4191.
58. Falconi, M.; Colonna, B.; Prosseda, G.; Micheli, G.; Gualerzi, C. O. Thermoregulation of *Shigella* and *Escherichia coli* EIEC pathogenicity. A temperature-dependent structural transition of DNA modulates accessibility of virF promoter to transcriptional repressor H-NS. *EMBO Journal* **1998**, 17, 7033-43.
59. Prosseda, G.; Fradiani, P. A.; Di, L. M.; Falconi, M.; Micheli, G.; Casalino, M.; Nicoletti, M.; Colonna, B. A role for H-NS in the regulation of the virF gene of *Shigella* and enteroinvasive *Escherichia coli*. *Research in Microbiology* **1998**, 149, 15-25.
60. Prosseda, G.; Falconi, M.; Giangrossi, M.; Gualerzi, C. O.; Micheli, G.; Colonna, B. The virF promoter in *Shigella*: more than just a curved DNA stretch. *Molecular Microbiology* **2004**, 51, 523-37.
61. Tobe, T.; Yoshikawa, M.; Sasakawa, C. Thermoregulation of virB transcription in *Shigella flexneri* by sensing of changes in local DNA superhelicity. *Journal of Bacteriology* **1995**, 177, 1094-7.
62. Kane, K. A.; Dorman, C. J. VirB-Mediated Positive Feedback Control of the Virulence Gene Regulatory Cascade of *Shigella flexneri*. *Journal of Bacteriology* **2012**, 194, 5264-5273.
63. Giangrossi, M.; Prosseda, G.; Tran, C. N.; Brandi, A.; Colonna, B.; Falconi, M. A novel antisense RNA regulates at transcriptional level the virulence gene icsA of *Shigella flexneri*. *Nucleic Acids Research* **2010**, 38, 3362-3375.
64. Dagberg, B.; Uhlin, B. E. Regulation of virulence-associated plasmid genes in enteroinvasive *Escherichia coli*. *Journal of Bacteriology* **1992**, 174, 7606-12.

65. Qi, M. S.; Yoshikura, H.; Watanabe, H. Virulence phenotypes of *Shigella flexneri* 2a virulent mutant 24570 can be complemented by the plasmid-coded positive regulator *virF* gene. *FEMS Microbiology Letters* **1992**, 92, 217-221.
66. Sasakawa, C.; Kamata, K.; Sakai, T.; Makino, S.; Yamada, M.; Okada, N.; Yoshikawa, M. Virulence-Associated Genetic Regions Comprising 31 Kilobases of the 230-Kilobase Plasmid in *Shigella flexneri* 2a. *Journal of Bacteriology* **1988**, 170, 2480-2484.
67. Mills, J. A.; Venkatesan, M. M.; Baron, L. S.; Buysse, J. M. Spontaneous Insertion of an IS1-Like Element into the *virF* Gene Is Responsible for Avirulence in Opaque Colonial Variants of *Shigella flexneri* 2a. *Infection & Immunity* **1992**, 60, 175-182.
68. Ashkenazi, S.; Cohen, D. An update on vaccines against Shigella. *Therapeutic Advances in Vaccines* **2013**, 1, 113-123.
69. Levine, M. M.; Kotloff, K. L.; Barry, E. M.; Pasetti, M. F.; Sztein, M. B. Clinical trials of Shigella vaccines: two steps forward and one step back on a long, hard road. *Nature reviews. Microbiology* **2007**, 5, 540-553.
70. Barnoy, S.; Baqar, S.; Kaminski, R. W.; Collins, T.; Nemelka, K.; Hale, T. L.; Ranallo, R. T.; Venkatesan, M. M. Shigella sonnei vaccine candidates WRSs2 and WRSs3 are as immunogenic as WRSS1, a clinically tested vaccine candidate, in a primate model of infection. *Vaccine* **2011**, 29, 6371-6378.
71. Barnoy, S.; Jeong, K. I.; Helm, R. F.; Suvarnapunya, A. E.; Ranallo, R. T.; Tzipori, S.; Venkatesan, M. M. Characterization of WRSs2 and WRSs3, new second-generation virG(icsA)-based Shigella sonnei vaccine candidates with the potential for reduced reactogenicity. *Vaccine* **2010**, 28, 1642-1654.
72. Ranallo, R. T.; Thakkar, S.; Chen, Q.; Venkatesan, M. M. Immunogenicity and characterization of WRSF2G11: A second generation live attenuated Shigella flexneri 2a vaccine strain. *Vaccine* **2007**, 25, 2269-2278.
73. Yoshikawa, M.; Sasakawa, C.; Okada, N.; Takasaka, M.; Nakayama, M.; Yoshikawa, Y.; Kohno, A.; Danbara, H.; Nariuchi, H.; Shimada, H.; Toriumi, M. Construction and evaluation of a virG thyA double mutant of Shigella flexneri 2a as a candidate live-attenuated oral vaccine. *Vaccine* **1995**, 13, 1436-1440.

74. Hurt, J. K.; McQuade, T. J.; Emanuele, A.; Larsen, M. J.; Garcia, G. A. High-Throughput Screening of the Virulence Regulator VirF: A Novel Antibacterial Target for Shigellosis. *Journal of Biomolecular Screening* **2010**, *15*, 379-387.

CHAPTER II

Small Molecule High-throughput Screening Campaign Targeting VirF

AraC family transcriptional activators regulate virulence pathways in a wide variety of bacterial pathogens¹ (e.g., ToxT from *Vibrio cholerae*,² LcrF from *Yersinia pestis*,³ InvF from *Salmonella typhimurium*,⁴ and ExsA from *Pseudomonas aeruginosa*⁵), as such, they have become popular targets for novel antibiotic discovery.^{6, 7} Many groups have utilized high-throughput screens (HTS) to identify compounds that inhibit these transcription factors.⁸⁻¹⁰ A common feature of these screens is the use of bacterial reporter strains that monitor the transcription factor of interest (TFI) activating the expression of a reporter gene under the control of the TFI's endogenous promoter. For example, Hung *et al.* constructed a screening strain of *V. cholera* where the tetracycline resistance gene was under the control of the cholera toxin promoter and used this strain to identify inhibitors of ToxT.¹⁰

To identify inhibitors of VirF, the main transcriptional activator of the *Shigella* spp. pathogenesis cascade, our lab previously constructed a *Shigella*-based, VirF-driven, β -galactosidase reporter system.⁹ For the reporter system, an avirulent strain of *S. flexneri*, BS103, was transformed with a reporter plasmid that had *lacZ* (gene encoding β -galactosidase) under the control of the *virB* promoter (see Figure II-1). In this system, β -galactosidase activity directly correlated to VirF activity and was monitored spectrophotometrically using the colorimetric substrate chlorophenol red β -D-galactopyranoside. Using this system, we carried out an initial 42,000 compound pilot

HTS at the Center for Chemical Genomics (Life Sciences Institute, University of Michigan Ann Arbor). Unfortunately, the pilot screen produced an artificially high hit rate (3%), a large degree of variability between plates, and hits that did not reconfirm. Also, the initial pilot HTS was modest in size and may not have sampled a large enough range of chemical diversity to identify an inhibitor of VirF.

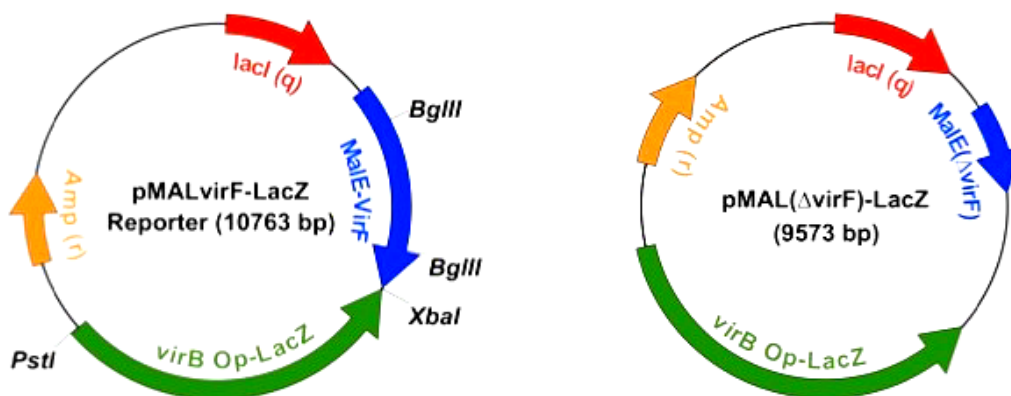


Figure II-1: Maps of the Reporter and Positive Control Plasmids Used in the HTS. Left map, pMALvirF-LacZ, depicts the reporter plasmid used in the HTS. The plasmid contained the *malEvirF* fusion gene as well as the *lacZ* gene under the control of the *virB* promoter. All compounds were screened against this plasmid. Right map, pMAL(Δ virF)-LacZ, depicts the positive control plasmid used in the HTS. This plasmid was used to determine the baseline value for 100% VirF inhibition.

To improve our chances of identifying an inhibitor of VirF, we decided to extend our small molecule screen to include ~100,000 more compounds, for a total small molecule screen of ~140,000 compounds. To address the variability issue seen in the pilot HTS and improve the overall accuracy of the screen, we initially contemplated switching from a bacteria-based assay to a biochemical assay. However, we could not develop a biochemical assay monitoring VirF activity at the time of the screen. This was largely due to the difficulty we had purifying VirF (see Chapter IV). Therefore, to lower the variance seen in the pilot HTS, we modified the *Shigella*-based assay to include

humidified overnight incubation. Using this modified assay, we were able to greatly reduce the variability of the screen and accurately test ~100,000 more compounds. Following a series of counter and reconfirmation screens, we were successfully able to identify five small molecules with VirF inhibitory properties.

Materials and Methods

Reagents

All reagents were purchased from Sigma-Aldrich (St. Louis, MO), unless otherwise specified. CPRG (chlorophenol red β -D-galactopyranoside) was purchased from Roche (Basel, Switzerland). Yeast extract, bactotryptone, carbenicillin, and Corning microtiter plates (384 and 96 well) were purchased from Fisher Scientific (Hampton, NH). Compounds selected for reconfirmation screening were purchased from ChemDiv (7 compounds, San Diego, CA) and Vitas-M Laboratory (3 compounds, Moscow, Russia).

Strains and Plasmids

Wild-type *Shigella flexneri* serotype 2a strain 2457T¹¹ and an isogenic, virulence plasmid-cured derivative, BS103,¹² were used in this study. HeLa cells and L2 mouse fibroblasts were used for virulence assays and were grown in Dulbecco's Modified Eagle Medium (Life Technologies, Grand Island, NY), supplemented with 10% heat-inactivated fetal bovine serum (Life Technologies, Grand Island, NY). The bacteria were grown in tryptic soy broth (TSB) or on agar plates supplemented with 0.025% Congo Red agar as necessary at 37°C. The construction of the reporter plasmids, pMAL*virF-lacZ* and pMAL(Δ *virF*)-*lacZ* (positive control), was previously described.⁹

Small Molecule Library

A 100,000 compound library produced by ChemDiv (San Diego, CA) was screened at the Center for Chemical Genomics (CCG, University of Michigan Ann Arbor).

High-throughput VirF-driven, β -galactosidase Reporter Assay

The construction and optimization of the reporter assay was previously described.⁹ Briefly, starter cultures of *S. flexneri* BS103 harboring either the reporter plasmid (pMAL*virF-lacZ*) or positive control plasmid (pMAL(Δ *virF*)-*lacZ*) were grown overnight at 37°C with shaking in 2xTY media (16 g bacto-tryptone, 10 g yeast extract, 5 g NaCl per liter of water supplemented with 100 μ g/mL carbenicillin). The next day, 20 μ L of 2xTY media supplemented with 100 μ g/mL carbenicillin was added to 384-well plates using a multidrop dispenser (Thermo Scientific, Waltham, MA). Compounds from the 100K ChemDiv library (13 μ M final, n=2, 0.2 μ L) were then added to appropriate wells using the Biomek HDR pintool instrument (Beckman, Fullerton, CA). Overnight starter cultures (reporter plasmid and positive control) were diluted to OD₆₀₀ = 0.012 using 2xTY media supplemented with 100 μ g/mL carbenicillin. The diluted cultures (10 μ L) were added to the appropriate wells of the plates via the multidrop dispenser (total volume 30 μ L). Plates were then spun-down at 1000 x g for one minute using a Beckman Coulter Allegra Series centrifuge. After centrifugation, plates were placed overnight (approximately 20 hours) in a humidified, 30°C incubator (VWR). The following day, 30 μ L of CPRG solution (0.5 mg/mL CPRG, 0.1% Triton X-100, 60 mM Na₂HPO₄, 40 mM NaH₂PO₄, 10 mM KCl, 1 mM MgSO₄, pH 7.0) was added to each well. Plates were incubated at room temperature for 10 minutes before measuring

chlorophenol red (CPR) absorbance (A_{570}) in a PHERAstar (BMG Labtech, Cary, NC) plate reader with a narrow bandpass filter.

Counter Screens

Potential hits identified from the primary high-throughput screen were subjected to a series of stringent control screens. First, compounds were assayed in a dose-response study ($n=2$) following the screening protocol described above. However, for the dose-response study, the concentration of the compounds was varied using 2-fold serial dilutions ranging from 100 to 0.78 μM . Also, directly prior to the addition of the CPRG solution, bacteria density (OD_{600}) was measured using the PHERAstar plate reader to determine if the compounds inhibited bacterial growth.

Compounds that inhibited VirF in a dose-dependent manner, but did not inhibit bacterial growth (e.g., $\text{MIC}_{50} > 100 \mu\text{M}$) were selected for β -galactosidase inhibition screening. For the β -galactosidase inhibition screening, cultures of *S. flexneri* BS103 harboring either *pMALvirF-lacZ* or *pMAL(Δ virF)-lacZ* were diluted to $\text{OD}_{600}=1.0$ using 2xTY media supplemented with 100 $\mu\text{g}/\text{mL}$ carbenicillin and added to appropriate wells of a 384-well microtiter plate using the multidrop dispenser (30 μL). Compounds were added to the plates in duplicate, and their concentrations were varied using 2-fold serial dilutions ranging from 100 to 0.78 μM . Immediately following compound addition, CPRG solution was added to each well (30 μL). After a 10-minute incubation period at room temperature, chlorophenol red absorbance (A_{570}) was measured using the PHERAstar plate reader to determine if the compounds directly inhibited β -galactosidase.

Reconfirmation Screen

Fresh samples of compounds identified as hits were ordered from commercial vendors for a reconfirmation dose-response study. For this study, the screening protocol was modified to a 96-well microtiter plate format. Working stocks of each compound were made using 2xTY media supplemented with 100 µg/mL carbenicillin. Working stocks were added to the plates in triplicate using a 2-fold serial dilution technique (60 µL). Cultures of *S. flexneri* BS103 harboring either pMAL*virF-lacZ* or pMAL(Δ *virF*)-*lacZ* were diluted to OD₆₀₀= 0.012 using 2xTY media supplemented with 100 µg/mL carbenicillin and added to appropriate wells of plate (30 µL). Final compound concentrations ranged from either 100 to 0.78 µM or 50 to 0.78 µM. For negative controls, compound vehicle (DMSO, 1% final concentration) was added to wells instead of compound. Plates were placed overnight (approximately 20 hours) in a humidified, 30°C incubator. The following day, bacteria density (OD₆₀₀) was measured using a BioTek Synergy H1 plate reader (Winooski, VT) then 90 µL of CPRG solution was added to each well. Plates were allowed to incubate for 7 minutes at room temperature (incubation time decreased, due to increase signal in 96-well plate format) then chlorophenol red absorbance (A₅₇₀) was read using the BioTek plate reader.

Data Analysis/Hit Selection

Three different sets of selection criteria were used to define active compounds in the initial high-throughput screen. Samples were defined as active if either: A) one of their A₅₇₀ readings was ≥ 3 times the standard deviation of the negative controls from the average A₅₇₀ of the negative controls (calculated on a plate by plate basis); or B) one of their A₅₇₀ readings was ≥ 3 times the standard deviation of the plate (not

including positive controls) from the average A_{570} of the plate (not including positive controls, calculated on a plate by plate basis); or C) if their percent effect value (calculated on a plate by plate basis using both negative and positive controls) was $\geq 30\%$ inhibition. Compounds that passed initial selection criteria were tested in a series of counter screens. Compounds that passed all counter screens were classified as hits. Counter screen selection criteria were as follows: $IC_{50} \leq 100 \mu\text{M}$ for VirF Inhibition dose-response study, $MIC_{50} > 100 \mu\text{M}$ for bacterial growth inhibition, and no direct β -galactosidase inhibition over the range of concentrations tested. For all dose-response studies, data were fit by non-linear regression to following equation using Kaleidagraph (Synergy Software, Essex, VT):

$$y = \text{lower} + \frac{(\text{upper} - \text{lower})}{(1 + 10^{(M_0 - M_1) * M_2})}$$

where $M_0 = \log$ of compound concentration, $M_1 = \log$ of IC_{50} , $M_2 =$ Hill slope, “lower” is defined to be the lower limit of the assay (lower = 0), and “upper” is defined to be the upper limit of the assay (upper = 100).

Results

Hit Identification

A summary of the hit identification process is shown in Figure II-2. The 100,000 compounds tested in the primary screen (in duplicate) produced 640 compounds that were considered active based on primary selection criteria (0.64% hit rate). Of the 640 active compounds, 592 met selection criterion A, 39 met selection criterion C, and 9 met selection criterion B. The average Z' factor per plate tested in the primary screen was equal to 0.66 ($Z' = 1 - ((3\sigma_{c+} + 3\sigma_{c-}) / (|\mu_{c+} - \mu_{c-}|))$), where σ_{c+} and σ_{c-} are the standard

deviations of the positive and negative controls and μ_{c+} and μ_{c-} are the means of the positive and negative controls, respectively).

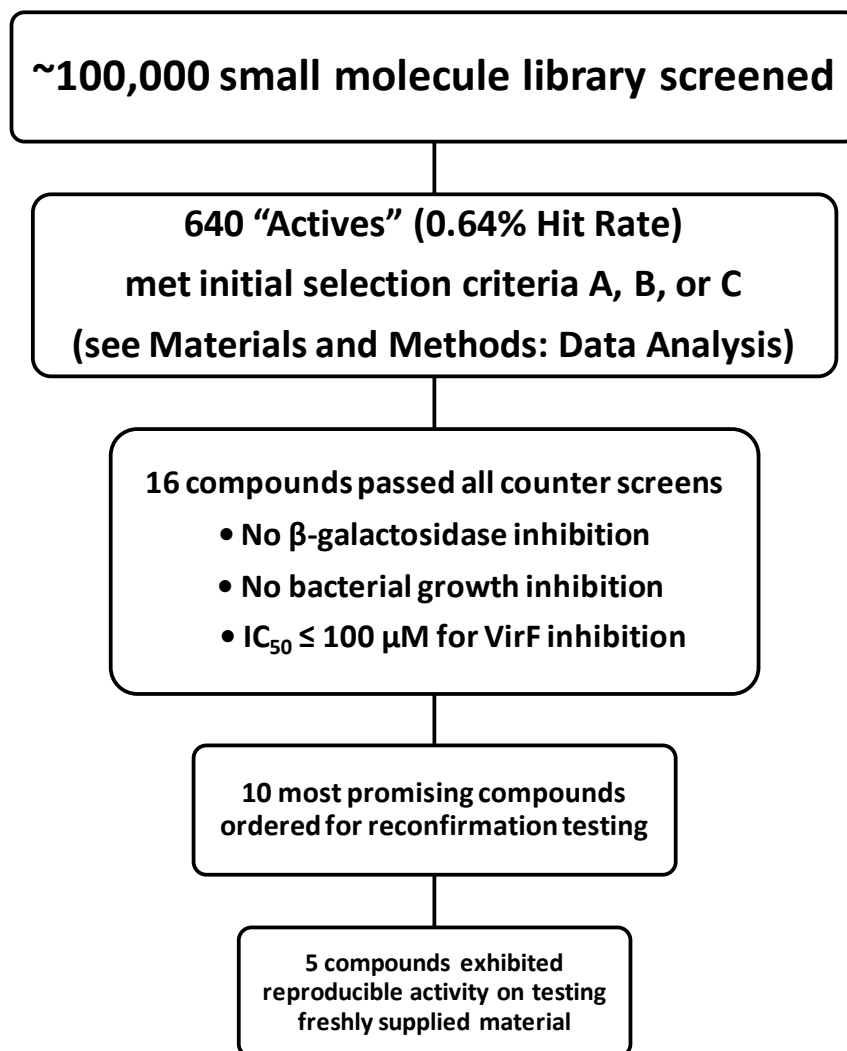
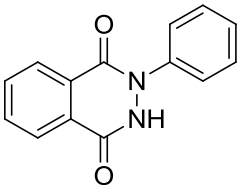
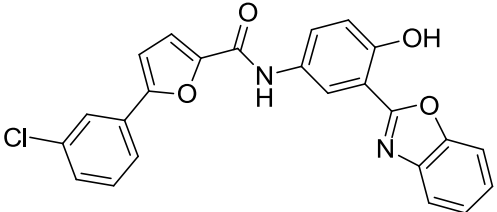
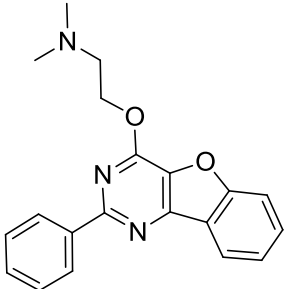
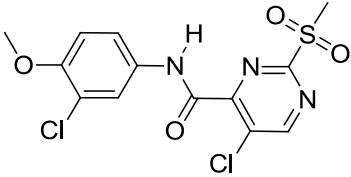


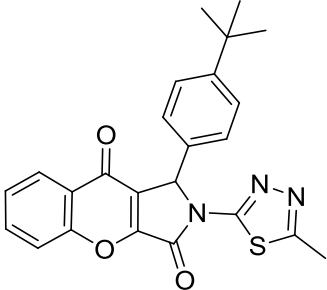
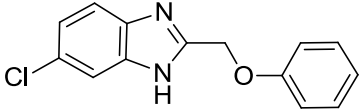
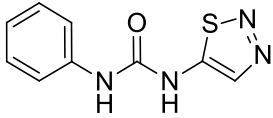
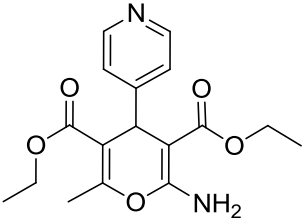
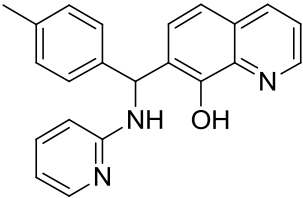
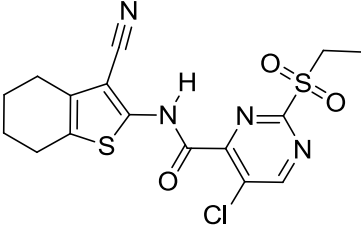
Figure II-2: Flow Chart Depicting the Hit Identification Process for the HTS.

The 640 active compounds were next tested in a dose-response study (in duplicate) monitoring both bacterial growth inhibition (optical density) and VirF inhibition (CPRG hydrolysis). Of the 640 active compounds, only 52 inhibited CPRG hydrolysis while not inhibiting bacterial growth over the range of concentrations tested (e.g., $MIC_{50} > 100 \mu M$). These 52 compounds were further tested for direct β -galactosidase inhibition and 17 of the 52 compounds inhibited β -galactosidase in a dose-dependent

manner. Therefore, only 35 of 640 active compounds appeared to inhibit the activity of VirF. Of the 35 compounds, only 16 had an $IC_{50} \leq 100 \mu\text{M}$ for VirF inhibition. Based on novelty of scaffold, availability, and potential toxicity concerns we eliminated 6 of the compounds from further study. Fresh samples of the remaining 10 compounds were ordered from commercial vendors (seven from ChemDiv, three from Vitas-M Laboratory) for the reconfirmation study (below). The structures of these 10 compounds are shown in Table II-1.

Table II-1. Hits from 100K ChemDiv Screen that were Rescreened from Fresh Samples.

Compound Name	HTS IC_{50} (μM)	Structure
*25354	6	
3776	12	
19615	21	
144092	31	

25073	45	
153578	58	
*24904	58	
16977	81	
*21496	89	
144143	91	

*These compounds were also hits in original 42,000 small molecule screen previously reported (Hurt *et al.*, 2010)

Reconfirmation

Each of the 10 compounds was tested in a modified 96-well plate version of the screening assay. Table II-2 shows the results from the modified dose-response study. Out of the 10 compounds tested, only five reconfirmed. The IC₅₀ values of these compounds ranged from 66 to 14 μM. Figure II-3 shows the dose-response curves for the two most potent compounds, 19615 and 144092. The dose-response curves for the rest of the compounds can be found in Appendix Figure II-1.

Table II-2. Reconfirmation Compound IC₅₀ Values and Toxicities from Fresh Samples.¹

Compound	Source	IC ₅₀ (μM) ²	Bacterial Growth Inhibition ³
19615	Vitas-M	14	2% @ 100 μM
144092	ChemDiv	23	13% @ 100 μM
144143	ChemDiv	23	14% @ 100 μM
153578	ChemDiv	37	19% @ 100 μM
24904	ChemDiv	66	13% @ 50 μM

¹ Compounds 25354, 3776, 25073, 16977 and 21496 did not reconfirm and were not tested for toxicity.

² Log (IC₅₀) values and their associated errors can be found in Appendix Table II-1. The estimated percent errors for each reconfirmed compound were ≤ 2%.

³ The % inhibition of bacterial growth values are averages of 3 determinations with standard errors of 3%.

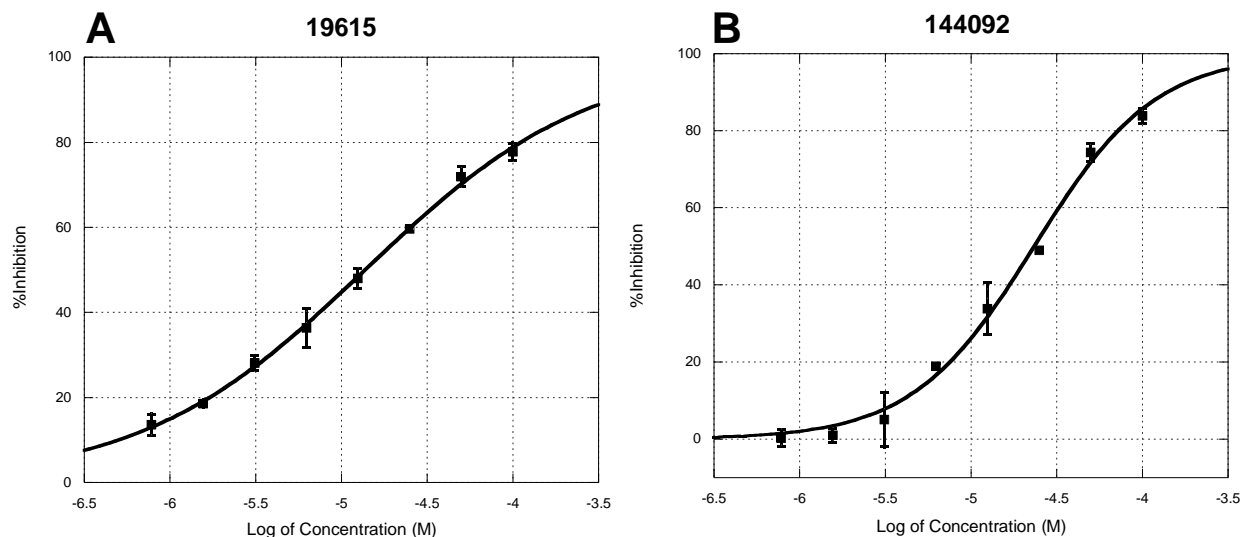


Figure II-3: Representative Dose-Response Curves from the Reconfirmation Study. All concentrations were tested in triplicate. The average %inhibition for each concentration is represented on the plots as solid black squares. Data were normalized for bacteria growth and background signal (positive control average: simulates complete VirF inhibition) was removed from data before plotting. Curves were fit to the equation listed in Materials and Methods and represented on the plots as solid black lines. **A)** Dose-response curve for compound 19615. Concentrations ranging from 100 to 0.78 μM were tested. **B)** Dose-response curve for compound 144092. Concentrations ranging from 100 to 0.78 μM were tested.

Discussion

A potential issue with any cell-based HTS is a problem with plate-to-plate/well-to-well variance. In our previous screen for inhibitors of VirF activity we had a problem with “edge effects”, evaporation around the perimeter of each microtiter plate, which produced a high degree of variability in the screen.⁹ This variability is evidenced by the low campaign Z' factor (≈ 0.45) and artificially high hit rate (3%) seen in the pilot screen. To improve upon our previous HTS, new humidified incubators were used for overnight bacterial growth in the HTS. The humidified incubation helped ameliorate the “edge effects” seen previously. The campaign Z' factor for the HTS increased significantly

(0.66) and a more reasonable hit rate was obtained (0.64%). Overall, the precision of the screen was much improved, as depicted in Figure II-4.

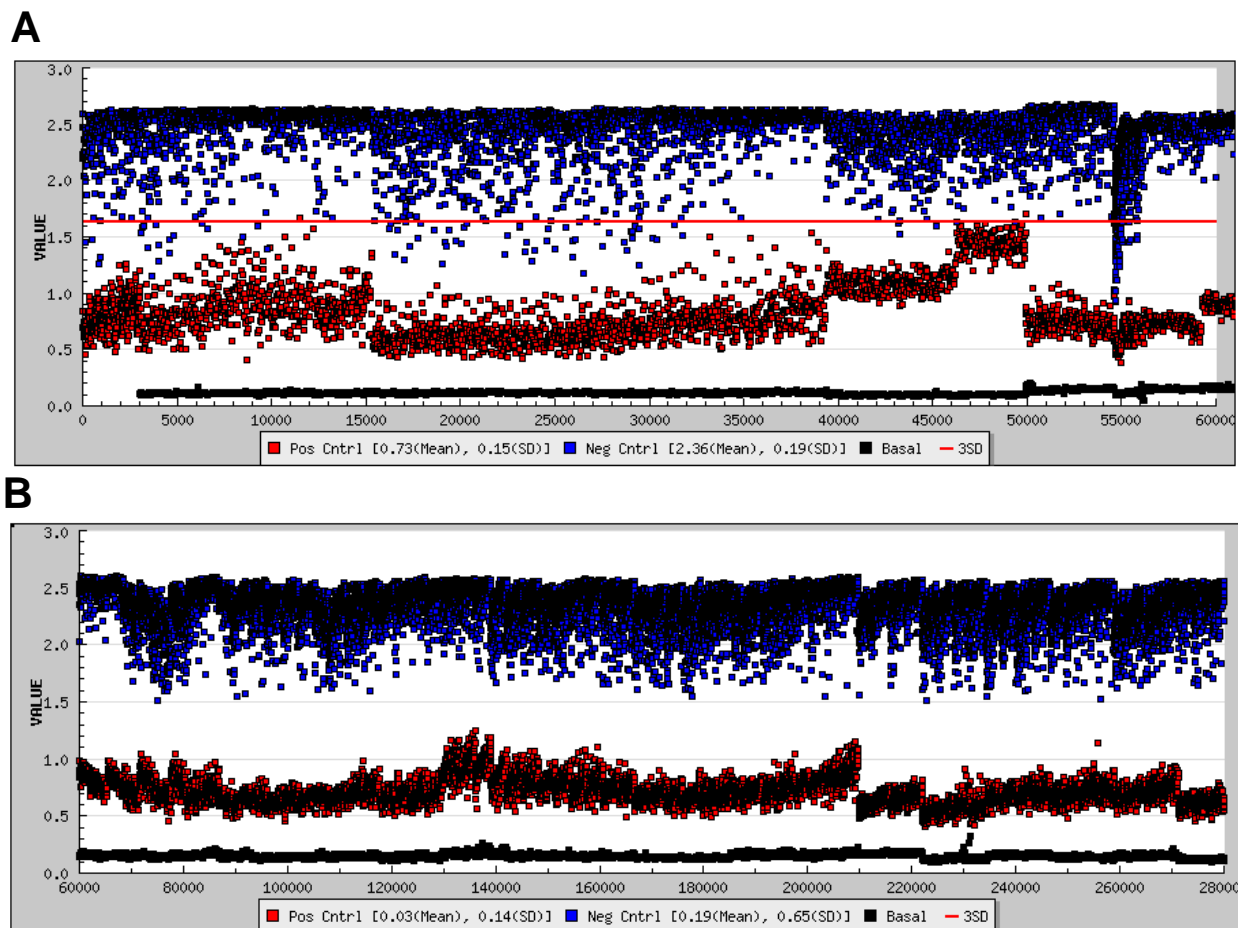


Figure II-4: Comparison of Controls for HTS Pilot Screen and 100K Small Molecule Screen. **A)** Graph depicts the A570 values generated for all controls during the pilot screen. The red dots represent the positive controls (*pMAL*($\Delta virF$)-*lacZ*) and the blue dots represent the negative controls (DMSO). **B)** Graph depicts the A570 values generated for all controls during the 100,000 small molecule screen. The red dots represent the positive controls (*pMAL*($\Delta virF$)-*lacZ*) and the blue dots represent the negative controls (DMSO).

The primary HTS identified 640 small molecules that met initial selection criteria for VirF inhibition, see Figure II-2. The 640 small molecules were tested in a series of counter screens to eliminate any false positives that inhibited bacterial growth or β -

galactosidase directly and to verify that the compounds exhibited dose-dependent activity. A total of 16 compounds passed all selection criteria and counter screens. Based on novelty of scaffold, availability, and potential toxicity concerns, we eliminated six of the compounds from further study. The remaining 10 compounds were ordered from commercial sources and tested in a dose-response study. The structures and HTS IC₅₀ values of the 10 compounds are shown in Table II-1. As Table II-1 shows, only 5 of the 10 compounds reconfirmed when fresh, pure samples were tested. Mass spectroscopy verified that the new samples of the five compounds that did not reconfirm were of the appropriate mass (data not shown) suggesting that the fresh samples were the correct compounds. Low reconfirmation rates are not uncommon in HTS follow-up studies.¹³ A variety of factors including library compound degradation, library compound impurities, and compound transfer errors can increase the number of false positive results obtained from an HTS. The most likely explanation for our low reconfirmation rate is that the active compounds from the HTS library are degradation products of the original compounds. The HTS library is stored in DMSO and has been subjected to multiple freeze-thaw cycles, which increases the likelihood of compound degradation. Due to the difficulty and unpredictable nature of determining the active degradation products from the HTS library, we decided to move forward with only the five compounds that reconfirmed from new, clean samples.

The reconfirmed compounds were considered promising for a variety of reasons. All of the compounds had IC₅₀ values for VirF inhibition less than 100 μM, with compound 19615 being the most potent (IC₅₀ = 14 μM). Since these IC₅₀ values were determined using a *Shigella*-based reporter system, we know each compound can

cross through the bacterial membrane and bind its target. Compounds 144092 and 144143 are close analogues and share a core pyrimidine scaffold, which makes them attractive candidates for future optimization via structure activity relationship (SAR) studies. Compound 153578 has a benzimidazole core that is similar to the benzimidazole compounds that were shown to inhibit the virulence regulator of *Yersinia pseudotuberculosis*, LcrF.¹⁴⁻¹⁶ Interestingly, LcrF and VirF are both members of the same class of transcriptional activators, the AraC family. Compound 24904 is a known plant defoliant, thidiazuron, that is reported to have low acute toxicity towards humans.¹⁷ Lastly, none of the compounds significantly inhibited bacterial growth when tested at 100 μ M which is necessary if they are to be further developed as anti-virulence therapies targeting shigellosis.

Although the results from the HTS are promising, further work must be done to characterize each compound. Given that a bacterial-based approach was used to identify the compounds, it is possible that the inhibition seen in the assay is a byproduct of an off-target effect. The most obvious off-target effects that would result in a reduction of β -galactosidase activity should have been caught by the control screens (direct inhibition of β -galactosidase, growth inhibition caused by RNA polymerase inhibition, or growth inhibition caused by ribosome inhibition). However, the mechanism of action of each compound should still be confirmed (see Chapter V). Furthermore, since our reporter assay only monitored VirF activation of the *virB* promoter, we do not know the effect the compounds have on VirF activation of the *icsA* promoter. Previous studies have identified compounds that selectively bind to specific promoter regions to prevent transcriptional activation without inducing toxicity.¹⁸ Although unlikely, it is

possible that our compounds may selectively inhibit one promoter over the other. To test this, we have attempted to make a similar β -galactosidase reporter system that monitors VirF activation of the *icsA* promoter. Unfortunately, we have not been successful; most likely due to the increased complexity of the *icsA* promoter (i.e. four potential VirF binding sites, VirF binding sites after the *icsA* transcription start site, and the presence of an antisense RNA regulator).¹⁹ In the future, we plan on constructing reporter systems that utilize full length IcsA-reporter protein fusions to ensure that the full *icsA* promoter is present.

In conclusion, we have developed a more precise HTS screening methodology and have used it to identify five small molecules with apparent VirF inhibitory properties. In the studies described in the next chapter, we will use these compounds to determine if a small molecule inhibitor of VirF can attenuate the virulence of *Shigella flexneri*, and thereby, validate VirF as a target for an anti-virulence therapy. In later chapters (Chapters IV and V), we will describe the development of methodologies to probe the mechanism of action of each compound.

Notes to Chapter II

Parts of this chapter have been published in Emanuele, et al. *Journal of Antibiotics* **2014**, 67, 379-386.²⁰ I would like to acknowledge Dr. Julie Hurt for the construction of the reporter plasmids used in this study and I would also like to thank her for her mentoring. I would also like to acknowledge Martha J. Larsen (Center for Chemical Genomics, Life Sciences Institute, University of Michigan), Tom McQuade (Center for Chemical Genomics, Life Sciences Institute, University of Michigan), and Dr. Yi-Chen Chen (Department of Medicinal Chemistry, University of Michigan) for their contributions to the high-throughput screening campaign.

References

1. Yang, J.; Tauschek, M.; Robins-Browne, R. M. Control of bacterial virulence by AraC-like regulators that respond to chemical signals. *Trends in Microbiology* **2011**, 19, 128-135.
2. Champion, G. A.; Neely, M. N.; Brennan, M. A.; DiRita, V. J. A branch in the ToxR regulatory cascade of *Vibrio cholerae* revealed by characterization of toxT mutant strains. *Molecular Microbiology* **1997**, 23, 323-331.
3. Hoe, N. P.; Minion, F. C.; Goguen, J. D. Temperature sensing in *Yersinia pestis*: regulation of yopE transcription by IcrF. *Journal of Bacteriology* **1992**, 174, 4275-4286.
4. Eichelberg, K.; Galán, J. E. Differential Regulation of *Salmonella typhimurium* Type III Secreted Proteins by Pathogenicity Island 1 (SPI-1)-Encoded Transcriptional Activators InvF and HilA. *Infection and Immunity* **1999**, 67, 4099-4105.
5. Yahr, T. L.; Wolfgang, M. C. Transcriptional regulation of the *Pseudomonas aeruginosa* type III secretion system. *Molecular Microbiology* **2006**, 62, 631-640.

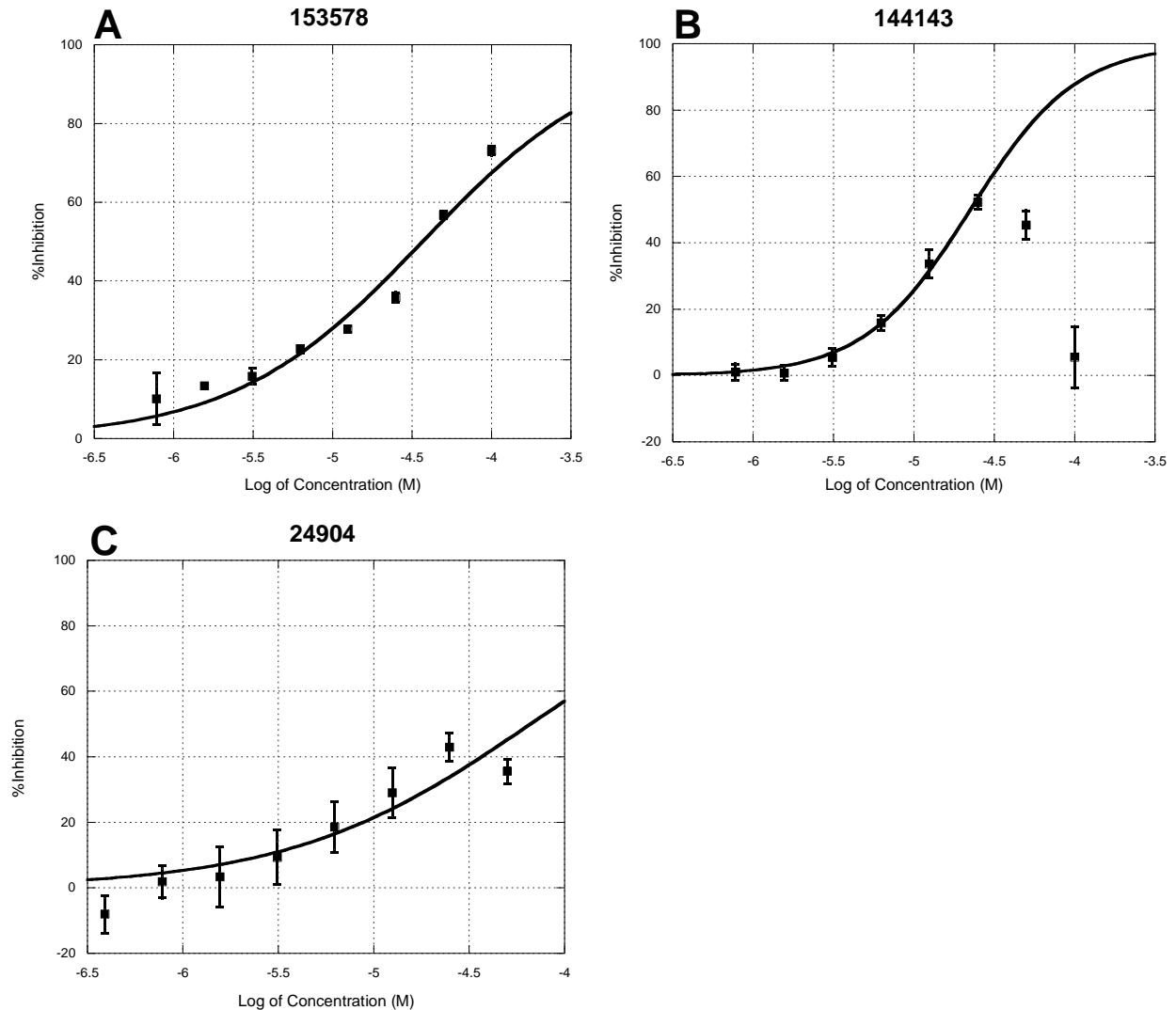
6. Allen, R. C.; Popat, R.; Diggle, S. P.; Brown, S. P. Targeting virulence: can we make evolution-proof drugs? *Nat Rev Micro* **2014**, 12, 300-308.
7. Clatworthy, A. E.; Pierson, E.; Hung, D. T. Targeting virulence: a new paradigm for antimicrobial therapy. *Nature Chemical Biology* **2007**, 3, 541-548.
8. Skredenske, J. M.; Koppolu, V.; Kolin, A.; Deng, J.; Kettle, B.; Taylor, B.; Egan, S. M. Identification of a Small-Molecule Inhibitor of Bacterial AraC Family Activators. *Journal of Biomolecular Screening* **2010**, 18.
9. Hurt, J. K.; McQuade, T. J.; Emanuele, A.; Larsen, M. J.; Garcia, G. A. High-Throughput Screening of the Virulence Regulator VirF: A Novel Antibacterial Target for Shigellosis. *Journal of Biomolecular Screening* **2010**, 15, 379-387.
10. Hung, D. T.; Shakhnovich, E. A.; Pierson, E.; Mekalanos, J. J. Small-Molecule Inhibitor of *Vibrio cholerae* Virulence and Intestinal Colonization. *Science* **2005**, 310, 670-674.
11. Formal, S. B.; Dammin, G. J.; Labrec, E. H.; Schneider, H. Experimental Shigella infections: characteristic of a fatal infection produced in guinea pigs. *Journal of Bacteriology* **1958**, 75, 604-610.
12. Maurelli, A. T.; Blackmon, B.; Curtiss III, R. Loss of pigmentation in *Shigella flexneri* 2a is correlated with loss of virulence and virulence associated plasmid. *Infection and Immunity* **1984**, 43, 397-401.
13. Zhang, J.; Chung, T.; Oldenburg, K. Confirmation of Primary Active Substances from High Throughput Screening of Chemical and Biological Populations: A Statistical Approach and Practical Considerations. *J Comb Chem* **2000**, 2, 258-265.
14. Bowser, T. E.; Bartlett, V. J.; Grier, M. C.; Verma, A. K.; Warchol, T.; Levy, S. B.; Alekshun, M. N. Novel anti-infection agents: small-molecule inhibitors of bacterial transcription factors. *Bioorganic & Medicinal Chemistry Letters* **2007**, 17, 5652-5.
15. Garrity-Ryan, L. K.; Kim, O. K.; Balada-Llasat, J. M.; Bartlett, V. J.; Verma, A. K.; Fisher, M. L.; Castillo, C.; Songsungthong, W.; Tanaka, S. K.; Levy, S. B.; Mecsas, J.; Alekshun, M. N. Small Molecule Inhibitors of LcrF, a *Yersinia pseudotuberculosis* Transcription Factor, Attenuate Virulence and Limit Infection in a Murine Pneumonia Model. *Infection and Immunity* **2010**, 78, 4683-4690.

16. Kim, O. K.; Garrity-Ryan, L. K.; Bartlett, V. J.; Grier, M. C.; Verma, A. K.; Medjanis, G.; Donatelli, J. E.; Maccone, A. B.; Tanaka, S. K.; Levy, S. B.; Alekshun, M. N. N-hydroxybenzimidazole inhibitors of the transcription factor LcrF in *Yersinia*: novel antivirulence agents. *J Med Chem* **2009**, *52*, 5626-34.
17. Edwards, D. *Reregistration Eligibility Decision (RED) Fact Sheet for Thidiazuron*; USA, Environmental Protection Agency: 2005.
18. Marín, S.; Mansilla, S.; García-Reyero, N.; Rojas, M.; Portugal, J.; Piña, B. Promoter-specific inhibition of transcription by daunorubicin in *Saccharomyces cerevisiae*. *Biochemical Journal* **2002**, *368*, 131-136.
19. Tran, C. N.; Giangrossi, M.; Prosseda, G.; Brandi, A.; Di Martino, M. L.; Colonna, B.; Falconi, M. A multifactor regulatory circuit involving H-NS, VirF and an antisense RNA modulates transcription of the virulence gene *icsA* of *Shigella flexneri*. *Nucleic acids research* **2011**, *39*, 8122-8134.
20. Emanuele, A. A.; Adams, N. E.; Chen, Y.-C.; Maurelli, A. T.; Garcia, G. A. Potential novel antibiotics from HTS targeting the virulence-regulating transcription factor, VirF, from *Shigella flexneri*. *Journal of Antibiotics* **2014**, *67*, 379-386.

Appendix

Appendix Table II-1. Log(IC₅₀) and associated error for the reconfirmation dose-response study.

Compound Name	Log(IC₅₀) (M)	Error
19615	-4.86	0.02
144092	-4.63	0.02
144143	-4.64	0.02
24904	-4.18	0.1
153578	-4.43	0.03



Appendix Figure II-1: Representative dose-response curves from reconfirmation study. All concentrations were tested in triplicate. The average %inhibition for each concentration is represented on the plots as solid black squares. Data were normalized for cell growth and background signal (positive control average: simulates complete VirF inhibition) was removed from data before plotting. Curves were fit to the equation listed in Materials and Methods and represented on the plots as solid black lines. **A)** Dose-response curve for compound 153578. Concentrations ranging from 100 to 0.78 μM were tested. **B)** Dose-response curve for compound 144143. Concentrations ranging from 100 to 0.78 μM were tested, but 100 μM and 50 μM points were excluded from fit due to toxicity to *S. flexneri* BS103. **C)** Dose-response curve for compound 24904. Concentrations ranging from 50 to 0.78 μM were tested, 100 μM was not tested due to solubility issues.

CHAPTER III

Tissue Culture-based Models of the *Shigella flexneri* Invasion Process

At the time of the studies reported herein, the VirF-activated *Shigella* spp. pathogenesis cascade had yet to be validated as a therapeutic target for small molecule inhibition. However, multiple studies highlighted the potential benefits and feasibility of targeting this pathway. Gene silencing studies of both the *virF* and *virB* genes, produced strains of *Shigella* that were viable but incapable of infecting eukaryotic cells.¹⁻
³ Similar studies targeting *icsA* produced strains of *Shigella* that were incapable of intra- or inter-cellular movement after initial host cell infection.^{4, 5} The potential for therapeutic intervention was further strengthened by the fact that several *icsA*-knockout strains of *Shigella* were being tested as live-attenuated vaccine candidates for the prevention of shigellosis.⁶⁻⁹ Lastly, other AraC family activated pathogenesis cascades had been targeted by small molecule inhibitors resulting in the attenuation of virulence of both *Vibrio cholerae*¹⁰ and *Yersinia pseudotuberculosis*,¹¹ which suggested a small molecule inhibitor of VirF may have a similar effect on *Shigella flexneri*.

To validate VirF as a target for small molecule therapeutic intervention, we screened the five small molecule VirF inhibitors identified in Chapter II in a series of tissue culture-based assays that model the *S. flexneri* infection process. With the help of our collaborators in the Maurelli lab (Prof. Anthony Maurelli, Uniformed Services University of the Health Sciences, Bethesda, MD), we initially screened the compounds in gentamicin protection invasion assays using HeLa cells (a human cervical cancer

epithelial cell line) and plaque formation assays using L2 cells (a rat lung epithelial cell line). The gentamicin protection assay serves as a model for initial bacterial invasion of the host cells, while the plaque formation assay serves as a model for the cell-to-cell spread of a bacterial infection. Since *Shigella* spp. are known to only naturally infect human or primate colonic cells *in vivo*,¹²⁻¹⁴ we subsequently repeated both assays in our own lab using Caco-2 cells (a human colonic cancer epithelial cell line); which we believe to be a more appropriate model for the *Shigella* infection process. Using the Caco-2 models, we determined that small molecule inhibitors of VirF activity can attenuate the virulence of *S. flexneri*.

Materials and Methods

Reagents

All reagents were purchased from Sigma-Aldrich (St. Louis, MO), unless otherwise specified. Yeast extract, bactotryptone, carbenicillin, and Corning microtiter plates (384 and 96 well) were purchased from Fisher Scientific (Hampton, NH). Compounds were purchased from ChemDiv (7 compounds, San Diego, CA) and Vitas-M Laboratory (3 compounds, Moscow, Russia).

Strains and Plasmids

Wild-type *Shigella flexneri* serotype 2a strain 2457T¹⁵ and an isogenic, virulence plasmid-cured derivative, BS103¹⁶, were used in this study. HeLa cells (Maurelli lab stock), Caco-2 cells (a generous gift from the Amidon Lab), and L2 mouse fibroblasts (Maurelli lab stock) were used for virulence assays and were grown in Dulbecco's Modified Eagle Medium (Life Technologies, Grand Island, NY), supplemented with 10% heat-inactivated fetal bovine serum (Life Technologies, Grand Island, NY). The bacteria

were grown in tryptic soy broth (TSB) or on agar plates supplemented with 0.025% Congo Red agar as necessary at 37°C. The construction of the reporter plasmids, pMAL*virF-lacZ* and pMAL(Δ *virF*)-*lacZ* (positive control), was previously described ¹⁷.

Growth Curves

Cultures of bacteria were grown overnight in TSB, washed in phosphate-buffered saline solution (PBS) (Lonza; Walkersville, MD), and diluted in TSB with appropriate concentration of drug. Approximately 2×10^4 colony forming units (CFU) were applied to individual wells in a 96 well plate for growth curve analysis. Growth curves were performed in a BioTek Synergy2 plate reader at 37°C with constant shaking. Readings of optical density at 600nm were recorded every 30 minutes for 24 hours, and data points were analyzed with Gen5 version 1.11.5 software.

Cell Toxicity

Serial dilutions of each compound were applied to 50% confluent monolayers of HeLa and L2 cells and monitored daily, up to 3 days, for growth phenotypes. Physical signs of cell health were monitored since an OD reading could not be done with adherent cells (SI-Table 2). The highest tolerable compound concentration with HeLa cells was then used to assess bacterial growth of wild-type *Shigella flexneri* 2457T, as well as a virulence plasmid-cured strain (BS103), by periodically measuring OD₆₀₀ over 24 hours.

MTT Assay

A MTT cell viability assay kit from Abnova (Taipei, Taiwan) was used for this study. Briefly, Caco-2 cells were seeded in 96-well microplates (25,000 cells per well) and incubated overnight at 37°C with 5% CO₂ in 80 μ L of Dulbecco's Modified Eagle

Medium (DMEM), supplemented with 10% heat-inactivated fetal bovine serum (Δ FBS). The next day 20 μ L of DMEM supplemented with 10% Δ FBS and either DMSO or test compound (concentrations ranged from 50 μ M to 0.8 μ M) was added to appropriate wells. Again, the plate was allowed to incubate overnight at 37°C with 5% CO₂. The following day, 15 μ L of MTT reagent was added to each well and the plate was allowed to incubate at 37°C with 5% CO₂. After a four hour incubation, 100 μ L of MTT solubilizer was added to each well and the plate was mixed gently on a rocker platform for one hour at room temperature (protected from light). Lastly, the optical density at 570 nm was measured using a BioTek Synergy H1 plate reader (Winooski, VT)

HeLa Cell Invasion Assay

Assays were performed as previously described¹⁸. Briefly, bacteria were grown overnight, subcultured into TSB supplemented with compound when appropriate, and grown with agitation until reaching mid-log phase. Cultures were standardized to an optical density at 600 nm of 0.35, washed in PBS and resuspended in Dulbecco's Modified Eagle Medium (DMEM) (Gibco; Grand Island, NY) supplemented with compound when appropriate. The input bacteria were titered on TSB Congo Red plates prior to applying to 6-well plates seeded to semi-confluence with HeLa cells. The plates were then centrifuged at 3,000 rpm for 10 minutes and then permitted to invade for 30 minutes at 37°C with 5% CO₂. The monolayers were washed with PBS, DMEM supplemented with 50 μ g/mL gentamicin was then applied, and plates were incubated at 37°C with 5% CO₂ for 30 minutes. After washing the monolayers again with PBS, infected cells were lysed with 0.5% Triton X-100, and the recovered bacteria were titered on TSB Congo Red plates after incubation at 37°C. Percent invasion was

determined by calculating the total recovered gentamicin-resistant CFU per well after lysis divided by the total number of input bacteria per well.

$$\text{Invasion \%} = (\text{total recovered bacteria}) / (\text{total input bacteria}) \times 100$$

Caco-2 Cell Invasion Assay

Assays were performed in the same manner as for the HeLa cell invasion assays with the following exceptions. Caco-2 cells were grown to near confluence prior to bacterial addition. After bacterial addition, the bacteria were permitted to invade for 2 hours at 37°C with 5% CO₂. After invasion, the monolayers were washed with PBS, DMEM supplemented with 50 µg/mL gentamicin was applied, and the plates were incubated at 37°C with 5% CO₂ for 90 minutes (after 30 minutes fresh DMEM supplemented with 50 µg/mL gentamicin was re-applied).

L2 Cell Plaque Assay

Assays were performed as previously described¹⁹. Briefly, bacteria were grown overnight, subcultured into TSB and grown with agitation until reaching mid-log phase. Cultures were standardized to an optical density at 600 nm of 0.35, washed in PBS and diluted in DMEM. The input bacteria were titered on TSB Congo Red plates prior to applying to 6-well plates seeded to confluence with L2 cells. The 6-well plates were then rocked at 37°C under 5% CO₂ for 2 hours. An agarose solution consisting of DMEM, 10% fetal bovine serum (FBS), 50 µg/mL gentamicin, 0.5% agarose (ISC Bioexpress; Kaysville, UT), and compound was then applied to the monolayers. The plates were incubated at 37°C under 5% CO₂ for three days and then stained with 0.5% Neutral Red (Sigma Aldrich; St. Louis, MO) and inverted to visualize plaques. Efficiency of plaque formation was calculated by dividing the total number of plaques observed

after staining by the total number of input bacteria. The average plaque size was determined by measuring 30 plaques.

$$\text{Plaque efficiency (\%)} = (\text{total number of plaques}) / (\text{total input bacteria}) \times 100$$

Caco-2 Cell Plaque Assay

Assays were performed in the same manner as for the HeLa cell invasion assays with the following exceptions. Prior to addition of bacteria, 60 mm dishes were seeded to confluence with Caco-2 cells. After bacterial addition, dishes were rocked and placed at 37°C under 5% CO₂ for 2 hours, and rocked again at the 1 hour time point. An agarose solution consisting of DMEM, 10% fetal bovine serum (FBS), 50 µg/mL gentamicin, 0.5% agarose, and compound was then applied to the monolayers. The plates were incubated at 37°C under 5% CO₂ for three days and then stained with 0.5% Neutral Red (Sigma Aldrich; St. Louis, MO) and inverted to visualize plaques. Efficiency of plaque formation was calculated by dividing the total number of plaques observed after staining by the total number of input bacteria.

$$\text{Plaque efficiency (\%)} = (\text{total number of plaques}) / (\text{total input bacteria}) \times 100$$

Results

Identifying the highest concentration of compound not affecting host cell or bacteria survival

As shown in Table III-1 and Appendix Figure III-1, the highest concentrations of compounds identified as having no significant effect on Caco-2 cell growth or bacterial survival were used for Caco-2 cell virulence assays, and are as follows: 144092 (6.25 µM), 144143 (6.25 µM), 19615 (6.25 µM), 153578 (6.25 µM), and 24904 (25 µM). As shown in Appendix Table III-1 and Appendix Figure III-1, the highest concentrations of

compounds identified as having no observable effect on HeLa cell, L2 cell, or bacterial survival were used for HeLa and L2 cell virulence assays, and are as follows: 144092 (6.25 μ M), 144143 (6.25 μ M), 19615 (6.25 μ M), 153578 (12.5 μ M), and 24904 (50 μ M).

Table III-1. MTT Cell Viability Assay Results for Caco-2 Cell Growth in Presence of Compounds.

Concentration (μ M)	153578 %Growth Inhibition	19615 %Growth Inhibition	144092 %Growth Inhibition	144143 %Growth Inhibition	24904 %Growth Inhibition
50.0	18% \pm 4%	65% \pm 6%	50% \pm 1%	45% \pm 1%	14% \pm 2%
25.0	15% \pm 3%	16% \pm 8%	45% \pm 1%	33% \pm 4%	8% \pm 1%
12.5	14% \pm 0%	20% \pm 8%	37% \pm 1%	0% \pm 3%	2% \pm 1%
6.25	10% \pm 9%	4% \pm 5%	8% \pm 4%	3% \pm 1%	-6% \pm 11%
3.13	-1% \pm 3%	1% \pm 3%	5% \pm 0%	1% \pm 2%	0% \pm 7%
1.56	0% \pm 4%	4% \pm 2%	-8% \pm 4%	2% \pm 0%	1% \pm 10%
0.78	0% \pm 10%	-6% \pm 8%	-5% \pm 7%	-5% \pm 9%	6% \pm 4%

Invasion assays

Invasion assays were performed to identify the compounds' effects on bacterial invasion of HeLa cells, by having compounds present during bacterial subculture and invasion period, or invasion period alone. As Figure III-1A shows, when present during bacterial subculture and invasion period, 144092 was the only compound that lowered invasion efficiency compared to wild-type *Shigella flexneri* 2457T (0.14% and 0.30% respectively); however, it displayed no effect on invasion when present during invasion period alone (0.30%). The remainder of the compounds, displayed hyper-invasion when compared to wild-type invasive bacteria (compounds 144143 and 19615, 2.1-fold increase; compound 153578, 9.6-fold increase; compound 24904, 9.8-fold increase). As a control, we tested the virulence plasmid-cured derivative of *Shigella flexneri* 2457T, BS103, in the invasion assay in the presence of compounds. The results show no BS103 surviving gentamicin treatment (data not shown).

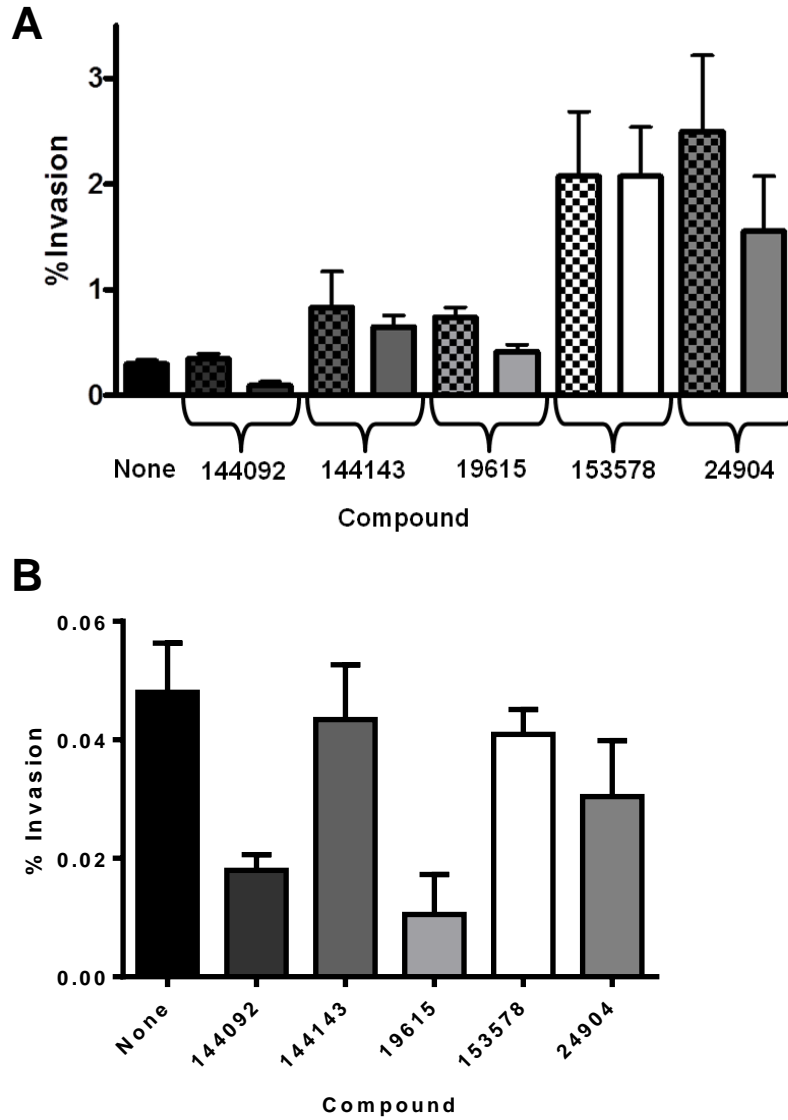


Figure III-1: *S. flexneri* 2457T Invasion Assay Results. A) Graph depicts %invasion of *S. flexneri* 2457T into monolayers of HeLa cells in the presence of compounds. Each compound was dosed at the highest concentration that had no effect on cell or bacterial survival as shown in Appendix Figure 1 and Appendix Table 1. Compounds were given during the invasion period only (checkered bar graphs) and during the exponential phase of bacterial growth and remained present during the invasion period (solid bar graphs). All experiments were conducted in duplicate. **B)** Graph depicts %invasion of *S. flexneri* 2457T into monolayers of Caco-2 cells in the presence of compounds. Each compound was dosed at the highest concentration that had no effect on cell or bacterial survival as shown in Table III-1 and Appendix Figure 1. Compounds were given during the exponential phase of bacterial growth and remained present during the invasion period (solid bar graphs). All experiments were conducted in duplicate.

Invasion assays were also performed to identify the compounds' effects on bacterial invasion of Caco-2 cells. Compounds were dosed during bacterial subculture and the invasion period. As shown in Figure III-1B, compounds 19615 and 144092 significantly lowered invasion efficiency (0.011% and 0.018%) when compared to wild-type *Shigella flexneri* 2457T (0.048%), while the other compounds appeared to have little to no effect on invasion efficiency. As a control, we tested the virulence plasmid-cured derivative of *Shigella flexneri* 2457T, BS103, in the invasion assay. The results show a very low amount BS103 surviving gentamicin treatment (0.0001% invasion efficiency).

Efficiency of Plaque Formation

Plaque assays were performed to identify the potential effects of the compounds on bacterial cell-to-cell spread using L2 cells, with compound present only in the agarose overlay. Overall, three compounds caused significant reductions in the efficiency of plaque formation for wild-type *Shigella flexneri* 2457T relative to the no compound control (144092: 77%, 19615: 81%, and 153578: 76% reductions), while 144143 had no effect on the efficiency of plaque formation, see Figure III-2A (Monolayers with 50 μ M 24904 did not survive the duration of the assay). The average plaque size for 144092 was reduced to 81% of wild-type plaque sizes (0.87 mm versus 1.08mm), while plaque sizes were unaffected by the other compounds, see Figure III-3.

Plaque assays were also performed to identify the potential effects of the compounds on bacterial cell-to-cell spread using Caco-2 cells, with compound present only in the agarose overlay. As shown in Figure III-2B, three compounds caused reductions in the efficiency of plaque formation for wild-type *Shigella flexneri* 2457T

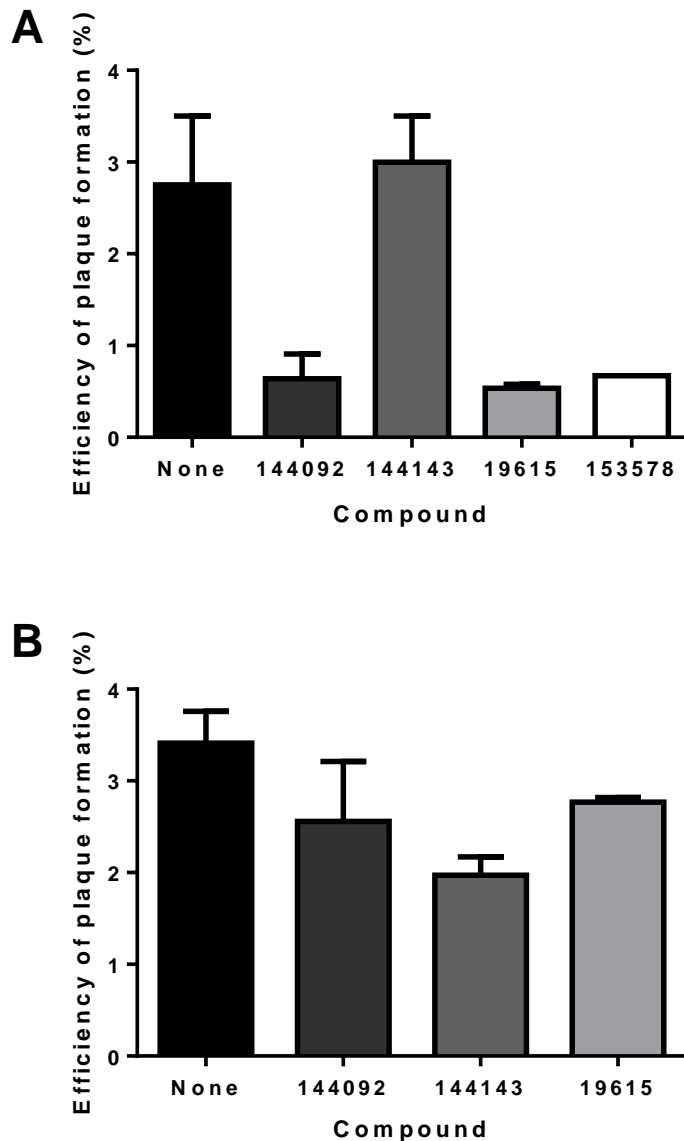


Figure III-2: *S. flexneri* 2457T Plaque Formation Assay Results. **A)** Graph depicts %efficiency of plaque formation of *S. flexneri* 2457T in the presence of compounds after initial infection into monolayers of L2 cells as described in Materials and Methods. Each compound was dosed at the highest concentration that had no effect on cell or bacterial survival as identified in Appendix Figure 1 and Appendix Table 1. Compound 24904 is not depicted on graph due to its toxicity towards the L2 monolayers over the duration of the assay. **B)** Graph depicts %efficiency of plaque formation of *S. flexneri* 2457T in the presence of compounds after initial infection into monolayers of Caco-2 cells as described in Materials and Methods. Each compound was dosed at the highest concentration that had no effect on cell or bacterial survival as shown in Table III-1 and Appendix Figure 1. Compounds 153578 and 24904 are not depicted on graph due to toxicity towards the Caco-2 monolayers over the duration of the assay. All experiments were conducted in duplicate.

relative to the no compound control (19615: 19%, 144092: 25%, 144143: 42% reductions), while 153578 and 24904 were toxic to the monolayers over the three day incubation period.

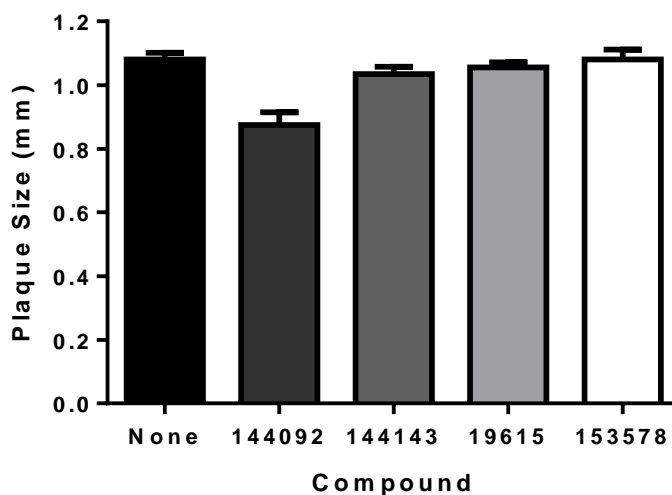


Figure III-3: Size of Plaques from Plaque Formation Assay with *S. flexneri* 2457T. The graph displays average plaque size of *S. flexneri* 2457T in the presence of compounds in L2 cells and visualized by Neutral Red staining as described in Materials and Methods. The concentration of each compound used in the assay was the highest concentration that demonstrated no effect on host or bacterial survival as identified in Appendix Figure 1 and Appendix Table 1. No compound was used as a control for wild-type *S. flexneri* 2457T plaque sizes.

Discussion

Recent outbreaks of multi-drug resistance strains of *Shigella* in developed nations have made evident the need for new, effective treatments for shigellosis.^{20, 21} Many studies have suggested that the VirF-activated, *Shigella* pathogenesis cascade could be a novel target for a small molecule anti-virulence therapy.¹⁻¹¹ A successful anti-virulence therapy targeting this pathway must be able to attenuate the virulence of *Shigella*, while not affecting bacterial viability or host cell health. To determine the

potential our previously identified (See Chapter II) small molecule inhibitors of VirF had as anti-virulence agents, we screened the compounds in a series of assays modeling the *S. flexneri* infection process. Before conducting these screens, we evaluated the cytotoxicity of each compound. Initial cytotoxicity determinations were performed using phenotypic screens (as shown in Appendix Table III-1), while later cytotoxicity determinations were done using an MTT assay (as shown in Table III-1). This change in methodology was due to a change in testing location (Uniformed Services University of the Health Sciences versus the University of Michigan). The maximum non-cytotoxic concentrations identified from either study were then screened against two strains of *S. flexneri*, BS103 and 2457T. As shown in Appendix Figure III-1, none of the compounds had any effect on bacterial growth at the concentrations tested.

Compounds were next evaluated in HeLa cell monolayer invasion and L2 cell monolayer plaque assays as models for the infection process. As shown in Figure III-1A, one compound, 144092, was able to reduce the %invasion relative to the no compound control when the compound was administered during the exponential growth phase of the bacterial subculture in addition to being present through the invasion period. The compound had no effect on %invasion when it was given at the time of invasion only. The lack of effect in the latter case is most likely due to VirF activating virulence genes during exponential growth in the absence of the compound. Those virulence proteins would then be already present when the compound was added during invasion, and the bacteria would still be able to invade the host cells. The ineffectiveness of the other four compounds was not unexpected because all of the compounds were administered at concentrations below their IC₅₀ values due to toxicity

towards the cell monolayers at higher concentrations. However, it was unexpected that the other four compounds displayed “hyper-invasion” relative to no compound controls. Control assays were performed to verify that compounds were not artificially raising %invasion by protecting the bacteria from gentamicin. It is possible that the compounds could be altering the HeLa cell monolayer in a non-observable manner making it more prone to bacterial infection. Further studies will need to be performed to determine the cause of the “hyper-invasion”.

Three of the compounds 144092, 19615, and 153578 lowered the efficiency of plaque formation by *S. flexneri* 2457T, indicating that the compounds attenuated the cell-to-cell spread of the bacteria (see Figure III-2A). This result was surprising since only compound 144092 lowered the invasion efficiency of *S. flexneri* 2457T during the invasion assays. However, only 144092 had any effect, albeit quite modest, on plaque size. Plaque size is dependent upon a number of factors including cell-to-cell spread and bacterial growth. Also, the plaque size is assessed after three days. The stability of the compounds over that period is not known, so it is hard to interpret effects on plaque size without further studies.

The hyperinvasive phenotypes seen in the HeLa cell invasion assay and the contradictory results obtained in the L2 plaque formation assay raised questions about the appropriateness of the cell lines used in these studies. The initial choice of HeLa and L2 cells were made based on the standard protocols used by the Maurelli lab. However, the Maurelli lab does not commonly use these assays to test the efficacy of small molecules and were also quite surprised by the initial results. The use of HeLa cells as a model for human cell biology has recently come into question due to large

genomic abnormalities discovered upon sequencing the full HeLa genome.^{22, 23} Also, the fact that *Shigella* spp. are known to infect only human or primate colonic cells *in vivo*,¹²⁻¹⁴ led to furthering questioning of the use of HeLa (a cervical cancer cell line) and L2 (a rat lung cell line) cells. A more appropriate cell line to use for modeling the *Shigella* spp. infection process would seem to be Caco-2. Caco-2 cells are derived from human colonic epithelial tissue and, unlike HeLa or L2 cells, are polarized in culture. To more accurately assess the anti-virulence properties of our small molecule VirF inhibitors, the invasion and plaque assays were repeated with Caco-2 cell monolayers. The use of the same cell line in both assays also allowed for more accurate comparisons to be made between the two studies.

As shown in Figure III-1B, two compounds, 144092 and 19615, were able to significantly reduce the %invasion relative to the no compound control, while the remaining compounds produced little to no effect. Interestingly, none of the compounds produced the hyperinvasive phenotype as seen in the HeLa cell invasion assay. It may be possible that the compounds do in fact make the HeLa cells more prone to bacterial infection, but further studies must be done to confirm this. Nevertheless, the Caco-2 invasion models are more physiologically appropriate and will continue to be used in future studies. Plaque formation assays with the Caco-2 cells also produced promising results. As shown in Figure III-2B, three compounds, 144092, 144143, and 19615, were able to modestly reduce the efficiency of plaque formation, while the remaining compounds were toxic to the Caco-2 cells over the three day exposure period. Unfortunately, plaque size could not be measured in the Caco-2 plaque assay due to a lack of equipment caused by a change in testing location. Unlike the previous HeLa/L2

cell studies, similar compounds were active in both assays. This suggests that small molecule inhibition of VirF transcriptional activation attenuates both the initial invasion and the cell-to-cell spread of *S. flexneri*, which is in agreement with previous gene disruption studies.¹⁻⁵ We believe that the lack of “hyper-invasion”, the consistency between assays (invasion and plaque), and the physiological appropriateness of the model make the results obtained in the Caco-2 studies more accurate and relevant.

It is worth noting that these compounds, directly from our HTS, have not yet been optimized in any way and were tested well below their IC₅₀ values for VirF inhibition (due to cytotoxicity). The fact that the compounds produced even modest attenuation of the infection process at the concentrations tested is encouraging. For example, compound 144092 had a significant effect on invasion at a concentration of about 25% of its IC₅₀ in the VirF screen. Our VirF screening assays involve overnight incubations whereas the invasion assays are only incubated for a total of 4-6 hours. The longer time frame of the screening assays may allow small amounts of active VirF to generate significant quantities of β-galactosidase, resulting in a higher IC₅₀. *In vivo* there is an amplification factor as VirF activates VirB, which in turn activates the invasion proteins. Inhibition of VirF could result in a much greater reduction in the invasion proteins due to this amplification, which is not present in our screening plasmid. The *Shigella* protein H-NS binds to both the *virB* and *icsA* promoter regions and represses their transcription. It may be that our artificial screening plasmid may be less susceptible to H-NS repression than the natural, 230 kb virulence plasmid making it harder to block VirF activation of gene expression. Finally, it is possible, but unlikely, that the compounds might accumulate in the eukaryotic cells to a higher concentration than in the media.

Compounds 19615 and 144092 are the most promising candidates for hit-to-lead development as they were able to reduce initial invasion efficiency (77% and 63% reductions, respectively) and plaque efficiency (19% and 25% reductions, respectively) in the Caco-2 studies at concentrations (6.25 μ M) that had no effect on bacterial or host cell viability. Furthermore, 144092 and 144143 share the same pyrimidine core. The differential activity of these analogs provides key insights into which regions of compound 144092 should be focused upon for analog development making it even more attractive. It is reasonable to expect that with further optimization of the chemical structures, an increase in efficacy in both the invasion and plaque efficiency assays as well as a decrease in cytotoxicity will be achieved.

Using our previously identified inhibitors of VirF-activated transcription (see Chapter II), we were able to attenuate the virulence of *S. flexneri* in models of bacterial invasion and cell-to-cell spread; thereby, validating VirF as an anti-virulence target for a small molecule therapeutic. At the time this work was completed, another study was published that described the testing of a small molecule inhibitor of AraC family transcriptional activators against VirF. Their results also confirmed that inhibition of VirF transcriptional activation results in the attenuation of *S. flexneri* virulence. Interestingly, they also showed that their small molecule inhibitor was active against a variety of AraC family regulators. In the future, we plan on testing our compounds against other AraC family members to determine their cross family activity. It is possible that our compounds could reduce the virulence of other pathogens.

Notes to Chapter III

Parts of this chapter have been published in Emanuele, et al. *Journal of Antibiotics* **2014**, 67, 379-386. ²⁴ Work described here was done in collaboration with the laboratory of Prof. Anthony Maurelli (Uniformed Services University of the Health Sciences, Bethesda, MD). I would specifically like to acknowledge Nancy Adams from the Maurelli lab for helping conduct the HeLa and L2 cell assays and for training me. Lastly, I would like to thank Dr. Arya Vijayalekshmi (Garner lab, University of Michigan) for help with setting up our tissue culture laboratory and Yasuhiro Tsume (Amidon lab, University of Michigan) for providing the Caco-2 cells used in this study.

References

1. Qi, M. S.; Yoshikura, H.; Watanabe, H. Virulence phenotypes of *Shigella flexneri* 2a virulent mutant 24570 can be complemented by the plasmid-coded positive regulator *virF* gene. *FEMS Microbiology Letters* **1992**, 92, 217-221.
2. Adler, B.; Sasakawa, C.; Tobe, T.; Makino, S.; Komatsu, K.; Yoshikawa, M. A dual transcriptional activation system for the 230 kb plasmid genes coding for virulence-associated antigens of *Shigella flexneri*. *Molecular Microbiology* **1989**, 3, 627-35.
3. Colonna, B.; Casalino, M.; Fradiani, P. A.; Zagaglia, C.; Naitza, S.; Leoni, L.; Prosseda, G.; Coppo, A.; Ghelardini, P.; Nicoletti, M. H-NS regulation of virulence gene expression in enteroinvasive *Escherichia coli* harboring the virulence plasmid integrated into the host chromosome. *Journal of Bacteriology* **1995**, 177, 4703-12.
4. Sansonetti, P. J.; Arondel, J.; Fontaine, A.; d'Hauteville, H.; Bernardini, M. L. OmpB (osmo-regulation) and icsA (cell-to-cell spread) mutants of *Shigella flexneri*: vaccine candidates and probes to study the pathogenesis of shigellosis. *Vaccine* **1991**, 9, 416-22.

5. Makino, S.; Sasakawa, C.; Kamata, K.; Kurata, T.; Yoshikawa, M. A genetic determinant required for continuous reinfection of adjacent cells on large plasmid in *S. flexneri* 2a. *Cell* **1986**, 46, 551-5.
6. Barnoy, S.; Jeong, K. I.; Helm, R. F.; Suvarnapunya, A. E.; Ranallo, R. T.; Tzipori, S.; Venkatesan, M. M. Characterization of WRSs2 and WRSs3, new second-generation virG(icsA)-based *Shigella sonnei* vaccine candidates with the potential for reduced reactogenicity. *Vaccine* **2010**, 28, 1642-1654.
7. Barnoy, S.; Baqar, S.; Kaminski, R. W.; Collins, T.; Nemelka, K.; Hale, T. L.; Ranallo, R. T.; Venkatesan, M. M. *Shigella sonnei* vaccine candidates WRSs2 and WRSs3 are as immunogenic as WRSS1, a clinically tested vaccine candidate, in a primate model of infection. *Vaccine* **2011**, 29, 6371-6378.
8. Ranallo, R. T.; Thakkar, S.; Chen, Q.; Venkatesan, M. M. Immunogenicity and characterization of WRSF2G11: A second generation live attenuated *Shigella flexneri* 2a vaccine strain. *Vaccine* **2007**, 25, 2269-2278.
9. Yoshikawa, M.; Sasakawa, C.; Okada, N.; Takasaka, M.; Nakayama, M.; Yoshikawa, Y.; Kohno, A.; Danbara, H.; Nariuchi, H.; Shimada, H.; Toriumi, M. Construction and evaluation of a virG thyA double mutant of *Shigella flexneri* 2a as a candidate live-attenuated oral vaccine. *Vaccine* **1995**, 13, 1436-1440.
10. Hung, D. T.; Shakhnovich, E. A.; Pierson, E.; Mekalanos, J. J. Small-Molecule Inhibitor of *Vibrio cholerae* Virulence and Intestinal Colonization. *Science* **2005**, 310, 670-674.
11. Garrity-Ryan, L. K.; Kim, O. K.; Balada-Llasat, J. M.; Bartlett, V. J.; Verma, A. K.; Fisher, M. L.; Castillo, C.; Songsunghong, W.; Tanaka, S. K.; Levy, S. B.; Mecsas, J.; Alekshun, M. N. Small Molecule Inhibitors of LcrF, a *Yersinia pseudotuberculosis* Transcription Factor, Attenuate Virulence and Limit Infection in a Murine Pneumonia Model. *Infection and Immunity* **2010**, 78, 4683-4690.
12. Philpott, D. J.; Edgeworth, J. D.; Sansonetti, P. J. The pathogenesis of *Shigella flexneri* infection: lessons from in vitro and in vivo studies. *Philosophical Transactions of the Royal Society of London B: Biological Sciences* **2000**, 355, 575-586.
13. Lee, J.-I.; Kim, S.-J.; Park, C.-G. *Shigella flexneri* infection in a newly acquired rhesus macaque (*Macaca mulatta*). *Laboratory Animal Research* **2011**, 27, 343-346.

14. Cooper, J. E.; Needham, J. R. An Outbreak of Shigellosis in Laboratory Marmosets and Tamarins (Family: Callithricidae). *The Journal of Hygiene* **1976**, 76, 415-424.
15. Formal, S. B.; Dammin, G. J.; Labrec, E. H.; Schneider, H. Experimental Shigella infections: characteristic of a fatal infection produced in guinea pigs. *Journal of Bacteriology* **1958**, 75, 604-610.
16. Maurelli, A. T.; Blackmon, B.; Curtiss III, R. Loss of pigmentation in *Shigella flexneri* 2a is correlated with loss of virulence and virulence associated plasmid. *Infection and Immunity* **1984**, 43, 397-401.
17. Hurt, J. K.; McQuade, T. J.; Emanuele, A.; Larsen, M. J.; Garcia, G. A. High-Throughput Screening of the Virulence Regulator VirF: A Novel Antibacterial Target for Shigellosis. *Journal of Biomolecular Screening* **2010**, 15, 379-387.
18. Hale, T. L.; Formal, S. B. Protein Synthesis in HeLa or Henle 407 cells infected with *Shigella dysenteriae* 1, *Shigella flexneri* 2a, or *Salmonella typhimurium* W118. *Infect Immun* **1981**, 32, 137-144.
19. Oaks, E. V.; Hale, T. L.; Formal, S. B. Plaque formation by virulent *Shigella flexneri*. *Infect Immun* **1985**, 48, 124-129.
20. Replogle, M. L.; Fleming, D. W.; Cieslak, P. R. Emergence of antimicrobial-resistant shigellosis in Oregon. *Clinical Infectious Diseases*. **2000**, 30, 515-9.
21. CDC. Importation and Domestic Transmission of *Shigella sonnei* Resistant to Ciprofloxacin - United States. *MMWR. Morbidity and Mortality Weekly Report* **2015**, 64.
22. Callaway, E. Most popular human cell line in science gets sequenced. *Nature News* **2013**.
23. Landry, J. J. M.; Pyl, P. T.; Rausch, T.; Zichner, T.; Tekkedil, M. M.; Stütz, A. M.; Jauch, A.; Aiyar, R. S.; Pau, G.; Delhomme, N.; Gagneur, J.; Korbel, J. O.; Huber, W.; Steinmetz, L. M. The Genomic and Transcriptomic Landscape of a HeLa Cell Line. *G3: Genes/Genomes/Genetics* **2013**, 3, 1213-1224.

24. Emanuele, A. A.; Adams, N. E.; Chen, Y.-C.; Maurelli, A. T.; Garcia, G. A. Potential novel antibiotics from HTS targeting the virulence-regulating transcription factor, VirF, from *Shigella flexneri*. *Journal of Antibiotics* **2014**, *67*, 379-386.

Appendix

Appendix Table III-1. Cytotoxicity Estimates of Compounds in HeLa and L2 Cells.

144092 (IC ₅₀ 23μM)			144143 (IC ₅₀ 23μM)		
Conc	Day 1	Day 3	Conc	Day 1	Day 3
25μM	Semi-confluent Membrane blebs L2's were also shriveled	Semi-confluent Membrane blebs Shriveled Hela's were also granular	25μM	Semi-confluent Membrane blebs Shriveled	Shriveled Only cell debris remains
12.5μM	Semi-confluent Membrane blebs L2's were also shriveled	Semi-confluent Membrane blebs Shriveled Hela's were also granular	12.5μM	Only cell debris remains	Shriveled Only cell debris remains
6.25μM	Hela's – Confluent L2's – Membrane blebs, shriveled	Semi-confluent Membrane blebs Shriveled Hela's were also granular	6.25μM	Hela's – Confluent L2's – Semi-confluent, membrane blebs, shriveled	Hela's – Over-confluent L2's – Semi-confluent, membrane blebs, shriveled, granular
3.1μM	Confluent	Over-confluent	3.1μM	Hela's – Confluent L2's – Semi-confluent, membrane blebs	Hela's – Over-confluent L2's – Semi-confluent, membrane blebs, shriveled, granular
1.5μM	Confluent	Over-confluent	1.5μM	Confluent	Over-confluent
0.75μM	Confluent	Over-confluent	0.75μM	Confluent	Over-confluent
0.38μM	Confluent	Over-confluent	0.38μM	Confluent	Over-confluent
0.19μM	Confluent	Over-confluent	0.19μM	Confluent	Over-confluent

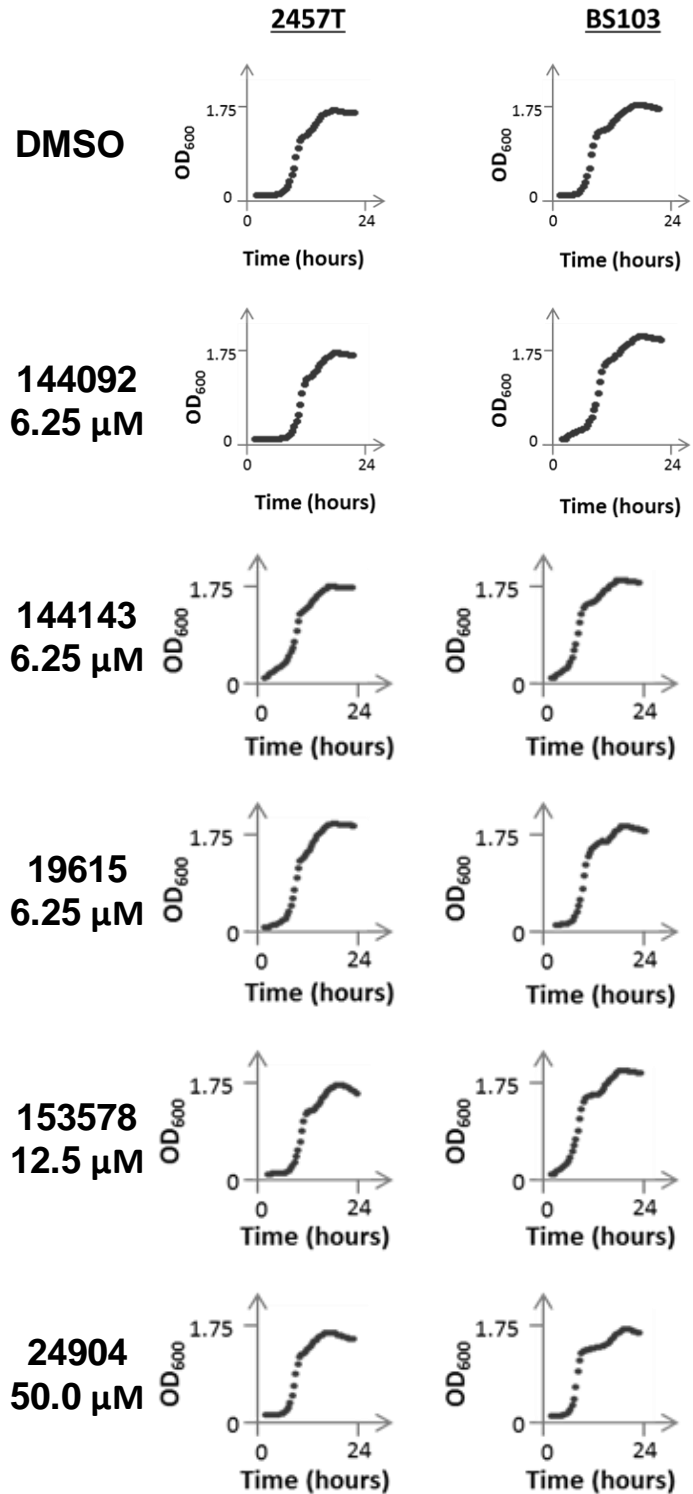
24904 (IC ₅₀ 66μM)			153578 (IC ₅₀ 37μM)		
Conc	Day 1	Day 3	Conc	Day 1	Day 3
50μM	Confluent	Confluent	50μM	Semi-confluent Membrane blebs Shriveled	Hela's – Only cell debris remains L2's – confluent
25μM	Confluent	Confluent	25μM	Semi-confluent Membrane blebs Shriveled	Hela's – Only cell debris remains L2's – confluent
12.5μM	Confluent	Over-confluent	12.5μM	Confluent	Hela's – Only cell debris remains L2's – confluent
6.25μM	Confluent	Over-confluent	6.25μM	Confluent	Hela's – Only cell debris remains L2's – confluent
3.1μM	Confluent	Over-confluent	3.1μM	Confluent	Over-confluent
1.5μM	Confluent	Over-confluent	1.5μM	Confluent	Over-confluent
0.75μM	Confluent	Over-confluent	0.75μM	Confluent	Over-confluent
0.38μM	Confluent	Over-confluent	0.38μM	Confluent	Over-confluent
0.19μM	Confluent	Over-confluent	0.19μM	Confluent	Over-confluent

19615 (IC ₅₀ 14μM)		
Conc	Day 1	Day 3
25μM	HeLa's – Confluent, granular L2's – Semi-confluent	Only cell debris remains
12.5μM	HeLa's – Confluent, granular L2's – Semi-confluent	HeLa's – Over-confluent L2's – Confluent, granular
6.25μM	Confluent	Over-confluent
3.1μM	Confluent	Over-confluent
1.5μM	Confluent	Over-confluent
0.75μM	Confluent	Over-confluent
0.38μM	Confluent	Over-confluent
0.19μM	Confluent	Over-confluent

HeLa and L2 cell toxicities were assessed by observing phenotype for 3 days. Physical signs of cell health were monitored since an OD reading could not be done with adherent cells. Phenotype descriptions are as follows: Membrane blebs: vacuole looking protrusions exuding from plasma membrane; Granular: dark punctate dots in cytoplasm; Shriveled: cells were condensed and smaller; Cell debris: no intact cells, only remnants of cells left behind; Confluent: >95% confluent, no obvious signs of cytotoxicity; Semi-confluent: ~70% confluent, no obvious signs of cytotoxicity; Over-confluent: cells growing on top of the monolayer, no obvious signs of cytotoxicity.

Appendix Figure III-1: Bacterial Toxicity of Compounds.

Dilutions of inhibitors were added to bacterial cultures and OD600 was monitored for 24 hours and plotted over time. Compound concentrations were chosen as the highest concentration that had no observable effect on host cells, as a result, the highest concentrations of compounds identified as having no observable effect on host cell or bacterial survival were: 144092 (6.25 μ M), 144143 (6.25 μ M), 19615 (6.25 μ M), 153578 (12.5 μ M), and 24904 (50 μ M).



CHAPTER IV

The Expression, Purification, and Characterization of VirF

“@#\$**^-#*~** AraC protein!”
-Dr. Robert Schleif

The quote above is taken from Dr. Robert Schleif's bio-essay on working with the AraC protein over the course of his career.¹ Dr. Schleif is the world's leading expert on AraC, as he has been credited with developing the first purification procedure for AraC,² identifying the DNA-looping mechanism used by AraC to regulate transcription,³ and solving the first crystal and solution state structures of AraC.^{4,5} Many other researchers who work with AraC family transcriptional regulators share Dr. Schleif's feelings (including this one), as AraC proteins are notably difficult to isolate. AraC proteins tend to be insoluble outside the cell, aggregate easily, and express poorly in recombinant systems.¹ VirF, the main transcriptional activator of the *Shigella* spp. pathogenesis cascade, is no different.

The first promising attempt to characterize VirF *in vitro* was done by Tobe *et al.*⁶ To purify VirF, a *malE* gene fusion tag (encodes for the *E. coli* maltose binding protein) was used to improve the solubility of the protein. Once purified, the MalE tag could not be cleaved from VirF without VirF precipitating out of solution. However, the MalE-VirF fusion could still bind to the *virB* promoter and activate transcription.⁶⁻⁹ Use of maltose-binding protein fusion tags to improve solubility is now a common method used by researchers to isolate AraC family transcriptional regulators.¹⁰⁻¹⁴ In most cases, the

fusion tag is added to the amino-terminus of the AraC family transcription factor and cannot be removed without deleterious effects. Surprisingly, the AraC family transcription factors remain active with the 43 kDa fusion tag.

Isolation of wildtype VirF has proved much more challenging. In fact, it has not been accomplished to this date. Dr. Julie Hurt, a former Garcia lab member, devoted a large portion of her dissertation work to isolating wildtype VirF. She tried many things including multiple different expression vectors, varying growth conditions, changing buffer systems, denaturing/refolding VirF, and co-expression with chaperones; yet, nothing proved successful.¹⁵ Although Dr. Hurt was not able to isolate wildtype VirF, she was able to optimize the purification procedure proposed by Tobe *et al.*⁶ and obtain MalE-VirF fusion protein that was ~70% pure.¹⁵ However, her yield was too low (≤ 0.5 mg of protein per liter of culture) to practically support the optimization and development of *in vitro* assays to characterize VirF.

In this chapter, we describe our efforts to develop an efficient and high-yielding purification procedure for the isolation of VirF. After initial attempts to optimize previous protocols proved unsuccessful, we engineered a novel *Shigella*-based homologous expression and purification system for MalE-VirF isolation. This system greatly improved the expression of MalE-VirF which highlights the importance of expressing VirF in its native environment. Once we isolated pure MalE-VirF, we developed and optimized two different *in vitro* assays which monitored VirF binding to the *virB* promoter (*pvirB*) and report the first dissociation constant (to our knowledge) for VirF binding to the *pvirB* ($2.8 \pm 1.0 \mu\text{M}$).

Materials and Methods

Reagents

All reagents and equipment were purchased from Fisher Scientific (Hampton, NH), unless otherwise specified.

Bacterial Strains

The following bacterial strains were used in this study: *Escherichia coli* BL21(DE3) (obtained from Novagen, Temcula, CA), *E. coli* KS1000 (obtained from New England Biolabs, Ipswich, MA), and a virulence plasmid-cured derivative of wildtype *S. flexneri*, BS103 (obtained from the laboratory of Dr. Anthony Maurelli, Uniformed Services University of the Health Sciences, Bethesda, MD).¹⁶

Plasmids

The sequences of all the following plasmids were confirmed by DNA sequencing (DNA Sequencing Core Facility, University of Michigan).

pMALvirF

pMALvirF encodes for a maltose binding protein – VirF fusion protein, MalE-VirF. pMALvirF was constructed by cloning the *virF* gene into the vector, pMAL-c2x (New England Biolabs), as previously described.^{6, 9, 15}

pET19b-VirF(154-263)

pET19b-VirF(154-263) encodes for the C-terminal, DNA-binding domain of VirF with a fused N-terminal 10X His-tag. pET19b-VirF(154-263) was a gift from Dr. Tappan Biswas (Tsodikov lab, University of Michigan, Ann Arbor, MI) and was constructed as previously described.¹⁵

pBAD202-MALvirF

pBAD202-MALvirF encodes for a maltose binding protein – VirF fusion, and was constructed using the pBAD directional TOPO® expression kit (Invitrogen, Carlsbad, CA). Briefly, the *malE-virF* fusion gene was amplified from pMALvirF via polymerase chain reaction to include a 5'-*NcoI* restriction site before the start codon of *malE-virF*. The amplified gene was then subcloned into pBAD202 via a directional TOPO® cloning reaction. The resulting vector was then subjected to *NcoI* restriction digestion (5 units, 1 hour, 37°C) to remove the N-terminal His-Patch thioredoxin leader sequence from pBAD202, and form pBAD202-MALvirF.

SDS-PAGE Analysis

Initial experiments were performed using the PhastSystem™ electrophoresis unit (GE Healthcare, United Kingdom). Samples were diluted 1:1 with SDS-PAGE buffer (60 mM Tris-HCl, 2% SDS, 10% Glycerol, 5% β-mercaptoethanol, 0.01% bromophenol blue, pH 6.8) and were boiled for 5 minutes along with the low molecular weight standard (LMW, GE Healthcare, contains 6 protein markers: 97 kDa, 66 kDa, 45, kDa, 30 kDa, 20.1 kDa, and 14.4 kDa). The samples and LMW were then loaded onto a pre-made denaturing 8-25% gradient polyacrylamide PhastGel™ (GE Healthcare) with SDS buffer strips (GE Healthcare). Samples were run under denaturing conditions and visualized by Coomassie Blue staining according to the PhastSystem™ protocol.

Later experiments were performed using the Owl™ dual-gel vertical electrophoresis unit. Samples and LMW were prepared as stated above but were loaded onto a denaturing polyacrylamide gel (5% stacking gel, 10% separating gel) and were ran in TGS running buffer (25 mM Tris, 192 mM glycine, 0.1% SDS) for 20

minutes at 100V followed by an additional 60 minutes at 150V. Gels were visualized via staining with Coomassie Blue solution (60% water, 30% methanol, 10% acetic acid, 0.1% Coomassie Brilliant Blue) for 30 minutes, followed by destaining for 2 hours in destain solution (60% water, 30% methanol, 10% acetic acid).

Protein Quantification

All purified protein samples were quantified utilizing the Bradford protein assay per vendor protocol (BioRad, Hercules, CA).

Expression and Purification of MalE-VirF from E. coli BL21(DE3)

The following protocol was based on the work done by Dr. Julie Hurt.¹⁵ First, pMALvirF was transformed into chemically competent *E. coli* BL21(DE3) cells. Starter cultures (5 mL) of pMALvirF BL21(DE3) were grown overnight in 2xTY broth (16 g bacto-tryptone, 10 g yeast extract, 5 g NaCl per liter of water) supplemented with carbenicillin (100 µg/mL) at 37°C with shaking. The following day the starter culture was used to inoculate 500 mL of 2xTY broth supplemented with carbenicillin. The culture was incubated at 37°C with shaking until an OD₆₀₀ of 0.6 was reached, upon which MalE-VirF expression was induced with 1 mM IPTG. Following an additional 4 hour incubation at 37°C with shaking, the cells were harvested via centrifugation (6000 X g, 15 min, 4°C) and stored overnight at -20°C. The next day the cells were resuspended in 10 mL of VirF storage buffer (20 mM Tris-HCl, 0.2 M NaCl, 1 mM EDTA, 10 mM β-mercaptoethanol, pH 7.5) supplemented with phenylmethylsulfonyl fluoride (0.1 mM) and 10 µL of lysonase bioprocessing reagent (EMD Millipore, Billerica, MA). Cells were slowly stirred for 10 minutes at room temperature and were immediately placed on ice and kept on ice or at 4°C for the remainder of the procedure.

Cells were lysed via sonication (6 cycles, 10 second pulse time, 2 minute intervals, max pulse setting) utilizing a ultrasonic XL2020 sonicator (Misonix, Farmingdale, NY). Following sonication, cellular debris was removed via centrifugation (20,000 X g, 4°C, 30 minutes). The resultant supernatant was brought up to 46 mL with VirF storage buffer and incubated with 4 mL of amylose resin (New England Biolabs) for 1 hour at 4°C with agitation. The mixture was applied to an empty 10 mL Econo-Pac® column (Bio-Rad), and washed via gravity flow with 12 column volumes of VirF storage buffer (48 mL). Male-VirF was eluted via gravity flow with 8 column volumes (1 mL fractions) of maltose elute buffer (VirF storage buffer + 10 mM Maltose). Fractions were analyzed by SDS-PAGE and samples containing Male-VirF were pooled and further purified by gel-filtration chromatography utilizing an S-200 column (GE Healthcare). Fractions were again analyzed by SDS-PAGE and samples containing Male-VirF were pooled and further purified by anion exchange chromatography utilizing a Mono-Q column (GE Healthcare). Lastly, fractions were analyzed by SDS-PAGE and pure samples containing only Male-VirF were pooled and concentrated utilizing Amicon Ultra-15 centrifugal units (EMD Millipore). Purified Male-VirF was stored in VirF storage buffer supplemented with 20% glycerol in liquid nitrogen.

Expression and Purification of VirF(154-263) from BL21(DE3)

The C-terminal domain of VirF, VirF(154-263), was expressed from pET19b-VirF(154-263) in *E. coli* BL21(DE3) cells. A 1L culture of 2xTY broth supplemented with carbenicillin (100 µg/mL) was inoculated with a pET19b-VirF(154-263) starter culture (1:100 inoculation). The culture was incubated at 37°C with shaking until an OD₆₀₀ of 0.6 was reached, upon which VirF(154-263) expression was induced with 0.5 mM IPTG.

Following induction, the culture was incubated overnight (~18 hours) at 19°C with shaking. The next day, the cells were harvested via centrifugation (6000 X g, 15 minutes, 4°C) and resuspended in 20 mL of Ni-resin bind buffer (50 mM NaH₂PO₄, 300 mM NaCl, 10 mM imidazole, 10 mM β-mercaptoethanol, pH 7.5). The cells were then lysed via sonication (7 cycles, 12 second pulse time, 2 minute intervals, setting 6). Following sonication, cellular debris was removed via centrifugation (25,500 X g, 4°C, 35 minutes). The resultant supernatant was incubated with 1 mL of Ni-NTA resin (Qiagen, Valencia, CA) for 1 hour at 4°C with agitation. Following the incubation, the mixture was applied to a 10 mL Econo-Pac ® column, and washed with 40 column volumes of Ni-resin wash buffer (50 mM NaH₂PO₄, 300 mM NaCl, 20 mM imidazole, 10 mM β-mercaptoethanol, pH 7.5). VirF(154-263) was eluted via gravity flow with 8 column volumes of Ni-resin elute buffer (50 mM NaH₂PO₄, 300 mM NaCl, 250 mM imidazole, 10 mM β-mercaptoethanol, pH 7.5). The eluate was concentrated to 3 mL utilizing Amicon Ultra-15 centrifugal units and applied to a Slide-A-Lyzer™ dialysis cassette (3.5K MWCO, 3 mL). The dialysis cassette was stirred for 1 hour at 4°C in 3 L of buffer A (10 mM NaH₂PO₄, 100 mM NaCl, 0.05 mM EDTA, pH 7.5), followed by an additional hour in a fresh 3 L of buffer A, and lastly overnight in 500 mL of buffer B (10 mM NaH₂PO₄, 100 mM NaCl, 0.05 mM EDTA, 10% glycerol, 0.01% Tween20, pH 7.5). Sample was removed from dialysis cassette and applied directly to a HiTrap Heparin HP 5 mL syringe column (GE Healthcare). The column was washed with 6 column volumes of heparin wash buffer (10 mM NaH₂PO₄, 100 mM NaCl, 0.05 mM EDTA, pH 7.5) and VirF(154-263) was eluted in 5 mL fractions of heparin wash buffer containing increasing concentrations of NaCl (10 fractions total that increased in NaCl

concentration 100 mM at a time from 100 mM to 1 M). Samples were analyzed by SDS-PAGE and fractions containing VirF(154-263) were pooled, concentrated, and stored in VirF(154-263) storage buffer (50 mM Tris, 100 mM NaCl, 0.05 mM EDTA, 20% glycerol, pH 7.5) in liquid nitrogen.

Expression and Purification of MalE-VirF from E. coli KS1000

Expression and purification experiments were conducted using pMALvirF and *E. coli* KS1000 as previously described.⁸

Expression and Purification of MalE-VirF from S. flexneri BS103

Experiments utilized pBAD202-MALvirF to express MalE-VirF in *S. flexneri* BS103 as follows. Using a MicroPulser electroporator (BioRad), pBAD202-MALvirF was transformed into electrocompetent *S. flexneri* BS103 cells. Starter cultures (10 mL) of pBAD202-MalVirF BS103 were grown overnight in 2xTY broth supplemented with kanamycin (50 µg/mL) at 37°C with shaking. The following day the starter culture was used to inoculate 1 L of 2xTY broth supplemented with kanamycin. The cells were grown to an OD₆₀₀ = 0.5. Expression of MalE-VirF was induced with the addition of arabinose (0.2% final concentration) and the culture continued to shake at 37°C for an additional 5 hours. Cells were then harvested via centrifugation (6000 X g, 4°C, 15 minutes) and were stored overnight at -20°C. The next day the cells were resuspended in 20 mL of amylose resin binding buffer (20 mM Tris-HCl, 500 mM NaCl, 1 mM EDTA, 1 mM, pH=7.4) supplemented with phenylmethylsulfonyl fluoride (0.1 mM) and 20 µL of lysonase bioprocessing reagent. Cells were slowly stirred for 10 minutes at room temperature and were then immediately placed on ice and kept on ice or at 4°C for the remainder of the procedure. Cells were lysed via sonication (8 cycles, 10 second pulse

time, 2 minute intervals, max pulse setting). Following sonication, cellular debris were removed via centrifugation (25,000 X g, 4°C, 40 minutes). The resultant supernatant was then applied to a 10 mL column of amylose resin (New England Biolabs) by gravity flow. Before addition of the supernatant the column was washed with 8 column volumes of amylose resin binding buffer. Following addition of the supernatant, the column was washed with 12 column volumes of amylose resin binding buffer. MalE-VirF was eluted from the column in 1 mL fractions of amylose resin elution buffer (amylose resin bind buffer plus 15% glycerol (wt/vol) and 10 mM maltose). Fractions were analyzed by SDS-PAGE. Fractions containing MalE-VirF were pooled, concentrated to approximately 6.5 mg/mL using Amicon Ultra-15 centrifugal units (EMD Millipore), and stored in liquid nitrogen for future use.

Analytical Gel Filtration

Analytical gel filtration chromatography was used to determine the oligomeric state of purified MalE-VirF. Briefly, MalE-VirF (0.75 mg/mL) was applied to a Superose 12 column, which was equilibrated with amylose resin binding buffer using an AKTA FPLC system (both from GE Healthcare Life Sciences, Piscataway, NJ). The sample was run through the column at a flow rate of 0.75 mL/min using amylose resin binding buffer. Eluted proteins were detected spectrophotometrically at 280 nm. The oligomeric state of MalE-VirF was determined by comparison to a previously generated 4-point molecular weight calibration curve specific to the Superose 12 column.

DNA Probe Hybridization

DNA probes were utilized in both EMSA and FP assays. The sequences of the oligonucleotides were based on previous studies^{8, 17} and are listed in Table IV-1. All

oligonucleotides were purchased from Invitrogen, except LUEGO which was purchased from Integrated DNA Technologies (Coralville, IA). Each oligonucleotide was brought up to a final concentration of 10 μ M in TE/NaCl buffer (10 mM Tris-HCl, 1 mM EDTA, 50 mM NaCl, pH = 8.0). For EMSA experiments, oligonucleotides were mixed at the following ratio: 10 volumes LUEGO, 5 volumes Top, 1 volume Bottom. For FP experiments, oligonucleotides were mixed 1:1 (Top:Bottom). Annealing was performed using a Mastercycler® Nexus thermocycler (Eppendorf, Hauppauge, NY) with the following program: 94°C for 2 minutes, cool down at 2°C/sec to 70°C and hold for 2 minutes, cool down at 0.1 °C/sec to 20°C and hold for 2 minutes.

Table IV-1. Oligonucleotides Used in EMSA and FP Experiments.

Name	Sequence (5'-3')	Modification	Length (bases)
<i>pvirB</i> Top EMSA	AGAATATTATTCTTTTATCCAAT AAAGATAAATTGCATCAATCCA GCTATTAATAATAGTA	None	60
<i>pvirB</i> Bottom EMSA	TACTATTTTAATAGCTGGATTGA TGCAATTTATCTTTATTGGATAA AAGAATAATATTCTCCAGACCA GGGCAC	None	74
<i>pScram</i> Top EMSA	TAAGTCCTAAATGGAAATTAAT TACGTAATTCACAAATATAGTAT GATCATTTATATCA	None	60
<i>pScram</i> Bottom EMSA	TGATATAAATGATCATACTATAT TTGTGAATTACGTAATTTAATTT CCATTTAGGACTTACCAGACCA GGGCAC	None	74
LUEGO	GTGCCCTGGTCTGG	5'-Cy5	14
<i>pvirB</i> Top FP	AGAATATTATTCTTTTATCCAAT AAAGATAAATTGCATCAATCCA GCTATTAATAATAGTA	5'-Fluorescein	60
<i>pvirB</i> Bottom FP	TACTATTTTAATAGCTGGATTGA TGCAATTTATCTTTATTGGATAA AAGAATAATATTCT	None	60
<i>pScram</i> Top FP	TAAGTCCTAAATGGAAATTAAT TACGTAATTCACAAATATAGTAT GATCATTTATATCA	5'-Fluorescein	60

<i>pScram</i> Bottom FP	TGATATAAATGATCATACTATAT TTGTGAATTACGTAATTTAATTT CCATTTAGGACTTA	None	60
-------------------------	--	------	----

DNA Binding via Electrophoretic Mobility Shift Assay (EMSA)

Reactions for the EMSAs were incubated in a 37°C water bath for 15 minutes. Reactions (15 µL total volume) were composed of 6 µL *pvirB* EMSA DNA probe (0.25 µM), 6 µL of either MalE-VirF (varying concentrations) or native gel loading buffer (Tris-HCl 0.3 M, 50% glycerol, 0.05% bromophenol blue, pH 7.0), 1.5 µL DMSO, 1 µL of salmon sperm DNA (0.7 mg/mL, Invitrogen), and 0.5 µL BSA (0.07 mg/mL). A 6% native polyacrylamide gel (29:1 acrylamide to bis-acrylamide ratio) was made with 0.25X TBE buffer (22 mM Tris Base, 22 mM boric acid, 0.5 mM EDTA, pH 9.5) for the EMSA. The gel was electrophoresed for 1 hour at 150 V in 0.25X TBE buffer at 4°C before samples were loaded. After the reaction solutions (12 µL) were loaded onto the gel, the gel was electrophoresed for an additional hour at 150 V and 4°C. The gel was then visualized using FluorChem M gel imager (Protein Simple, Santa Clara, CA) with a 607 nm excitation wavelength and a 710 nm emission filter.

DNA Binding via Fluorescence Polarization (FP)

The FP assays were conducted in duplicate in black, half-area, 96-well plates (Corning, Tewksbury, MA). First, 30 µL of 5'-Fluorescein-*pvirB* DNA probe working standard was added to appropriate wells of the microplate. The *pvirB* DNA working standard was in TE/NaCl buffer (see above) supplemented with BSA (0.07 mg/mL) and salmon sperm DNA (0.7 mg/mL). Next, 30 µL of varying concentrations of MalE-VirF in amylose resin elution buffer (see above) was added to appropriate wells of the microplate. The final concentration of *pvirB* DNA was either 50 nM (for test wells) or

none (for blank wells) and the final concentrations of MalE-VirF ranged from 45 μ M to 0.12 μ M (for test wells) or none (for control wells). For each concentration of MalE-VirF tested, a blank well was also set up that included all reagents except *pvirB* DNA. The microplate was then incubated for 20 minutes at 37°C and anisotropy was determined using a SpectraMax M5 plate reader (Molecular Devices, Sunnyvale, CA). Data was acquired using an excitation wavelength equal to 490 nm and an emission wavelength equal to 520 nm. To determine anisotropy the following equation was used:

$$\text{Anisotropy} = (F_{\parallel} - G \cdot F_{\perp}) / (F_{\parallel} + 2 \cdot G \cdot F_{\perp}) \cdot 1000$$

where: F_{\parallel} = fluorescence intensity parallel to excitation source after blanking, F_{\perp} = fluorescence intensity perpendicular to excitation source after blanking, and G = G-factor (correction for polarization bias of the detection system). After anisotropy was determined, data were plotted using GraphPad Prism (La Jolla, Ca) and fit to the following equation:

$$Y = B_{\text{MAX}} \cdot (X / (K_D + X)) + b$$

where Y = specific binding, K_D = dissociation constant, B_{MAX} = maximum binding, X = MalE-VirF concentration, and b = y-intercept.

On average, there was a 65% increase in anisotropy when VirF was added to the DNA. Within a single set of experiments, the DNA (alone) fluorescence anisotropy values varied ~4%, whereas, between experiments these anisotropy values varied ~15%. The latter variation is most likely due to differences in the efficiency of duplex DNA formation.

Results

MalE-VirF Purification from E. coli BL21(DE3)

Initial attempts to purify VirF relied upon expressing MalE-VirF from the expression vector pMALvirF in *E. coli* BL21(DE3) cells. The first purification step used amylose resin chromatography to isolate MalE-VirF from the cellular lysate. As shown in Figure IV-1A, the amylose resin did capture MalE-VirF, but also captured a variety of other proteins with MalE being the main impurity. To further purify MalE-VirF, gel filtration chromatography was used. The gel filtration chromatography was successful at eliminating the major MalE impurity, but did not eliminate the other minor impurities, see Figure IV-1B. Bradford assay analysis indicated a total protein yield of 0.5 to 0.75 mg per liter of culture with MalE-VirF making up approximately 60% - 70% of the sample (based on SDS-PAGE analysis). Lastly, anion exchange chromatography was used to remove all other impurities from the sample (as shown in Figure IV-1C). Although the sample was pure at this point, the overall yield of MalE-VirF was poor. Typical purifications with this procedure yielded approximately 0.2 to 0.3 mg of MalE-VirF per liter of culture.

VirF(154-263) Purification

The C-terminal domain of VirF was also expressed in and purified from *E. coli* BL21(DE3) cells. The purification procedure involved two chromatography steps: batch Ni-resin affinity chromatography and heparin affinity chromatography. The initial Ni-resin purification isolated VirF(154-263) from the cellular lysate while the heparin affinity chromatography removed a majority of the contaminating proteins (See Figure IV-2). As shown in Figure IV-2, the 800 mM NaCl fraction from the heparin column contained the

most VirF(154-263) and was stored in liquid nitrogen for later use. Based on SDS-PAGE analysis, the isolated VirF(154-263) was approximately 75% pure with Bradford assay analysis indicating a total protein yield of 0.1 to 0.2 mg per liter of culture.

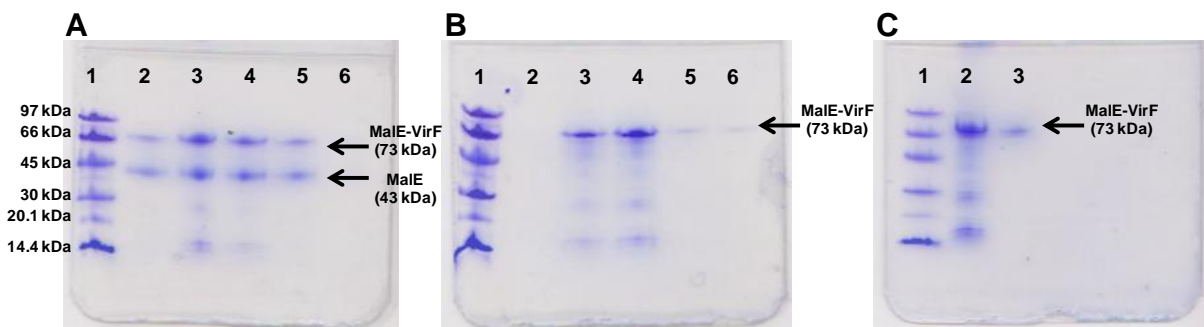


Figure IV-1: SDS-PAGE Analysis of the MalE-VirF Purification from pMALvirF in *E. coli* BL21(DE3) Cells. All samples visualized with Coomassie Blue staining. **A)** Phastgel™ depicting the contents of the amylose resin chromatography fractions. Lane 1: LMW ladder, Lane 2: fraction 1 off column, Lane 3: fraction 2 off column, Lane 4: fraction 3 off column, Lane 5: fraction 4 off column, Lane 6: fraction 5 off column. **B)** Phastgel™ depicting the contents of the gel filtration chromatography fractions. Lane 1: LMW ladder, Lane 2: fraction 12 off column, Lane 3: fraction 15 off column, Lane 4: fraction 18 off column, Lane 5: fraction 23 off column, Lane 6: fraction 27 off column. **C)** Phastgel™ comparing the pooled and concentrated gel filtration chromatography fractions to the pooled and concentrated anion exchange chromatography fractions. Lane 1: LMW Ladder, Lane 2: Pooled fractions 13-30 from gel filtration, Lane 3: Pooled fractions 4-36 from anion exchange.

MalE-VirF Purification from KS1000 and BS103

Attempts to isolate MalE-VirF using pMALvirF as an expression vector in *E. coli* KS1000 cells, followed by purification via amylose resin chromatography produced poor results. SDS-PAGE analysis showed a small amount of MalE-VirF was isolated along with a large amount of MalE in all fractions (See Figure IV-3A). To improve the purification, an arabinose-inducible vector, pBAD202-MALvirF was constructed to express MalE-VirF in *S. flexneri* BS103 cells. Following purification by amylose resin

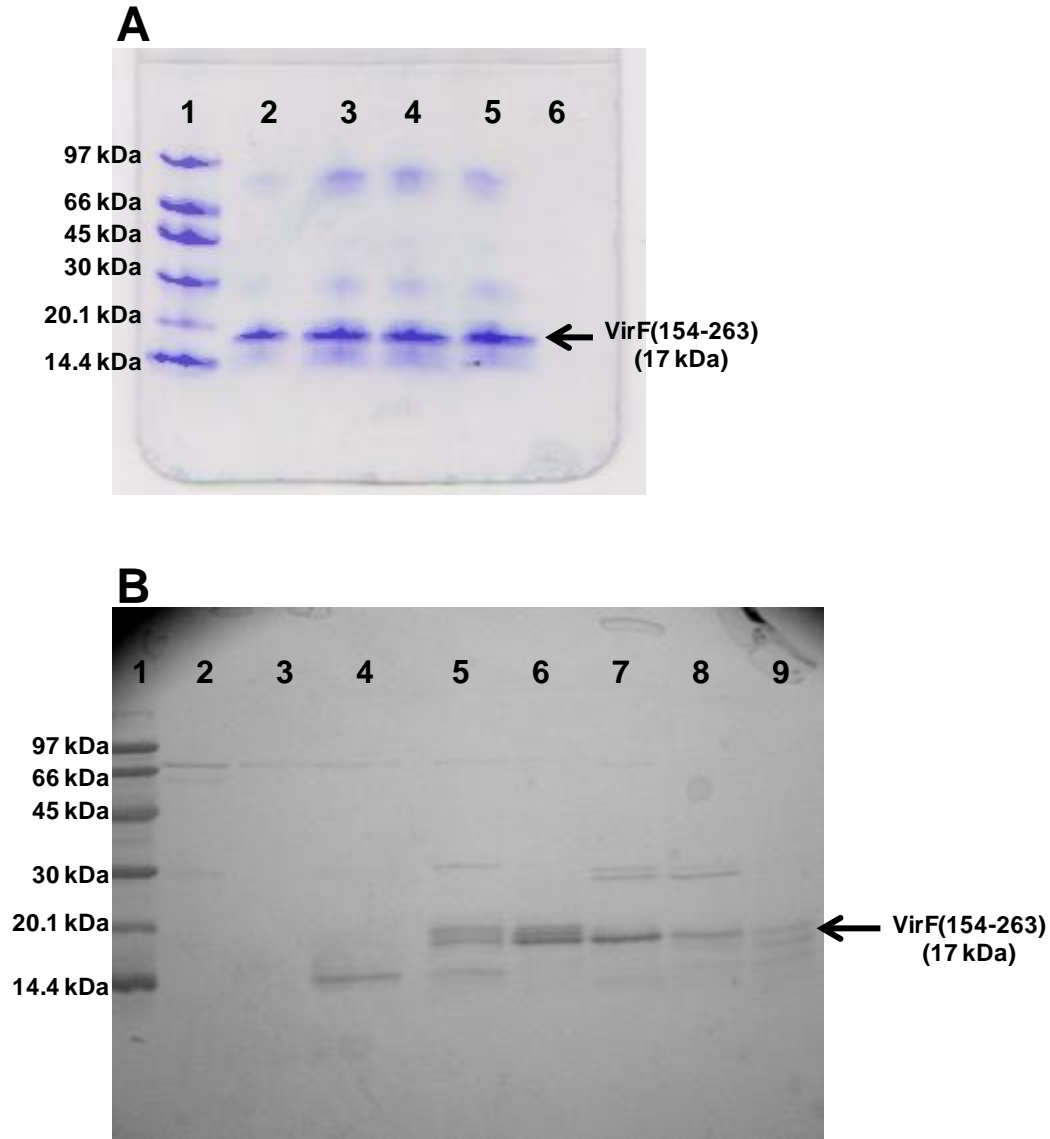


Figure IV-2: SDS-PAGE Analysis of the VirF(154-264) Purification from pET19b-VirF(154-263) in *E. coli* BL21(DE3) Cells. All samples visualized with Coomassie Blue staining. **A)** Phastgel™ depicting the contents of the Ni-resin chromatography fractions. Lane 1: LMW ladder, Lane 2: fraction 1 off column, Lane 3: fraction 2 off column, Lane 4: fraction 3 off column, Lane 5: fraction 4 off column, Lane 6: fraction 5 off column. **B)** Denaturing 10% acrylamide gel depicting the contents of the heparin resin chromatography fractions. Lane 1: LMW ladder, Lane 2: 300 mM NaCl fraction, Lane 3: 400 mM NaCl fraction, Lane 4: 500 mM NaCl fraction, Lane 5: 600 mM NaCl fraction, Lane 6: 700 mM NaCl fraction, Lane 7: 800 mM NaCl fraction, Lane 8: 900 mM NaCl fraction, Lane 9: 1 M NaCl fraction.

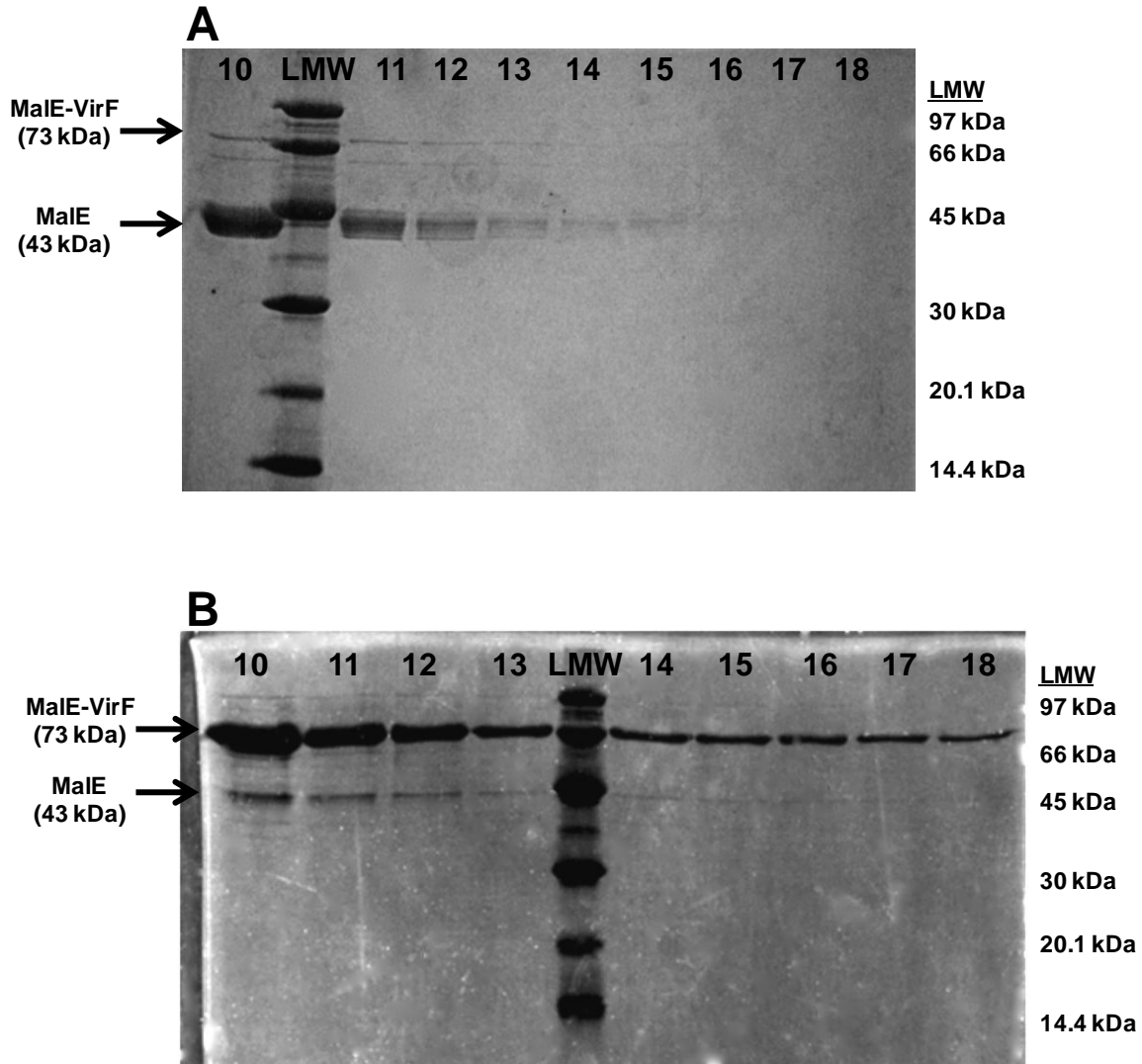


Figure IV-3: SDS-PAGE Analysis of MalE-VirF Purifications (KS1000 vs. BS103 Expression). All samples visualized with Coomassie Blue staining and captured utilizing FluorChem M gel imager. **A)** Denaturing 10% acrylamide gel depicting MalE-VirF expression in *E. coli* KS1000 cells via pMALvirF expression vector. MalE-VirF is 73 kDa in weight and the main impurity, MalE, is 43 kDa in weight. Numbers at the top of the gel represent the fraction (1 mL volume) number eluting off the amylose resin column. The numbers on the right-hand side of the gel correspond to the sizes of the LMW bands. **B)** Denaturing 10% acrylamide gel depicting MalE-VirF expression in *S. flexneri* BS103 cells via pBAD202-MALvirF expression vector. MalE-VirF is 73 kDa in weight and the main impurity, MalE, is 43 kDa in weight. Numbers at the top of the gel represent the fraction (1 mL volume) number eluting off the amylose resin column. The numbers on the right-hand side of the gel correspond to the sizes of the LMW bands.

chromatography, pure and soluble MalE-VirF was isolated. SDS-PAGE analysis shows that the fractions saved for later experiments were over 80% pure (see Figure IV-3B). Typical yields for the BS103 expression system varied between 1.5 – 2.5 mg of MalE-VirF per liter of culture. This expression/purification system was used to isolate MalE-VirF for all *in vitro* studies. Analytical gel filtration chromatography indicates that the purified MalE-VirF exists in solution as a monomer at concentrations used in further experiments, see Appendix Figure IV-1.

MalE-VirF DNA Binding via Electrophoretic Mobility Shift Assay (EMSA)

To monitor MalE-VirF binding to the *virB* promoter, an EMSA was optimized. Control experiments were conducted to verify that MalE-VirF was specifically binding to the 5'Cy5-labeled *pvirB* DNA probe (see Figure IV-4A) and that this binding was dose-dependent (see Figure IV-4B). Binding of MalE-VirF to the *virB* promoter could not be monitored unless the pH of the gel/running buffer was 9.5. If the pH was lower than 9.5, the protein/DNA complex would not enter the gel matrix (data not shown). This EMSA was also used to test VirF(154-263) binding to the *virB* promoter, however, interaction with the *virB* promoter could not be visualized under these conditions (data not shown).

DNA Binding via Fluorescence Polarization (FP)

For the FP assay reaction conditions from the EMSA assay were scaled to a 96-well plate format. Control experiments were conducted to verify equilibrium was reached (anisotropy signal did not increase after 20 minutes), binding was specific (MalE-VirF binding to labeled *pvirB* DNA probe could be competed by unlabeled *pvirB* DNA probe and MalE-VirF would not bind to sequence scrambled DNA probe as shown in Appendix Figure IV-2), and maximum anisotropy signal was achieved. The

anisotropy signal generated from MalE-VirF binding to the *pvirB* DNA probe was shown to be dose-dependent (see Figure IV-5). The FP assay was then used to determine the dissociation constant for MalE-VirF and the *pvirB* DNA probe. The data shown in Figure IV-5 was fitted with a specific binding equation (see Materials and Methods) and the dissociation constant was determined to $2.8 \pm 1.0 \mu\text{M}$.

Discussion

To enable the *in vitro* characterization of VirF, we sought to optimize a VirF purification procedure that could isolate pure, active VirF at concentrations practical for assay development. Based on the previous work done by Dr. Julie Hurt, we decided to focus on optimizing the purification of MalE-VirF rather than trying to isolate wildtype VirF.¹⁵ Her work, and the work of others,^{6, 8, 18} showed that wildtype VirF is insoluble outside of the cell and is prone to aggregation. To isolate MalE-VirF, Dr. Hurt used an *E. coli* BL21(DE3) expression system and two chromatography steps, batch purification with amylose affinity resin and gel filtration chromatography. As shown in Figure IV-1, we were able to replicate her work and obtain MalE-VirF that was approximately 60-70% pure with a yield of 0.5 to 0.75 mg per liter of culture. Although the yield of this prep was not ideal, it was practical upon scaling for assay development. However, the prep was not pure enough for accurate *in vitro* characterization studies of VirF.

The isoelectric point for VirF is predicted to be at pH 9.8 (SerialCloner Software), which means at physiological pH VirF is cationic. To improve the purity of our MalE-VirF preparations, we decided to take advantage of VirF's cationic nature by utilizing anion exchange chromatography after gel filtration. We chose anion exchange

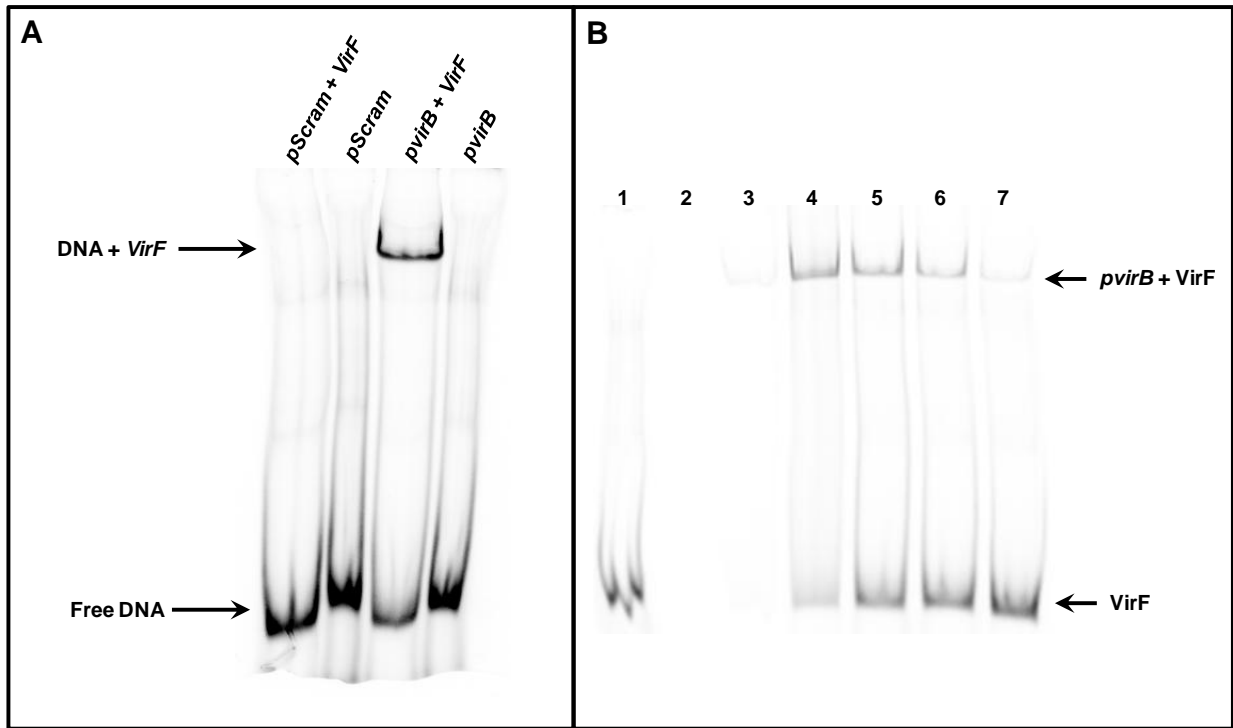


Figure IV-4: Electrophoretic Mobility Shift Assay (EMSA) PAGE of MalE-VirF Binding to *pvirB* DNA Probe. All reactions contained varying concentrations of probe DNA, varying concentration of MalE-VirF, 0.7 mg/mL salmon sperm DNA, and 0.07 mg/mL BSA. **A)** EMSA image shows the retardation of the 5'Cy5-*pvirB* DNA probe (0.25 μ M) when incubated in the presence of MalE-VirF (1 μ M) and shows no retardation of the 5'Cy5-*pScram* DNA probe (0.25 μ M) when incubated in the presence of MalE-VirF (1 μ M). **B)** EMSA image shows the dose-dependent binding relationship between MalE-VirF and the *pvirB* probe. Lane 1: 5'Cy5-*pvirB* DNA probe (0.25 μ M), Lane 2: MalE-VirF (11 μ M), Lane 3: 5'Cy5-*pvirB* DNA probe (0.025 μ M) + MalE-VirF (11 μ M), Lane 4: 5'Cy5-*pvirB* DNA probe (0.25 μ M) + MalE-VirF (11 μ M), Lane 5: 5'Cy5-*pvirB* DNA probe (0.25 μ M) + MalE-VirF (1 μ M), Lane 6: 5'Cy5-*pvirB* DNA probe (0.25 μ M) + MalE-VirF (0.25 μ M), Lane 7: 5'Cy5-*pvirB* DNA probe (0.25 μ M) + MalE-VirF (0.1 μ M).

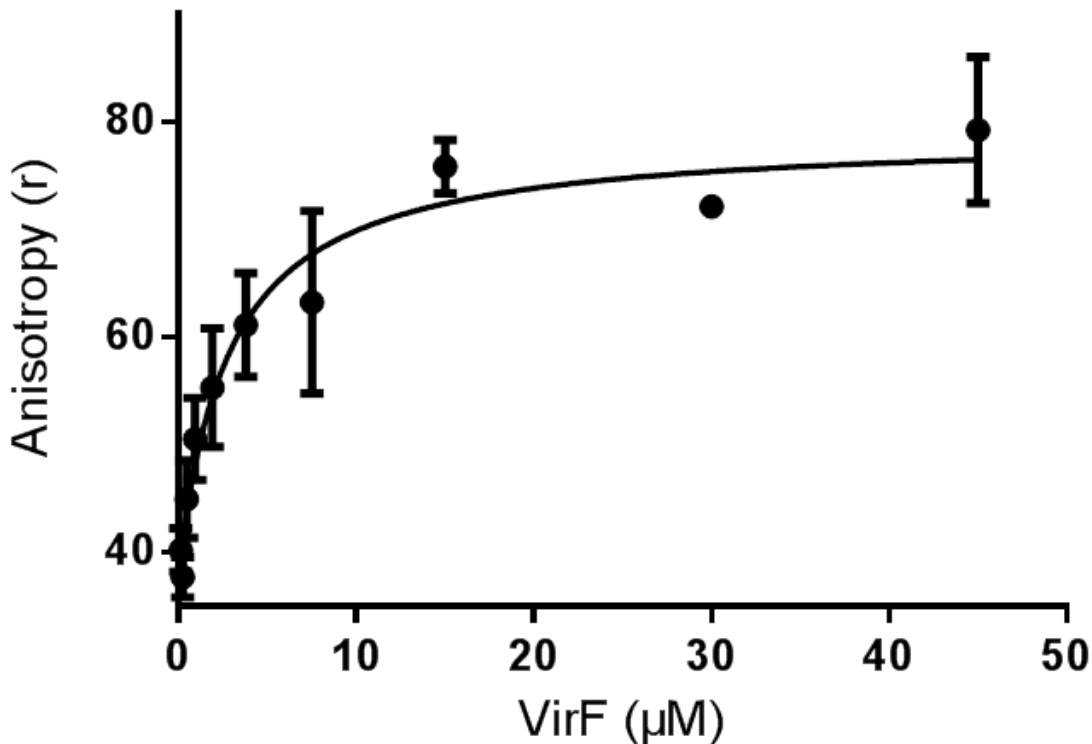


Figure IV-5: Plot of Male-VirF Binding to the *pvirB* DNA probe. For the assay, 5'Fluorescein-*pvirB* DNA probe concentration was held constant at 50 nM, while Male- VirF concentration was varied from 45 μ M to 0.12 μ M. The observed binding max for Male-VirF binding was approximately $r = 75$, while the observed baseline (no Male-VirF, only free *pvirB* DNA probe) was $r = 42$. The assay was conducted in duplicate.

chromatography over cation exchange chromatography in hopes of minimizing the loss of Male-VirF caused by poor column resolution or co-elution with other impurities. By utilizing anion exchange chromatography, we ensured that all the Male-VirF in the sample would quickly elute in the void volume, which it did. As shown in Figure IV-1C, the addition of anion exchange chromatography drastically improved sample purity; however, the overall yield was reduced to approximately 0.2 mg per liter of culture. It is possible that this was the actual amount of VirF present in the sample before anion

exchange chromatography, but the previous yield was artificially raised by the presence of impurities. At this point, the purification was a week long process that produced a very small amount of protein that was not practical for assay development studies.

Previous studies have shown that AraC family regulators that function as monomers tend to be more soluble and can be over-expressed at higher levels.^{1, 19, 20} This, combined with the fact that N-terminal truncations of AraC family members have been shown to still bind to their promoter regions *in vitro*,^{21, 22} led us to explore purifying the C-terminal domain of VirF(154-263) as an alternative to MalE-VirF. The VirF(154-263) purification was based on previous work done by Dr. Tappan Biswas (unpublished, Tsodikov lab, University of Michigan) and utilized an N-terminal 10X His-tag to purify the protein via Ni-resin affinity and heparin chromatographies. Initial one liter culture preparation yielded approximately 0.15 mg of VirF(154-263) at 75% purity. To increase yield, later preparations were scaled to eight liters of culture and produced a total of approximately 0.8 mg of VirF(154-263). As similar to previous MalE-VirF preparations, the purification of VirF(154-263) was long, inefficient, and produced low yields.

During the time that the VirF(154-263) purification was being optimized, Egan and co-workers reported a MalE-VirF purification protocol.⁸ In their protocol, MalE-VirF was expressed in *E. coli* KS1000 from an IPTG-inducible pMALvirF vector and purified in one-step via a 10 mL amylose affinity resin column. The only differences between this protocol and our previous attempts at purifying MalE-VirF were the *E. coli* strain used for expression, KS1000, and the use of an amylose resin column instead of batch purification. KS1000 is a Prc protease (a periplasmic protease) deficient strain of *E. coli*²³ that is quite similar to the expression strains we used in previous protocols (e.g.

BL21, K12, TG2, etc.). Unsurprisingly, when we used the KS1000 expression/purification system to isolate MalE-VirF, we obtained results that we had typically seen for other *E. coli* heterologous expression systems: low overall yield and large amounts of MalE impurity (as shown via SDS-PAGE analysis in Figure VI-3A). However, the amylose resin column did eliminate a significant amount of other contaminating proteins that the batch purification procedure previously did not.

A common feature in all previous attempts to isolate VirF (in any form) was the use of an *E. coli* heterologous expression system. It is possible, although seemingly unlikely due to the extremely close genetic relationship between *E. coli* and *Shigella*, that VirF does not express or fold properly in *E. coli*. To probe this possibility, we sought to develop a homologous, *Shigella*-based expression system. Researchers studying virulence factor expression in *Streptococcus pneumoniae* had recently shown that a *S. pneumoniae* homologous expression system greatly improved the overall yield of isolated proteins.²⁴ In an effort to mimic their results, an arabinose-inducible vector, pBAD202-MALvirF was constructed that allowed for homologous expression of MalE-VirF in *S. flexneri* BS103 cells. Arabinose-inducible vectors had previously been shown to be compatible with the *Shigella* transcription machinery.²⁵ As shown in Figure IV-3B, this expression system, when used with the same amylose resin column purification procedure, greatly improved overall yield (approximately 1.5 - 2.5 mg per liter of culture) and purity of the MalE-VirF preparation (over 80% pure). It was by far the most successful preparation of MalE-VirF to date and it provided adequate amounts of protein for the development of *in vitro* binding assays.

The complexity of the *icsA* promoter¹⁸ prompted us to focus our efforts on developing *in vitro* assays to monitor MalE-VirF binding to the *virB* promoter. Since we did not know if our MalE-VirF preparations were active, we wanted to first optimize an assay with an easy to visualize readout. Therefore, we chose an electrophoretic mobility shift assay (EMSA), a platform commonly used to visualize protein-DNA interactions. The EMSA utilized a fluorescently-labeled *pvirB* DNA fragment which was 74 bp long, with 60 bp corresponding to the previously determined *pvirB* region,^{6, 8, 9} and 14 bp corresponding to a 5'-Cy5 labeled LUEGO (labeled universal electrophoretic gel shift oligonucleotide) site.¹⁷ Interestingly, while determining the optimal pH for the assay, it was observed that MalE-VirF could not enter the polyacrylamide gel matrix if the pH of the gel or running buffer was less than 9.5 (data not shown). We hypothesize that at pH less than 9.5, the protein is too positively charged (pI ~ 9.8) to be attracted to the cathode that is pulling other biomolecules into the gel matrix. Following further optimization of buffer and reaction conditions, the interaction between MalE-VirF and the *pvirB* was successfully visualized. It was later shown that MalE-VirF was specifically binding to the 5'-Cy5-labeled *pvirB* DNA probe and that this binding was dose-dependent, see Figure IV-4. It is also worth noting that as expected the MalE tag did not prevent binding to the *pvirB*.

To confirm and quantitate the results of the EMSA, a Fluorescence Polarization (FP) assay was developed. The FP assay utilized reaction conditions similar to the EMSA, with the only major change being to the *pvirB* DNA fragment. For the FP assay, the *pvirB* fragment was shortened to 60 bp with the LUEGO site being removed and was labeled with a 5'-Fluorescein instead of Cy5. These changes increased the FP

signal generated in the assay by decreasing the molecular weight of the fragment and increasing the fluorescent lifetime of the probe. After control experiments were completed, the FP assay was used to determine the K_D of MalE-VirF binding to the *pvirB* DNA probe. The data shown in Figure IV-5 was fitted and an experimental K_D was calculated to be $2.8 \pm 1.0 \mu\text{M}$. To our knowledge this is the first reported K_D for VirF binding either of its promoter regions. It has been shown that VirF only activates the transcription of the *virB* gene when supercoiled DNA is used as a template.²⁶ Therefore, we should note that it is possible that our experimental K_D , determined with a linear DNA fragment may be different than the *in vivo* K_D , under physiological conditions where VirF is activating supercoiled DNA.

In conclusion, we have successfully developed tools (an efficient homologous expression system and two DNA-binding assays) to study the interaction between VirF and the *virB* promoter. In the future, we plan on developing other assays that monitor different aspects of the VirF transcriptional activation process, such as dimerization and binding to the *icsA* promoter. These tools will then be used to determine the mechanism of action for each of our previously identified small molecule VirF inhibitors (see Chapter V).

Notes to Chapter IV

The work presented in this chapter required a great amount of time, effort, and sanity. I would like to acknowledge the following people who made contributions along the way: Eric Lachacz (Department of Medicinal Chemistry, University of Michigan) for contributions made to the construction of the homologous expression vector for VirF, Gordon Kane (University of Michigan REU program, home institution: Beloit College, Wisconsin) for contributions made to the VirF(154-263) expression trials, Dr. Amanda Garner (Department of Medicinal Chemistry, University of Michigan) for the use of the SpectraMax M5 plate reader and gel imager in her laboratory, and Dr. Jennifer Meagher (Center of Structural Biology, Life Sciences Institute, University of Michigan) for use of the analytical gel filtration chromatography system. Some of the work presented here was published in Emanuele and Garcia, *PLoS ONE* **2015**, 10, e0137410.²⁷

References

1. Schleif, R. AraC protein: a love-hate relationship. *Bioessays* **2003**, 25, 274-82.
2. Schleif, R. F.; Favreau, M. A. Hyperproduction of araC protein from *Escherichia coli*. *Biochemistry* **1982**, 21, 778-782.
3. Dunn, T. M.; Hahn, S.; Ogden, S.; Schleif, R. F. An operator at -280 base pairs that is required for repression of araBAD operon promoter: addition of DNA helical turns between the operator and promoter cyclically hinders repression. *Proceedings of the National Academy of Sciences* **1984**, 81, 5017-5020.
4. Soisson, S. M.; MacDougall-Shackleton, B.; Schleif, R.; Wolberger, C. The 1.6 Å crystal structure of the AraC sugar-binding and dimerization domain complexed with d-fucose. *Journal of Molecular Biology* **1997**, 273, 226-237.

5. Rodgers, M. E.; Schleif, R. Solution Structure of the DNA Binding Domain of AraC Protein. *Proteins* **2009**, *77*, 202-208.
6. Tobe, T.; Yoshikawa, M.; Mizuno, T.; Sasakawa, C. Transcriptional control of the invasion regulatory gene *virB* of *Shigella flexneri*: activation by *virF* and repression by H-NS. *Journal of Bacteriology* **1993**, *175*, 6142-9.
7. Emanuele, A. A.; Adams, N. E.; Chen, Y.-C.; Maurelli, A. T.; Garcia, G. A. Potential novel antibiotics from HTS targeting the virulence-regulating transcription factor, *VirF*, from *Shigella flexneri*. *Journal of Antibiotics* **2014**, *67*, 379-386.
8. Koppolu, V.; Osaka, I.; Skredenske, J. M.; Kettle, B.; Hefty, P. S.; Li, J.; Egan, S. M. Small-molecule inhibitor of the *Shigella flexneri* master virulence regulator *VirF*. *Infection & Immunity* **2013**, *81*, 4220-31.
9. Hurt, J. K.; McQuade, T. J.; Emanuele, A.; Larsen, M. J.; Garcia, G. A. High-Throughput Screening of the Virulence Regulator *VirF*: A Novel Antibacterial Target for Shigellosis. *Journal of Biomolecular Screening* **2010**, *15*, 379-387.
10. Munson, G. P.; Scott, J. R. Binding Site Recognition by Rns, a Virulence Regulator in the AraC Family. *Journal of Bacteriology* **1999**, *181*, 2110-2117.
11. Tramonti, A.; Visca, P.; De Canio, M.; Falconi, M.; De Biase, D. Functional Characterization and Regulation of *gadX*, a Gene Encoding an AraC/XylS-Like Transcriptional Activator of the *Escherichia coli* Glutamic Acid Decarboxylase System. *Journal of Bacteriology* **2002**, *184*, 2603-2613.
12. Ibarra, J. A.; Villalba, M. I.; Puente, J. L. Identification of the DNA Binding Sites of *PerA*, the Transcriptional Activator of the *bfp* and *per* Operons in Enteropathogenic *Escherichia coli*. *Journal of Bacteriology* **2003**, *185*, 2835-2847.
13. Michel, L.; González, N.; Jagdeep, S.; Nguyen-Ngoc, T.; Reimmann, C. PchR-box recognition by the AraC-type regulator *PchR* of *Pseudomonas aeruginosa* requires the siderophore pyochelin as an effector. *Molecular Microbiology* **2005**, *58*, 495-509.

14. Thomson, J. J.; Withey, J. H. Bicarbonate Increases Binding Affinity of *Vibrio cholerae* ToxT to Virulence Gene Promoters. *Journal of Bacteriology* **2014**, 196, 3872-3880.
15. Hurt, J. K. Modulation of Expression and Antibacterial Targeting of *Shigella flexneri* VirF. Ph.D. Dissertation, University of Michigan, Ann Arbor, 2010.
16. Maurelli, A. T.; Blackmon, B.; Curtiss III, R. Loss of pigmentation in *Shigella flexneri* 2a is correlated with loss of virulence and virulence associated plasmid. *Infection and Immunity* **1984**, 43, 397-401.
17. Jullien, N.; Herman, J.-P. LUEGO: a cost and time saving gel shift procedure. *BioTechniques* **2011**, 51, 267-269.
18. Tran, C. N.; Giangrossi, M.; Prosseda, G.; Brandi, A.; Di Martino, M. L.; Colonna, B.; Falconi, M. A multifactor regulatory circuit involving H-NS, VirF and an antisense RNA modulates transcription of the virulence gene *icsA* of *Shigella flexneri*. *Nucleic acids research* **2011**, 39, 8122-8134.
19. Rhee, S.; Martin, R. G.; Rosner, J. L.; Davies, D. R. A novel DNA-binding motif in MarA: The first structure for an AraC family transcriptional activator. *Proceedings of the National Academy of Sciences of the United States of America* **1998**, 95, 10413-10418.
20. Kwon, H. J.; Bennik, M. H.; Demple, B.; Ellenberger, T. Crystal structure of the *Escherichia coli* Rob transcription factor in complex with DNA. *Nature Structural Biology* **2000**, 7, 424-30.
21. Menon, K. P.; Lee, N. L. Activation of *ara* operons by a truncated AraC protein does not require inducer. *Proceedings of the National Academy of Sciences of the United States of America* **1990**, 87, 3708-3712.
22. Kolin, A.; Balasubramaniam, V.; Skredenske, J. M.; Wickstrum, J. R.; Egan, S. M. Differences in the mechanism of the allosteric l-rhamnose responses of the AraC/XylS family transcription activators RhaS and RhaR. *Molecular Microbiology* **2008**, 68, 448-461.
23. Silber, K. R.; Keiler, K. C.; Sauer, R. T. Tsp: a tail-specific protease that selectively degrades proteins with nonpolar C termini. *Proceedings of the*

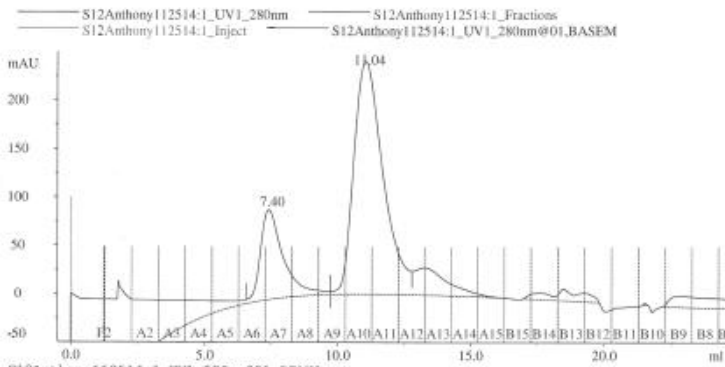
National Academy of Sciences of the United States of America **1992**, 89, 295-299.

24. Lo Sapio, M.; Hilleringmann, M.; Barocchi, M. A.; Moschioni, M. A novel strategy to over-express and purify homologous proteins from *Streptococcus pneumoniae*. *Journal of Biotechnology* **2012**, 157, 279-286.
25. Wing, H. J.; Yan, A. W.; Goldman, S. R.; Goldberg, M. B. Regulation of IcsP, the Outer Membrane Protease of the *Shigella* Actin Tail Assembly Protein IcsA, by Virulence Plasmid Regulators VirF and VirB. *Journal of Bacteriology* **2004**, 186, 699-705.
26. Tobe, T.; Yoshikawa, M.; Sasakawa, C. Thermoregulation of virB transcription in *Shigella flexneri* by sensing of changes in local DNA superhelicity. *Journal of Bacteriology* **1995**, 177, 1094-7.
27. Emanuele, A. A.; Garcia, G. A. Mechanism of Action and Initial, In Vitro SAR of an Inhibitor of the *Shigella flexneri* Virulence Regulator VirF. *PLoS ONE* **2015**, 10, e0137410.

Appendix

A

Chromatogram Questions
 No 1: Sample Volume and Type
 NoLE-VirF Analytical GP Anthony 11/25/14
 No 2: Column
 Superose 12
 No 3: Eluent A
 20mM tris 7.4, 500mM NaCl, 1mM DTT, 1mM EDTA
 No 4: Eluent B
 No 5: Remarks



S12Anthony112514:1_UV1_280nm@01, PRAK1

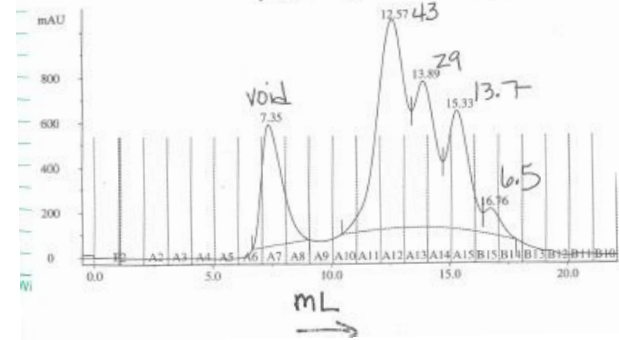
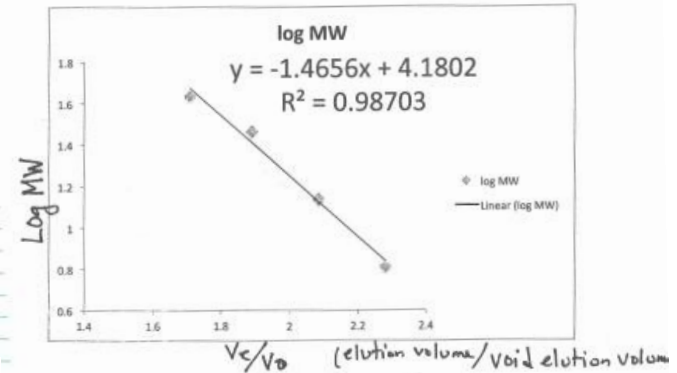
No	Ret ml	Area mAU*ml	Height mAU
1	7.40	93.3798	93.121
2	11.04	309.0499	240.889

Total number of detected peaks = 14
 Total area = 932.0859 mAU*ml
 Area in evaluated peaks = 402.4297 mAU*ml
 Ratio peak area / total area = 0.431752
 Total peak width = 6.22 ml
 Column height = 30.00 cm
 Column void = 7.77 ml
 Calculated from : S12Anthony112514:1_UV1_280nm
 Baseline : S12Anthony112514:1_UV1_280nm@01, BASEM
 Peak rejection on:
 Maximum number of peaks: 20
 Current peak filter settings:
 Maximum number of peaks: 20

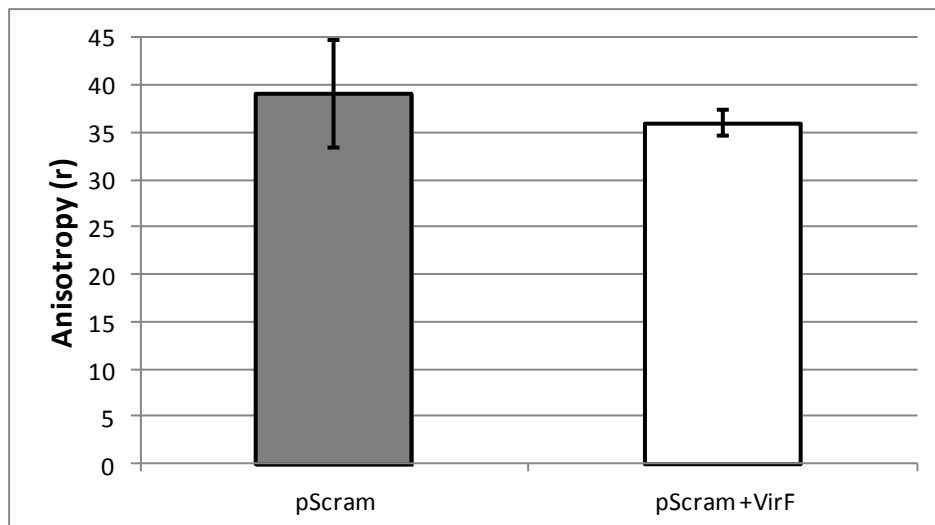
B

Calibration of Superose 12 July 30, 2014
 Buffer: 20mM hepes 7.5, 100mM KCl, 0.5mM EDTA
 Flow Rate 0.75 ml/min

Elution Vol	Ve/Vo	MW void	log MW void	Ve/Vo	log MW
7.35	void			1.71020408	1.63346846
12.57	1.710	43	1.633	1.88979592	1.462398
13.89	1.890	29	1.462	2.08571429	1.13672057
15.33	2.086	13.7	1.137	2.28027211	0.81291336
16.76	2.280	6.5	0.813		



Appendix Figure IV-1: Analytical Gel Filtration Results. A) Chromatogram depicting elution of MalE-VirF (11.04 mL) from Superose 12 column. B) Chromatogram and four-point calibration curve for Superose 12 column used to determine molecular weight of MalE-VirF in "A".



Appendix Figure IV-2: Negative Controls for FP assay. B) Graph depicting the anisotropy values generated in the FP assay for the 5'Fluorescein *pScram* probe alone ($r = 39$) and in the presence of MalE-VirF ($r = 36$). Experiments were conducted in duplicate with 50 nM *pScram* and 20 μ M MalE-VirF.

CHAPTER V

Mechanism of Inhibition Determination and Resulting SAR Studies

Chapters II and III detail the identification of five promising small molecule inhibitors of VirF from a high-throughput screening campaign and a series of follow-up assays, including tissue-culture based invasion and cell-to-cell spread assays that model aspects of the *Shigella* infection process. All five compounds inhibited VirF-driven transcriptional activation in a *Shigella*-based, β -galactosidase reporter assay with IC₅₀ values in the low micromolar range (14-66 μ M). Furthermore, at concentrations at or below their IC₅₀s in the reporter assay, two of the compounds (19615 and 144143) significantly inhibited the spread of an active *S. flexneri* infection in a tissue-culture based plaque efficiency assay, and two of the compounds (19615 and 144092) also significantly inhibited initial *S. flexneri* invasion in a gentamicin protection assay. These results, supported by similar results recently published by other groups,¹⁻³ validate our approach by providing proof of principle that small molecules can attenuate virulence; however, the mechanism by which our compounds inhibit the VirF transcriptional activation process remains unclear.

The exact mechanism by which VirF activates transcription is not presently understood. Like AraC and most AraC family members, VirF has two domains, an N-terminal dimerization domain and C-terminal DNA binding domain. Both of these domains are necessary for *in vivo* transcriptional activation.⁴ As shown in Figure V-1, in order for VirF to activate transcription it must bind to the correct promoter region (either

the *virB* promoter (*pvirB*) or the *icsA* promoter (*picsA*), dimerize, and recruit RNA polymerase. The order of these events, indeed if they are ordered at all, is presently unknown. Our small molecule inhibitors could be disrupting any of these steps of the VirF gene activation process. In fact, there have been reports indicating that VirF, and/or homologous AraC family members, can be inhibited through the blockade of DNA binding^{1, 3} or self-dimerization.² A clearer understanding of the mechanism of action of the VirF inhibitors would provide critical insight for furthering their development.

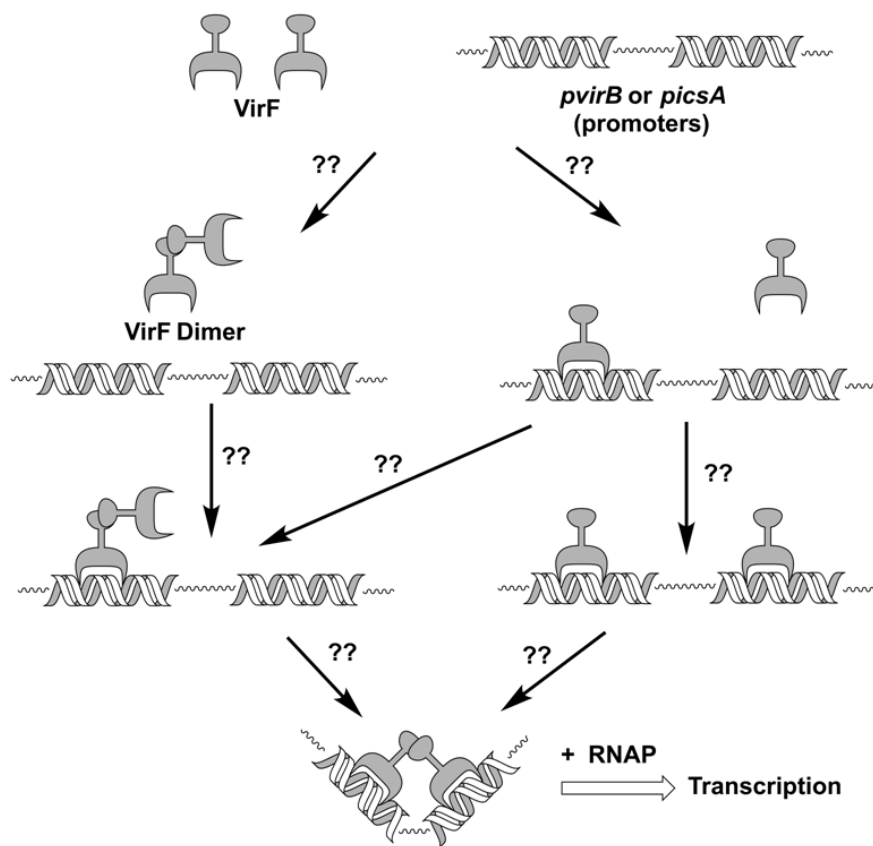


Figure V-1: Schematic Depicting Presumptive Steps in the Activation of Transcription by VirF. By analogy to AraC and family members, it is presumed that two VirF proteins bind to two proximal DNA binding sites in a dimeric form to activate transcription. The question marks indicate that the exact steps in this process and their order (if ordered) are not yet understood.

In the studies herein reported, we probed the mechanism of action of our small molecule VirF inhibitors. We hypothesized that our inhibitors were preventing VirF-driven transcriptional activation by either blocking VirF from binding to DNA or by preventing VirF dimerization. Using the *in vitro* DNA-binding studies described in Chapter IV, we determined that one of our small molecule inhibitors (19615) blocked VirF from binding to the *virB* promoter. To probe the ability of our inhibitors to block VirF dimerization, we also attempted (albeit unsuccessfully) to develop a VirF-driven, split-GFP reassembly assay. Lastly, we screened a series of analogs of our most promising chemical scaffolds (19615 and 144143/144092) and deduced initial structure-activity relationship trends that we will use as a basis to further optimize our inhibitors and work towards achieving our goal of developing a novel therapy for treating shigellosis.

Materials and Methods

Reagents

All reagents and equipment were purchased from Fisher Scientific (Hampton, NH), unless otherwise specified. All restriction enzymes were purchased from New England Biolabs (Ipswich, MA).

Bacterial Strains

The following bacterial strains were used in this study: *Escherichia coli* BL21(DE3) (obtained from Novagen, Temcula, CA).⁵

Plasmids

The following plasmids were generous gifts from the laboratory of Dr. Lynne Regan (Department of Chemistry, Yale University): pET11a-NGFP-link, pMRBAD-link-

CGFP, pET11a-NGFP-link-Z, and pMRBAD-Z-link-CGFP. The other plasmids used in the study were constructed as described below.

Various TOPO Plasmids

Plasmids were constructed using the TOPO® TA Cloning® kit (Invitrogen, Carlsbad, CA). Briefly, the primers listed in Table V-1 were used to amplify the DNA fragment of interest with the appropriate 5' and 3' restriction sites via polymerase chain reaction. The amplified DNA fragments were then subcloned into pCR2.1TOPO via a directional TOPO® TA cloning reaction resulting in the formation of the plasmids listed in Table V-2.

Table V-1. Primers Used in TOPO Plasmid Construction.

Primer Name	Sequence (5'-3')	Purpose
XhoI-VirF For NGFP	CTCGAGCATGTCTGGGACATAAAAACAAAAT	Used to TOPO clone <i>virF</i> and N-term <i>virF</i> with 5'- <i>XhoI</i> site
NcoI-VirF For CGFP	CCATGGCTATGTCTGGGACATAAAAACAAAAT	Used to TOPO clone <i>virF</i> and N-term <i>virF</i> with 5'- <i>NcoI</i> site
XhoI-MalEVirF For NGFP	CTCGAGCATGAAAATCGAAGAAGGT	Used to TOPO clone <i>malEvirF</i> with 5'- <i>XhoI</i> site
BamHI-MalEVirF Rev NGFP	GGATCCTTAAAATTTTTTATGATATAAGTAA	Used to TOPO clone <i>malEvirF</i> and <i>virF</i> with 3'- <i>BamHI</i> site
NcoI-MalEVirF For CGFP	CCATGGCTATGAAAATCGAAGAAGGT	Used to TOPO clone <i>malEvirF</i> with 5'- <i>NcoI</i> site
AatII-MalEVirF Rev CGFP	GACGTCCCAAATTTTTTATGATATAAGTAA	Used to TOPO clone <i>malEvirF</i> and <i>virF</i> with 3'- <i>AatII</i> site
BamHI-NTermVirF Rev NGFP	GGATCCTTATATCGATATCGAAGTATA	Used to TOPO clone N-term <i>virF</i> with 3'- <i>BamHI</i> site
AatII-	GACGTCCCTATCGATATCGAAGTATA	Used to TOPO

NtermVirF Rev CGFP		clone N-term <i>virF</i> with 3'- <i>AatII</i> site
SgrAI-pvirB For NGFP	CGCCGGTGATCACACCCTGTTTATTC	Used to TOPO clone <i>pvirB</i> with 3'- <i>SgrAI</i> site
XbaI-pvirB Rev NGFP	TCTAGACTCACATCAGAGCTCCAC	Used to TOPO clone <i>pvirB</i> with 5'- <i>XbaI</i> site

Table V-2. Constructed TOPO Vectors.

pCR-TOPO-2.1-XhoI-VirF-BamHI
pCR-TOPO-2.1-NcoI-VirF-AatII
pCR-TOPO-2.1-XhoI-MalEVirF-BamHI
pCR-TOPO-2.1-NcoI-MalEVirF-AatII
pCR-TOPO-2.1-XhoI-NTermVirF-BamHI
pCR-TOPO-2.1-NcoI-NTermVirF-AatII
pCR-TOPO-2.1-XbaI-pvirB-SgrAI

pMRBAD-X-link-CGFP Plasmids

pMRBAD-X-link-CGFP plasmids encode for a VirF-CGFP fusion protein (with the C-terminal fragment of GFP(158-238) fused to the C-terminal of either MalE-VirF, VirF, or the N-terminal domain of VirF(1-153)). The pMRBAD-X-link-CGFP plasmids were constructed by first treating pMRBAD-link-CGFP and the appropriate TOPO vector (see Table V-2) with *NcoI* and *AatII* in a double restriction enzyme digestion (20 U each, 40 μ L volume) at 37°C for 1 hour. The digestion products were then separated on a 1% low-melting (Seaplaque) agarose gel for 2 hours at 70V. The gel was visualized via ethidium bromide staining and UV light. Bands containing linearized pMRBAD-link-CGFP and the appropriate *virF* gene were excised and gel-purified with Gelase™ (Epicentre, Madison, WI) according to vendor's protocol. Following the purification, the *virF* insert was incubated with digested pMRBAD-link-CGFP in a 5:1 ratio overnight at 16°C in the presence of T4 DNA Ligase (400 units, NEB, Ipswich, MA). pMRBAD-VirF-

link-CGFP was later used to make pMRBAD-CGFP-link-VirF which encodes for a CGFP-VirF fusion protein (with the C-terminal fragment of GFP(158-238) fused to the N-terminal of VirF).

pET11a-NGFP-link-X Plasmids

pET11a-NGFP-link-X plasmids encode for a NGFP-VirF fusion protein (with the N-terminal fragment of GFP(1-157) fused to the N-terminal of either MalE-VirF, VirF, or the N-terminal domain of VirF(1-153)). The pET11a-NGFP-link-X plasmids were constructed by first treating pET11a-NGFP-link and the appropriate TOPO vector (see Table V-2) with *XhoI* and *BamHI* in a double restriction enzyme digestion (20 U each, 40 μ L volume) at 37°C for 1 hour. The digestion products were then separated on a 1% low-melting (Seaplaque) agarose gel for 2 hours at 70V. The gel was visualized via ethidium bromide staining and UV light. Bands containing linearized pET11a-NGFP-link and the appropriate *virF* gene were excised and gel-purified with Gelase™ (Epicentre, Madison, WI) according to vendor's protocol. Following the purification, the *virF* insert was incubated with digested pET11a-NGFP-link in a 5:1 ratio overnight at 16°C in the presence of T4 DNA Ligase (400 units, NEB, Ipswich, MA).

pET11a-NGFP-link-VirF+pvirB

The *virB* promoter (-130 to +54) was subcloned into pET11a-NGFP-link-VirF. Briefly, pCR-TOPO-2.1-XbaI-pvirB-SgrAI and pET11a-NGFP-link-VirF were treated with *SgrAI* and *XbaI* in a double restriction enzyme digestion (20 U each, 40 μ L volume) at 37°C for 1 hour. The digestion products were then separated on a 1% low-melting (Seaplaque) agarose gel for 2 hours at 70V. The gel was visualized via ethidium bromide staining and UV light. Bands containing linearized pET11a-NGFP-link-VirF and

the *virB* promoter were excised and gel-purified with Gelase™ (Epicentre, Madison, WI) according to vendor's protocol. Following the purification, the *virB* promoter insert was incubated with digested pET11a-NGFP-link-VirF in a 5:1 ratio overnight at 16°C in the presence of T4 DNA Ligase (400 units, NEB, Ipswich, MA).

DNA Probe Hybridization

The DNA probes used in the EMSA, FP, and FID assays were hybridized as described in Chapter IV. The sequences of the oligonucleotides used in these studies are listed in Table V-3.

Table V-3. Oligonucleotides Used in EMSA, FP, and FID Experiments.

Name	Sequence (5'-3')	Modification	Length (bases)
<i>pvirB</i> Top EMSA	AGAATATTATTCTTTTATCCAAT AAAGATAAATTGCATCAATCCA GCTATTAATAATAGTA	None	60
<i>pvirB</i> Bottom EMSA	TACTATTTTAATAGCTGGATTGA TGCAATTTATCTTTATTGGATAA AAGAATAATATTCTCCAGACCA GGGCAC	None	74
LUEGO	GTGCCCTGGTCTGG	5'-Cy5	14
<i>pvirB</i> Top FP	AGAATATTATTCTTTTATCCAAT AAAGATAAATTGCATCAATCCA GCTATTAATAATAGTA	5'-Fluorescein	60
<i>pvirB</i> Bottom FP	TACTATTTTAATAGCTGGATTGA TGCAATTTATCTTTATTGGATAA AAGAATAATATTCT	None	60
<i>pvirB</i> Top FID	AGAATATTATTCTTTTATCCAAT AAAGATAAATTGCATCAATCCA GCTATTAATAATAGTA	None	60
<i>pvirB</i> Bottom FID	TACTATTTTAATAGCTGGATTGA TGCAATTTATCTTTATTGGATAA AAGAATAATATTCT	None	60
<i>pvirB</i> (51-60) Top FID	TAAAATAGTA	None	10
<i>pvirB</i> (51-60) Bottom FID	TACTATTTTA	None	10

Monitoring Inhibition of VirF DNA binding via Electrophoretic Mobility Shift Assay (EMSA)

EMSAs were performed as described in Chapter IV but with compounds (100 μ M) present during appropriate reactions.

Monitoring Inhibition of VirF DNA Binding via Fluorescence Polarization (FP)

The FP protocol described in Chapter IV was adapted to determine the IC₅₀ of the small molecule hit compounds. Compounds (ranging from 200 μ M to 3.1 μ M) or DMSO for controls (1% final concentration) were added to the *pvirB* DNA probe working standard prior to addition to the microplates. For IC₅₀ determination, the MalE-VirF and *pvirB* DNA probe concentrations were held constant at 20 μ M and 50 nM, respectively. Positive controls were established to determine 100% VirF inhibition (no MalE-VirF present, 50 nM *pvirB* DNA probe) and negative controls were set up to determine no VirF inhibition (1% DMSO, 20 μ M MalE-VirF, and 50 nM *pvirB* DNA probe). Once again blanks were set up to include all reagents, except *pvirB* DNA probe. All reactions were run in duplicate. Anisotropy was calculated as listed in Chapter IV and data were plotted using GraphPad Prism then fit to the following equation:

$$Y = \text{Bottom} + (\text{Top} - \text{Bottom}) / (1 + 10^{(X - \log(\text{IC}_{50}))})$$

where: Y = anisotropy, X=log of compound concentration, Top and Bottom = plateaus in anisotropy units, and log(IC₅₀) = log of the concentration that inhibits 50% of VirF binding.

Fluorescence Intercalator Displacement (FID) Assay

The FID protocol was based on previously published studies^{6, 7} and was conducted in triplicate. For the assay, black, half-area, 96-well plates (Corning,

Twerksbury, MA) were used. First, 70 μL of ethidium bromide in Tris Buffer (0.1 M Tris HCl, 0.1 M NaCl, pH 8.0) was added to all wells. The concentration of ethidium bromide was contingent upon the length of the DNA probe that was used. For the 60 bp *pvirB* FID DNA probe, the final ethidium bromide concentration used was 45 μM ; whereas, for the 10 bp *pvirB* (51-60) FID DNA probe, the final ethidium bromide concentration used was 7.5 μM . Next, 10 μL of either *pvirB* FID DNA probes (10 or 60 bp) in TE/NaCl buffer (see above) or 10 μL of TE/NaCl buffer (background fluorescence control) were added to the appropriate wells of the plate. The final concentrations of the *pvirB* FID DNA probes were 1.5 μM . Lastly, 20 μL of test compound (either 19615 or Berenil) in 10% DMSO Tris Buffer or 20 μL of 10% DMSO Tris Buffer (100% fluorescence control) were added to the appropriate wells of the plate. The final concentrations of each test compound ranged from 12.5 μM to 100 μM . After the addition of all reagents, the plates were protected from light and allowed to equilibrate for 30 min on an orbital shaker at room temperature. Following equilibration, fluorescence was measured (545 nm emission, 595 nm excitation) using a BioTek Synergy H1 plate reader (Winooski, VT). The average background fluorescence was subtracted from all data generated and %fluorescence was calculated for all wells containing compound via the following formula:

$$\% \text{ fluorescence} = F_{\text{test}}/F_{100\%} * 100$$

where: F_{test} = the average fluorescence value obtained for each test compound and $F_{100\%}$ = the average fluorescence value obtained for each 100% fluorescence control.

GFP Reassembly Assay

The GFP reassembly assay was based on previously published methods.⁸ First, matching pairs of NGFP and CGFP plasmids were co-transformed into electrocompetent *E. coli* BL21(DE3) cells using a MicroPulser electroporator (BioRad) and grown overnight on LB plates containing carbenicillin (100 µg/mL) and kanamycin (35 µg/mL) at 37°C. The next day, a single colony was selected and used to grow a 5 mL starter culture of 2XTY supplemented with carbenicillin (100 µg/mL) and kanamycin (35 µg/mL). After overnight growth at 37°C with agitation, a loopful of culture was streaked onto an LB plate supplemented with carbenicillin (100 µg/mL), kanamycin (35 µg/mL), IPTG (100 µM), and arabinose (0.2%). The plate was incubated at 37°C for one day, wrapped with parafilm, and then incubated another 48 hours at room temperature. GFP-containing colonies were then visualized by placing the plate under UV light and monitoring fluorescence.

Structure-Activity Relationship (SAR) Study utilizing VirF-Driven, β -galactosidase Reporter Assay

The 96-well plate version of the β -galactosidase reporter assay was used to test 33 commercially available analogs of compounds 144092 and 144143 (obtained from Vitas-M Laboratory: Moscow, Russia and ChemDiv: San Diego, CA). The assay was performed as described in Chapter II Material and Methods Reconfirmation Screen.

Results

Monitoring the Inhibition of VirF DNA binding by EMSA

Using the optimized EMSA conditions described in Chapter IV, the assay was used to determine if our five previously identified hits (see Chapter II) could inhibit the

binding of MalE-VirF to the *virB* promoter at 100 μ M. As shown in Figure V-2, only one compound, 19615, dramatically reduced binding, while the other four compounds were indistinguishable from the DMSO negative control.

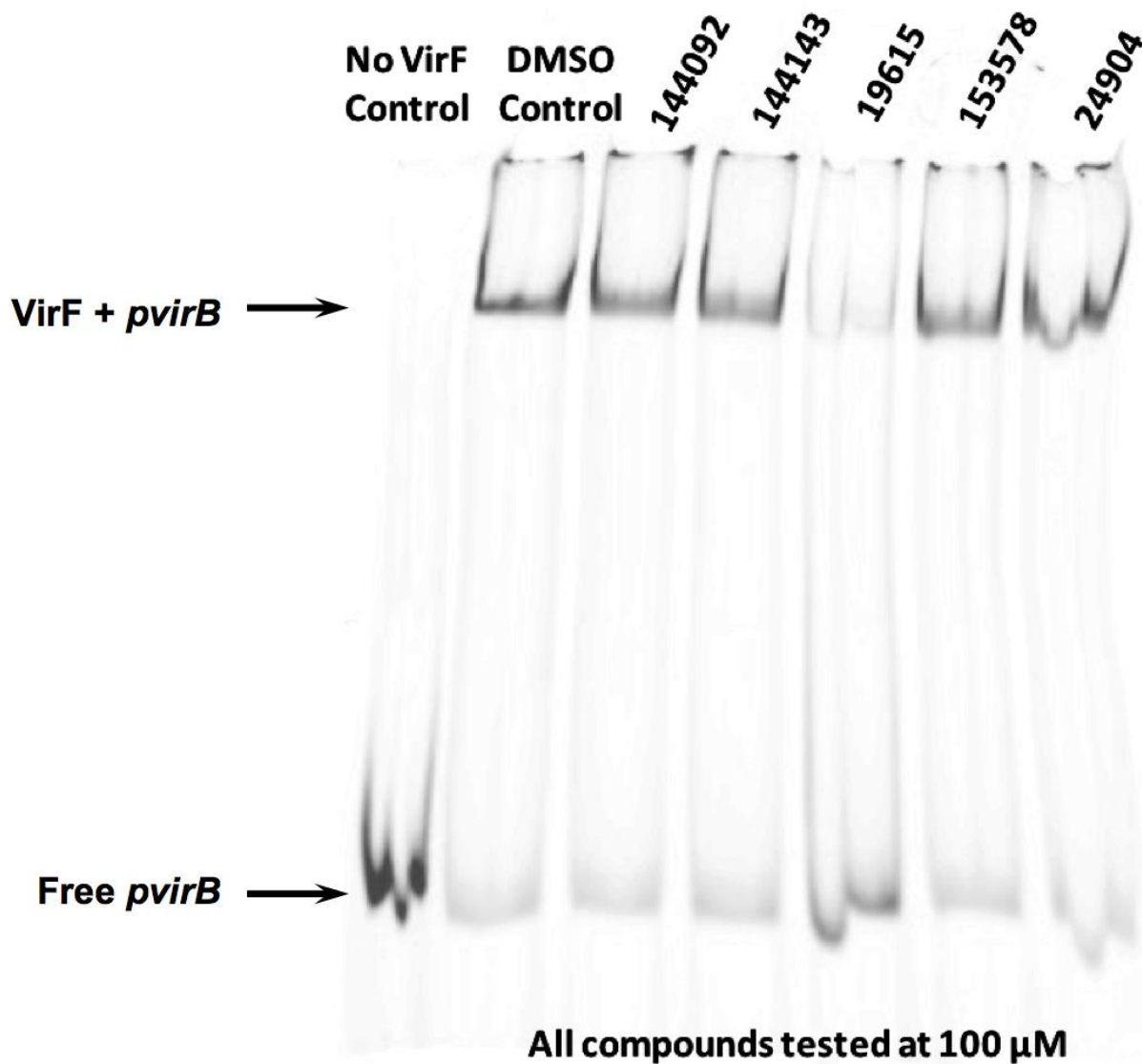
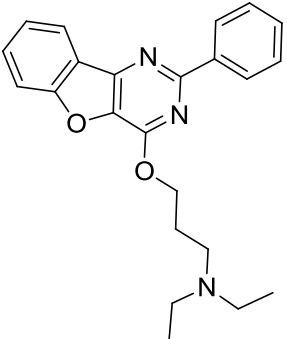


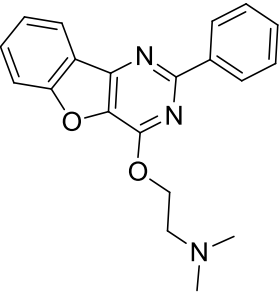
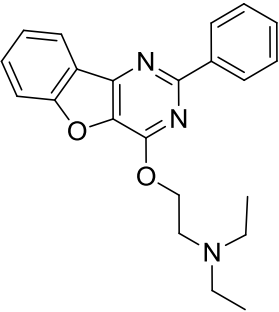
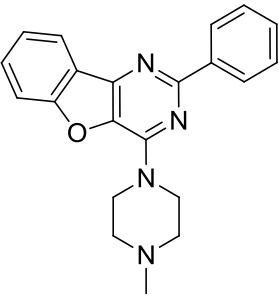
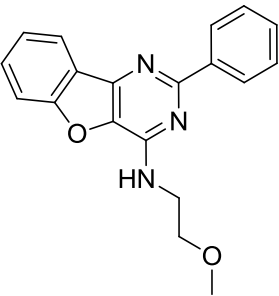
Figure V-2: Electrophoretic Mobility Shift Assay (EMSA) PAGE of MalE-VirF Binding to *pvirB* DNA Probe in Presence of Small Molecule Hit Compounds. EMSA image shows the retardation of the 5'Cy5-*pvirB* DNA probe (0.25 μ M) when incubated in the presence of MalE-VirF (1 μ M). Image also shows the effect each of the five hit compounds have on MalE-VirF binding. All compounds were dosed at 100 μ M, and only one compound, 19615, appeared to inhibit MalE-VirF binding to the *pvirB* DNA probe.

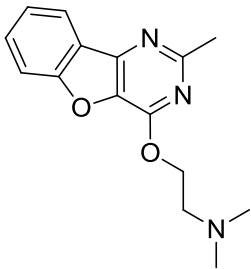
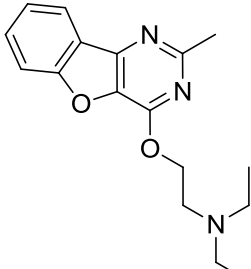
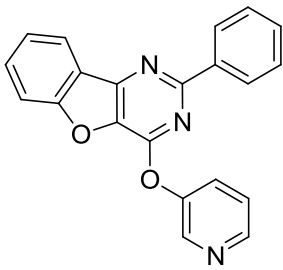
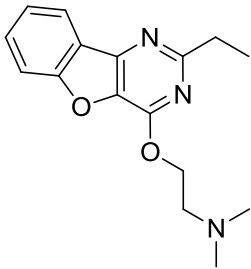
Monitoring Inhibition of VirF DNA Binding Via FP Assay

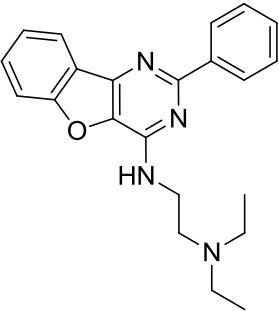
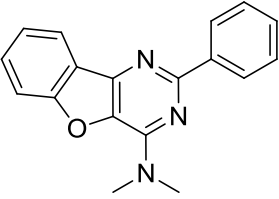
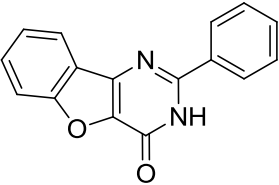
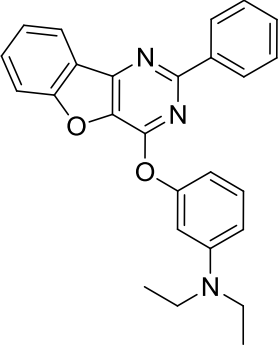
The FP assay was used to confirm and quantify the results of the EMSA. Consistent with the EMSA study, the five compounds were tested at 100 μM , and only 19615 inhibited DNA binding (63% inhibition, see Table V-4). Next, a small library of analogs of 19615 were purchased and screened in the FP assay. As shown in Table V-4, one of the 19615 analogs (598089) was essentially equal in potency to 19615 (68% versus 63% inhibition, respectively) and the rest of the compounds displayed lower %inhibition values (ranging from 43% to -5%). Lastly, to further evaluate the potency of 19615 in the FP assay, a dose-response study was performed (see Figure V-3); from which an IC_{50} of $46 \pm 2.2 \mu\text{M}$ was determined. Applying this IC_{50} to the Cheng-Prusoff equation, $K_i = \text{IC}_{50} / (1 + ([\text{Ligand}] / K_D))$, produces a K_i for 19615 of 5.6 μM .

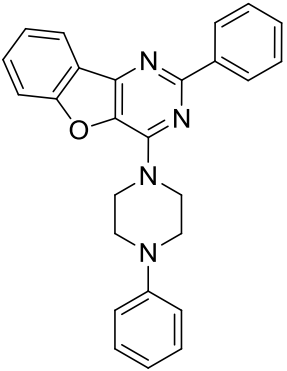
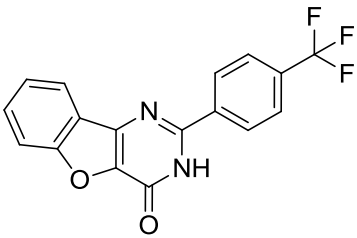
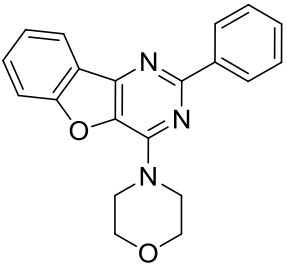
Table V-4. Results of 19615 Analog Testing in FP Assay.

Name	Structure	% Inhibition at 100 μM	Physical Properties
598089		68 ± 5	MW: 375.46 CLogP: 6.39 tPSA: 46.42

<p>19615 (original HTS hit)</p>		<p>63 ± 0.7</p>	<p>MW: 333.38 CLogP: 4.99 tPSA: 46.42</p>
<p>587109</p>		<p>43 ± 1</p>	<p>MW: 361.44 CLogP: 6.05 tPSA: 46.42</p>
<p>078044</p>		<p>42 ± 0.4</p>	<p>MW: 344.41 CLogP: 4.70 tPSA: 40.43</p>
<p>048181</p>		<p>31 ± 0.6</p>	<p>MW: 319.36 CLogP: 4.75 tPSA: 55.21</p>

582610		24 ± 0.3	MW: 271.31 CLogP: 3.39 tPSA: 46.42
050908		18 ± 0.4	MW: 299.37 CLogP: 4.45 tPSA: 46.42
9660232		17 ± 2	MW: 339.35 CLogP: 4.54 tPSA: 55.54
587469		16 ± 0.4	MW: 285.34 CLogP: 3.92 tPSA: 46.42

048373		15 ± 0.4	MW: 360.45 CLogP: 6.02 tPSA: 49.22
569084		11 ± 0.3	MW: 289.33 CLogP: 4.85 tPSA: 37.19
098754		6 ± 0.1	MW: 262.26 CLogP: 2.96 tPSA: 50.69
9660235		5 ± 0.2	MW: 409.48 CLogP: 7.26 tPSA: 46.42

568180		2 ± 0.1	MW: 406.48 CLogP: 6.13 tPSA: 40.43
765345		1 ± 0.1	MW: 330.26 CLogP: 3.87 tPSA: 50.69
9111063		-5 ± 0.1	MW: 331.37 CLogP: 4.14 tPSA: 46.42

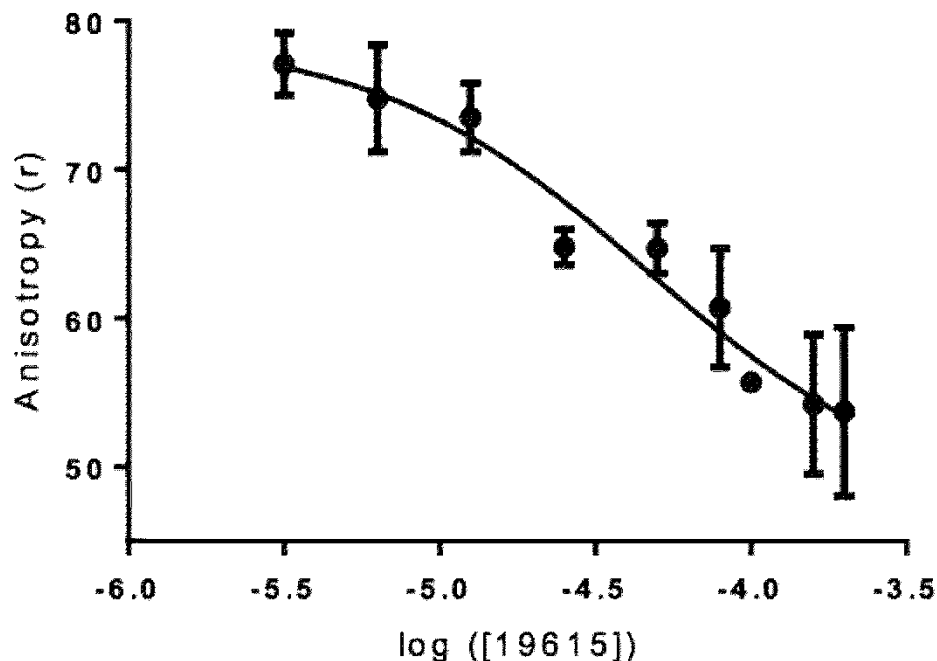


Figure V-3: Characterization of Compound 19615. Plot of inhibition of MalE-VirF binding to the *pvirB* DNA probe by 19615. Assay conducted with the MalE-VirF concentration constant at 20 μM . An IC_{50} of $46 \pm 2.2 \mu\text{M}$ for DNA binding was determined, which, by the Cheng-Prusoff equation, yields a derived $K_i = 5.6 \mu\text{M}$. The assay was conducted in duplicate.

DNA Affinity Determination via Fluorescence Intercalator Displacement (FID) Assay

To determine if 19615 was inhibiting VirF from binding to the *virB* promoter by directly binding to the DNA a fluorescence intercalator displacement (FID) assay was conducted. Berenil, a known minor groove binder with a preference for AT-rich sequences,^{6, 9} was used as a positive control. Two different *pvirB* probes were used in the study: a full length 60 bp probe, *pvirB* FID, and a 10 bp probe, *pvirB* 51-60 FID. A preliminary FID screen was conducted to determine which segment of the *virB* promoter to use for the 10 bp probe and the results are shown in Appendix Table V-1. As shown in Table V-5, Berenil was able to displace ethidium bromide from the *pvirB* DNA probes and lower the fluorescence signal generated in the assay to produce low %fluorescence values for all experimental conditions; on the other hand, **19615** was not able to

displace ethidium bromide from the *pvirB* DNA probes resulting in high %fluorescence values for all experimental conditions.

Table V-5. Results of the FID Assay.

Compound	60 bp <i>pvirB</i> FID probe %fluorescence	10 bp <i>pvirB</i> 51-60 FID probe %fluorescence
12.5 μ M 19615	93% \pm 3%	97% \pm 2%
25 μ M 19615	97% \pm 2%	97% \pm 3%
50 μ M 19615	95% \pm 2%	97% \pm 2%
100 μ M 19615	93% \pm 3%	95% \pm 1%
12.5 μ M Berenil	76% \pm 2%	52% \pm 1%
25 μ M Berenil	67% \pm 2%	51% \pm 2%
50 μ M Berenil	58% \pm 1%	51% \pm 1%
100 μ M Berenil	48% \pm 2%	46% \pm 1%

GFP Reassembly Assay

A split-GFP reassembly assay was used to try and monitor VirF dimerization. A variety of plasmids were constructed that expressed various VirF proteins (MalE-VirF, VirF, or the N-terminal domain of VirF (1-153)) fused to either an N-terminal GFP fragment (1-157) or a C-terminal GFP fragment (158-238). Plasmids were also designed to include the *virB* promoter and flip the fusion site of the C-terminal GFP fragment. Maps of all plasmids, including positive (leucine zipper fusions) and negative (GFP fragments alone) controls, are shown in Figures V-4 and V-5. The sequences of all plasmids used in this study were confirmed by DNA sequencing (DNA Sequencing Core, University of Michigan Ann Arbor).

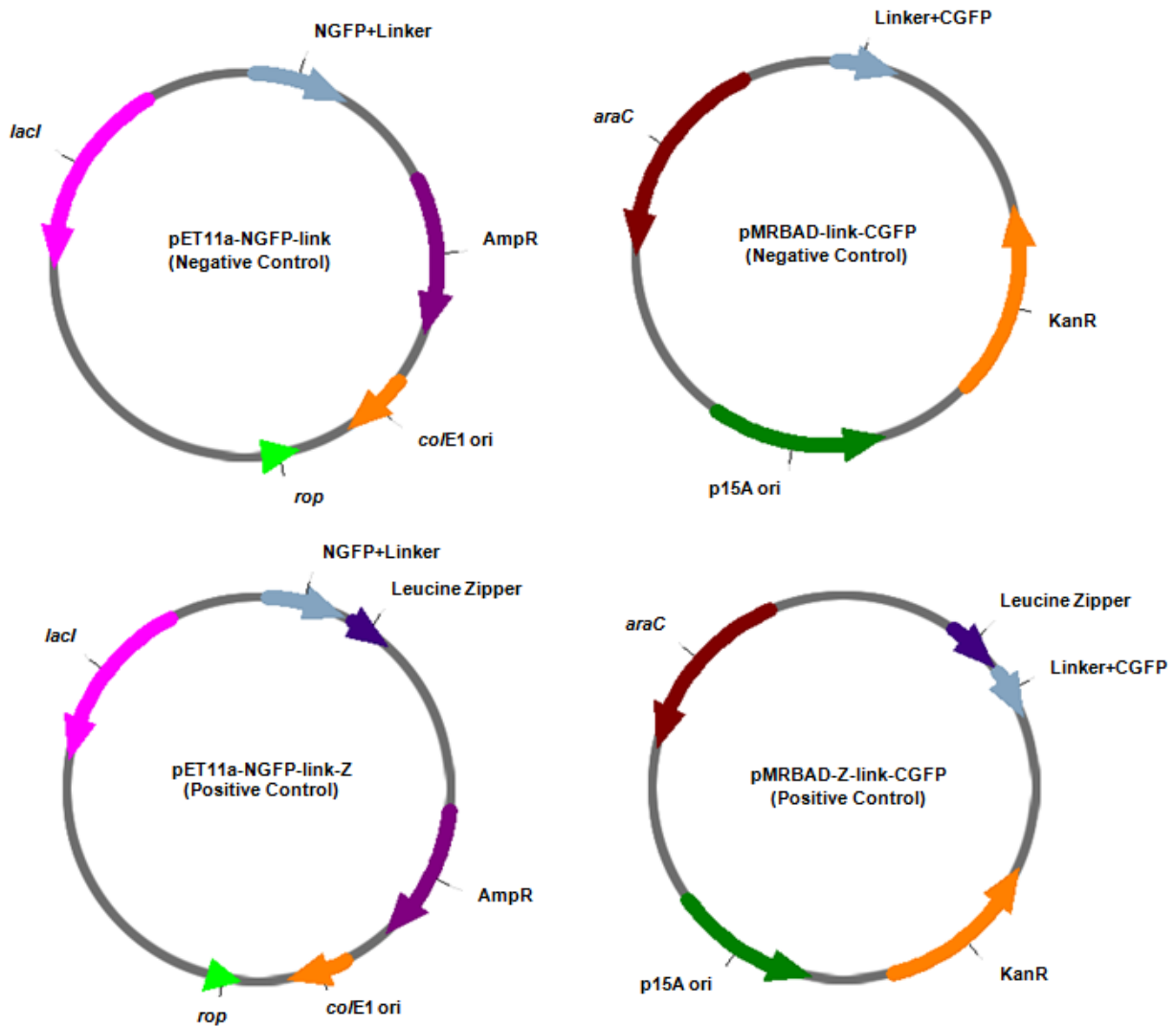


Figure V-4: Maps of Control Plasmids Used in GFP Reassembly Assay.

Appropriate pairs of GFP control and test vectors were co-transformed into *E. coli* BL21(DE3) cells. Following a 3 day induction period on LB_{CARB/KAN} plates containing 10 μM IPTG and 0.2% arabinose, fluorescent colonies were visualized using a UV transilluminator. Typical results from the GFP reassembly assay are shown in Figure V-6. In all trials, the GFP positive control strain would fluoresce, the GFP negative control strain would not fluoresce, and any VirF test strain would also not fluoresce. Table V-6 lists the results of all the different plasmid combinations that were used in the assay.

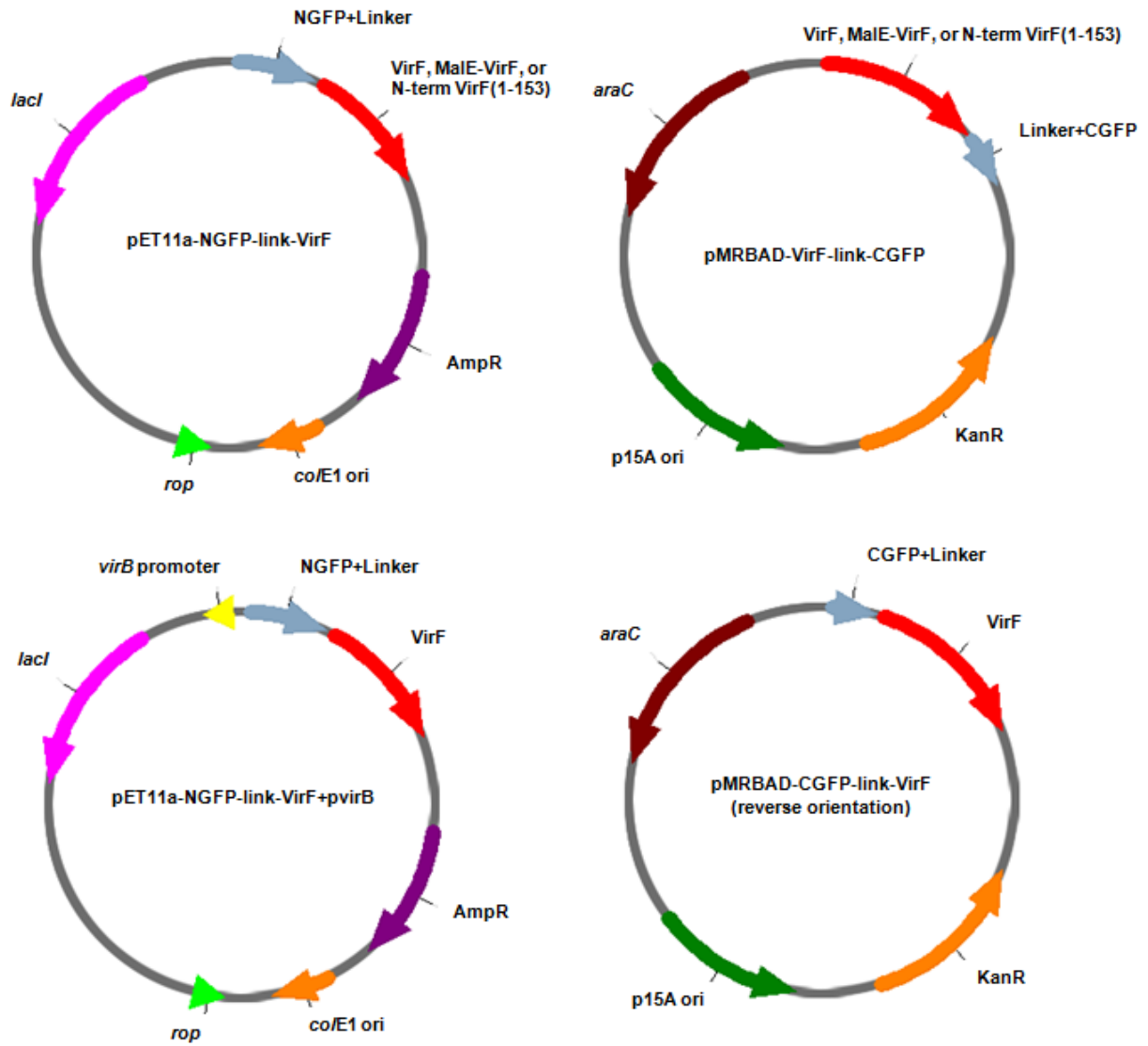


Figure V-5: Maps of Test Plasmids Used in the GFP Reassembly Assay.

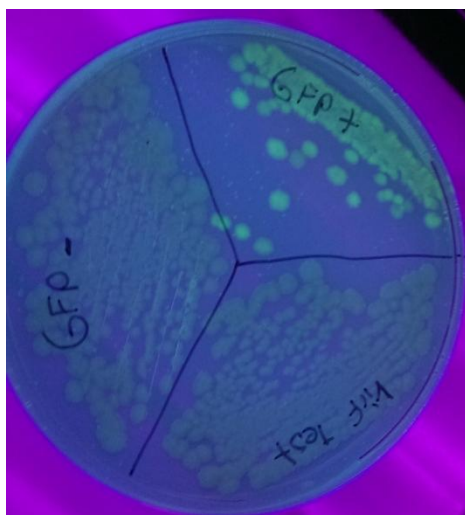


Figure V-6: Typical Results Seen in GFP Reassembly Assay.

Table V-6. List of all Plasmid Combinations Used in GFP Reassembly Assay.

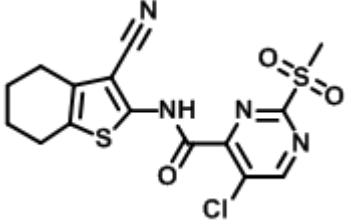
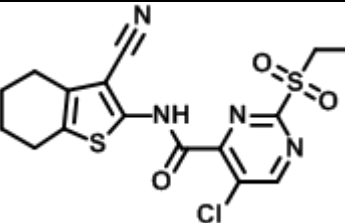
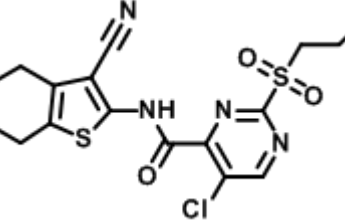
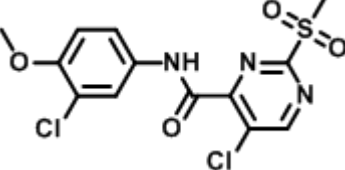
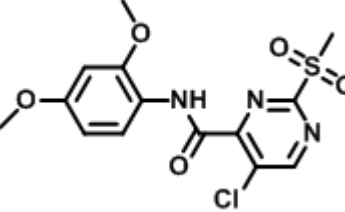
Plasmids	Type	Fluorescence
pET11a-NGFP-link and pMRBAD-link-CGFP	Negative Control	Negative
pET11a-NGFP-link-Z and pMRBAD-Z-link-CGFP	Positive Control	Positive
pET11a-NGFP-link-MalEVirF and pMRBAD-MalEVirF-link-CGFP	MalE-VirF Test	Negative
pET11a-NGFP-link-VirF and pMRBAD-VirF-link-CGFP	VirF Test	Negative
pET11a-NGFP-link-NTermVirF and pMRBAD-NTermVirF-link-CGFP	VirF(1-153) Test	Negative
pET11a-NGFP-link-VirF+pvirB and pMRBAD-VirF-link-CGFP	VirF with <i>pvirB</i> Test	Negative
pET11a-NGFP-link-VirF+pvirB and pMRBAD-CGFP-link-VirF (reverse)	VirF with <i>pvirB</i> Test	Negative

Testing of 144092/144143 Analogs

The *Shigella*-based, VirF-driven, β -galactosidase reporter assay was used to screen 33 analogs of compounds 144092 and 144143 in dose-response studies. Appendix Tables V-2 through V-4 provide the IC₅₀ values generated for each compound. The IC₅₀ values ranged from no inhibition to 23 μ M. Some compounds displayed toxicity towards the bacteria during the course of the assay and produced no

reporter signal. Lastly, the solubility of select compounds was determined after all 33 analogs were screened and these data are shown in Table V-7.

Table V-7. Solubility of Selected 144092/144143 Analogs.

Compound	IC ₅₀ (μM)	Solubility (mg/mL)	Assay Dilution (mg/mL)
	78	0.12	0.04
	23	0.14	0.04
	560	0.04	0.04
	45	0.23	0.04
	No Inhibition	0.01	0.04

Discussion

Researchers at Paratek Pharmaceuticals recently identified a series of benzimidazole compounds,¹⁰ similar to 153578, that inhibited the ability of LcrF, an AraC family transcriptional activator in *Yersinia* (and subsequently inhibited a number of other AraC family proteins), to bind to its DNA promoter region.¹ Egan and co-workers also recently found a small molecule that inhibited the ability of multiple AraC family members, including VirF, to bind DNA.³ These studies prompted us to focus our initial efforts on determining the effect our compounds had on VirF binding to its promoter.

To probe the mechanism of action of our five inhibitors we first screened them in modified versions of the EMSA and FP assay described in Chapter IV. The EMSA and FP assays were slightly modified to include 100 μM of compound in the reaction mixtures. This concentration (well above IC_{50} values for VirF transcriptional activation) was selected to ensure that if the compounds were acting through inhibition of DNA binding, it would be clearly evident in the assays. In the FP assay the MalE-VirF concentration was held constant at 20 μM , a concentration higher than its DNA-binding K_D value (2.8 μM , see Chapter IV) while still sub-saturating, to balance the magnitude of the anisotropy signal and the sensitivity to inhibition. As shown in Figure V-2 and Table V-4, only one compound, 19615, inhibited the binding of MalE-VirF to the *pvirB*. Surprisingly, 153578, the benzimidazole-derivative hit from our HTS, had little to no effect on DNA binding under these conditions. These results suggest that the other four compounds are inhibiting VirF activity at different steps of the gene activation process subsequent to DNA binding. (Another, albeit unlikely possibility is that the four other compounds may be metabolized *in vivo* to species that do inhibit VirF-DNA binding.

This will be determined as we continue to investigate their mechanisms of action.) If different molecular mechanisms of inhibition for the different compounds are confirmed, then the development of multiple compounds may circumvent any resistance and/or toxicity issues that could arise during further optimization of any one of the compounds.

Next, the mechanism of inhibition of compound 19615 was further probed. To determine if 19615 is a non-specific inhibitor of protein-DNA binding, a control EMSA was performed that revealed 19615 had no effect on *E. coli* RNA polymerase binding to the *lac* promoter (see Appendix Figure V-1). An FID assay was performed to ensure 19615 was not acting through DNA intercalation (see Table V-5), and lastly, a dose-response study was performed using the FP assay. As shown in Figure V-3, the dose-response study produced an IC_{50} of $46 \pm 2.2 \mu\text{M}$, which when applied to the Cheng-Prusoff equation produces a K_i for 19615 of $5.6 \mu\text{M}$. In Chapters II and III, we determined an IC_{50} for 19615 in the *Shigella*-based, VirF-driven, β -galactosidase reporter assay to be $14 \mu\text{M}$ and showed that 19615 inhibited the initial invasion of *S. flexneri* into Caco-2 monolayers by $\sim 75\%$ at $6.25 \mu\text{M}$. The correlation between these results and the K_i for inhibition of VirF binding to DNA strongly suggest that 19615 attenuates the virulence of *S. flexneri* by decreasing VirF-driven transcriptional activation via inhibition of VirF-DNA binding. This, combined with the fact that 19615 was not toxic to mammalian cells or *S. flexneri* at the tested concentrations makes 19615 an attractive candidate for further exploration.

The next logical step in developing 19615 into an anti-virulence therapy for treating shigellosis is to improve its potency through structural optimization. To construct an initial SAR, a small library of analogs of 19615 were purchased and

screened in the FP assay. The FP assay was chosen over other assays previously developed (e.g., *Shigella*-based reporter assay, tissue culture-based virulence assays) because it eliminates a number of complicating factors associated with measuring efficacy in the other assays, such as permeability and cytotoxicity. Unfortunately, none of the compounds tested proved to be significantly more potent than 19615, see Table V-4. It is worth noting that the goal of testing this panel of analogs was primarily to provide supporting evidence for the mechanism of action of 19615 and secondarily to find a compound that was more potent than compound 19615. Some notable trends identified from the data shown in Table V-4 (see p.105 - 109) include (a) preference of a phenyl ring substituent over smaller alkyl chains attached to the pyrimidine (e.g., 19615 vs. 582610 or 587469), (b) preference of side chain ether rather than amine linkage to pyrimidine (e.g., 587109 vs. 048373), and (c) preference for the dimethyl amine over the diethyl amine on the ether side chain (19615 vs. 587109 and 582610 vs. 050908). The data also suggest that there is considerable space for favorable SAR development through the installation of additional basic side chain ethers and aromatic moieties off the pyrimidine ring. Figure V-7 depicts the most promising trends that will serve as the starting point for later generations of 19615 analogs with the goal of developing a more potent inhibitor.

To probe the mechanism of inhibition of the other four compounds, we sought to develop assays that monitored the dimerization of VirF. Analytical gel filtration studies showed that purified MalE-VirF exists as a monomer under the conditions the EMSA and FP assays are conducted (see Chapter IV Appendix). Our previous struggles with purified VirF aggregation and solubility prompted us to develop a bacteria-based

method to monitor dimerization. We chose to use a split-GFP reassembly assay. Split-GFP reassembly assays have been used by many groups to monitor protein-protein interactions inside the cell,¹¹⁻¹⁵ including monitoring homodimerization.¹⁶ The bacteria-based split-GFP assay was first developed by the laboratory of Dr. Lynne Regan,^{8, 17} who used it to monitor the interaction between anti-parallel leucine zippers. They showed that GFP fragments could not reassemble unless they were fused to interacting proteins; they also predicted that the assay was sensitive enough to monitor interactions with dissociation constants as high as 1 mM.

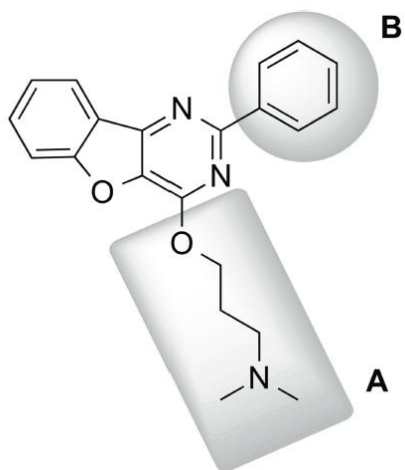


Figure V-7: Figure Depicting Deduced SAR. Structure shown is a hybrid compound containing most promising substituents and will serve as a starting point for future synthetic SAR studies that will probe the core heterocycle. Region A: SAR data suggest the preferred substituent at this position is an ether chain with a 2-3 carbon spacer and small aminoalkyl headpiece. Region B: SAR data suggest the preferred substituent at this position is an aromatic ring, although further probing with substituted phenyl and heteroaromatic moieties is needed.

The split-GFP reassembly assay offered us many advantages. For one, it allowed us the flexibility to test multiple different forms of VirF (MalE-VirF, wildtype VirF, and the N-terminal fragment of VirF(1-153)) in the presence and absence of the *virB*

promoter through simple cloning procedures. It is still not known if VirF needs to bind to its promoter region before it can dimerize. The split-GFP platform, in theory, offered a way to answer this question. Also, it provided a read-out that could be easily visualized during the development phase but could also be measured quantitatively for more accurate measurements of each compounds' inhibitory effects. Lastly, Dr. Lynne Regan was kind enough to send us the positive control vectors, negative control vectors, and empty test vectors which greatly simplified the development process.

Unfortunately, as shown in Table V-6, no combinations of VirF test vectors were able to promote GFP reassembly. Therefore, VirF dimerization could not be monitored with this platform. Initial GFP assay trials had the N-Terminal GFP fragment attached to the N-terminal of VirF (either MalE-VirF, wildtype VirF, or VirF(1-153)) and the C-terminal GFP fragment attached to the C-terminal of VirF (either MalE-VirF, wildtype VirF, or VirF(1-153)). These trials were later repeated with the *virB* promoter cloned into the N-terminal GFP plasmid. Lastly, the C-terminal GFP fragment was moved to the N-terminal of VirF to probe if the GFP fragment orientation was preventing VirF dimerization; still no fluorescence was achieved. It is still possible that with further optimization (e.g. alteration of the linker lengths between GFP fragments and VirF, moving GFP fragments to the C-terminal of VirF) VirF dimerization could be monitored with this assay; however, it is also likely that VirF dimerization will never be able to drive the reassembly of GFP. Statistically, only one third of all successful VirF homodimerization events would allow for GFP reassembly in the assay; at best the GFP signal would be attenuated. Therefore, in future studies, we plan on switching to an

SPR approach to monitor VirF dimerization and hopefully identify the mechanisms of inhibition of the remaining four compounds.

Although we were not able to identify the mechanism of inhibition of compounds 144092 and 144143, we were still intrigued by their properties. In previous studies, both compounds inhibited VirF transcriptional activation and both inhibited either the initial invasion or the cell-to-cell spread of *S. flexneri* in Caco-2 monolayers at concentrations that were not toxic to the bacteria or the cells. The compounds also appear to be perfect candidates for a SAR campaign since they share a core pyrimidine scaffold. To identify potential SAR trends, we ordered a library of 144092/144143 analogs and screened them in the *Shigella*-based, VirF-driven, β -galactosidase reporter assay. The results of the screen are shown in Appendix Tables V-2 to V-4. Unfortunately, complicating factors such as cell permeability, cytotoxicity, and solubility (could not increase organic solvent content over 1% without deleterious effects on assay) prevented activity trends from being identified. For example, as shown in Table V-7, there appears to be an increase in activity associated with increasing the length of the alkyl chain off of the sulfone until the solubility of the next compound prevents accurate testing in the assay. It is now clear, that an *in vitro* assay will be needed to identify any SAR trends. We are currently optimizing an *in vitro* transcription assay to re-screen this library of analogs.

In this report, we have determined the mechanism of VirF inhibition by compound 19615 and have constructed an initial SAR to be used for further development. However, at the present time, we do not yet have direct evidence to indicate that 19615's effects are specific to VirF versus other AraC family transcription factors,

although we have determined that 19615 does not interfere with RNA polymerase binding to DNA. There is precedent for small molecules to exhibit cross-reactivity against multiple AraC family members.^{10, 18, 19} To examine the specificity of 19615, we plan to test it (or a more potent analogue) in EMSAs against a variety of other AraC family regulators, such as ToxT (virulence) from *Vibrio cholera*, MarA (multi-drug resistance) from *E. coli*, and AraC (arabinose operon) from *E. coli*. Once specificity is determined, we will conduct mutagenesis studies to further probe the interactions between the compound and its target(s). We also plan on determining the mechanism of action of the other hits from our high-throughput screen, conducting a synthetic SAR study of 19615 to probe the core heterocyclic structure, and continuing our work towards the development of an anti-virulence therapy to treat shigellosis.

Notes to Chapter V

I would like to acknowledge the following people who contributed to the work presented in this chapter: Justin Arrendondo-Guerrero (University of Michigan REU program, home institution: University of the Incarnate Word, San Antonio, Texas) for contributions made to the GFP reassembly assay, Dr. Amanda Garner (Department of Medicinal Chemistry, University of Michigan) for the use of the SpectraMax M5 plate reader and gel imager in her laboratory, and Dr. Hollis Showalter (Department of Medicinal Chemistry, University of Michigan) for his organic chemistry knowledge. Some of the work presented here was published in Emanuele and Garcia, *PLoS ONE* **2015**, 10, e0137410.²⁰

References

1. Garrity-Ryan, L. K.; Kim, O. K.; Balada-Llasat, J. M.; Bartlett, V. J.; Verma, A. K.; Fisher, M. L.; Castillo, C.; Songsunthong, W.; Tanaka, S. K.; Levy, S. B.; Meccas, J.; Alekshun, M. N. Small Molecule Inhibitors of LcrF, a *Yersinia pseudotuberculosis* Transcription Factor, Attenuate Virulence and Limit Infection in a Murine Pneumonia Model. *Infection and Immunity* **2010**, 78, 4683-4690.
2. Hung, D. T.; Shakhnovich, E. A.; Pierson, E.; Mekalanos, J. J. Small-Molecule Inhibitor of *Vibrio cholerae* Virulence and Intestinal Colonization. *Science* **2005**, 310, 670-674.
3. Koppolu, V.; Osaka, I.; Skredenske, J. M.; Kettle, B.; Hefty, P. S.; Li, J.; Egan, S. M. Small-molecule inhibitor of the *Shigella flexneri* master virulence regulator VirF. *Infection & Immunity* **2013**, 81, 4220-31.
4. Porter, M. E.; Dorman, C. J. In vivo DNA-binding and oligomerization properties of the *Shigella flexneri* AraC-like transcriptional regulator VirF as identified by random and site-specific mutagenesis. *Journal of Bacteriology* **2002**, 184, 531-9.

5. Maurelli, A. T.; Blackmon, B.; Curtiss III, R. Loss of pigmentation in *Shigella flexneri* 2a is correlated with loss of virulence and virulence associated plasmid. *Infection and Immunity* **1984**, 43, 397-401.
6. Tse, W. C.; Boger, D. L. A Fluorescent Intercalator Displacement Assay for Establishing DNA Binding Selectivity and Affinity. *Accounts of Chemical Research* **2004**, 37, 61-69.
7. Tse, W. C.; Boger, D. L. A Fluorescent Intercalator Displacement Assay for Establishing DNA Binding Selectivity and Affinity. *Current Protocols in Nucleic Acid Chemistry* **2005**, 8.5.1-8.5.11.
8. Wilson, C. G.; Magliery, T. J.; Regan, L. Detecting protein-protein interactions with GFP-fragment reassembly. *Nature Methods* **2004**, 1, 255-262.
9. Nguyen, B.; Hamelberg, D.; Bailly, C.; Colson, P.; Stanek, J.; Brun, R.; Neidle, S.; Wilson, W. D. Characterization of a Novel DNA Minor-Groove Complex. *Biophysical Journal* **2004**, 86, 1028-1041.
10. Kim, O. K.; Garrity-Ryan, L. K.; Bartlett, V. J.; Grier, M. C.; Verma, A. K.; Medjanis, G.; Donatelli, J. E.; Maccone, A. B.; Tanaka, S. K.; Levy, S. B.; Alekshun, M. N. N-hydroxybenzimidazole inhibitors of the transcription factor LcrF in *Yersinia*: novel antivirulence agents. *J Med Chem* **2009**, 52, 5626-34.
11. Lindman, S.; Johansson, I.; Thulin, E.; Linse, S. Green fluorescence induced by EF-hand assembly in a split GFP system. *Protein Science* **2009**, 18, 1221-1229.
12. Jackrel, M. E.; Cortajarena, A. L.; Liu, T. Y.; Regan, L. Screening Libraries To Identify Proteins with Desired Binding Activities Using a Split-GFP Reassembly Assay. *ACS Chemical Biology* **2010**, 5, 553-562.
13. Barnard, E.; McFerran, N. V.; Trudgett, A.; Nelson, J.; Timson, D. J. Detection and localisation of protein-protein interactions in *Saccharomyces cerevisiae* using a split-GFP method. *Fungal Genetics and Biology* **2008**, 45, 597-604.
14. Sarkar, M.; Magliery, T. J. Re-engineering a split-GFP reassembly screen to examine RING-domain interactions between BARD1 and BRCA1 mutants observed in cancer patients. *Molecular BioSystems* **2008**, 4, 599-605.

15. Chun, W.; Waldo, G.; Johnson, G. W. Split GFP Complementation Assay for Quantitative Measurement of Tau Aggregation In Situ. In *Alzheimer's Disease and Frontotemporal Dementia*, Roberson, E. D., Ed. Humana Press: 2011; Vol. 670, pp 109-123.
16. Han, X.; Liu, D.; Zhang, Y.; Li, Y.; Lu, W.; Chen, J.; Songyang, Z. Akt regulates TPP1 homodimerization and telomere protection. *Aging Cell* **2013**, 12, 1091-1099.
17. Magliery, T. J.; Wilson, C. G. M.; Pan, W.; Mishler, D.; Ghosh, I.; Hamilton, A. D.; Regan, L. Detecting Protein-Protein Interactions with a Green Fluorescent Protein Fragment Reassembly Trap: Scope and Mechanism. *Journal of the American Chemical Society* **2005**, 127, 146-157.
18. Skredenske, J. M.; Koppolu, V.; Kolin, A.; Deng, J.; Kettle, B.; Taylor, B.; Egan, S. M. Identification of a Small-Molecule Inhibitor of Bacterial AraC Family Activators. *Journal of Biomolecular Screening* **2010**, 18.
19. Bowser, T. E.; Bartlett, V. J.; Grier, M. C.; Verma, A. K.; Warchol, T.; Levy, S. B.; Alekshun, M. N. Novel anti-infection agents: small-molecule inhibitors of bacterial transcription factors. *Bioorganic & Medicinal Chemistry Letters* **2007**, 17, 5652-5.
20. Emanuele, A. A.; Garcia, G. A. Mechanism of Action and Initial, In Vitro SAR of an Inhibitor of the *Shigella flexneri* Virulence Regulator VirF. *PLoS ONE* **2015**, 10, e0137410.

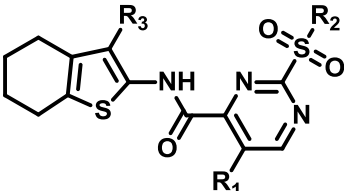
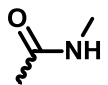
Appendix

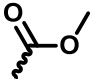
Appendix Table V-1. FID Assay with 10 bp *pvirB* Probes.

10 bp <i>pvirB</i> Fragment	19615 (2 μ M) %fluorescence	Berenil (2 μ M) %fluorescence
<i>pvirB</i> 1-10 (5'-AGAATATTAT-3')	93% \pm 6%	45% \pm 2%
<i>pvirB</i> 11-20 (5'-TCTTTTATCC -3')	95% \pm 3%	66% \pm 0%
<i>pvirB</i> 21-30 (5'-AATAAAGATA -3')	92% \pm 1%	81% \pm 4%
<i>pvirB</i> 31-40 (5'-AATTGCATCA -3')	94% \pm 2%	89% \pm 5%
<i>pvirB</i> 41-50 (5'-ATCCAGCTAT -3')	94% \pm 1%	96% \pm 2%
<i>pvirB</i> 51-60 (5'-TAAAATAGTA -3')*	92% \pm 0%	67% \pm 0%

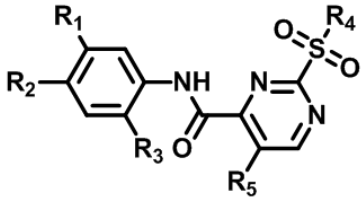
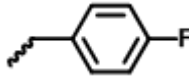
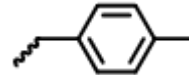
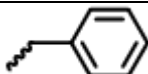
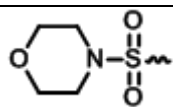
**pvirB* 51-60 was selected for use in the dose-response FID assay since it was sensitive to Berenil (67%) and was the most sensitive to 19615 (92%) in this study. The differential affinity of Berenil for the various 10 BP fragments reflects its preference for specific AT-rich sequences.

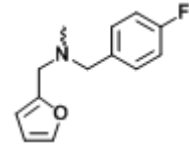
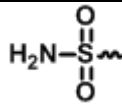
Appendix Table V-2. SAR Table for 144143 Analogs.

				
Compound	IC ₅₀ (μ M)	R ₁	R ₂	R ₃
144143	23	Cl	CH ₂ CH ₃	$\text{---}\equiv\text{N}$
D053-0233	78	Cl	CH ₃	$\text{---}\equiv\text{N}$
D053-0411	560	Cl	CH ₂ CH ₂ CH ₃	$\text{---}\equiv\text{N}$
STK518484	79	Br	CH ₂ CH ₃	$\text{---}\equiv\text{N}$
D053-0337	No Inhibition	Cl	CH ₂ CH ₃	

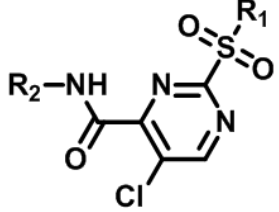
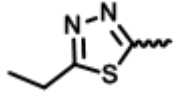
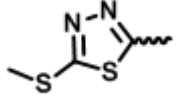
D053-0332	No Inhibition	Cl	CH ₂ CH ₃	
-----------	---------------	----	---------------------------------	---

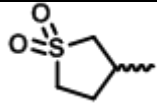
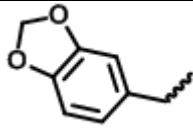
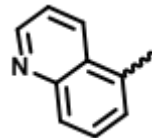
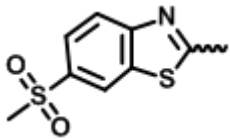


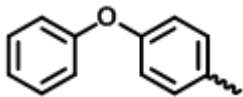
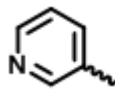
Appendix Table V-3. SAR Table for 144092 Analogs.

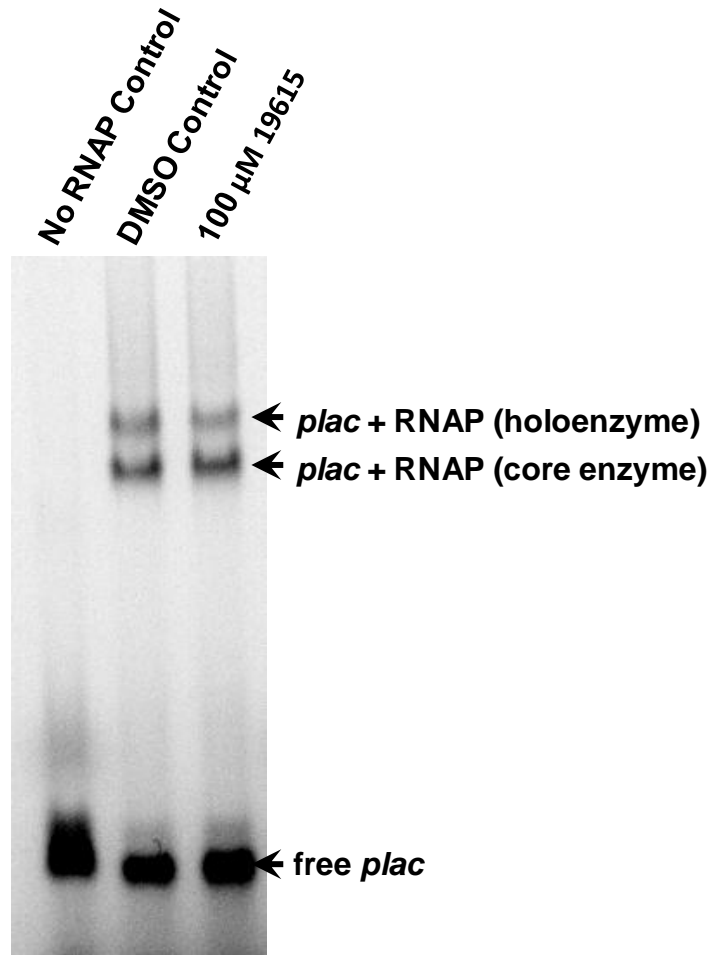
						
Compound	IC ₅₀ (μM)	R ₁	R ₂	R ₃	R ₄	R ₅
144092	23	Cl	OCH₃	H	CH₃	Cl
D053-0099	110	Cl	OCH ₃	H	CH ₂ CH ₃	Cl
D053-0184	194	Cl	OCH ₃	H	CH ₂ CH ₂ CH ₃	Cl
D233-0313	207	H	OCH ₃	H		Cl
D233-0369	195	H	OCH ₃	H		Cl
D233-0481	570	H	OCH ₃	H		Cl
D053-0102	165	Cl	CH ₃	H	CH ₂ CH ₃	Cl
D053-0008	112	H	NO ₂	H	CH ₃	Cl
D053-0244	115	H		H	CH ₃	Cl

D299-0375	232	Cl	OCH ₃	H	CH ₃	
D053-0089	No Inhibition	H		H	CH ₂ CH ₃	Cl
D053-0106	No Inhibition	Cl	H	O-CH ₃	CH ₂ CH ₃	Cl
D053-0022	No Inhibition	H	OCH ₃	O-CH ₃	CH ₃	Cl
D053-0003	Cytotoxic	H	OCH ₃	H	CH ₃	Cl
D053-0006	Cytotoxic	Cl	H	H	CH ₃	Cl
STK518445	Cytotoxic	Cl	H	H	CH ₂ CH ₃	Br

Appendix Table V-4. SAR Table for Pyrimidine Analogs.

			
Compound	IC ₅₀ (μM)	R ₁	R ₂
D053-0260	61	CH ₃	
D053-0292	70	CH ₃	

D053-0094	116	CH ₂ CH ₃	
D053-0037	59	CH ₃	
STK938588	285	CH ₃	
D053-0239	No Inhibition	CH ₃	
STK938480	No Inhibition	CH ₃	
STK936637	No Inhibition	CH ₃	
STK934554	Cytotoxic	CH ₂ CH ₃	
D053-0024	Cytotoxic	CH ₃	
STK787063	Cytotoxic	CH ₃	H



Appendix Figure V-1: EMSA depicting *E. coli* RNA Polymerase (RNAP) Binding to the *lac* Promoter (*plac*) in the Presence of 19615. EMSA image shows the retardation of a 5'Cy5-*plac* DNA probe (0.25 μ M) when incubated in the presence of *E. coli* RNAP (2.7 μ M) and also shows that compound 19615 has no effect on RNAP binding when tested at 100 μ M. For the EMSA a hybrid 2% acrylamide, 1% agarose gel was used which was made with and ran in a 1X TGE buffer (25 mM Tris base, 190 mM glycine, 1 mM EDTA, pH 8.3). The sequence of the 5'Cy5-*plac* DNA probe is as follows: 5'-gtgccctggtctggTTAGGCACCCCAGGCTTTACACTTTATGCTTCCGGCTCGTATAATGTGTGGAATTGTGAG-3' (lowercase text represents LUEGO sequence, uppercase text represents *lac* promoter sequence).

CHAPTER VI

HTS of ~20,000 Marine Natural Product Extracts Against *Shigella flexneri*:

Identification of Globomycin and Desferrioxamine E

As detailed in Chapter II and as previously reported,^{1, 2} we have successfully screened over 140,000 small molecules utilizing a *Shigella*-based, VirF-driven, β -galactosidase reporter assay in an attempt to identify small-molecule virulence inhibitors of *S. flexneri*. From the small molecule high-throughput screening (HTS) campaign, we identified five promising small molecule VirF inhibitors with IC₅₀ values ranging from 14 to 66 μ M.¹ While the results of our small molecule screen were promising, we believed a more potent VirF inhibitor scaffold might be identified by sampling a larger range of chemical diversity.

Nature's small molecules, which possess biological activities and are obtained from natural resources, e.g. plants, animals, and microorganisms, are defined as *Natural Products (NPs)*. Over the past century, the complexity and diversity of these natural product scaffolds and appended functional groups have been an inspiration to chemists involved in pharmaceutical discovery, developing spectroscopic technology and devising principles and strategies for total synthesis, both biomimetic and abiotic.³ Interestingly, mankind has known for at least several thousand years that marine organisms contain substances capable of potent biological activity, but in contrast to investigations on terrestrial NPs the first serious work on marine organisms started about 60 years ago with the pioneering work of Werner Bergman, when he published

reports of unusual *arabino*- and *ribo*-pentosyl nucleosides obtained from marine sponges collected in Florida, USA.⁴⁻⁶ Moreover, NPs have been used by human societies for millennia. Many NPs and synthetically modified NP derivatives have been successfully developed for clinical use to treat human diseases, particularly as anticancer drugs and antibiotics.⁷

To take advantage of the wealth of chemical diversity found within NPs, we conducted a follow-up HTS on a natural product extracts (NPEs) library developed in the laboratory of Dr. David Sherman (Life Sciences Institute, University of Michigan Ann Arbor). This NPE library contains over 20,000 NPEs derived from a collection of marine organisms (e.g., sponges, sediments, and cyanobacteria) taken from across the globe (Papua New Guinea, Costa Rica, US Virgin Islands, Panama, Lake Erie, Lake Huron and Antarctica). For the screening of the NPE library, the small molecule HTS was altered to include an optical density reading to monitor bacterial growth levels. This alteration allowed for the detection of both bactericidal/bacteriostatic agents and potential virulence inhibitors from the NPE library.

In this report, we first detail the results of our NPE HTS. During the HTS, we observed not only extracts that inhibited bacterial growth and VirF activity, but also extracts that stimulated an increase in β -galactosidase activity, apparently by increasing the VirF-driven expression of β -galactosidase. Investigation of these apparent VirF activator extracts might provide insight into the mechanism VirF uses to activate transcription. Therefore, in the second part of this we report, we describe our efforts to identify and characterize the active components from an extract that stimulated β -galactosidase activity and an extract that inhibited β -galactosidase activity.

Materials and Methods

Reagents and General Methods

All reagents were purchased from Sigma-Aldrich (St. Louis, MO), unless otherwise specified. CPRG (chlorophenol red β -D-galactopyranoside) was purchased from Roche (Basel, Switzerland). Yeast extract, bactotryptone, carbenicillin, and Corning microtiter plates (384 and 96 well) were purchased from Fisher Scientific (Hampton, NH). All NMR spectra were acquired on a Varian INOVA 500 MHz and a Varian INOVA 700 MHz spectrometer at the NMR Facility, Department of Chemistry, University of Michigan. High-resolution MS spectra were measured at the University of Michigan core facility in the Department of Chemistry using Agilent 6520 Quadruple-Time of Flight mass spectrometer equipped with Agilent 1290 HPLC system. RP-HPLC was performed using Waters Atlantis® Prep T3 OBD™ 5 μ m 19 \times 250 mm column and Waters XBridge™ 5 μ M 19 \times 150 mm C18 column using solvent system of ACN and H₂O. The LCMS analysis of HPLC fractions was performed on a Shimadzu 2010 EV APCI spectrometer.

Strains and Plasmids

The avirulent strain of *S. flexneri*, BS103, used in the HTS and reconfirmation testing was a generous gift from Dr. Anthony Maurelli (Uniformed Services University of the Health Sciences, Bethesda, MD). The construction of the reporter plasmid, pMALvirF-LacZ, and positive control plasmid, pMAL(Δ virF)-LacZ was previously reported.² The following strains used in the minimum inhibitory concentration (MIC) study were a generous gift from Dr. Sylvie Garneau-Tsodikova (currently at the University of Kentucky): *Bacillus subtilis* 168, *Bacillus cereus* ATCC1778, *Bacillus*

anthracis 34F2 Sterne, *Escherichia coli* MC1061, *Enterococcus faecalis* ATCC29212, *Listeria monocytogenes* ATCC19115, and *Salmonella enterica* ATCC14028. The *E. coli* EC2880 strain (permeable strain with *tolC* and *imp*⁻ mutations) used in the MIC study was a generous gift from Dr. Michael Hubbard (Pfizer Scientific). A Vancomycin-resistant *Enterococcus* strain and a methicillin-resistant *Staphylococcus aureus* strain were contributed by the Sherman laboratory (University of Michigan, Ann Arbor) and were also screened in the MIC study.

Natural Product Extract Library

The NPE library contained 20,061 extracts that were derived from a collection of various marine organisms sampled from across the globe. Microbes found in the collection of samples were carefully cultured and grown to a suitable cell mass for organic extraction. Each culture underwent organic extractions with three different solvents: methanol, acetone, and ethyl acetate. The extracts generated from the cultures were dried, dissolved in DMSO (to a final concentration of 15 mg/mL), and stored in plates amenable to high-throughput screening. The NPE library is stored and was screened at the Center for Chemical Genomics (Life Sciences Institute, University of Michigan Ann Arbor).

High-throughput, VirF-driven, β -galactosidase Reporter Assay

The NPE HTS was performed as previously described² with a few modifications. Samples containing *Shigella flexneri* BS103 harboring pMALvirF-LacZ (or the positive control for no β -galactosidase activity, pMAL(Δ virF)-LacZ) were grown to saturation in 2xTY at 37°C with shaking. Extracts from the NPE library were added to 20 μ L 2xTY in the appropriate wells of each 384-well plate (0.1 mg/mL, $n=2$, 0.2 μ L) by Biomek HDR

(Beckman). Cells were diluted with 2xTY supplemented with 100 µg/mL carbenicillin to a final OD₆₀₀ = 0.004 and 10 µL was added to the 384-well microtiter plates with the Multidrop dispenser (Thermo Scientific) (30 µL total volume). Plates were then centrifuged at 1000 rpm for one minute using a Beckman Coulter Allegra Series centrifuge before being incubated for 20 hours at 30°C in a humidified incubator (VWR). Cell density (OD₆₀₀) was measured prior to addition of an equal volume (30 µL) of 0.5 mg/mL CPRG and 0.1% Triton X-100 in Miller's Z-buffer (60 mM Na₂HPO₄, pH 7.0; 40 mM NaH₂PO₄; 10 mM KCl; 1 mM MgSO₄).⁸ The samples were incubated at room temperature for 10 minutes before measuring chlorophenol red (CPR) absorbance (A₅₇₀) in a PHERAstar (BMG Labtech) plate reader with a narrow band pass filter.

Selection Criteria

See Figure VI-1 for a flowchart of the selection and counter screen process. For the VirF inhibition high-throughput screen, extracts were considered hits if they produced ≥25% VirF inhibition or their minimum standard deviation was ≥3.0 (calculated on a plate by plate basis using the negative controls only) and if they exhibited ≤25% cell growth inhibition and ≤25% β-galactosidase inhibition. Extracts were selected for reconfirmation testing if they produced ≥45% VirF inhibition or if two or more extracts taken from the same culture both produced ≥30% VirF inhibition.

For the cell growth inhibition screen, extracts were considered hits if they produced ≥25% cell growth inhibition against *S. flexneri* BS103 cells harboring pMALvirF-LacZ. Extracts were selected for reconfirmation testing if they also produced ≥25% cell growth inhibition against *S. flexneri* BS103 cells harboring pMAL(ΔvirF)-LacZ.

Extracts were considered hits for VirF activation if they produced a rapid, visual increase in CPRG cleavage compared to the negative controls. Extracts were selected for reconfirmation testing if in the dose-response study their pAC₅₀ for VirF activation was 0.5 larger than their pAC₅₀ for cell growth inhibition. Note: pAC₅₀ = -log(AC₅₀)

Counter Screens

All extracts that met the selection criteria for VirF inhibition were subjected to a β -galactosidase inhibition screening. For the screen, cultures of *S. flexneri* BS103 harboring either pMALvirF-LacZ or pMAL(Δ virF)-LacZ were diluted to OD₆₀₀=1.0 using 2xTY media supplemented with 100 μ g/mL carbenicillin and added to appropriate wells of a 384-well plate using the multidrop dispenser (30 μ L). Extracts were added to the plates in duplicate at a concentration of 0.1 mg/mL. Immediately following extract addition, CPRG solution was added to each well (30 μ L). After a 10-minute incubation period at room temperature, chlorophenol red absorbance (A₅₇₀) was measured using a PHERAstar plate reader to determine if the extracts directly inhibited β -galactosidase. All extracts that met the selection criteria for cell growth inhibition were screened again against the control strain, *S. flexneri* BS103 harboring pMAL(Δ virF)-LacZ, using the screening protocol described above.

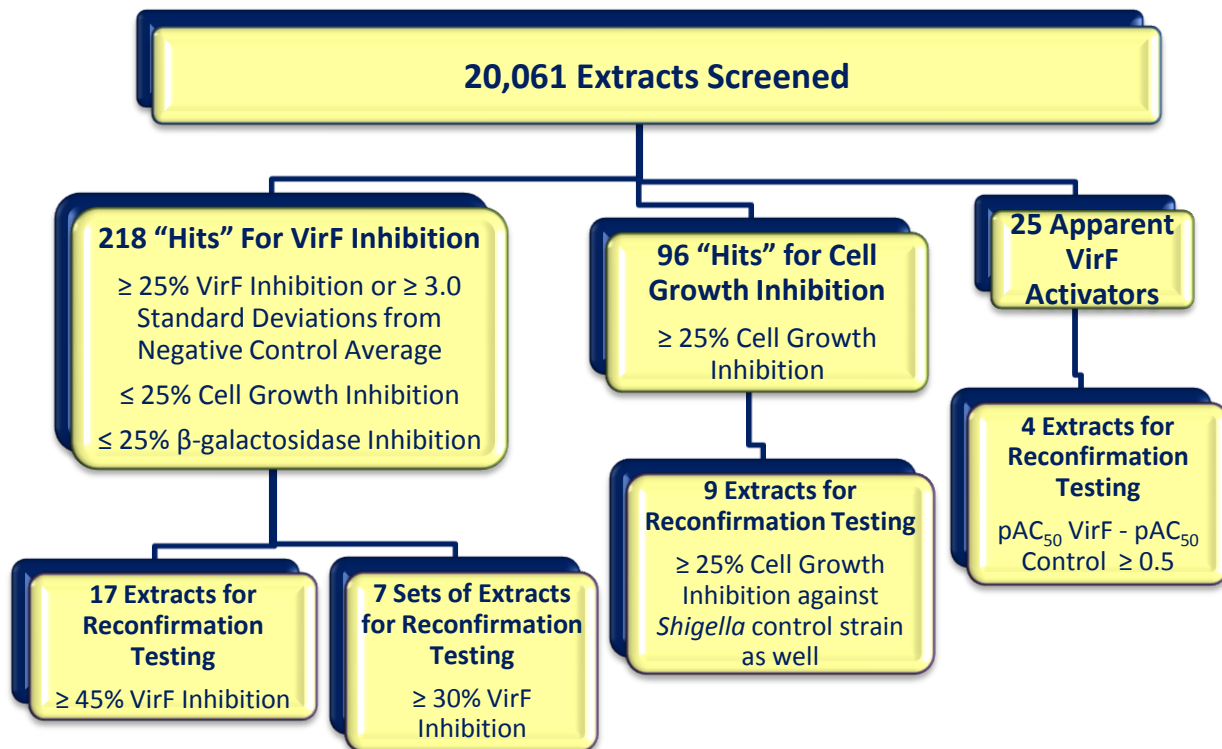


Figure VI-1: Flow Chart Depicting the Results of the HTS Campaign. See Materials and Methods for details regarding the selection criteria.

All extracts that produced apparent VirF activation in the HTS were subjected to two different counter screens. The first counter screen verified that the extracts were not chemically cleaving CPRG. For this screen 30 μL of 2xTY media supplemented with 100 $\mu\text{g}/\text{mL}$ carbenicillin was added to appropriate wells of a 384-well plate using the multidrop dispenser. Extracts were added to the plates in duplicate at a concentration of 0.1 mg/mL . Immediately following extract addition, CPRG solution was added to each well (30 μL). After a 10-minute incubation period at room temperature, chlorophenol red absorbance (A_{570}) was measured using a PHERAstar plate reader to determine if the extracts could directly cleave CPRG. The second counter was a dose-

response study that followed the screening protocol described above. However, for the dose-response study, the concentration of the extracts was varied using 2-fold serial dilutions ranging from 0.3 mg/mL to 0.002 mg/mL. Note: for the dose response study the CPRG incubation time was lowered from 10 min to 2.5 min to ensure that the upper detection limit of the spectrophotometer was not reached.

Active Natural Product Extract Strain Regrowth

Streptomyces sp. 34443-A2 and *Streptomyces* sp. 44306-A41 were isolated from marine sediments collected at a depth of 15 m during a scuba diving expedition at Playa Langosta, Costa Rica (-85°51'41", 10°16'24.9") near Diria National Park, Costa Rica. The procedure for the isolation of actinomycetes from these samples was previously described by Magarvey et al.⁹ Maintenance and propagation of cultures were performed using standard media and protocols where 500 mg of wet sediment was diluted in 10 mL of sterile water and vortexed for 10 min. One mL of this suspension was then applied directly to the top of the discontinuous sucrose gradient and centrifuged for 30 minutes at 300 x g. Next, 500 µL of the 20%, 30%, and 40% layers were plated on HVA agar supplemented with 10 µg/mL chlortetracycline, 25 µg/mL cyclohexamide, and 25 µg/mL of nalidixic acid. The plates were then incubated at 28 °C for one month. A colony was picked off the plate and streaked onto ISP2 agar until pure. Seed cultures were grown in 17 mL dual position cap tubes containing 2 mL of ISP2 and grown for 4 days on a rotary shaker at 200 rpm. The seed culture was then poured into a 250 mL baffled flask containing 100 mL of ISP2 and grown for 10 days on a rotary shaker at 200 rpm. The culture was centrifuged at 4000 rpm for 10 min to remove the cells and 2 g of XAD16 resin (Sigma-Aldrich, St. Louis, Mo.) contained

within a polypropylene mesh bag was added to the broth and incubated overnight on the rotary shaker. The resin bag was removed and placed into 10 mL of MeOH followed by 10 mL of acetone and 10 mL of ethyl acetate. Each of the three fractions was dried *in vacuo* and reconstituted to a final concentration of 15 mg/mL in DMSO.

Culture Maintenance and Fermentation

Seed cultures of 100 mL (x5) of ISP2 media (1% malt extract, 0.4% yeast extract, 0.4% dextrose, 3% NaCl) were inoculated with a loopful of vegetative cells from an oatmeal plate (6% oatmeal, 1.25% agar, 3% NaCl) culture of *Streptomyces* sp. 34443-A2 or *Streptomyces* sp. 44306-A41 and incubated with shaking (200 rpm) at 28°C for 8 days. A 25 mL portion of the seed cultures were transferred to a 2.8 L Fernbach flask containing 1.5 L of the ISP2 medium, and the fermentation was carried out on a rotary shaker (200 rpm) at 28 °C. After 8-10 days of growth, the cultures were harvested by centrifugation. The resulting cell free broth was subjected to solid phase extraction using 15 g of Amberlite XAD-16. The resin was then separated by filtration and subjected to organic extraction using MeOH: EtOAc (1:1).

Isolation and Purification of Globomycins A-C (1-3)

The organic extract from *Streptomyces* sp. 34443-A2 was concentrated under vacuum to afford the crude extracts (~3.2 g). Crude extracts were dissolved in 30 mL of H₂O and were applied to a C18-silica gel column (20 × 2.6 cm, YMC Gel ODS-A, 12 nm, S-150 μm). The C-18 column was eluted with a stepwise gradient of H₂O/ACN (100:0 → 0:100) to give eight fractions, which were concentrated *in vacuo* to yield fractionated organic materials, respectively. All eight fractions were assayed as described above. The bio-active fractions 4 and 5 were further purified by RP-HPLC on

an isocratic 50% ACN in H₂O and was followed by UV/Vis photodiode array detection at 210 nm and 254 nm to yield semi-pure compounds **1** (11.2 mg), **2** (6.9 mg) and **3** (5.3 mg). These compounds were subjected to re-purification over RP-HPLC using isocratic elution with 48% ACN on a Waters XBridge™ 5μM 19 × 150 mm C18 column to yield compounds **1** (7.6 mg), **2** (4.3 mg) and **3** (3.6 mg) (Figure VI-2).

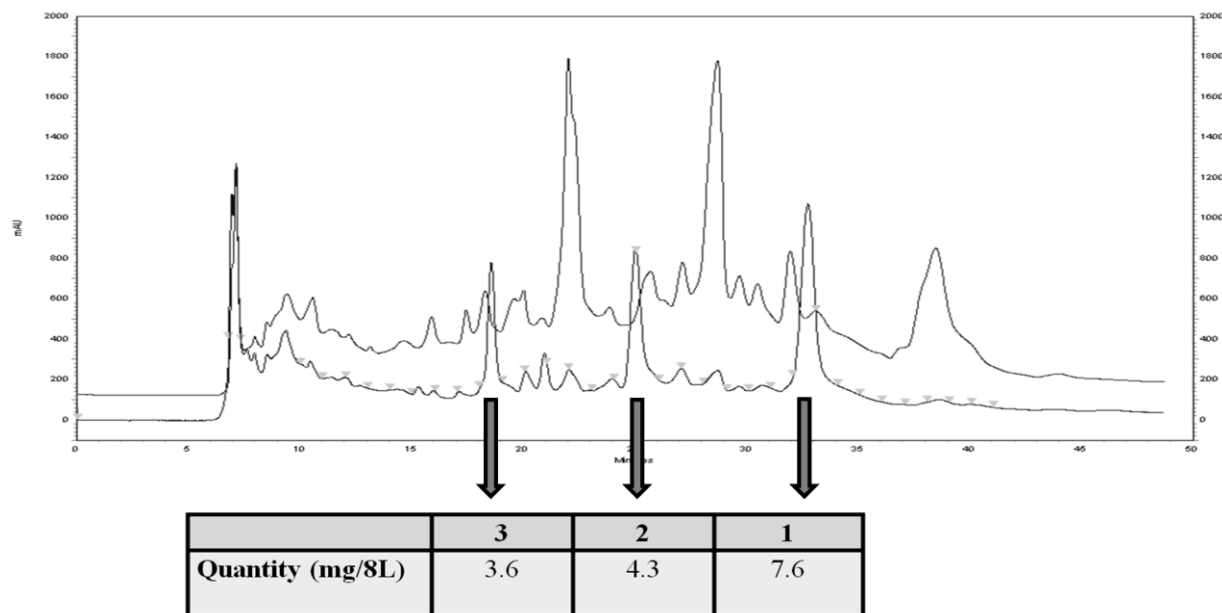


Figure VI-2: HPLC Trace and Yield of Active Peptidic Molecules.

X-ray Crystallography of Globomycin A (1)

The entire isolated yield of **1** was dissolved in a small amount of filtered ACN, and then MeOH was added at 50 °C until the saturation point was reached. Colorless needles of **1** were grown from evaporation of an acetonitrile/methanol solution of the compound at 4°C. A crystal of dimensions 0.12 x 0.02 x 0.02 mm was mounted on a Rigaku AFC10K Saturn 944+ CCD-based X-ray diffractometer equipped with a low temperature device and Micromax-007HF Cu-target micro-focus rotating anode ($\lambda = 1.54187 \text{ \AA}$) operated at 1.2 kW power (40 kV, 30 mA). The X-ray intensities were

measured at 85°K with the detector placed at a distance 42.00 mm from the crystal. A total of 2911 images were collected. The exposure time was 5 sec. for the low angle images, 15 sec. for high angle. The integration of the data yielded a total of 128099 reflections to a maximum 2θ value of 136.48° of which 7433 were independent and 7205 were greater than 2σ . The final cell constants (Appendix Table VI-1) were based on the xyz centroids 86072 reflections above 10σ . Analysis of the data showed negligible decay during data collection; the data were processed with CrystalClear 2.0 (Rigaku Americas and Rigaku Corporation (2011)) and corrected for absorption. The structure was solved and refined with the Bruker SHELXTL (version 2008/4) software package, using the space group P6(1) with Z = 6 for the formula $C_{37}H_{57}N_5O_9$, C_2H_3N , H_2O , 1.25(H_2O). Full matrix least-squares refinement based on F^2 converged at $R_1 = 0.0409$ and $wR_2 = 0.1030$ [based on $I > 2\sigma(I)$], $R_1 = 0.0422$ and $wR_2 = 0.1041$ for all data.

Isolation and Purification of Desferrioxamine E

Desferrioxamine E was isolated and purified from the organic extract of *Streptomyces* sp. 44306-A41 as previously described.¹⁰ Structure was confirmed via HRMS, 1H NMR, ^{13}C NMR, and 2D COSY NMR.

Activation versus Growth Inhibition Dose-Response Study

For this study, the screening protocol was modified to a 96-well microtiter plate format. Briefly, starter cultures (3 mL) of *S. flexneri* BS103 harboring either the reporter plasmid (pMALvirF-LacZ) or positive control plasmid (pMAL(Δ virF)-LacZ) were grown overnight at 37°C with shaking in 2xTY media (16 g bactotryptone, 10 g yeast extract, 5 g NaCl per liter of water supplemented with 100 μ g/mL carbenicillin). The following day

each culture was diluted with similar media to $OD_{600}=0.005$ and then added to appropriate wells of a 96-well microtiter plate (85 μ L). Working stocks of each compound were made in 25% DMSO using a two-fold serial dilution approach: 5 μ L of each compound were added in triplicate to appropriate wells of a 96-well plate resulting in final concentrations ranging from 43 μ M to 0.34 μ M. For the negative controls, compound vehicle (25% DMSO) was added to the wells instead of compound. Plates were grown overnight at 37°C for 20 hours in a humidified incubator. The following day the cell density (OD_{600}) for all samples was measured using a BioTek Synergy H1 plate reader (Winooski, VT) then 90 μ L of CPRG solution was added to each well. Plates were allowed to incubate for 2.5 minutes at room temperature then chlorophenol red absorbance (A_{570}) was determined using the BioTek plate reader.

Minimum Inhibitory Concentration Testing

Starter cultures (3 mL) of the following strains were grown overnight at 37°C in the indicated media:

S. aureus (MRSA): TSB media (17 g casein peptone, 2.5 g dipotassium hydrogen phosphate, 2.5 g glucose, 3 g soya peptone, 5 g sodium chloride/L of water)

B. cereus ATCC1778, *E. faecalis* ATCC29212, *L. monocytogenes* ATCC19115,

Vancomycin-Resistant *Enterococcus* (VRE): BHi media (5 g beef heart, 12.5 g calf brains, 2.5 g disodium hydrogen phosphate, 2 g glucose, 10 g peptone, 5 g sodium chloride/L of water)

B. subtilis 168, *E. coli* MC1061, *E. coli* EC2880, *S. enterica* ATCC14028, *S. flexneri* BS103, *B. anthracis*: LB media (10 g bactotryptone, 5 g yeast extract, 5 g sodium chloride/L of water)

The following day each culture was diluted with similar media to $OD_{600}=0.005$ and then added to appropriate wells of a 96-well microtiter plate (85 μ L). Working stocks of each compound were made in 25% DMSO using a two-fold serial dilution approach; 5 μ L of each compound were added in triplicate to appropriate wells of a 96-well plate resulting in final concentrations ranging from 50 μ M to 0.39 μ M (note: EC2880 was also tested with lower compound concentrations ranging from 670 nM to 5 nM). For the negative controls, compound vehicle (25% DMSO) was added to the wells instead of compound. Plates were grown overnight at 37°C for 20 hours in a humidified incubator. The following day the cell density (OD_{600}) for all samples was measured using a M5 SpectraMax plate reader (Molecular Devices, Sunnyvale, CA).

Desferrioxamine E Electrophoretic Mobility Shift Assay (EMSA)

EMSAs were performed as described in Chapter IV but with Desferrioxamine E (100 μ M) present in appropriate reactions.

Siderophore VirF Inhibition Testing

Desferrioxamine E and 2,2-bipyridine were tested in the 96-well plate version of the β -galactosidase reporter assay. Both compounds were tested alone (17 μ M and 50 μ M, respectively) and in the presence of ferric citrate (20 μ M). The assay was performed as described in Chapter II Material and Methods Reconfirmation Screen.

Results

Hit Identification

For the high-throughput screen, 20,061 natural product extracts were tested. As shown in Figure VI-1, the screen produced 218 initial “hits” for VirF inhibition (Z' factor =0.59, average Z' factor per plate = 0.65, 1.09% hit rate). Application of more stringent

selection criteria (see Figure VI-1) yielded 24 strains (17 single extracts, 7 sets of extracts) for reconfirmation testing and extract fractionation. Of the strains selected for reconfirmation only one, 44306-A41, maintained activity throughout the regrowth and fractionation process. The screen also produced 96 “hits” for cell growth inhibition (0.48% hit rate). Of the 96 “hits”, nine inhibited cell growth in both *S. flexneri* BS103 cells harboring pMALvirF-LacZ and *S. flexneri* BS103 cells harboring pMAL(Δ virF)-LacZ. These nine extracts were selected for reconfirmation testing and fractionation; however, none displayed activity after regrowth. The initial screen also identified 25 extracts that stimulated a greater amount of CPRG cleavage compared to the negative controls. These extracts were further tested in two counter screens. The first counter screen determined if the extracts were chemically cleaving CPRG. None of the 25 extracts exhibited CPRG cleavage. The 25 extracts were then tested in dose-response studies similar to the HTS assay. Of the 25 extracts, four had a pAC₅₀ for VirF activation that was at least 1.5-fold larger than their pAC₅₀ for cell growth inhibition (e.g., their AC₅₀ for activation was at least 3-fold less than that for toxicity). These extracts were selected for further reconfirmation testing and fractionation, and only one, 34443-A2, maintained activity throughout the regrowth and fractionation process.

Isolation and Identification of Globomycins

The marine actinomycete strain 34443-A2 was isolated from Costa Rica marine sediments as described in Material and Methods. The marine microbe was grown at a large scale (6 L) and the active organic extracts were subjected to C18 chromatography followed by *in vitro* biological activity assessment. The VirF-based β -galactosidase reporter assay revealed fractions eluting with 3:2 and 1:1 (H₂O: ACN) to contain the

active fraction (Figure VI-2). Both fractions were pooled together based on their similar activities and being consecutive C18 fractions. The pooled active fraction was then subjected to RP-18 HPLC purification to yield three active peptidic molecules (**1-3**) (Figure VI-2).

Compound **1** was purified in greater yield, as a white amorphous solid and showed $[M+H]^+$ ion peak at m/z 656.4308 possessing molecular formula of $C_{32}H_{57}N_5O_9$ as suggested by HRMS (Appendix Figure VI-1). The 1H NMR data recorded in DMSO- d_6 , indicated the peptidic nature of **1** and suggested the presence of at least two *N*-methyl amide groups at δ 3.29 and eight *NH* groups at δ 7.23, 7.45, 7.77, 7.96, 8.27, 8.36 and 8.61 ppm (Appendix Figure VI-4). Interestingly, the molecular formula indicated only five *N* atoms to be present in molecule. Furthermore, the ^{13}C NMR spectrum (in DMSO- d_6 , Appendix Figure VI-5) of **1** exhibited the presence of six clear carbonyl carbons (with equal number of minor carbonyl carbon signals) attributable to ester/amide functionalities along with the possibility of molecule showing conformational flexibility in DMSO- d_6 . Analyses of 1D and 2D NMR spectra of **1** (Appendix Figures VI-4 to VI-6) led to the establishment of a hybrid structural framework consisting of five proteinogenic amino acids, namely leucine, isoleucine, serine, threonine and glycine along with an aliphatic moiety of polyketidic origin. However, NMR spectra were also suggesting double signals for each moiety making it difficult to tether the data with HRMS.

In order to resolve the issue, we resorted to crystallization efforts for the active molecule using drops of MeOH in saturated solution of **1** in ACN at 50 °C followed by slow evaporation at 4°C to produce a small amount of crystals that were adequate for X-

ray diffraction studies (see Material and Methods). The resulting structure (Figure VI-3) was essentially super-imposable to the predicted residues, which led to the identification of **1** as the earlier reported molecule Globomycin A.^{11, 12}

Globomycins B (**2**) and C (**3**) were also isolated from RP-18 HPLC of the same C18 fractions containing compound **1**. The HRMS of the molecules provided molecular formulas of $C_{32}H_{55}N_5O_9$ and $C_{30}H_{53}N_5O_9$, showing $[M+H]^+$ ion peaks at 628.3938 and 642.4130 respectively (Appendix Figures VI-2 and 3). Both these molecules differ by a CH_2 group and share near identical NMR spectra leading them to be identified as reported analogs isolated along with Globomycin A (**1**), see Figure VI-4.^{11, 12}

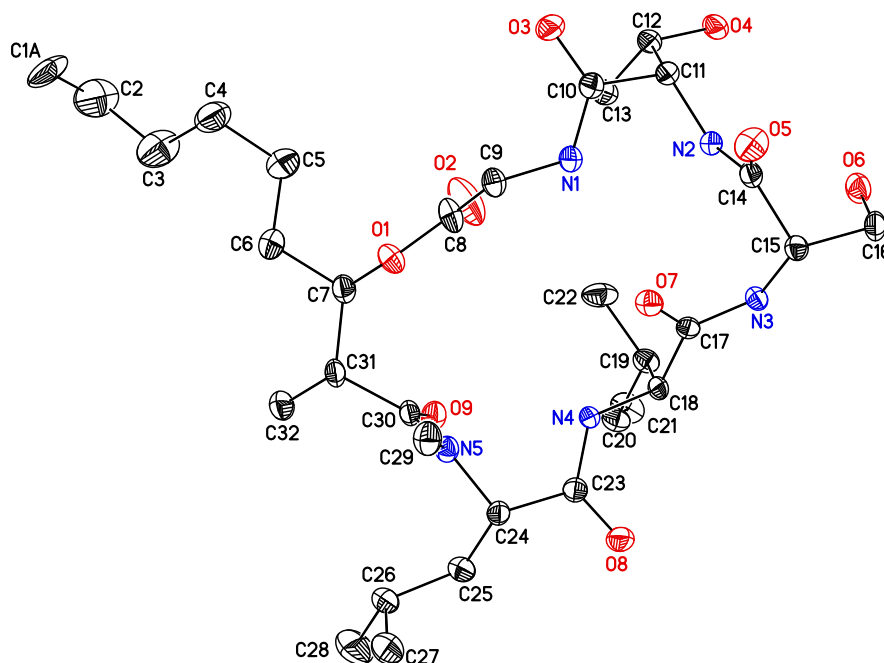


Figure VI-3: Crystal Structure (Ellipsoid) of Globomycin A (1).

Isolation and Identification of Desferrioxamine E

The marine actinomycete strain 44306-A41 was isolated from Costa Rica marine sediments as described in Material and Methods. The marine microbe was grown at a

large scale (6 L) and the active organic extracts were subjected to C18 chromatography followed by *in vitro* biological activity assessment. A total of three rounds of RP-18 HPLC purification, followed by *in vitro* biological activity assessment were needed to produce a single active peak. The structure of the purified compound was then determined via 1D and 2D NMR studies and HRMS (see Appendix Figures 7-10). The structure is shown in Figure VI-5.

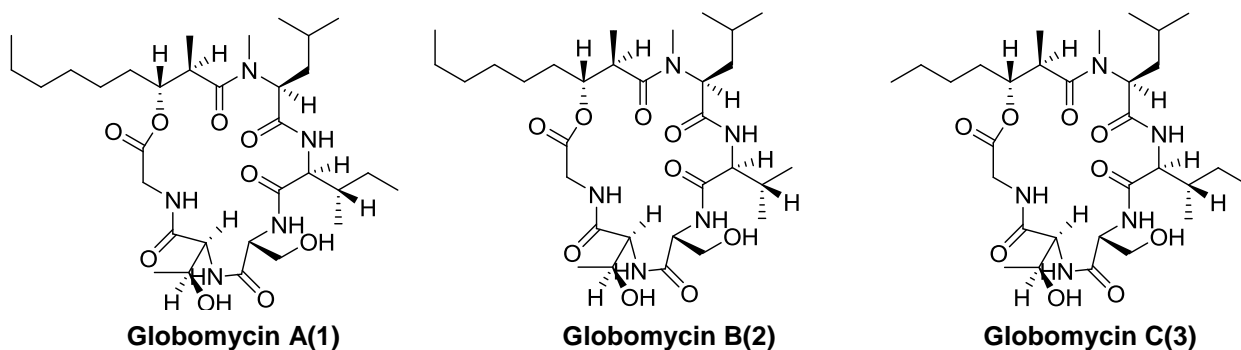


Figure VI-4: Chemical Structures of Globomycins A-C (1, 2, and 3).

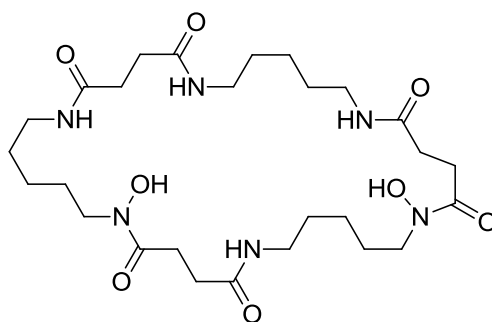


Figure VI-5: Chemical Structure of Desferrioxamine E.

Activation versus Growth Inhibition Dose-Response Studies with Globomycins

Pure samples of compounds **1**, **2**, and **3** were tested in dose-response studies with a modified 96-well microtiter plate version of the screening assay. Both cell growth inhibition and apparent VirF activation were monitored. As shown in Figure VI-6, as the concentration of each compound increased, there was a steep rise in VirF activation followed by a steep drop-off due to growth inhibition. At higher concentrations

(approximately 20 μM) no VirF activation was seen due to the toxicity of the compounds.

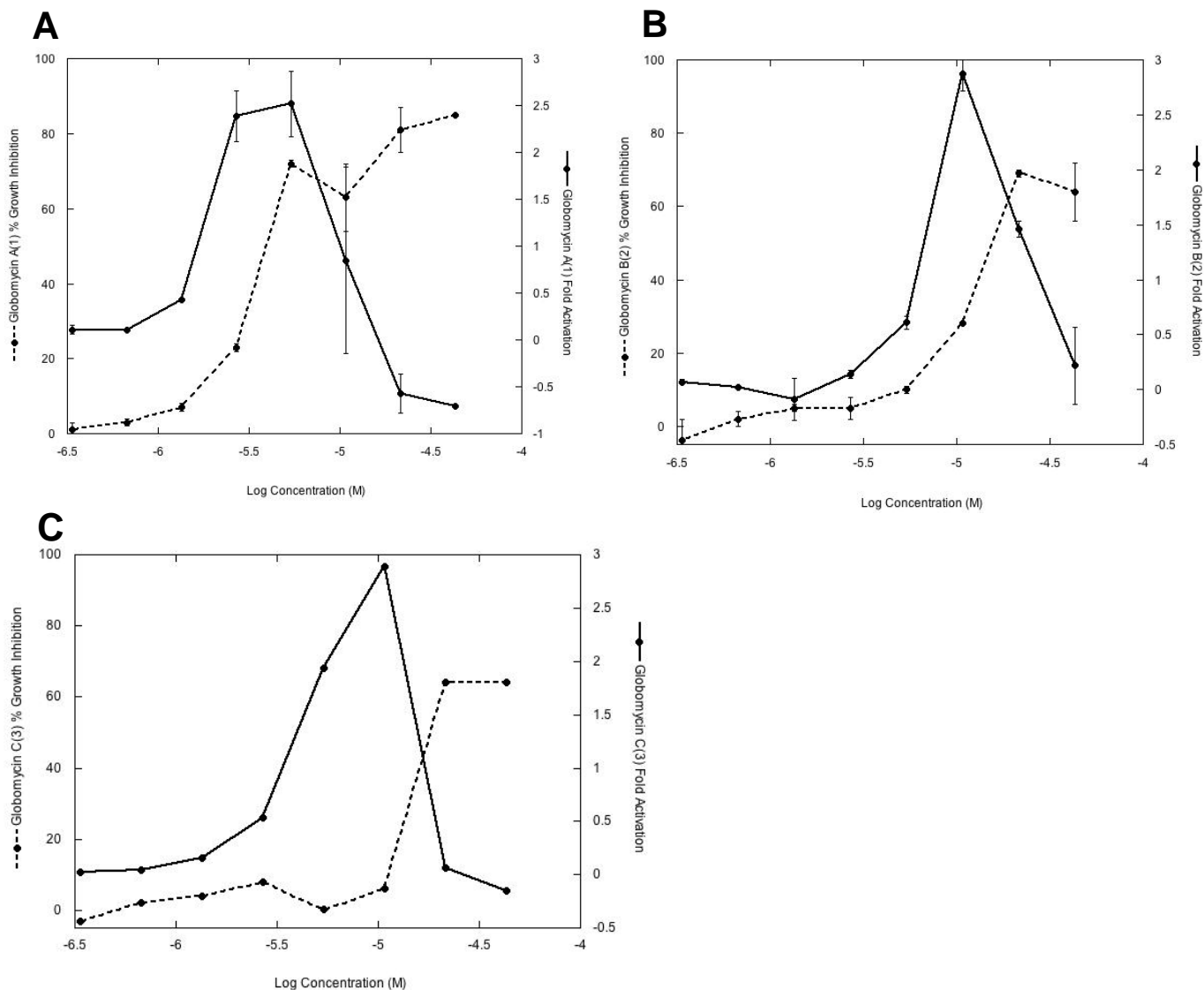


Figure VI-6: Plots Depicting Fold VirF Activation (solid-line, right y-axis) Versus % Growth Inhibition (dotted-line, left y-axis) for Globomycins A-C (1, 2, and 3). Each concentration was tested in triplicate (two-fold serial dilutions 43-0.33 μM). A) Plot for Globomycin A (1), fold activation peaks at 2.7 μM B) Plot for Globomycin B (2), fold activation peaks at 11 μM . C) Plot for Globomycin C (3), fold activation peaks at 5.4 μM .

Minimum Inhibitory Concentration Determination of Globomycin Compounds

Minimum inhibitory concentration studies were performed with compounds **1**, **2**, and **3** against a panel of bacteria. Table VI-1 shows the results for the MIC studies.

The concentrations listed in Table VI-1 refer to the concentration of each compound that produced 90% growth inhibition. As shown in the table, the compounds were primarily active against *E. coli* and *S. flexneri*, with slight activity against the various *Bacillus* strains. The bactericidal effect of each compound against *E. coli* increased in *E. coli* EC2880, an *E. coli* strain with the gene encoding for the TolC efflux pump removed. The MIC₉₀ of compound **1** decreased approximately 300-fold, the MIC₉₀ of compound **2** decreased approximately 35-fold, and the MIC₉₀ compound **3** decreased approximately 70-fold for the *tolC* knockout strain versus wild-type.

Desferrioxamine E Electrophoretic Mobility Shift Assay (EMSA)

Using the optimized EMSA conditions described in Chapter IV, the assay was used to determine if Desferrioxamine E at 100 μ M could inhibit the binding of MalE-VirF to the *virB* promoter. As shown in Figure VI-7, Desferrioxamine E had no effect on the binding of MalE-VirF and was indistinguishable from the DMSO negative control.

Siderophore Testing in the Presence of Ferric Citrate

The *Shigella*-based, VirF-driven, β -galactosidase assay was used to determine the effects of 2,2-bipyridine and purified Desferrioxamine E on VirF-driven transcription of the *virB* promoter with and without excess ferric citrate. As shown in Table VI-2, both 2,2-bipyridine and Desferrioxamine E had inhibitory effects in the assay. However, these inhibitory effects were offset by the addition of ferric citrate in both cases. Table VI-2 also shows that ferric citrate alone had a negligible effect on VirF-driven transcription at the concentrations used in this study.

Table VI-1. MIC₉₀ Values for Compounds 1, 2, and 3.

Organism	MIC ₉₀ (μM)		
	1	2	3
<i>E. coli</i> MC1061	6.3	25.0	12.5
<i>E. coli</i> EC2880 (<i>tolC</i> ⁻ , <i>imp</i> ⁻)	0.02	0.67	0.17
<i>S. flexneri</i> BS103	25.0	25.0	25.0
<i>B. subtilis</i> 168	>50.0	>50.0	>50.0
<i>B. anthracis</i> 34F2 Sterne	Not Active	>50.0	50.0
<i>B. cereus</i> ATCC1778	>50.0	>50.0	50.0
MRSA	Not Active	Not Active	>50.0
<i>S. enterica</i> ATCC14028	>50.0	Not Active	Not Active
VRE	Not Active	Not Active	Not Active
<i>L. monocytogenes</i> ATCC19115	Not Active	Not Active	Not Active
<i>E. faecalis</i> ATCC29212	Not Active	Not Active	Not Active

Note: The highest compound concentration tested was 50 μM. Therefore, a “Not Active” result is defined as a compound producing no growth inhibition at 50 μM, while a “>50.0 μM” result is defined as a compound producing some level growth inhibition at 50 μM but <90%.

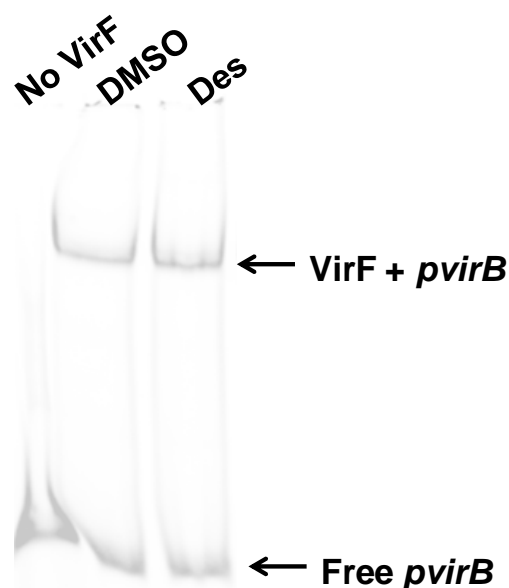


Figure VI-7: Electrophoretic Mobility Shift Assay (EMSA) of MalE-VirF Binding to *pvirB* DNA Probe in Presence of Desferrioxamine E (Des). EMSA image shows the retardation of the 5'Cy5-*pvirB* DNA probe (0.25 μ M) when incubated in the presence of MalE-VirF (1 μ M). Image also shows the effect Desferrioxamine E (100 μ M) has on MalE-VirF binding.

Table VI-2. Results of Siderophore Testing in Presence of Iron.

% Inhibition in the Shigella-Based, VirF-Driven, β -Galactosidase Reporter Assay				
<u>Des*</u> (17 μ M)	<u>Des* (17 μM) + Ferric Citrate (20 μM)</u>	<u>2,2-B*</u> (50 μ M)	<u>2,2-B* (50 μM) + Ferric Citrate (20 μM)</u>	<u>Ferric Citrate (20 μM)</u>
77% \pm 2%	22% \pm 8%	63% \pm 3%	43% \pm 1%	4% \pm 2%

*Des = Desferrioxamine

*2,2-B = 2,2-bipyridine

Discussion

The initial objective of the NPE HTS was to identify extracts that either had VirF inhibitory properties or bactericidal/bacteriostatic properties. As shown in Figure VI-1, we were able to identify 218 “hits” for VirF inhibition and 96 “hits” for cell growth

inhibition from the HTS. However, during the screen we also observed 25 extracts that appeared to increase VirF activity. This apparent increase in VirF activity was evidenced by the rapid turnover of the β -galactosidase substrate, CPRG, to chlorophenol red. Typically, after CPRG is added to each microtiter plate, it is allowed to incubate at room temperature for 10 minutes before absorbance is measured at 570 nm. During this incubation time, the yellow substrate slowly turns a deep red upon hydrolysis by β -galactosidase. However, for samples containing the apparent VirF activating extracts, the red color appeared very rapidly and in most cases reached the upper detection limit of the plate reader within five minutes. Control screens showed that the extracts were not chemically cleaving CPRG or directly activating β -galactosidase (data not shown). Combined, these results suggested that there was a greater amount of β -galactosidase present in these samples, presumably due to an increase in VirF activity.

As with all NPE screens, the extracts contain multiple compounds. Therefore, once a promising extract has been identified, the active component must be isolated from the extract and characterized. To isolate the active component, the producing organism is grown on a larger scale and the extraction procedure is repeated. A series of bioassay-guided fractionations on the large-scale extraction are then used to isolate the active compounds. To narrow down our list of hits for reconfirmation and fractionation studies, tighter selection criteria were applied to all three sets of hits (as shown in Figure VI-1 and described in Methods). The tighter selection criteria yielded 24 strains that produced extracts with VirF inhibitory properties, nine strains that

produced extracts with bactericidal/bacteriostatic properties, and four strains that produced extracts with apparent VirF activation properties.

Although not the original goal of our HTS, we decided to first follow-up on the apparent VirF activators in an attempt to gain insight into the mechanism VirF uses to activate transcription. VirF is classified as a homodimeric, AraC-type transcriptional regulator. There are three classes of AraC-type regulators: chemically-modulated, physically-modulated, and monomeric.¹³ AraC is a member of the first class since it is positively regulated by arabinose¹⁴, whereas VirF is a member of the second class owing to the fact that VirF is constitutively active and its expression is modulated by temperature, pH and osmolarity.¹⁵ The exact mechanism and order of events VirF uses to activate transcription is poorly understood, but it is clear that VirF must dimerize, bind DNA, and recruit RNA polymerase to turn on transcription. We hypothesized that a natural product could be acting as a positive modulator at any of the above listed steps for VirF transcriptional activation, much like arabinose is a positive modulator for AraC. Identification of a positive modulator of VirF activity would change the current understanding of how VirF functions.

To identify the active component from the hits for apparent VirF activation, the four strains that produced the extracts were cultured and the extraction procedures were repeated. Unfortunately, only one of the four strains (a marine actinomycete) reconfirmed and produced an extract with apparent VirF activating properties. This strain was subjected to scaled-up growth conditions and a large-scale extraction. The large-scale extract underwent a series of bioassay guided fractionations until three active compounds (**1**, **2**, and **3**) were isolated via C-18 HPLC. Once each compound

was purified and their molecular weights were determined via high-resolution mass spectrometry, the concentration of each compound could be accurately varied in the VirF-driven, β -galactosidase reporter assay. When the pure compounds were tested at higher concentrations, there was a sharp drop-off in apparent VirF activation due to *S. flexneri* growth inhibition as shown in Figure VI-6. These results suggested that the apparent VirF activation might be a side effect/response from the cellular stress the compounds placed on the bacteria prior to bacteriostasis. To determine if *S. flexneri* growth inhibition was VirF specific or if the compounds inhibited the growth of other bacterial species, minimum inhibitory concentration (MIC) studies were performed against a panel of bacteria. As shown in Table VI-1, the compounds were able to successfully inhibit the growth of different bacterial species (primarily *E. coli* and *Bacillus* strains) that do not express VirF. This result proved that the growth inhibition was not VirF-specific and further suggested that the apparent VirF activation may be a side effect from a stress response.

To confirm the structures of the compounds, compound **1** was successfully crystallized and analyzed by X-ray crystallography. From the crystal structure and a series of NMR experiments, the chemical structures of all three compounds were determined, see Figure VI-4. Compound **1** is a known bactericidal agent named Globomycin A, while compounds **2** and **3** are also previously discovered naturally occurring derivatives, Globomycins B and C. Globomycin A was initially isolated in 1978 from a terrestrial actinomycete^{11, 12}, while its congeners were later isolated in 1981.¹⁶ Globomycin A and its derivatives are known to block prolipoprotein processing through the inhibition of signal peptidase II.¹⁷ The known antibacterial properties of

Globomycin A and its derivatives are similar to the properties we have reported in Table VI-1.¹⁸⁻²¹ However, the data in Table VI-1 suggests that Globomycins are substrates for one or more of the *E. coli* TolC efflux pumps. TolC forms the outer-membrane channel for the majority of pumps associated with the efflux of antibacterial agents in *E. coli*.²² The MIC₉₀ values for the Globomycins (**1**, **2**, and **3**) were much lower when tested against the *tolC* genetic knockout strain, EC2880, than when tested against wild type *E. coli* (300-fold, 35-fold, and 70-fold lower, respectively). This characteristic of Globomycins has not been previously reported and could aid in developing a more potent Globomycin derivative effective against Gram-negative bacteria.

Globomycin is also a known inducer of the phage shock response pathway in *E. coli*.²³ The phage shock response pathway activates the transcription of effector proteins to help overcome stressors affecting cell membrane function.²⁴ It is likely that the apparent VirF activation seen during the HTS was actually a general upregulation of transcription caused by the activation of the phage shock pathway or a similar stress response pathway and not a direct effect of the compounds upon VirF.

After the identification and characterization of the Globomycins, we followed up on the hits that displayed VirF inhibition. A total of 15 of the 24 strains that produced VirF inhibitory extracts were regrown, extracted, and fractionated. Unfortunately, only one strain, 44306-A41 (a marine actinomycete) reconfirmed and produced an extract with VirF inhibitory properties. This strain was subjected to scaled-up growth conditions and large-scale extraction. The large-scale extract underwent a series of bioassay guided fractionations until an active compound was isolated via C-18 HPLC. A series of

NMR and HRMS experiments confirmed the active compound was a known siderophore, Desferrioxamine E.^{10, 25}

Previous studies have determined that iron concentration plays a role in VirF transcriptional activation of *virB*.^{26, 27} Specifically, when iron levels are depleted, a small regulatory RNA, RhyB (encoded on genome), is produced and inhibits VirB expression by decreasing the amount of *virB* mRNA. Currently, it is believed that RhyB regulates VirB expression at the level of *virB* transcription and that this regulation may be directly linked to sequence complementarity to the template strand of *virB*.²⁶ Yet, there have been no reports of iron-levels specifically affecting the activation of the *virB* promoter. Therefore, the inhibition seen in the reporter assay (inhibition of VirF activating *pvirB-lacZ*) suggested that Desferrioxamine E could have a direct effect on VirF not related to iron chelation.

To probe if Desferrioxamine E was directly blocking VirF from binding to the *virB* promoter, an EMSA that monitored MalE-VirF binding to the *virB* promoter was performed. As shown in Figure VI-7, Desferrioxamine E had no effect on VirF binding to the *virB* promoter. To verify that the depletion of iron was causing the inhibition seen in the reporter assay, and not Desferrioxamine E directly, the reporter assay was repeated in the presence of excess ferric citrate, as well as, a known iron-chelator, 2,2-bipyridine, in place of Desferrioxamine E. Unfortunately, as shown in Table VI-2, 2,2-bipyridine had the same effect on the reporter assay as Desferrioxamine E, and that both of these effects could be offset by the addition of excess ferric citrate. This confirmed that the inhibition seen in the reporter assay was due to the depletion of iron and not a direct interaction between Desferrioxamine E and VirF.

Unfortunately, we were not able to identify any novel compounds from our NPE HTS campaign. This can be attributed to many factors, including poor luck and a very low reconfirmation rate when the “active” strains from the HTS were regrown. It is possible that with further optimization of growth conditions, a novel compound may still yet be identified. However, the high-rate at which known natural products are currently identified from bacterial HTS,²⁸ has lead us to move on from this endeavor. The novel information that can be taken away from this study is that it appears Globomycin is substrate for the *E. coli* TolC efflux pump and that iron depletion reduces VirF-driven transcription of a reporter gene from the *virB* promoter.

Notes to Chapter VI

The work described in this chapter was based on a collaboration between the Sherman laboratory (Life Sciences Institute, University of Michigan Ann Arbor) and the Garcia laboratory (College of Pharmacy, University of Michigan Ann Arbor). All structure elucidation work presented in this chapter was done in the Sherman laboratory, by Dr. Ashootosh Tripathi. The remaining experiments (screening and biological activity testing) were performed in the Garcia lab, by Anthony Emanuele. Other contributors to acknowledge, include: Martha J. Larsen and Tom McQuade at Center of Chemical Genomics, Life Sciences Institute, University of Michigan, for high throughput screening automation and NPE sample management; Dr. Yi-Chen Chen, for technical assistance; and Dr. Jeff W. Kampf, Director, X-ray Services, Department of Chemistry, University of Michigan for help with the Globomycin crystal structure determination.

References

1. Emanuele, A. A.; Adams, N. E.; Chen, Y.-C.; Maurelli, A. T.; Garcia, G. A. Potential novel antibiotics from HTS targeting the virulence-regulating transcription factor, VirF, from *Shigella flexneri*. *Journal of Antibiotics* **2014**, 67, 379-386.
2. Hurt, J. K.; McQuade, T. J.; Emanuele, A.; Larsen, M. J.; Garcia, G. A. High-Throughput Screening of the Virulence Regulator VirF: A Novel Antibacterial Target for Shigellosis. *Journal of Biomolecular Screening* **2010**, 15, 379-387.
3. Davies, J. In Praise of Antibiotics. *ASM News* **1999**, 65, 304.
4. Bergmann, W.; Burke, D. C. Contributions to the Study of Marine Products. XL. The Nucleosides of Sponges. IV. Spongosine. *J Org Chem* **1956**, 21, 226-228.

5. Bergmann, W.; Feeney, R. J. Contributions to the study of marine products. XXXII. The nucleosides of sponges. I. *J Org Chem* **1951**, 16, 981-987.
6. Bergmann, W.; Stempien Jr., M. F. Contributions to the Study of Marine Products. XLIII. The Nucleosides of Sponges. V. The Synthesis of Spongocine. *J Org Chem* **1957**, 22, 1575-1577.
7. Newman, D. J.; Cragg, G. M. Natural products as sources of new drugs over the 30 years from 1981 to 2010. *J Nat Prod* **2012**, 75, 311-335.
8. Miller, J. H. *Experiments in Molecular Genetics*. CSH Laboratory Press: Cold Spring Harbor, NY, 1972.
9. Magarvey, N. A.; Keller, J. M.; Bernan, V.; Dworkin, M.; Sherman, D. H. Isolation and characterization of novel marine-derived actinomycete taxa rich in bioactive metabolites. *Appl Environ Microbiol* **2004**, 70, 7520-7529.
10. Yamanaka, K.; Oikawa, H.; Ogawa, H.-o.; Hosono, K.; Shinmachi, F.; Takano, H.; Sakuba, S.; Beppu, T.; Ueda, K. Desferrioxamine E produced by *Streptomyces griseus* stimulates growth and development of *Streptomyces tanashiensis*. *Microbiology* **2005**, 151, 2899-2905.
11. Inukai, M.; Enokita, R.; Torikata, A.; Nakahara, M.; Iwado, S.; Arai, M. Globomycin, A New Peptide Antibiotic with Spheroplast-Forming Activity I. Taxonomy of Producing Organisms and Fermentation. *J Antibiot* **1978**, 31, 410-420.
12. Nakajima, M.; Inukai, M.; Haneishi, T.; Terahara, A.; Arai, M.; Kinoshita, T.; Tamura, C. Globomycin, A New Peptide Antibiotic With Spheroplast-Forming Activity III. Structural Determination of Globomycin. *J Antibiot* **1978**, 31, 426-432.
13. Dorman, C. J.; Porter, M. E. The Shigella virulence gene regulatory cascade: a paradigm of bacterial gene control mechanisms. *Molecular Microbiology* **1998**, 29, 677-684.
14. Gallegos, M. T.; Schleif, R.; Bairoch, A.; Hofmann, K.; Ramos, J. L. Arac/XylS family of transcriptional regulators. *Microbiology & Molecular Biology Reviews* **1997**, 61, 393-410.

15. Tobe, T.; Yoshikawa, M.; Sasakawa, C. Thermoregulation of *virB* transcription in *Shigella flexneri* by sensing of changes in local DNA superhelicity. *Journal of Bacteriology* **1995**, 177, 1094-7.
16. Omoto, S.; Ogino, H.; Inouye, S. Studies on SF-1902 A2~A5, Minor Components of SF-1902 (globomycin). *J Antibiot* **1981**, 34, 1416-1423.
17. Dev, I. K.; Harvey, R. J.; Ray, P. H. Inhibition of prolipoprotein signal peptidase by globomycin. *J Biol Chem* **1985**, 260, 5891-5894.
18. Banaiee, N.; Jacobs, W. R.; Ernst, J. D. LspA-independent action of globomycin on *Mycobacterium tuberculosis*. *J Antimicrob Chemother* **2007**, 60, 414-416.
19. Hayashi, S.; Wu, H. C. Biosynthesis of *Bacillus licheniformis* penicillinase in *Escherichia coli* and in *Bacillus subtilis*. *J Bacteriol* **1983**, 156, 773-777.
20. Kiho, T.; Nakayama, M.; Yasuda, K.; Inukai, M.; Kogen, H. Synthesis and antimicrobial activity of novel globomycin analogues. *Bioorg Med Chem Lett* **2003**, 13, 2315-2318.
21. Kiho, T.; Nakayama, M.; Yasuda, K.; Miyakoshi, S.; Inukai, M.; Kogen, H. Structure-activity relationships of globomycin analogues as antibiotics. *Bioorg Med Chem* **2004**, 12, 337-361.
22. Li, X. Z.; Nikaido, H. Efflux-mediated drug resistance in bacteria. *Drugs* **2004**, 64, 159-204.
23. Bergler, H.; Abraham, D.; Aschauer, H.; Turnowsky, F. Inhibition of lipid biosynthesis induces the expression of the *pspA* gene. *Microbiology* **1994**, 140, 1937-1944.
24. Joly, N.; Engl, C.; Jovanovic, G.; Huvet, M.; Toni, T.; Sheng, X.; Stumpf, M. P.; Buck, M. Managing membrane stress: the phage shock protein (Psp) response, from molecular mechanisms to physiology. *Fems Microbiology Reviews* **2010**, 34, 797-827.
25. Rateb, M. E.; Houssen, W. E.; Harrison, W. T. A.; Deng, H.; Okoro, C. K.; Asenjo, J. A.; Andrews, B. A.; Bull, A. T.; Goodfellow, M.; Ebel, R.; Jaspars, M.

Diverse Metabolic Profiles of a *Streptomyces* Strain Isolated from a Hyper-arid Environment. *Journal of Natural Products* **2011**, 74, 1965-1971.

26. Broach, W. H.; Egan, N.; Wing, H. J.; Payne, S. M.; Murphy, E. R. VirF-independent regulation of *Shigella* virB transcription is mediated by the small RNA RyhB. *PLoS ONE [Electronic Resource]* **2012**, 7, e38592.
27. Murphy, E. R.; Payne, S. M. RhyB, an Iron-Responsive Small RNA Molecule, Regulates *Shigella dysenteriae* Virulence. *Infection and Immunity* **2007**, 75, 3470-3477.
28. Watve, M. G.; Tickoo, R.; Jog, M. M.; Bhole, B. D. How many antibiotics are produced by the genus *Streptomyces*? *Archives of Microbiology* **2001**, 176, 386-390.

Appendix

Appendix Table VI-1. Crystal Data and Structure Refinement for Globomycin A (1).

Identification code:	Globomycin A (1)
Empirical formula:	C ₃₄ H _{65.12} N ₆ O _{11.25} (with residual solvents)
Formula weight:	738.05 (with residual solvents)
Temperature:	85° K
Wavelength:	1.54178 Å
Crystal system, space group:	Hexagonal, P 6(1)
Unit cell dimensions:	a = 26.7741(4) Å alpha = 90 deg. b = 26.7741(4) Å beta = 90 deg. c = 9.8770(7) Å gamma = 120 deg.
Volume:	6131.8(5) Å ³
Z, Calculated density:	6, 1.199 Mg/m ³
Absorption coefficient:	0.739 mm ⁻¹
F(000):	2407
Crystal size:	0.12 x 0.02 x 0.02 mm
Theta range for data collection:	4.87 to 68.22 deg.
Limiting indices:	-32<=h<=32, -32<=k<=32, -11<=l<=11
Reflections collected / unique:	128099 / 7433 [R(int) = 0.0657]
Completeness to theta:	68.22 99.9 %
Absorption correction:	Semi-empirical from equivalents
Max. and min. transmission:	0.986 and 0.830
Refinement method:	Full-matrix least-squares on F ₂
Data / restraints / parameters:	7433 / 22 / 539
Goodness-of-fit on F ² :	1.072
Final R indices [I>2sigma(I)]:	R ₁ = 0.0409, wR ₂ = 0.1030
R indices (all data):	R ₁ = 0.0422, wR ₂ = 0.1041
Absolute structure parameter:	0.06(14)
Largest diff. peak and hole:	0.671 and -0.251 Å ⁻³

Appendix Table VI-2. Atomic Coordinates ($\times 10^4$) and Equivalent Isotropic Displacement Parameters ($A^2 \times 10^3$) for Globomycin A (1).

	x	y	z	U(eq)
O(1)	8517(1)	2956(1)	3528(1)	24(1)
O(2)	7666(1)	2145(1)	3859(2)	53(1)
O(3)	7780(1)	1102(1)	1355(1)	31(1)
O(4)	6463(1)	-293(1)	3638(1)	25(1)
O(5)	8444(1)	490(1)	4130(1)	29(1)
O(6)	7323(1)	-397(1)	6843(1)	28(1)
O(7)	8549(1)	1569(1)	6099(1)	21(1)
O(8)	8970(1)	2620(1)	9879(1)	27(1)
O(9)	8276(1)	3238(1)	7028(1)	25(1)
O(11)	7370(1)	200(1)	-351(1)	28(1)
O(10A)	9390(1)	345(1)	4635(5)	58(1)
O(10B)	9290(1)	160(1)	4206(5)	62(1)
N(1)	8162(1)	1485(1)	3399(1)	21(1)
N(2)	7605(1)	450(1)	4662(1)	18(1)
N(3)	8046(1)	777(1)	7361(1)	18(1)
N(4)	8540(1)	2303(1)	7844(1)	18(1)
N(5)	9175(1)	3392(1)	6653(1)	19(1)
N(6)	7781(1)	-558(1)	747(2)	48(1)
C(1A)	7757(2)	4298(2)	-1653(4)	59(1)
C(1B)	7580(4)	4136(3)	-1852(6)	120(2)
C(2)	7299(1)	4069(1)	-552(3)	63(1)
C(3)	7499(1)	3886(1)	694(2)	53(1)
C(4)	7650(1)	3426(1)	456(2)	43(1)
C(5)	7745(1)	3171(1)	1734(2)	43(1)
C(6)	8207(1)	3601(1)	2686(2)	31(1)
C(7)	8286(1)	3326(1)	3954(2)	23(1)
C(8)	8166(1)	2385(1)	3525(2)	28(1)
C(9)	8470(1)	2080(1)	2974(2)	23(1)
C(10)	7820(1)	1048(1)	2593(2)	21(1)
C(11)	7454(1)	457(1)	3248(2)	20(1)
C(12)	6811(1)	270(1)	3102(2)	21(1)
C(13)	6639(1)	662(1)	3827(2)	26(1)
C(14)	8100(1)	463(1)	4997(2)	19(1)
C(15)	8221(1)	447(1)	6494(2)	19(1)
C(16)	7928(1)	-173(1)	6977(2)	24(1)
C(17)	8274(1)	1345(1)	7157(2)	17(1)
C(18)	8183(1)	1701(1)	8221(2)	18(1)
C(19)	7545(1)	1533(1)	8393(2)	22(1)
C(20)	7500(1)	1930(1)	9437(2)	24(1)
C(21)	6902(1)	1682(1)	10049(2)	36(1)
C(22)	7268(1)	1539(1)	7053(2)	35(1)

C(23)	8905(1)	2712(1)	8677(2)	20(1)
C(24)	9270(1)	3323(1)	8102(2)	20(1)
C(25)	9224(1)	3758(1)	9024(2)	26(1)
C(26)	9590(1)	4386(1)	8594(2)	36(1)
C(27)	10232(1)	4588(1)	8591(2)	45(1)
C(28)	9466(1)	4769(1)	9509(3)	59(1)
C(29)	9655(1)	3528(1)	5727(2)	26(1)
C(30)	8702(1)	3431(1)	6288(2)	21(1)
C(31)	8715(1)	3746(1)	4990(2)	22(1)
C(32)	8554(1)	4201(1)	5390(2)	30(1)
C(33)	7918(1)	-727(1)	1657(2)	42(1)
C(34)	8078(1)	-940(1)	2828(3)	76(1)
O(99)	10854(6)	795(6)	5340(19)	146(6)
O(99A)	10779(13)	544(10)	6230(40)	112(11)

Appendix Table VI-3. Bond Lengths [Å] and Angles [deg] for Globomycin A (1).**Bond Lengths**

O(1)-C(8)	1.3348(17)
O(1)-C(7)	1.468(2)
O(2)-C(8)	1.206(2)
O(3)-C(10)	1.2425(19)
O(4)-C(12)	1.4195(17)
O(4)-H(4A)	0.86(2)
O(5)-C(14)	1.2348(19)
O(6)-C(16)	1.4228(18)
O(6)-H(6A)	1.04(3)
O(7)-C(17)	1.2470(17)
O(8)-C(23)	1.2423(19)
O(9)-C(30)	1.2306(18)
O(11)-H(11B)	0.77(3)
O(11)-H(11C)	0.98(2)
N(1)-C(10)	1.3300(18)
N(1)-C(9)	1.4417(18)
N(1)-H(1A)	0.94(2)
N(2)-C(14)	1.3491(19)
N(2)-C(11)	1.4561(19)
N(2)-H(2A)	0.992(19)
N(3)-C(17)	1.3402(17)
N(3)-C(15)	1.4639(19)
N(3)-H(3A)	0.91(2)
N(4)-C(23)	1.3280(18)
N(4)-C(18)	1.4527(16)
N(4)-H(4B)	0.88(2)
N(5)-C(30)	1.3710(19)
N(5)-C(29)	1.467(2)
N(5)-C(24)	1.480(2)
N(6)-C(33)	1.146(3)
C(1A)-C(2)	1.520(5)
C(1A)-H(1B)	0.9800
C(1A)-H(1C)	0.9800
C(1A)-H(1D)	0.9800
C(1B)-C(2)	1.453(7)
C(1B)-H(1E)	0.9800
C(1B)-H(1F)	0.9800
C(1B)-H(1G)	0.9800
C(2)-C(3)	1.518(3)
C(2)-H(2B)	0.9900
C(2)-H(2C)	0.9900
C(2)-H(2D)	0.9900
C(2)-H(2E)	0.9899

C(3)-C(4)	1.496(3)
C(3)-H(3B)	0.9900
C(3)-H(3C)	0.9900
C(4)-C(5)	1.515(3)
C(4)-H(4C)	0.9900
C(4)-H(4D)	0.9900
C(5)-C(6)	1.521(2)
C(5)-H(5A)	0.9900
C(5)-H(5B)	0.9900
C(6)-C(7)	1.520(2)
C(6)-H(6B)	0.9900
C(6)-H(6C)	0.9900
C(7)-C(31)	1.530(2)
C(7)-H(7A)	1.0000
C(8)-C(9)	1.513(2)
C(9)-H(9A)	0.9900
C(9)-H(9B)	0.9900
C(10)-C(11)	1.5288(19)
C(11)-C(12)	1.541(2)
C(11)-H(11A)	1.0000
C(12)-C(13)	1.521(2)
C(12)-H(12A)	1.0000
C(13)-H(13A)	0.9800
C(13)-H(13B)	0.9800
C(13)-H(13C)	0.9800
C(14)-C(15)	1.519(2)
C(15)-C(16)	1.5161(19)
C(15)-H(15A)	1.0000
C(16)-H(16A)	0.9900
C(16)-H(16B)	0.9900
C(17)-C(18)	1.517(2)
C(18)-C(19)	1.5443(19)
C(18)-H(18A)	1.0000
C(19)-C(22)	1.521(2)
C(19)-C(20)	1.528(2)
C(19)-H(19A)	1.0000
C(20)-C(21)	1.519(2)
C(20)-H(20A)	0.9900
C(20)-H(20B)	0.9900
C(21)-H(21A)	0.9800
C(21)-H(21B)	0.9800
C(21)-H(21C)	0.9800
C(22)-H(22A)	0.9800
C(22)-H(22B)	0.9800
C(22)-H(22C)	0.9800
C(23)-C(24)	1.5340(19)

C(24)-C(25)	1.530(2)
C(24)-H(24A)	1.0000
C(25)-C(26)	1.524(2)
C(25)-H(25A)	0.9900
C(25)-H(25B)	0.9900
C(26)-C(27)	1.522(3)
C(26)-C(28)	1.523(3)
C(26)-H(26A)	1.0000
C(27)-H(27A)	0.9800
C(27)-H(27B)	0.9800
C(27)-H(27C)	0.9800
C(28)-H(28A)	0.9800
C(28)-H(28B)	0.9800
C(28)-H(28C)	0.9800
C(29)-H(29A)	0.9800
C(29)-H(29B)	0.9800
C(29)-H(29C)	0.9800
C(30)-C(31)	1.525(2)
C(31)-C(32)	1.532(2)
C(31)-H(31A)	1.0000
C(32)-H(32A)	0.9800
C(32)-H(32B)	0.9800
C(32)-H(32C)	0.9800
C(33)-C(34)	1.446(4)
C(34)-H(34A)	0.9800
C(34)-H(34B)	0.9800
C(34)-H(34C)	0.9800

Bond Angles

C(8)-O(1)-C(7)	118.72(11)
C(12)-O(4)-H(4A)	107.7(14)
C(16)-O(6)-H(6A)	109.1(16)
H(11B)-O(11)-H(11C)	105(2)
C(10)-N(1)-C(9)	124.06(13)
C(10)-N(1)-H(1A)	121.1(12)
C(9)-N(1)-H(1A)	114.7(12)
C(14)-N(2)-C(11)	120.69(12)
C(14)-N(2)-H(2A)	117.3(12)
C(11)-N(2)-H(2A)	119.3(11)
C(17)-N(3)-C(15)	119.66(12)
C(17)-N(3)-H(3A)	121.4(13)
C(15)-N(3)-H(3A)	117.7(13)
C(23)-N(4)-C(18)	124.21(12)
C(23)-N(4)-H(4B)	113.0(12)
C(18)-N(4)-H(4B)	122.7(12)
C(30)-N(5)-C(29)	123.01(13)

C(30)-N(5)-C(24)	119.05(12)
C(29)-N(5)-C(24)	116.81(12)
C(2)-C(1A)-H(1B)	109.5
C(2)-C(1A)-H(1C)	109.5
C(2)-C(1A)-H(1D)	109.5
C(2)-C(1B)-H(1E)	109.5
C(2)-C(1B)-H(1F)	109.5
H(1E)-C(1B)-H(1F)	109.5
C(2)-C(1B)-H(1G)	109.5
H(1E)-C(1B)-H(1G)	109.5
H(1F)-C(1B)-H(1G)	109.5
C(1B)-C(2)-C(3)	120.8(4)
C(1B)-C(2)-C(1A)	9.0(3)
C(3)-C(2)-C(1A)	111.5(3)
C(1B)-C(2)-H(2B)	116.6
C(3)-C(2)-H(2B)	109.3
C(1A)-C(2)-H(2B)	109.3
C(1B)-C(2)-H(2C)	90.3
C(3)-C(2)-H(2C)	109.3
C(1A)-C(2)-H(2C)	109.3
H(2B)-C(2)-H(2C)	108.0
C(1B)-C(2)-H(2D)	106.9
C(3)-C(2)-H(2D)	107.5
C(1A)-C(2)-H(2D)	125.7
H(2B)-C(2)-H(2D)	91.1
H(2C)-C(2)-H(2D)	19.4
C(1B)-C(2)-H(2E)	106.7
C(3)-C(2)-H(2E)	107.4
C(1A)-C(2)-H(2E)	95.9
H(2B)-C(2)-H(2E)	16.4
H(2C)-C(2)-H(2E)	122.7
H(2D)-C(2)-H(2E)	106.9
C(4)-C(3)-C(2)	115.01(19)
C(4)-C(3)-H(3B)	108.5
C(2)-C(3)-H(3B)	108.5
C(4)-C(3)-H(3C)	108.5
C(2)-C(3)-H(3C)	108.5
H(3B)-C(3)-H(3C)	107.5
C(3)-C(4)-C(5)	114.59(18)
C(3)-C(4)-H(4C)	108.6
C(5)-C(4)-H(4C)	108.6
C(3)-C(4)-H(4D)	108.6
C(5)-C(4)-H(4D)	108.6
H(4C)-C(4)-H(4D)	107.6
C(4)-C(5)-C(6)	115.44(15)
C(4)-C(5)-H(5A)	108.4

C(6)-C(5)-H(5A)	108.4
C(4)-C(5)-H(5B)	108.4
C(6)-C(5)-H(5B)	108.4
H(5A)-C(5)-H(5B)	107.5
C(7)-C(6)-C(5)	113.61(13)
C(7)-C(6)-H(6B)	108.8
C(5)-C(6)-H(6B)	108.8
C(7)-C(6)-H(6C)	108.8
C(5)-C(6)-H(6C)	108.8
H(6B)-C(6)-H(6C)	107.7
O(1)-C(7)-C(6)	107.36(14)
O(1)-C(7)-C(31)	105.88(12)
C(6)-C(7)-C(31)	115.50(12)
O(1)-C(7)-H(7A)	109.3
C(6)-C(7)-H(7A)	109.3
C(31)-C(7)-H(7A)	109.3
O(2)-C(8)-O(1)	124.55(16)
O(2)-C(8)-C(9)	124.40(14)
O(1)-C(8)-C(9)	110.97(12)
N(1)-C(9)-C(8)	109.02(12)
N(1)-C(9)-H(9A)	109.9
C(8)-C(9)-H(9A)	109.9
N(1)-C(9)-H(9B)	109.9
C(8)-C(9)-H(9B)	109.9
H(9A)-C(9)-H(9B)	108.3
O(3)-C(10)-N(1)	123.25(13)
O(3)-C(10)-C(11)	119.28(12)
N(1)-C(10)-C(11)	117.46(13)
N(2)-C(11)-C(10)	112.40(11)
N(2)-C(11)-C(12)	110.99(12)
C(10)-C(11)-C(12)	109.30(12)
N(2)-C(11)-H(11A)	108.0
C(10)-C(11)-H(11A)	108.0
C(12)-C(11)-H(11A)	108.0
O(4)-C(12)-C(13)	107.03(12)
O(4)-C(12)-C(11)	110.03(12)
C(13)-C(12)-C(11)	113.98(11)
O(4)-C(12)-H(12A)	108.6
C(13)-C(12)-H(12A)	108.6
C(11)-C(12)-H(12A)	108.6
C(12)-C(13)-H(13A)	109.5
C(12)-C(13)-H(13B)	109.5
H(13A)-C(13)-H(13B)	109.5
C(12)-C(13)-H(13C)	109.5
H(13A)-C(13)-H(13C)	109.5
H(13B)-C(13)-H(13C)	109.5

O(5)-C(14)-N(2)	121.78(14)
O(5)-C(14)-C(15)	120.92(13)
N(2)-C(14)-C(15)	117.30(13)
N(3)-C(15)-C(16)	109.28(12)
N(3)-C(15)-C(14)	114.51(13)
C(16)-C(15)-C(14)	109.64(11)
N(3)-C(15)-H(15A)	107.7
C(16)-C(15)-H(15A)	107.7
C(14)-C(15)-H(15A)	107.7
O(6)-C(16)-C(15)	106.82(12)
O(6)-C(16)-H(16A)	110.4
C(15)-C(16)-H(16A)	110.4
O(6)-C(16)-H(16B)	110.4
C(15)-C(16)-H(16B)	110.4
H(16A)-C(16)-H(16B)	108.6
O(7)-C(17)-N(3)	119.73(14)
O(7)-C(17)-C(18)	121.32(12)
N(3)-C(17)-C(18)	118.94(12)
N(4)-C(18)-C(17)	107.26(11)
N(4)-C(18)-C(19)	111.67(12)
C(17)-C(18)-C(19)	113.26(11)
N(4)-C(18)-H(18A)	108.2
C(17)-C(18)-H(18A)	108.2
C(19)-C(18)-H(18A)	108.2
C(22)-C(19)-C(20)	111.88(14)
C(22)-C(19)-C(18)	111.99(13)
C(20)-C(19)-C(18)	109.44(11)
C(22)-C(19)-H(19A)	107.8
C(20)-C(19)-H(19A)	107.8
C(18)-C(19)-H(19A)	107.8
C(21)-C(20)-C(19)	113.38(12)
C(21)-C(20)-H(20A)	108.9
C(19)-C(20)-H(20A)	108.9
C(21)-C(20)-H(20B)	108.9
C(19)-C(20)-H(20B)	108.9
H(20A)-C(20)-H(20B)	107.7
C(20)-C(21)-H(21A)	109.5
C(20)-C(21)-H(21B)	109.5
H(21A)-C(21)-H(21B)	109.5
C(20)-C(21)-H(21C)	109.5
H(21A)-C(21)-H(21C)	109.5
H(21B)-C(21)-H(21C)	109.5
C(19)-C(22)-H(22A)	109.5
C(19)-C(22)-H(22B)	109.5
H(22A)-C(22)-H(22B)	109.5
C(19)-C(22)-H(22C)	109.5

H(22A)-C(22)-H(22C)	109.5
H(22B)-C(22)-H(22C)	109.5
O(8)-C(23)-N(4)	123.10(13)
O(8)-C(23)-C(24)	119.24(12)
N(4)-C(23)-C(24)	117.64(13)
N(5)-C(24)-C(25)	113.45(13)
N(5)-C(24)-C(23)	115.70(11)
C(25)-C(24)-C(23)	109.85(12)
N(5)-C(24)-H(24A)	105.6
C(25)-C(24)-H(24A)	105.6
C(23)-C(24)-H(24A)	105.6
C(26)-C(25)-C(24)	114.89(14)
C(26)-C(25)-H(25A)	108.5
C(24)-C(25)-H(25A)	108.5
C(26)-C(25)-H(25B)	108.5
C(24)-C(25)-H(25B)	108.5
H(25A)-C(25)-H(25B)	107.5
C(27)-C(26)-C(28)	110.35(16)
C(27)-C(26)-C(25)	112.51(15)
C(28)-C(26)-C(25)	109.96(16)
C(27)-C(26)-H(26A)	108.0
C(28)-C(26)-H(26A)	108.0
C(25)-C(26)-H(26A)	108.0
C(26)-C(27)-H(27A)	109.5
C(26)-C(27)-H(27B)	109.5
H(27A)-C(27)-H(27B)	109.5
C(26)-C(27)-H(27C)	109.5
H(27A)-C(27)-H(27C)	109.5
H(27B)-C(27)-H(27C)	109.5
C(26)-C(28)-H(28A)	109.5
C(26)-C(28)-H(28B)	109.5
H(28A)-C(28)-H(28B)	109.5
C(26)-C(28)-H(28C)	109.5
H(28A)-C(28)-H(28C)	109.5
H(28B)-C(28)-H(28C)	109.5
N(5)-C(29)-H(29A)	109.5
N(5)-C(29)-H(29B)	109.5
H(29A)-C(29)-H(29B)	109.5
N(5)-C(29)-H(29C)	109.5
H(29A)-C(29)-H(29C)	109.5
H(29B)-C(29)-H(29C)	109.5
O(9)-C(30)-N(5)	120.67(14)
O(9)-C(30)-C(31)	119.37(13)
N(5)-C(30)-C(31)	119.88(13)
C(30)-C(31)-C(7)	110.78(11)
C(30)-C(31)-C(32)	106.58(13)

C(7)-C(31)-C(32)	110.57(13)
C(30)-C(31)-H(31A)	109.6
C(7)-C(31)-H(31A)	109.6
C(32)-C(31)-H(31A)	109.6
C(31)-C(32)-H(32A)	109.5
C(31)-C(32)-H(32B)	109.5
H(32A)-C(32)-H(32B)	109.5
C(31)-C(32)-H(32C)	109.5
H(32A)-C(32)-H(32C)	109.5
H(32B)-C(32)-H(32C)	109.5
N(6)-C(33)-C(34)	178.4(3)
C(33)-C(34)-H(34A)	109.5
C(33)-C(34)-H(34B)	109.5
H(34A)-C(34)-H(34B)	109.5
C(33)-C(34)-H(34C)	109.5
H(34A)-C(34)-H(34C)	109.5
H(34B)-C(34)-H(34C)	109.5

Symmetry transformations used to generate equivalent atoms

Appendix Table VI-4. Hydrogen Coordinates ($\times 10^4$) and Isotropic Displacement Parameters ($\text{Å}^2 \times 10^3$) for Globomycin A (1).

	x	y	z	U(eq)
H(4A)	6427(9)	-536(9)	3020(20)	45(6)
H(6A)	7105(11)	-807(11)	7280(30)	77(9)
H(11B)	7440(10)	-32(11)	-100(30)	66(8)
H(11C)	7550(8)	514(8)	310(20)	35(5)
H(1A)	8206(8)	1425(8)	4320(20)	41(6)
H(2A)	7299(7)	314(8)	5360(20)	29(5)
H(3A)	7844(8)	604(8)	8120(20)	35(5)
H(4B)	8524(8)	2435(8)	7040(20)	34(5)
H(1B)	8119	4610	-1284	89
H(1C)	7630	4446	-2405	89
H(1D)	7816	3986	-1979	89
H(1E)	7919	4522	-1913	179
H(1F)	7310	4083	-2582	179
H(1G)	7700	3846	-1937	179
H(2B)	7207	4372	-298	76
H(2C)	6942	3734	-906	76
H(2D)	6885	3786	-685	76
H(2E)	7326	4444	-344	76
H(3B)	7841	4230	1071	63
H(3C)	7190	3747	1385	63
H(4C)	8006	3590	-98	52
H(4D)	7337	3112	-74	52
H(5A)	7851	2879	1471	52
H(5B)	7376	2969	2235	52
H(6B)	8578	3802	2193	37
H(6C)	8103	3894	2956	37
H(7A)	7903	3084	4400	28
H(9A)	8483	2102	1973	27
H(9B)	8871	2269	3317	27
H(11A)	7523	173	2745	24
H(12A)	6720	263	2117	25
H(13A)	6240	548	3595	39
H(13B)	6896	1063	3547	39
H(13C)	6671	629	4808	39
H(15A)	8646	614	6604	22
H(16A)	8051	-400	6420	29
H(16B)	8028	-191	7934	29
H(18A)	8325	1640	9108	21

H(19A)	7332	1131	8758	26
H(20A)	7781	2007	10172	29
H(20B)	7607	2303	8999	29
H(21A)	6620	1594	9326	54
H(21B)	6896	1965	10670	54
H(21C)	6806	1329	10547	54
H(22A)	6859	1407	7196	52
H(22B)	7307	1281	6410	52
H(22C)	7461	1932	6688	52
H(24A)	9679	3414	8170	24
H(25A)	8815	3660	9060	31
H(25B)	9339	3716	9952	31
H(26A)	9476	4422	7650	43
H(27A)	10448	4991	8291	67
H(27B)	10307	4347	7973	67
H(27C)	10354	4558	9508	67
H(28A)	9598	4760	10430	88
H(28B)	9051	4628	9519	88
H(28C)	9671	5166	9167	88
H(29A)	9508	3425	4801	39
H(29B)	9843	3309	5991	39
H(29C)	9935	3942	5772	39
H(31A)	9112	3940	4598	26
H(32A)	8623	4460	4622	44
H(32B)	8791	4425	6161	44
H(32C)	8145	4010	5643	44
H(34A)	8459	-644	3149	115
H(34B)	8091	-1288	2580	115
H(34C)	7793	-1033	3548	115

Appendix Table VI-5. Torsion Angles [deg] for Globomycin A (1).

C(1B)-C(2)-C(3)-C(4)	-40.6(4)
C(1A)-C(2)-C(3)-C(4)	-59.2(3)
C(2)-C(3)-C(4)-C(5)	-169.52(17)
C(3)-C(4)-C(5)-C(6)	-57.1(2)
C(4)-C(5)-C(6)-C(7)	179.85(17)
C(8)-O(1)-C(7)-C(6)	-105.26(15)
C(8)-O(1)-C(7)-C(31)	130.83(14)
C(5)-C(6)-C(7)-O(1)	66.40(18)
C(5)-C(6)-C(7)-C(31)	-175.78(16)
C(7)-O(1)-C(8)-O(2)	-0.5(3)
C(7)-O(1)-C(8)-C(9)	176.38(13)
C(10)-N(1)-C(9)-C(8)	104.00(18)
O(2)-C(8)-C(9)-N(1)	-22.3(3)
O(1)-C(8)-C(9)-N(1)	160.81(13)
C(9)-N(1)-C(10)-O(3)	7.7(3)
C(9)-N(1)-C(10)-C(11)	-170.88(14)
C(14)-N(2)-C(11)-C(10)	-73.04(17)
C(14)-N(2)-C(11)-C(12)	164.21(12)
O(3)-C(10)-C(11)-N(2)	172.65(14)
N(1)-C(10)-C(11)-N(2)	-8.7(2)
O(3)-C(10)-C(11)-C(12)	-63.65(19)
N(1)-C(10)-C(11)-C(12)	114.99(15)
N(2)-C(11)-C(12)-O(4)	-58.71(16)
C(10)-C(11)-C(12)-O(4)	176.77(12)
N(2)-C(11)-C(12)-C(13)	61.52(16)
C(10)-C(11)-C(12)-C(13)	-63.01(17)
C(11)-N(2)-C(14)-O(5)	1.0(2)
C(11)-N(2)-C(14)-C(15)	-179.28(11)
C(17)-N(3)-C(15)-C(16)	177.04(12)
C(17)-N(3)-C(15)-C(14)	-59.54(16)
O(5)-C(14)-C(15)-N(3)	141.69(13)
N(2)-C(14)-C(15)-N(3)	-38.06(16)
O(5)-C(14)-C(15)-C(16)	-95.09(15)
N(2)-C(14)-C(15)-C(16)	85.17(15)
N(3)-C(15)-C(16)-O(6)	61.85(15)
C(14)-C(15)-C(16)-O(6)	-64.42(15)
C(15)-N(3)-C(17)-O(7)	12.8(2)
C(15)-N(3)-C(17)-C(18)	-167.87(12)
C(23)-N(4)-C(18)-C(17)	-129.21(15)
C(23)-N(4)-C(18)-C(19)	106.15(16)
O(7)-C(17)-C(18)-N(4)	-8.80(18)
N(3)-C(17)-C(18)-N(4)	171.87(12)
O(7)-C(17)-C(18)-C(19)	114.87(14)

N(3)-C(17)-C(18)-C(19)	-64.46(17)
N(4)-C(18)-C(19)-C(22)	68.28(16)
C(17)-C(18)-C(19)-C(22)	-52.94(17)
N(4)-C(18)-C(19)-C(20)	-56.38(16)
C(17)-C(18)-C(19)-C(20)	-177.60(12)
C(22)-C(19)-C(20)-C(21)	75.82(18)
C(18)-C(19)-C(20)-C(21)	-159.45(14)
C(18)-N(4)-C(23)-O(8)	-1.1(2)
C(18)-N(4)-C(23)-C(24)	177.47(13)
C(30)-N(5)-C(24)-C(25)	-49.31(15)
C(29)-N(5)-C(24)-C(25)	118.92(13)
C(30)-N(5)-C(24)-C(23)	78.97(17)
C(29)-N(5)-C(24)-C(23)	-112.80(14)
O(8)-C(23)-C(24)-N(5)	178.51(14)
N(4)-C(23)-C(24)-N(5)	-0.1(2)
O(8)-C(23)-C(24)-C(25)	-51.46(19)
N(4)-C(23)-C(24)-C(25)	129.91(15)
N(5)-C(24)-C(25)-C(26)	-51.42(17)
C(23)-C(24)-C(25)-C(26)	177.34(13)
C(24)-C(25)-C(26)-C(27)	-61.8(2)
C(24)-C(25)-C(26)-C(28)	174.78(16)
C(29)-N(5)-C(30)-O(9)	169.87(13)
C(24)-N(5)-C(30)-O(9)	-22.66(19)
C(29)-N(5)-C(30)-C(31)	-13.5(2)
C(24)-N(5)-C(30)-C(31)	153.96(12)
O(9)-C(30)-C(31)-C(7)	-69.67(18)
N(5)-C(30)-C(31)-C(7)	113.66(15)
O(9)-C(30)-C(31)-C(32)	50.68(16)
N(5)-C(30)-C(31)-C(32)	-125.99(14)
O(1)-C(7)-C(31)-C(30)	-68.50(15)
C(6)-C(7)-C(31)-C(30)	172.86(14)
O(1)-C(7)-C(31)-C(32)	173.56(12)
C(6)-C(7)-C(31)-C(32)	54.92(18)

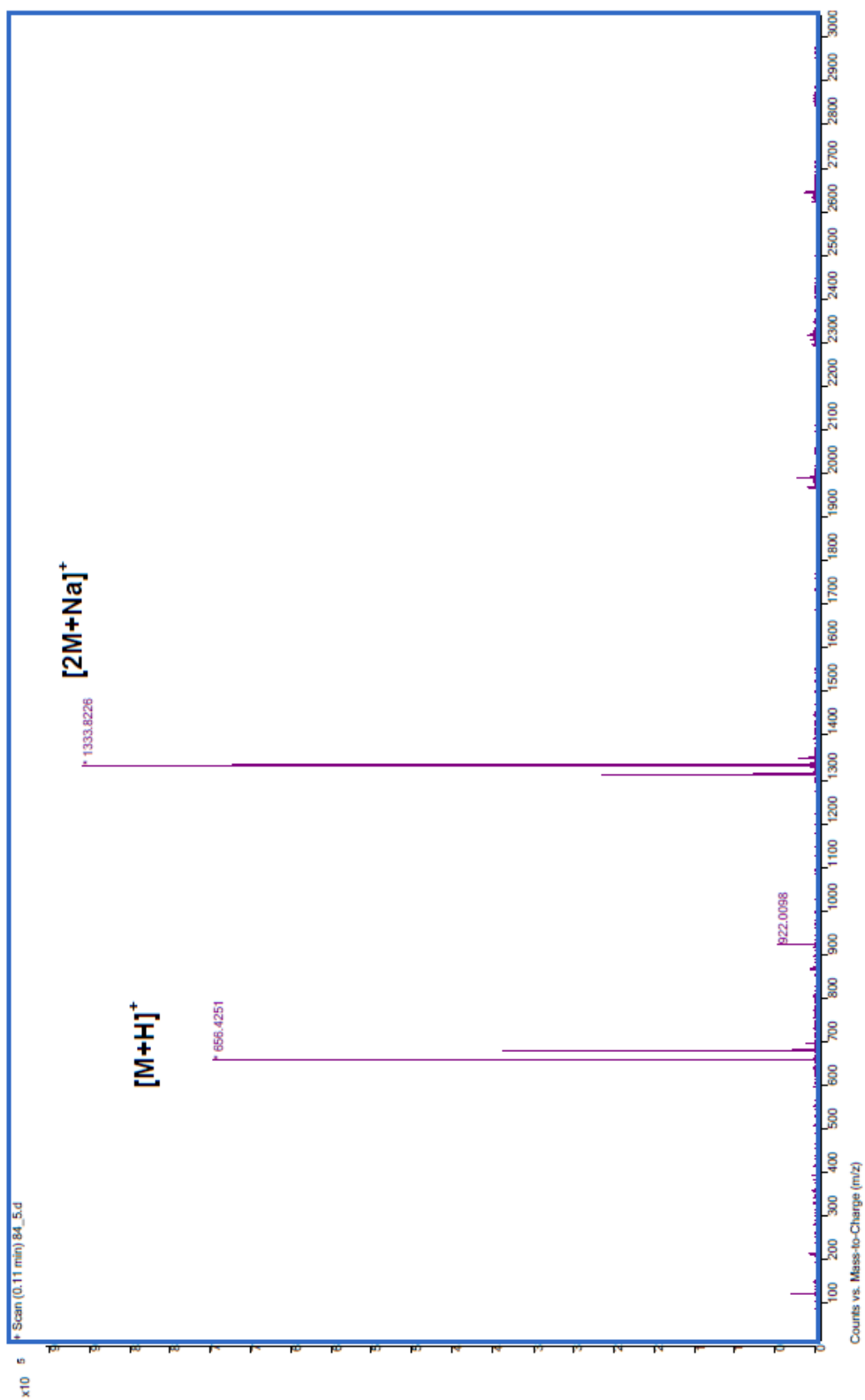
Symmetry transformations used to generate equivalent atoms

Appendix Table VI-6. Hydrogen Bonds for Globomycin A (1) [d = Å and < = deg.].

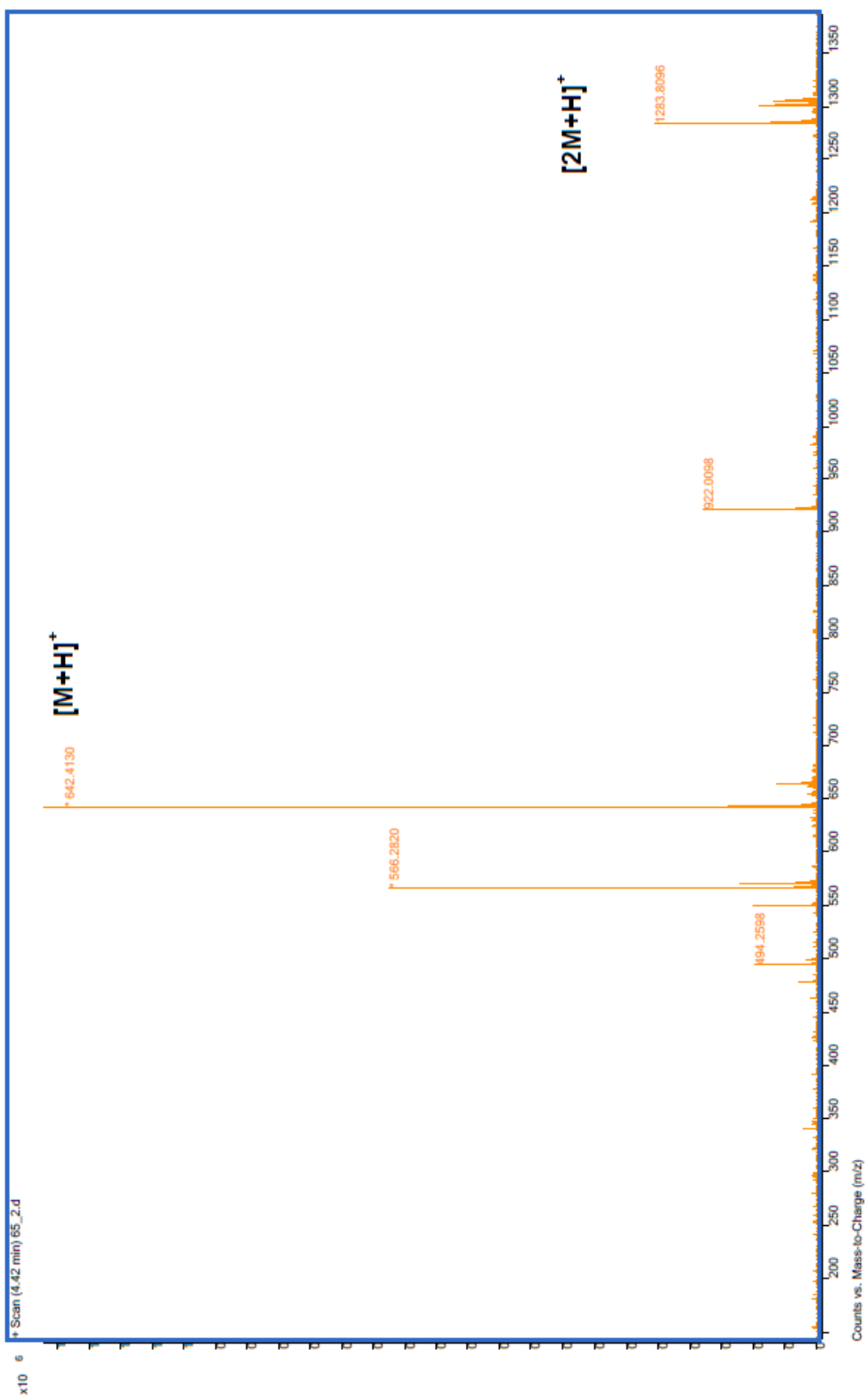
D-H...A	d(D-H)	d(H...A)	d(D...A)	<(DHA)
O(4)-H(4A)...O(8)#1	0.86(2)	1.91(2)	2.7679(15)	175(2)
O(6)-H(6A)...O(7)#2	1.04(3)	1.66(3)	2.6534(14)	158(3)
N(1)-H(1A)...O(7)	0.94(2)	1.93(2)	2.8300(17)	159.0(16)
N(3)-H(3A)...O(11)#3	0.91(2)	1.92(2)	2.8238(16)	175.9(18)
N(4)-H(4B)...N(5)	0.88(2)	2.299(18)	2.7965(16)	115.9(15)
N(4)-H(4B)...O(9)	0.88(2)	2.55(2)	3.0330(17)	115.5(17)

Symmetry transformations used to generate equivalent atoms

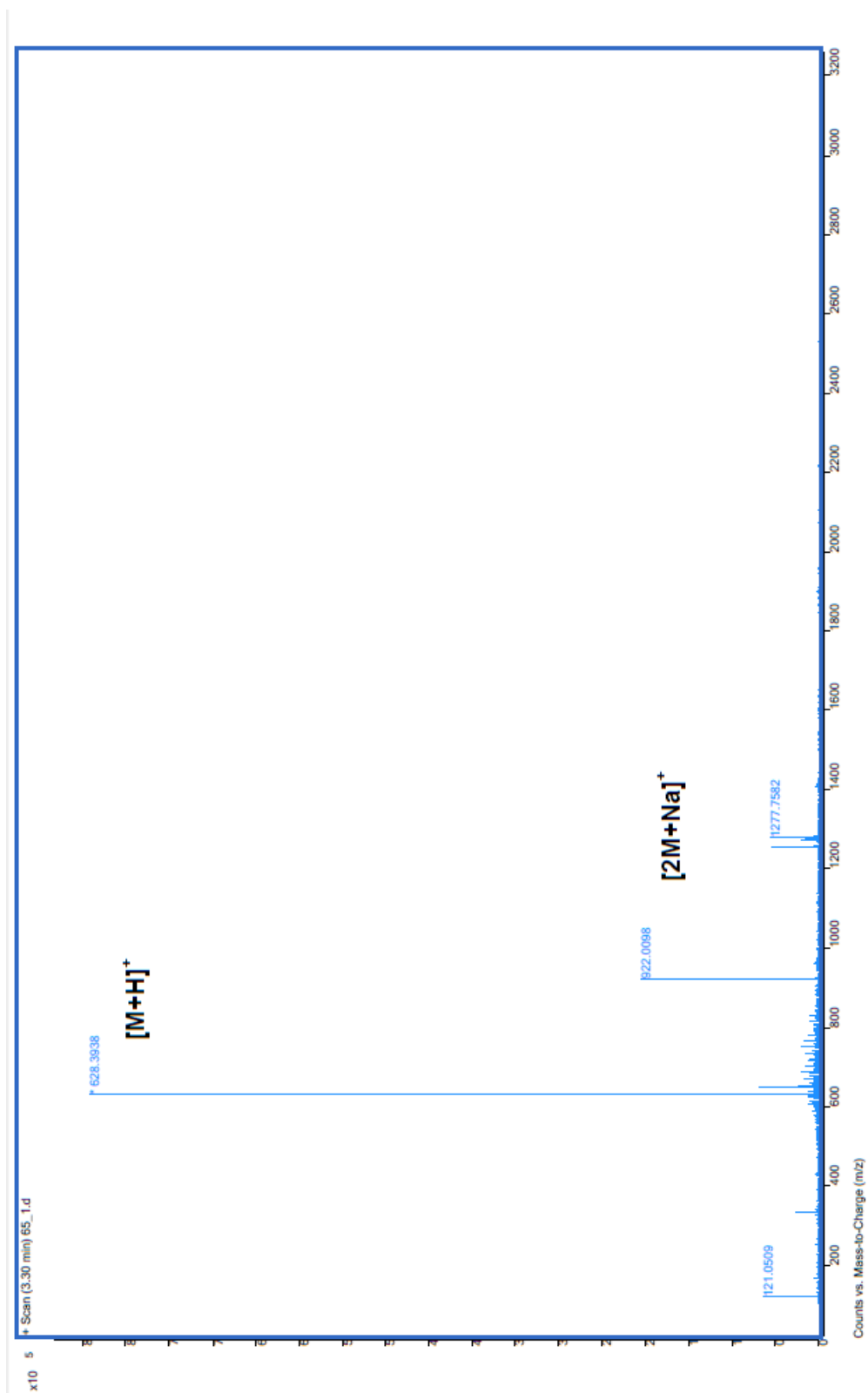
Appendix Figure VI-1: HRMS Spectrum of Globomycin A (1).



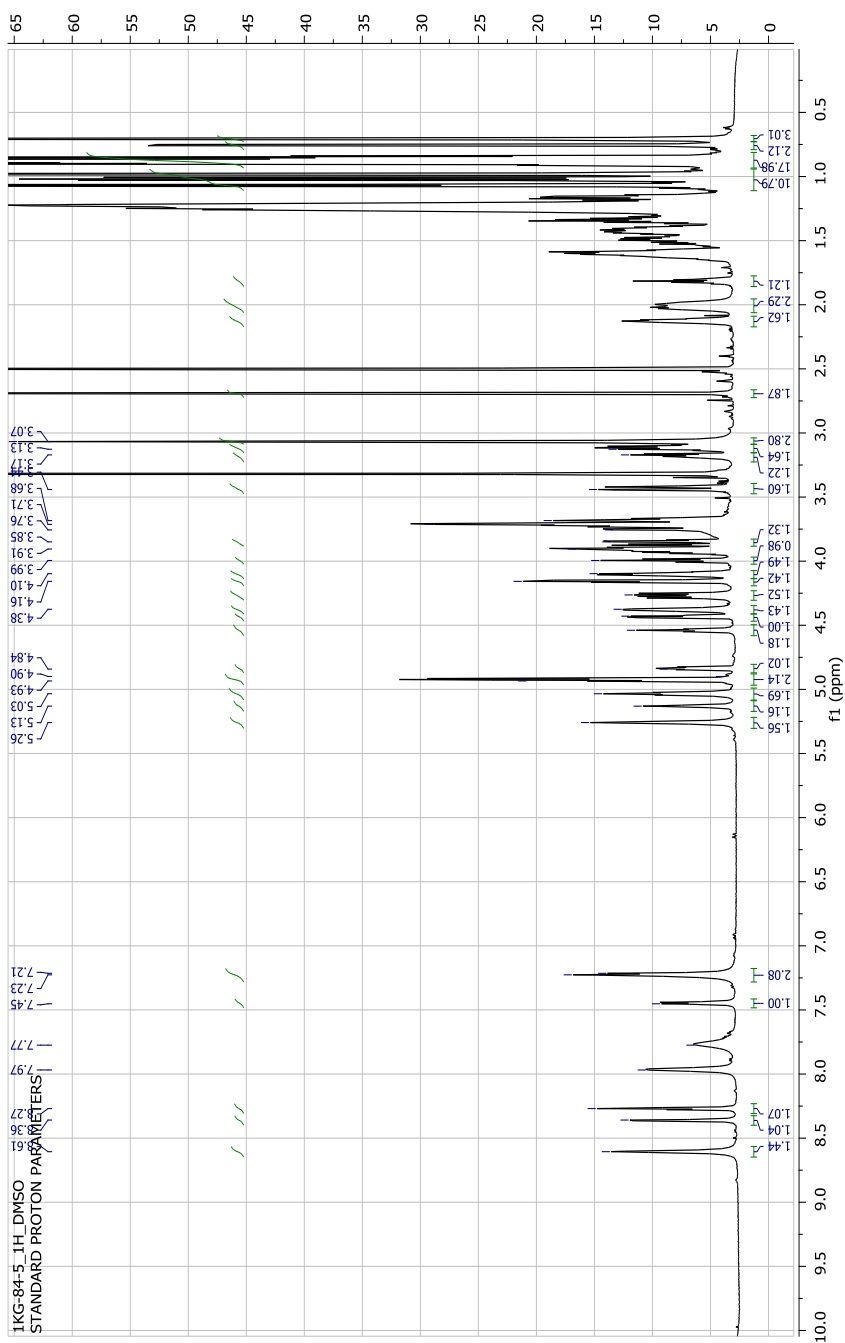
Appendix Figure VI-2: HRMS Spectrum of Globomycin B (2).



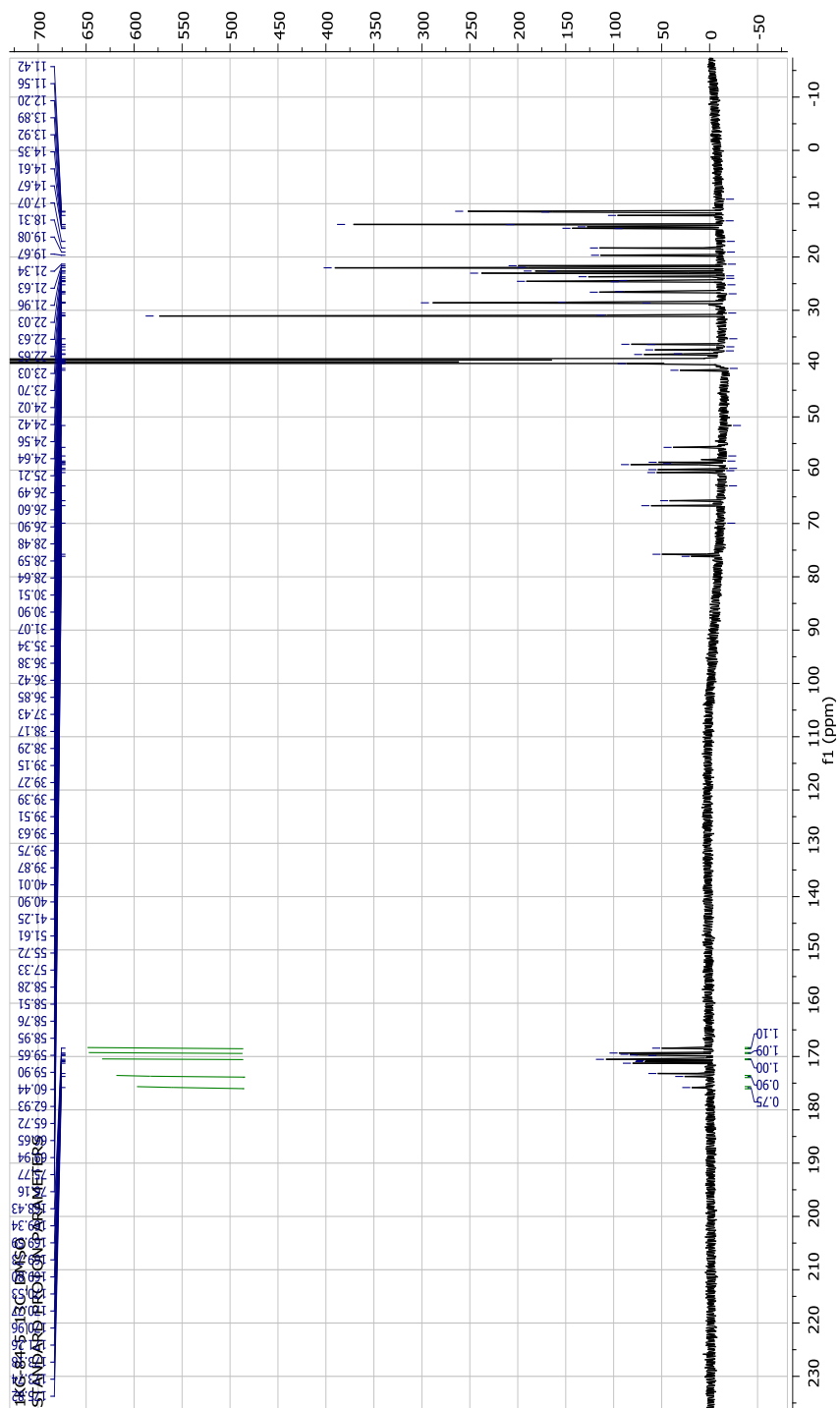
Appendix Figure VI-3: HRMS Spectrum of Globomycin C (3).



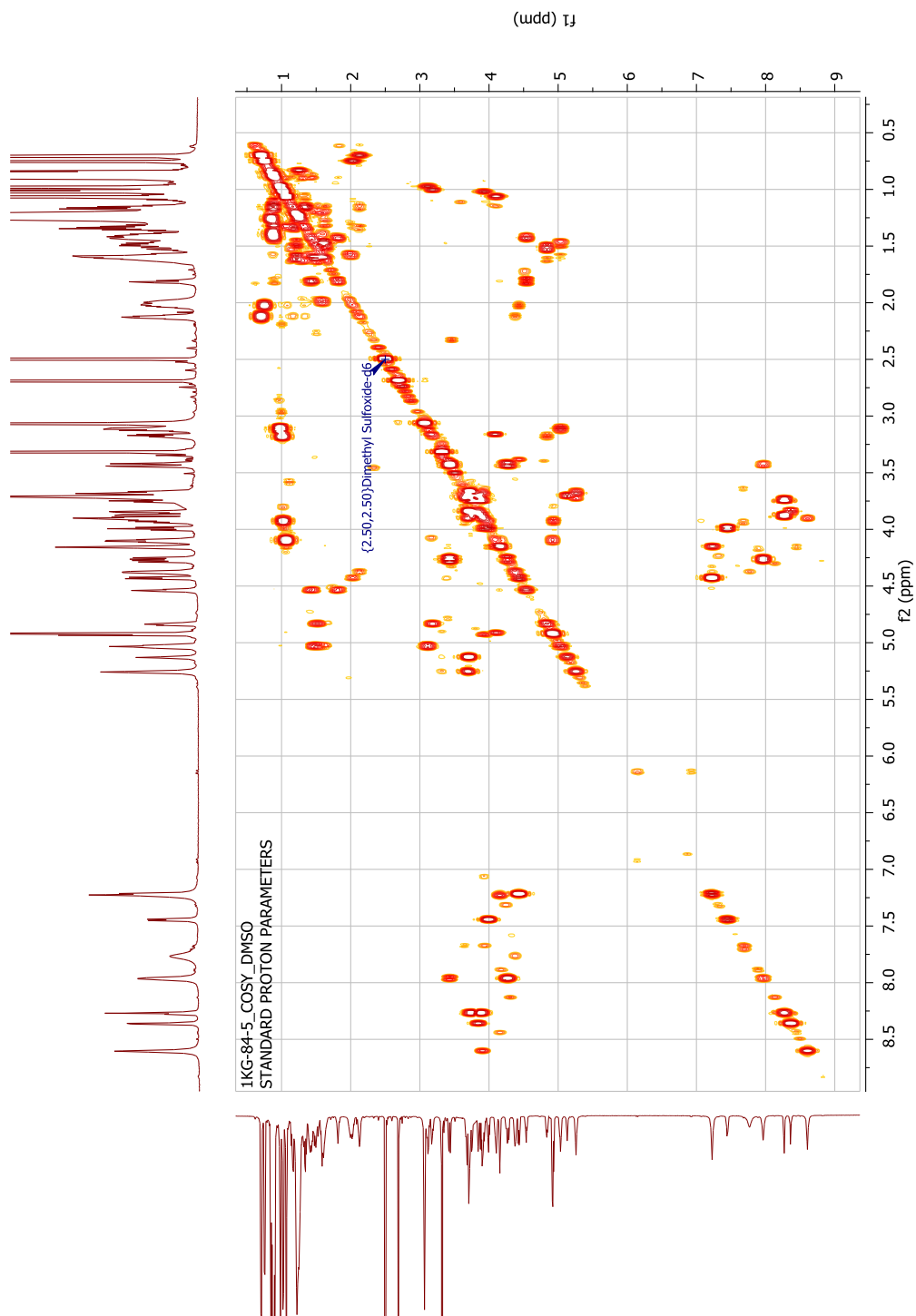
Appendix Figure VI-4: ¹H NMR Spectrum of Globomycin A (1) Recorded at 700 MHz (in DMSO-d6).



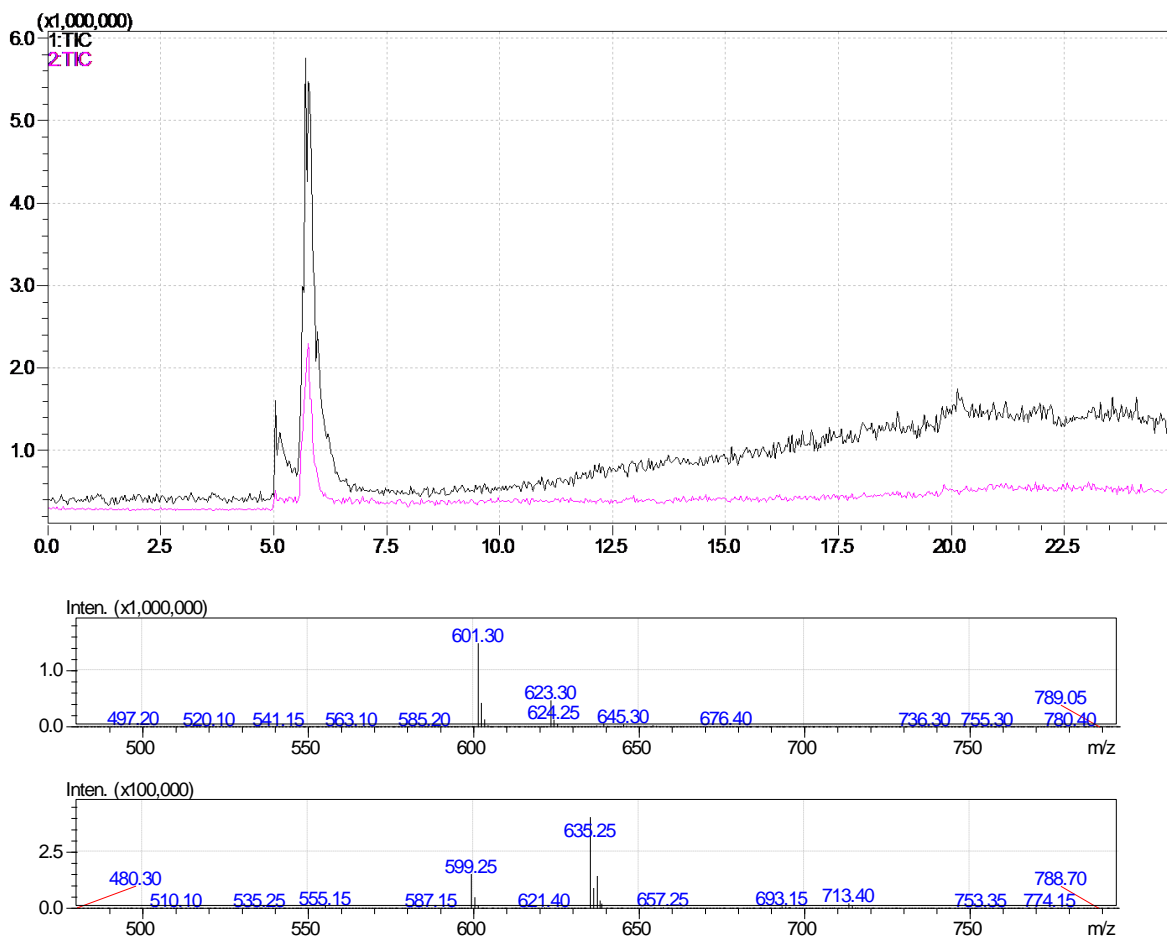
Appendix Figure VI-5: ^{13}C NMR Spectrum of Globomycin A (1) Recorded at 700 MHz (in DMSO-d₆).



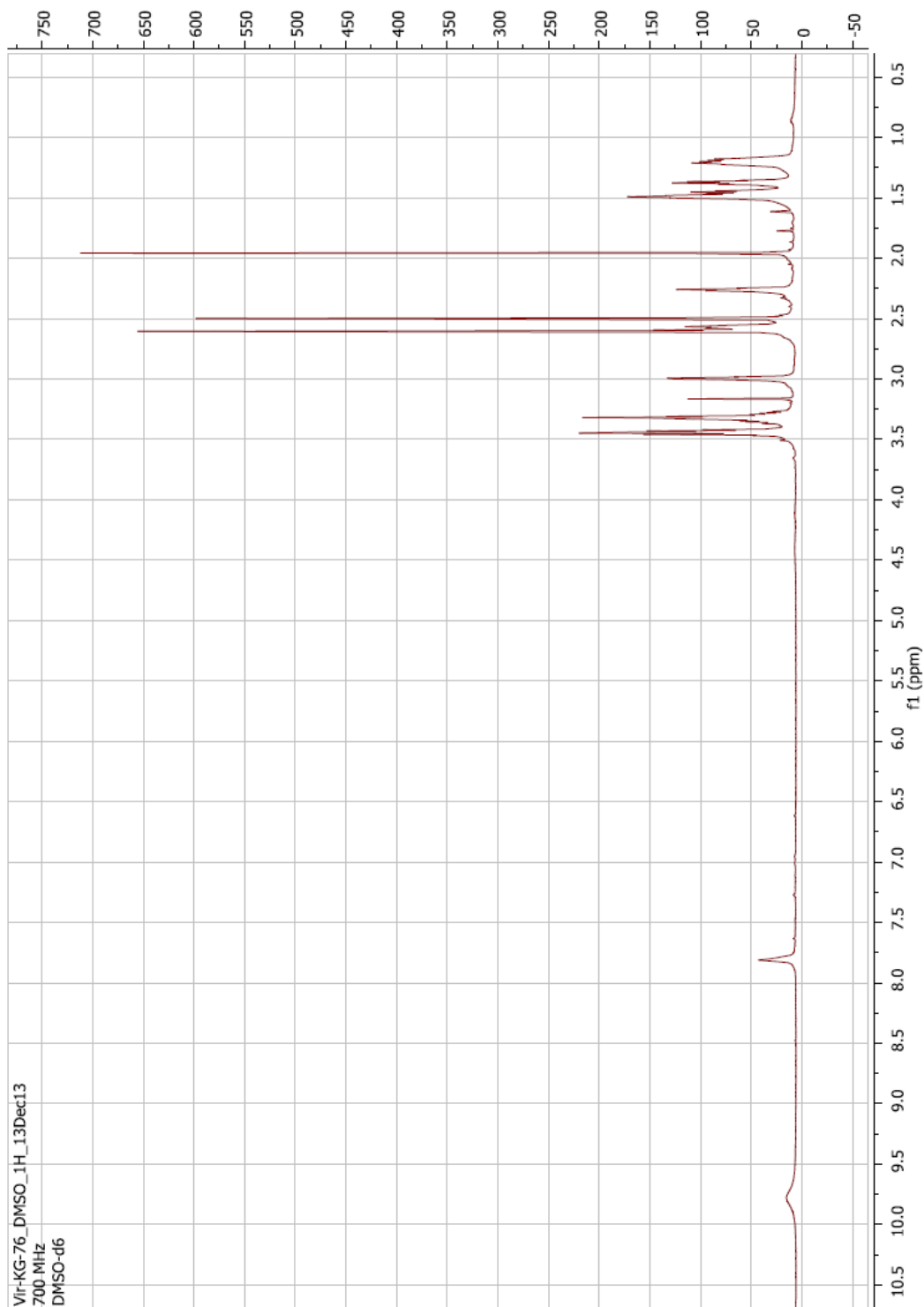
Appendix Figure VI-6: g-COSY Spectrum of Globomycin A (1) Recorded at 700 MHz (in DMSO-d6).



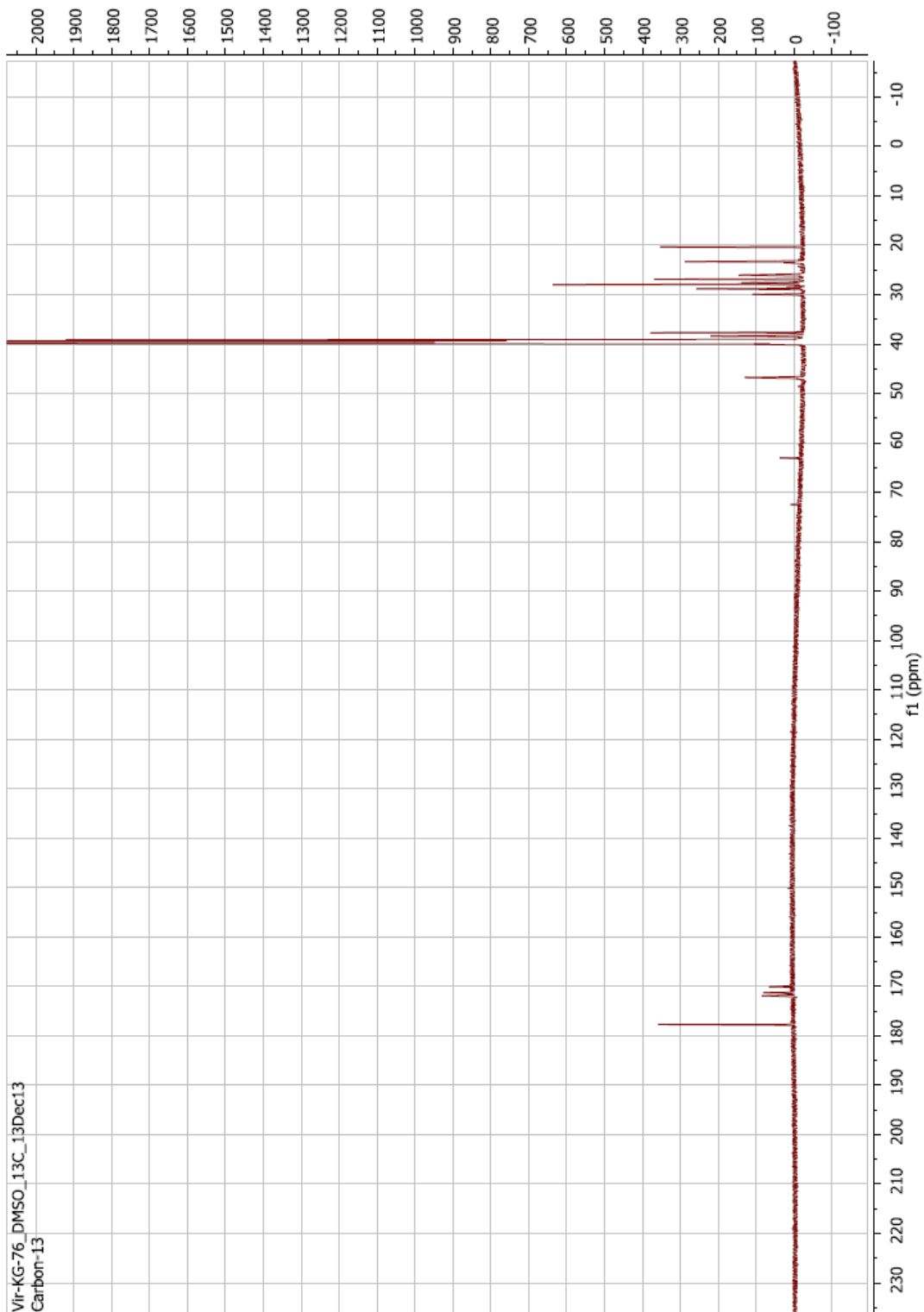
Appendix Figure VI-7: HRMS Spectrum of Desferrioxamine E.



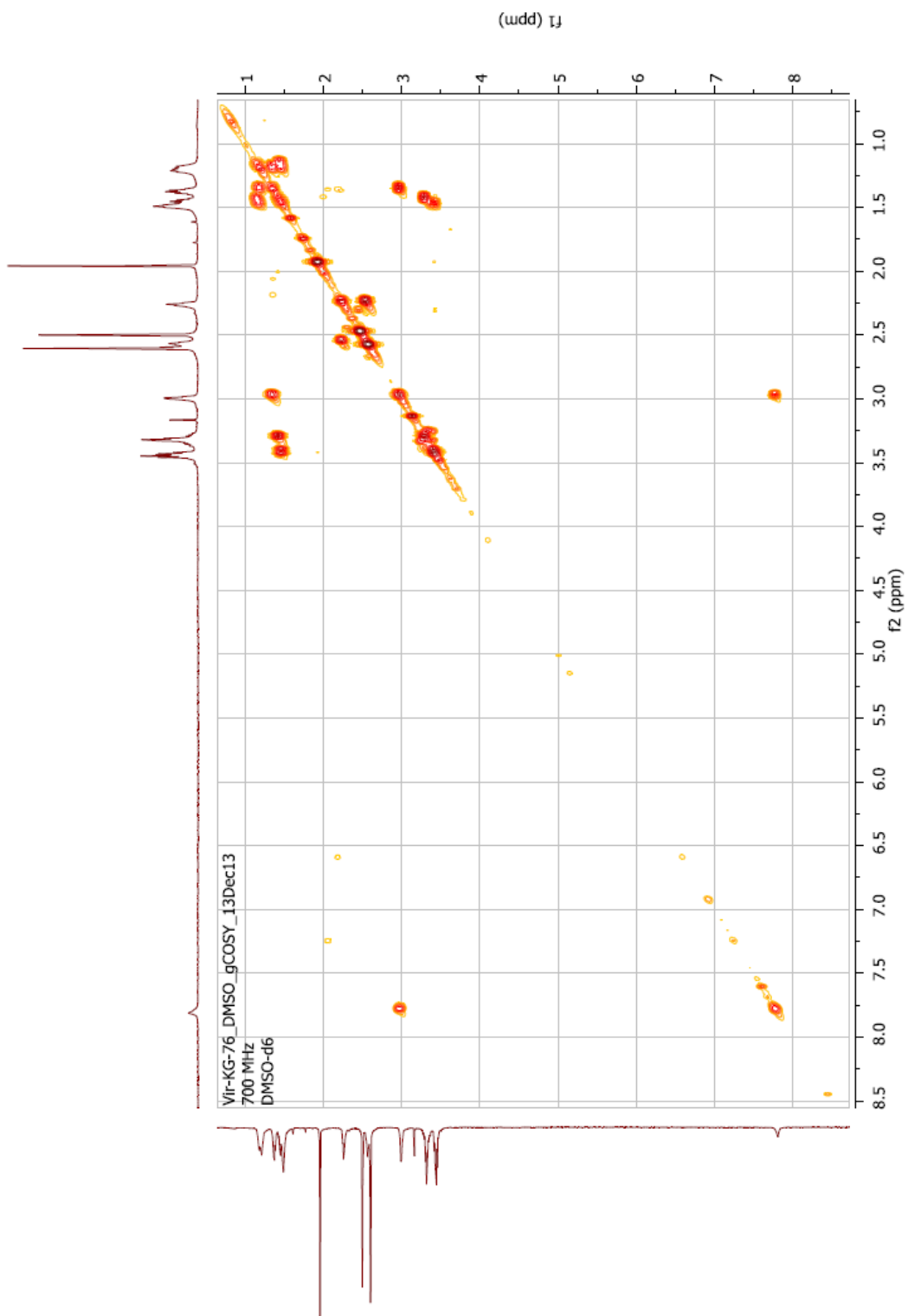
Appendix Figure VI-8: ^1H NMR Spectrum of Desferrioxamine E Recorded at 700 MHz (in DMSO-d6).



Appendix Figure VI-9: ^{13}C NMR Spectrum of Desferrioxamine E Recorded at 700 MHz (in DMSO-d6).



Appendix Figure VI-10: g-COSY Spectrum of Desferrioxamine E Recorded at 700 MHz (in DMSO-d6).



CHAPTER VII

Concluding Summary

In developing nations, diarrheal diseases are a leading cause of illness for children under five years of age and are responsible for 10% of all deaths of children in this age group.¹ It is estimated that 20% of all diarrheal diseases are caused by *Shigella* spp. infections.² Recent outbreaks of multi-drug resistant strains of *Shigella* in day care centers across developed nations has made evident that drug-resistant shigellosis is no longer a concern for only the developing world.³⁻⁶ Clearly, new treatments are needed. A recent trend in discovering new treatments for bacterial infections is to target virulence over bacterial viability.⁷ In theory, targeting virulence will produce less selective pressure for the emergence of resistance since virulence is not required for bacterial viability and anti-virulence therapies should not affect non-pathogenic organisms. Based on previous gene disruption studies,⁸⁻¹² we hypothesize that inhibiting VirF, the main transcriptional activator of the *Shigella* spp. pathogenesis cascade, with a small molecule will attenuate the virulence of *Shigella flexneri* and not affect bacterial viability. The purpose of this dissertation study was to identify and characterize inhibitors of VirF and determine their potential as anti-virulence agents for treating shigellosis.

As shown in Figure VII-1, VirF is known to activate the transcription of two genes, *virB* (encodes for a secondary transcriptional activator necessary for activating virulence

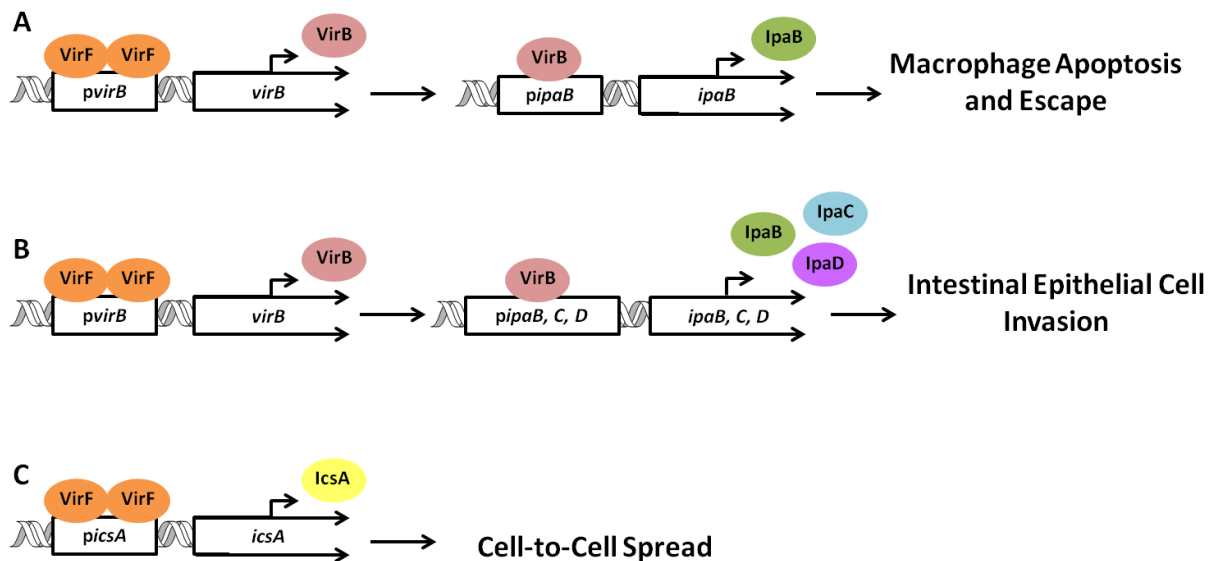


Figure VII-1: Genes Regulated by VirF and their Roles in Pathogenesis.

genes responsible for host cell invasion and macrophage escape) and *icsA* (encodes for an outer membrane protein that assembles actin polymerase and allows the bacterium to spread to adjacent host cells).^{13, 14} To identify inhibitors of VirF, we utilized a *Shigella*-based, VirF-driven, β -galactosidase reporter assay that monitored the transcriptional activation from the *virB* promoter. Using this assay, we followed up on our 42,000 compound pilot high-throughput screen (HTS),¹⁵ and screened an additional 100,000 compounds and 20,000 natural product extracts. Following a series of control screens and reconfirmation assays, we identified five compounds with IC_{50} values for VirF transcriptional activation ranging from 14 to 66 μ M. Although the compounds do not have great potency, we believe that their efficacy could be increased in future structure optimization studies. Also, previous studies have shown that if VirF expression levels are lowered by only 60% that *S. flexneri* displays an avirulent phenotype;¹⁶ therefore, it might not be necessary to have an extremely potent compound to produce a therapeutic effect *in vivo*.

S. flexneri is known to only infect the colonic epithelium in human and nonhuman primates. Therefore, to validate our HTS approach and test our hypothesis, we screened our inhibitors in Caco-2 monolayer models (derived from human epithelial colorectal adenocarcinoma cells) of the *S. flexneri* infection process. The compounds were tested in two different assays, a gentamicin protection invasion assay (model for initial host cell invasion) and a plaque formation assay (model for the cell-to-cell spread of an active infection). At concentrations that were not toxic to the bacteria or the Caco-2 monolayers, two compounds, 19615 and 144092, significantly reduced the ability of *S. flexneri* to initially invade the monolayers, while three compounds 19615, 144092, and 144143, modestly reduced the ability of *S. flexneri* to spread from cell-to-cell after initial invasion. Interestingly, compound 144143 only showed activity in the plaque formation assay. It is possible, since the cell-to-cell spread of an active infection relies on activation of the *icsA* promoter, that compound 144143 may have a preferential effect on inhibiting VirF transcriptional activation of the *icsA* promoter over the *virB* promoter. Our initial HTS assay only monitored activation of the *virB* promoter (required for initial host cell invasion, but not cell-to-cell spread). In the future, we plan on constructing an assay similar to our HTS reporter that monitors activation of the *icsA* promoter to test this theory. Nevertheless, the fact that the compounds attenuated the virulence of *S. flexneri* validates our HTS approach and confirms our hypothesis.

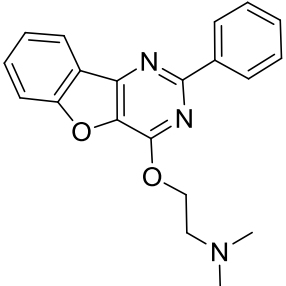
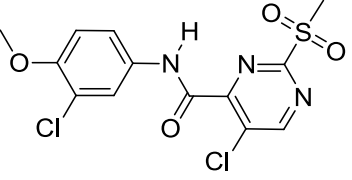
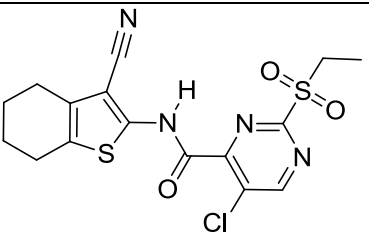
Next, to further characterize our compounds we sought to identify their mechanisms of inhibition. The exact process of how VirF activates transcription is not known. It is predicted that VirF must bind to its promoter region, dimerize, and recruit RNA polymerase. It is possible that our compounds could be inhibiting any of these

steps. The lack of information regarding VirF transcriptional activation is partly due to how difficult VirF is to study outside of the bacterial cell. VirF expresses poorly in recombinant systems, has a tendency to aggregate, and is fairly insoluble. To enable *in vitro* studies of isolated VirF, we developed a novel *Shigella*-based homologous expression system to express and purify MalE-VirF. Using this system, we were able to obtain pure MalE-VirF preparations with sufficient yields to enable the development of two *in vitro* DNA binding assays (an EMSA and FP assay) and report the first K_D (to our knowledge) for VirF binding to the *virB* promoter ($2.8 \pm 1.0 \mu\text{M}$). Using these assays, along with a fluorescence intercalator displacement assay, we were able to demonstrate that 19615 attenuates the virulence of *S. flexneri* by decreasing VirF transcriptional activation via direct inhibition of VirF-DNA binding. Using the FP assay we were also able to determine a K_i for 19615 ($5.6 \mu\text{M}$) and identify valuable structure-activity relationship trends to be incorporated into future generations of 19615 analogs. Unfortunately, we were unable to identify the mechanisms of inhibition of the remaining four compounds. It is possible that they could be inhibiting VirF dimerization, RNA polymerase recruitment, or acting through an unpredicted mechanism. We are currently developing assays to probe the other potential mechanisms of inhibition (e.g. an SPR platform that monitors VirF dimerization and/or RNA polymerase recruitment, an *in vitro* transcription assay, and other reporter systems).

In conclusion, we have developed tools, a novel homologous expression system and multiple assays, that have enabled us to study the activity of VirF at multiple levels (i.e. biochemical, bacterial, and cellular). Using these tools we have identified/characterized inhibitors of VirF transcriptional activation (see Table VII-1 for

summary of most promising compounds) and validated VirF as an anti-virulence target for a small molecule therapeutic to treat shigellosis. In the future, we plan on conducting synthetic structure-activity relationship studies to improve the potency of our leads, developing assays to probe the mechanisms of inhibition of our remaining compounds, and screening our inhibitors against additional AraC family regulators that control virulence in other organisms. Previous studies have shown that inhibitors of AraC family regulators have the potential to inhibit multiple different family members.¹⁷⁻²¹ It is possible that our lead compounds could not only be developed into an anti-virulence therapy to treat shigellosis, but into a broad-spectrum anti-virulence therapeutic agent.

Table VII-1. Summary of Most Promising Compounds Identified in this Work.

Compound	Reporter Assay IC ₅₀	%Inhibition at 6.25 μM in Invasion Assay	%Inhibition at 6.25 μM in Plaque Assay	Inhibits VirF from binding to <i>virB</i> promoter?
 19615	14 μM	77%	19%	Yes (K _i = 5.6 μM)
 144092	23 μM	63%	25%	No, negligible effect
 144143	23 μM	Negligible effect	42%	No, negligible effect

References

1. WHO/UNICEF. *Ending preventable child deaths from pneumonia and diarrhoea by 2025*; Geneva, Switzerland, 2013; pp 1-64.
2. Keusch, G. T.; Fontaine, O.; Bhargava, A.; Boschi-Pinto, C.; Bhutta, Z. A.; Gotuzzo, E.; Rivera, J.; Chow, J.; Shahid-Salles, S.; Laxminarayan, R. Diarrheal Diseases. In *Disease Control Priorities in Developing Countries*, 2nd ed.; Jamison, D. T.; Breman, J. G.; Measham, A. R., Eds. World Bank: Washington DC, 2006.
3. CDC. Outbreaks of multidrug-resistant *Shigella sonnei* gastroenteritis associated with day care centers-Kansas, Kentucky, and Missouri, 2005. *MMWR Morb Mortal Wkly Rep* **2006**, 55, 1068-1071.
4. Replogle, M. L.; Fleming, D. W.; Cieslak, P. R. Emergence of antimicrobial-resistant shigellosis in Oregon. *Clinical Infectious Diseases*. **2000**, 30, 515-9.
5. Shimosako, J.; Onaka, T.; Yamaguchi, M.; Yokota, M.; Nakamura, T.; Fujii, F.; Matsumoto, E.; Shibata, H.; Fukuda, M.; Tanaka, T. An Outbreak of Extended-Spectrum Beta-Lactamase (ESBL)-Producing *Shigella sonnei* at a Day Care Nursery in Sakai City, 2006. *Japanese Journal of Infectious Diseases* **2007**, 60, 408-409.
6. CDC. Importation and Domestic Transmission of *Shigella sonnei* Resistant to Ciprofloxacin - United States. *MMWR. Morbidity and Mortality Weekly Report* **2015**, 64.
7. Clatworthy, A. E.; Pierson, E.; Hung, D. T. Targeting virulence: a new paradigm for antimicrobial therapy. *Nature Chemical Biology* **2007**, 3, 541-548.
8. Qi, M. S.; Yoshikura, H.; Watanabe, H. Virulence phenotypes of *Shigella flexneri* 2a virulent mutant 24570 can be complemented by the plasmid-coded positive regulator *virF* gene. *FEMS Microbiology Letters* **1992**, 92, 217-221.
9. Adler, B.; Sasakawa, C.; Tobe, T.; Makino, S.; Komatsu, K.; Yoshikawa, M. A dual transcriptional activation system for the 230 kb plasmid genes coding for virulence-associated antigens of *Shigella flexneri*. *Molecular Microbiology* **1989**, 3, 627-35.

10. Colonna, B.; Casalino, M.; Fradiani, P. A.; Zagaglia, C.; Naitza, S.; Leoni, L.; Prosseda, G.; Coppo, A.; Ghelardini, P.; Nicoletti, M. H-NS regulation of virulence gene expression in enteroinvasive *Escherichia coli* harboring the virulence plasmid integrated into the host chromosome. *Journal of Bacteriology* **1995**, *177*, 4703-12.
11. Sansonetti, P. J.; Arondel, J.; Fontaine, A.; d'Hauteville, H.; Bernardini, M. L. OmpB (osmo-regulation) and icsA (cell-to-cell spread) mutants of *Shigella flexneri*: vaccine candidates and probes to study the pathogenesis of shigellosis. *Vaccine* **1991**, *9*, 416-22.
12. Makino, S.; Sasakawa, C.; Kamata, K.; Kurata, T.; Yoshikawa, M. A genetic determinant required for continuous reinfection of adjacent cells on large plasmid in *S. flexneri* 2a. *Cell* **1986**, *46*, 551-5.
13. Tobe, T.; Yoshikawa, M.; Mizuno, T.; Sasakawa, C. Transcriptional control of the invasion regulatory gene *virB* of *Shigella flexneri*: activation by *virF* and repression by H-NS. *Journal of Bacteriology* **1993**, *175*, 6142-9.
14. Tran, C. N.; Giangrossi, M.; Prosseda, G.; Brandi, A.; Di Martino, M. L.; Colonna, B.; Falconi, M. A multifactor regulatory circuit involving H-NS, *VirF* and an antisense RNA modulates transcription of the virulence gene *icsA* of *Shigella flexneri*. *Nucleic acids research* **2011**, *39*, 8122-8134.
15. Hurt, J. K.; McQuade, T. J.; Emanuele, A.; Larsen, M. J.; Garcia, G. A. High-Throughput Screening of the Virulence Regulator *VirF*: A Novel Antibacterial Target for Shigellosis. *Journal of Biomolecular Screening* **2010**, *15*, 379-387.
16. Durand, J. M. B.; Dagberg, B.; Uhlin, B. E.; Bjork, G. R. Transfer RNA modification, temperature and DNA superhelicity have a common target in the regulatory network of the virulence of *Shigella flexneri*: the expression of the *virF* gene. *Molecular Microbiology* **2000**, *35*, 924-935.
17. Bowser, T. E.; Bartlett, V. J.; Grier, M. C.; Verma, A. K.; Warchol, T.; Levy, S. B.; Alekshun, M. N. Novel anti-infection agents: small-molecule inhibitors of bacterial transcription factors. *Bioorganic & Medicinal Chemistry Letters* **2007**, *17*, 5652-5.
18. Kim, O. K.; Garrity-Ryan, L. K.; Bartlett, V. J.; Grier, M. C.; Verma, A. K.; Medjanis, G.; Donatelli, J. E.; Maccone, A. B.; Tanaka, S. K.; Levy, S. B.; Alekshun, M. N. N-hydroxybenzimidazole inhibitors of the transcription factor LcrF in *Yersinia*: novel antivirulence agents. *J Med Chem* **2009**, *52*, 5626-34.

19. Garrity-Ryan, L. K.; Kim, O. K.; Balada-Llasat, J. M.; Bartlett, V. J.; Verma, A. K.; Fisher, M. L.; Castillo, C.; Songsungthong, W.; Tanaka, S. K.; Levy, S. B.; Mecsas, J.; Alekshun, M. N. Small Molecule Inhibitors of LcrF, a *Yersinia pseudotuberculosis* Transcription Factor, Attenuate Virulence and Limit Infection in a Murine Pneumonia Model. *Infection and Immunity* **2010**, 78, 4683-4690.
20. Skredenske, J. M.; Koppolu, V.; Kolin, A.; Deng, J.; Kettle, B.; Taylor, B.; Egan, S. M. Identification of a Small Molecule Inhibitor of Bacterial AraC Family Activators. *Journal of biomolecular screening* **2013**, 18, 588-598.
21. Koppolu, V.; Osaka, I.; Skredenske, J. M.; Kettle, B.; Hefty, P. S.; Li, J.; Egan, S. M. Small-molecule inhibitor of the *Shigella flexneri* master virulence regulator VirF. *Infection & Immunity* **2013**, 81, 4220-31.